

Belief Distortions and Unemployment Fluctuations*

Do Lee[†]

October 23, 2025

[Click here for the latest version](#)

Abstract

This paper studies the dynamics of asset prices and unemployment when expectations deviate from a rational benchmark. Using machine learning forecasts as a benchmark for rational and efficient beliefs, I quantify distortions in survey forecasts of firms' future cash flows and discount rates. Survey forecasts overreact to cash flow news, while machine forecasts do not. These distortions explain a large share of variation in aggregate and firm-level hiring. Following positive idiosyncratic shocks, firms with distorted beliefs overhire relative to realized profits, while rational firms do not. Results suggest that distorted beliefs about firms' future cash flows can provide a unified explanation for volatility in aggregate unemployment and dispersion in firm-level hiring. A search model in which firms learn about the long-run mean of their cash flows with fading memory can reproduce these patterns by generating a large share of observed volatility in unemployment and asset valuations.

JEL Classification: E71, E24, E27, G41, J64

Keywords: Behavioral, Beliefs, Risk premia, Business Cycles, Unemployment

*I am grateful to Jaroslav Borovička, Sophia Chen, Daniel Greenwald, Sydney Ludvigson, Virgiliu Midrigan, and participants at seminars and conferences for their valuable comments. All errors remain my own.

[†]New York University, 19 West 4th Street, 6th Floor, New York, NY 10012. Email: dql204@nyu.edu.

1 Introduction

Why is unemployment so volatile? Unemployment is a key indicator of the business cycle and a central target of macroeconomic policy. Yet the standard search-and-matching (DMP) framework generates unemployment volatility an order of magnitude smaller than observed in the data, a disconnect known as the “unemployment volatility puzzle” (Shimer, 2005). Recent rational models have proposed rationalizing this disconnect with time-varying discount rates inferred from asset prices, with the assumption that recessions bring high risk premia that depress the present value of the long-term cash flows generated from firms’ hiring decisions (e.g., Hall, 2017; Borovickova and Borovička, 2017; Kehoe et al., 2023). However, there is a growing body of evidence finding that stock market investors and firm managers are neither perfectly rational nor efficient at processing information. Despite this evidence, little research has attempted to quantify the extent to which distortions in subjective beliefs (if any) can explain the unemployment volatility puzzle.

This paper addresses this gap in the literature. I measure firms’ subjective expectations using consensus survey forecasts from equity research analysts and CFOs, which proxy for the beliefs of corporate managers who make hiring decisions. I then construct a real-time measure of non-distorted and efficient expectation formation using the machine learning methodology developed in Bianchi et al. (2025) (BLLM, hereafter) that can identify distortions and inefficiencies in subjective beliefs. For brevity, I refer to such deviation, whether due to nonrational expectation or informational inefficiency, as a belief distortion of subjective beliefs from the non-distorted and efficient machine benchmark, and use the BLLM methodology to quantify the extent to which these belief distortions explain fluctuations in the labor market.

I document several results showing that belief distortions in expected cash flows, measured by corporate earnings, can quantitatively account for much of the observed variation in aggregate unemployment and firm-level hiring. First, I find that subjective beliefs implied by survey forecasts systematically overreact to cash flow news while machine forecasts do not, confirming the presence of belief distortions. Second, these distortions make hiring excessively sensitive to perceived cash flow changes, explaining more than 60% of variation in both aggregate and firm-level hiring. Third, following positive idiosyncratic shocks, firms with distorted beliefs overreact to the shock and overhire relative to realized profits, leading to lower subsequent profits per worker. Fourth, I develop a calibrated search-and-matching model with constant-gain learning about the long-run mean of firms’ cash flow process that is consistent with the documented overreaction. The learning model explains 60% of U.S. unemployment volatility and 66% of

hiring rate dispersion, compared with 16% and 30% explained by the standard rational search model without time-varying discount rates, respectively (Shimer, 2005). These results suggest that unemployment is volatile because firms' subjective expectations about future cash flows are distorted. In general I find that, when firms form expectations about their future cash flows, they overreact to recent information by interpreting good and bad news alike as more persistent than a non-distorted perspective would imply. Overoptimism about future cash flows in transitory booms inflates the perceived value of hiring and leads firms to post more vacancies than warranted, tightening labor markets. In recessions, pessimism overshoots, reducing the perceived value and leading to a collapse in hiring.

This paper makes two contributions to understanding unemployment fluctuations. First, I go beyond documenting violations of full information rational expectations (FIRE) to quantifying their importance for labor market fluctuations. While previous work has investigated whether forecast errors made by survey respondents deviate from FIRE, knowing whether a deviation exists does not necessarily quantify its importance for hiring behavior. To do so, I construct a benchmark for objective beliefs using a machine learning algorithm that makes out-of-sample forecasts of firms' cash flows and discount rates. I use the algorithm of BLLM to train a neural network that can diverge from the survey only if the machine finds evidence of predictable mistakes in survey responses. Crucially, the machine operates entirely out of sample using only historical data available when firms make their hiring decisions. Comparing survey forecasts to this rational benchmark therefore isolates belief distortions, which I find arise from overreaction or underreaction to cash-flow news, shaping firm hiring behavior.

Second, belief distortions provide a unified explanation for both aggregate and firm-level hiring behavior. Because belief distortions lead firms to overreact to both aggregate and idiosyncratic shocks, the same mechanism can explain both aggregate unemployment volatility and cross-sectional hiring dispersion. Good news about idiosyncratic cash flows triggers overoptimism, leading to overhiring and reduced profitability per worker. This contrasts with rational models that explain fluctuations in hiring using time-varying discount rates, where idiosyncratic shocks are diversifiable in the absence of additional frictions and should not affect discount rates or hiring.

Several additional points about these findings bear noting. First, the evidence for survey overreaction comes from comparing survey forecasts against machine-based predictions, which serve as a rational benchmark. The wedge between these two measures arises specifically from survey overreaction to news rather than from any systematic errors in the machine forecasts. This pattern holds consistently both in the aggregate time series and across individual firms,

providing evidence that the distortions reflect genuine biases in expectation formation rather than measurement error. Using the firm's hiring condition in a search-and-matching model, I link this belief distortion to hiring behavior by decomposing the value of hiring into expected cash flows, measured by expected earnings, and discount rates, measured by expected stock returns. The structure of this decomposition is analogous to the present-value identity of Campbell and Shiller (1988), which attributes fluctuations in valuation ratios in asset markets to revisions in expected cash flows versus discount rates. Comparing the decomposition under survey and machine forecasts quantifies how much of the variation in hiring arises from biased beliefs.

Under subjective beliefs, hiring is excessively sensitive to news about cash flows when compared against my measure of objective beliefs. In models that rely on rational expectations with time-varying discount rates, it is perhaps unsurprising that objective measures of discount rates dominate, explaining 69% of aggregate variation and 60% of cross-sectional dispersion in hiring. By contrast, under subjective beliefs, distorted cash flow expectations account for 97% of aggregate variation and 79% of cross-sectional dispersion. A key result is that it is not the subjective belief *per se*, but rather the identified distortion in these beliefs that drives the greatest part of this excess sensitivity. This finding demonstrates that labor market fluctuations reflect how firms perceive, not how they discount, future cash flows.

Third, rational and subjective beliefs have qualitatively different implications for how firms respond to idiosyncratic shocks. Using local projections, I estimate how actual profits per worker respond to forecast revisions under both rational and subjective beliefs. To isolate idiosyncratic variation, I sort firms into portfolios based on idiosyncratic shocks estimated as residuals from a firm-level autoregressive model with firm and industry-time fixed effects. Under rational beliefs using machine forecasts, profits per worker remain stable after idiosyncratic shocks, consistent with no overreaction in discount rates where the machine correctly identifies these shocks as largely temporary. Under subjective beliefs using survey forecasts, however, profits per worker drop significantly following positive idiosyncratic news. This occurs because subjective beliefs overreact by becoming overly optimistic, inflating the expected value of hiring and causing firms to overhire relative to actual profits. The belief distortion thus provides a unified explanation for why hiring responds to not only aggregate shocks but also idiosyncratic shocks.

Fourth, the constant-gain learning model generates overreaction because firms place excessive weight on recent observations when updating beliefs about the long-run mean of their cash flow process. When firms observe positive cash flow shocks, they mistakenly interpret them as more persistent than they actually are, leading to excessive optimism about future hiring value. Conversely, negative shocks generate excessive pessimism. This distorted belief about expected

cash flows then drives excessive fluctuations in the value of hiring, which allows the model to generate the large subjective cash flow component in the variance decomposition. The model also produces realistic cross-sectional dispersion as firms react differently to their histories of idiosyncratic shocks.

Related Literature This paper contributes to the literature on unemployment fluctuations, labor markets, asset prices, and expectation formation by quantifying the extent to which distorted beliefs relevant to asset prices can explain labor market fluctuations.

First, it relates to the literature on the unemployment volatility puzzle in search-and-matching models under the Diamond, Mortensen, and Pissarides (DMP) framework (Shimer, 2005).¹ The search model struggles to generate sufficient volatility in unemployment unless firms' responses to shocks are amplified through mechanisms such as time-varying discount rates (Hall, 2017; Borovickova and Borovička, 2017; Kehoe et al., 2023).² Another strand of the labor search literature attributes high unemployment volatility to wage rigidity arising from credible bargaining (Hall, 2005; Hall and Milgrom, 2008), staggered negotiations (Gertler and Trigari, 2009), or incentive contracts (Gaur et al., 2023). Existing work in this literature generally assumes that firms rationally process information about cash flows and discount rates. My paper complements this approach by highlighting distortions in subjective beliefs as a distinct mechanism generating large unemployment fluctuations. My contribution is to show that firms' overreaction to cash flow news can generate aggregate unemployment volatility and the cross-sectional dispersion in hiring, a dimension that existing aggregate models with time-varying discount rates miss.

A growing literature embeds nonrational expectations in macro models with labor market frictions (Venkateswaran, 2014; Acharya and Wee, 2020; Mueller et al., 2021; Menzio, 2023; Faberman et al., 2022; Bhandari et al., 2024; Jäger et al., 2024; Du et al., 2025). Notably, Bhandari et al. (2024) show that pessimism in households and firms can explain the volatility of unemployment fluctuations. Du et al. (2025) document stickiness in workers' job finding and separation expectations, showing that belief stickiness attenuates precautionary saving and leads workers to under-insure during recessions. My paper extends this work by providing a new estimate that quantifies the importance of distorted beliefs, showing that overreaction to cash flow news, which can mean either excessive pessimism or excessive optimism depending on the

¹See also Hagedorn and Manovskii (2008), Hall and Milgrom (2008), Pissarides (2009), Elsby and Michaels (2013), Kudlyak (2014), Chodorow-Reich and Karabarbounis (2016), and Ljungqvist and Sargent (2017).

²Related work that takes an asset pricing perspective on the labor market under rational expectations includes Merz and Yashiv (2007), Donangelo (2014), Belo et al. (2014), Favilukis and Lin (2015), Kuehn et al. (2017), Kilic and Wachter (2018), Mitra and Xu (2019), Donangelo et al. (2019), Kehoe et al. (2019), Liu (2021), Belo et al. (2023), and Meeuwis et al. (2023).

news, is the main driver of unemployment volatility. The cross-sectional analysis in my paper adds another dimension to belief-driven labor market volatility by showing that firms with more distorted beliefs exhibit greater fluctuations in hiring.

The empirical analysis builds on survey-based evidence on firm expectations. Ben-David et al. (2013) document persistent overoptimism in CFO forecasts. Gennaioli et al. (2016) document that extrapolative CFO expectations of earnings growth predict corporate investment. Ma et al. (2020) link biases in managerial forecasts to distortions in firm investment. Coibion et al. (2018) and Candia et al. (2020) find that firm managers' inflation expectations adjust slowly and display substantial dispersion. My paper builds on this work by showing how distortions in survey expectations shape labor markets.

The variance decomposition and learning model in this paper builds on recent work using survey-based expectations to reassess the drivers of asset prices.³ The approach adapts the present-value identity framework from Campbell and Shiller (1988) and Cochrane (2007), which attributes variation in valuation ratios to expected cash flows and discount rates. Recent survey-based applications challenge the traditional view that discount-rate variation dominates asset price fluctuations. De La O and Myers (2021) show that subjective expectations of cash flow growth explain most of the variation in valuation ratios, while Bordalo et al. (2024a) find that overreaction in long-term earnings expectations drives return predictability. My contribution is to construct an explicit measure of objective beliefs that can quantify the overall magnitude of distortions in subjective beliefs about firms' cash flows and demonstrate that they not only drive asset prices but also shape real decisions such as hiring.

I adopt the machine learning approach to using a dynamic real-time forecasting framework (of BLLM, and the others) to measuring the magnitude of distortions in subjective beliefs. The algorithm uses high-dimensional prediction models estimated on rolling samples of real-time data to produce a benchmark that is free from human cognitive biases and look-ahead bias, while also addressing overfitting and structural change. As in Bianchi et al. (2022) and BLLM, I structure the algorithm so that the machine's forecasts can differ from the survey forecasts only if the machine finds evidence of predictable mistakes in the survey responses immediately prior to the machine making a true out-of-sample forecast. The method uses tools from machine learning by training LSTM networks with recursive re-estimation and hyperparameter tuning (Gu et al., 2020, Cong et al., 2020, Nagel, 2021, Bybee et al., 2024). The resulting forecasts are fully ex-

³Related work includes Timmermann (1993), Barberis et al. (1998), Chen et al. (2013), Greenwood and Shleifer (2014), Collin-Dufresne et al. (2016), Adam et al. (2016), De La O and Myers, 2021, Giglio et al. (2021), Nagel and Xu (2022), Jin and Sui (2022), Bordalo et al., 2024a, De La O et al. (2024), Adam and Nagel (2023), Décaire and Graham (2024), and Bastianello et al. (2024).

ante and provide high-dimensional empirical counterparts to rational expectations for evaluating belief distortions. The machine learning algorithm in this paper differs from these studies in that it is expressly designed to uncover and quantify distortions in subjective beliefs.

The rest of the paper proceeds as follows. Section 3 describes the data used in the empirical analysis. Section 4 documents overreaction in survey expectations and compares the predictive performance of machine and survey forecasts. Section 5 presents a search and matching model with belief distortions and derives a decomposition of the vacancy filling rate. Section 6 presents the estimated variance decomposition of the aggregate vacancy filling rate. Section 7 presents cross-sectional evidence motivated by a firm-level extension of the baseline model. Section 8 introduces a model of constant-gain learning about future earnings that could match the decompositions estimated from the data. Section 9 discusses model extensions and robustness checks. Finally, section 10 concludes.

2 Data

This section describes the data used to estimate the time-series and cross-sectional variance decompositions. For each outcome, I measure subjective expectations with survey forecasts $\mathbb{F}_t[\cdot]$ and rational expectations with machine learning forecasts $\mathbb{E}_t[\cdot]$. The estimation sample is quarterly, 2005Q1-2023Q4. Throughout, t indexes quarters and i indexes firms.⁴

Labor Market Outcomes *Aggregate level: Vacancy Filling Rate.* The vacancy filling rate q_t measures the probability that a posted vacancy is filled in period t :

$$q_t \equiv \frac{\text{Total Hires}}{\text{Total Job Vacancies}} = \frac{f_t U_t}{V_t},$$

where V_t is total job vacancies from JOLTS job openings (available since 2000:12; earlier periods use the help-wanted index, Barnichon, 2010), and U_t is the unemployment level (BLS). The job finding rate f_t measures the probability that an unemployed worker finds a job within the month. Following Shimer (2005), I infer how many people must have exited unemployment each period from the decline in total unemployment after removing very short-term unemployed workers:

$$f_t = 1 - \frac{U_t - U_t^s}{U_{t-1}},$$

where U_t^s is short-term unemployment less than 5 weeks (UEMPLT5). The job separation rate δ_t is from JOLTS. Variables are constructed monthly, aggregated to quarterly averages, and detrended with an HP filter ($\lambda = 10^5$) following Shimer (2005).

⁴Appendix C provides additional details. Figure A.1 and Table A.1 report stylized facts.

Firm level: Hiring Rate. Since firm-level vacancies are not readily observable, I proxy hiring at the firm level by the net hiring rate,

$$hl_{i,t} \equiv \log\left(\frac{L_{i,t+1} - (1 - \delta_{i,t})L_{i,t}}{L_{i,t}}\right) = \log\left(\frac{\text{Total Hires}}{\text{Total Employment}}\right),$$

where $L_{i,t}$ is employment for firm i , recorded at fiscal year-end and carried forward to quarterly frequency. $\delta_{i,t}$ is the separation rate of firm i 's NAICS2 industry (from JOLTS). Including job separations ensures the hiring rate captures total hires needed to both replace departing workers and expand employment. The firm-level sample includes publicly listed firms with common stocks (share codes 10, 11) on NYSE/AMEX/NASDAQ with IBES analyst coverage of expected earnings and stock price targets.

Earnings (Realized Cash Flows) *Firm level.* Firm-level earnings $E_{i,t}^*$ are constructed from IBES street earnings per share (EPS), converted to total earnings by multiplying by each firm's shares outstanding (1983Q4-2023Q4). Street earnings exclude one-off items that are not informative for ongoing operations and better proxy expected cash flows (Hillenbrand and McCarthy, 2024). To handle instances where firm earnings may be zero or negative, which would make log transformations undefined, I follow the approach of Vuolteenaho (2002) and define a transformed measure of earnings that is strictly positive. Specifically, each firm is treated as a portfolio consisting of a fraction $(1 - \lambda)$ of equity and a small fraction λ of risk-free assets, such that

$$E_{i,t} = (1 - \lambda)E_{i,t}^* + \lambda r_t^f P_{i,t-1}, \quad \lambda = 0.10,$$

where $P_{i,t-1}$ is lagged equity value and r_t^f is the one-year Treasury bill rate. The risk-free component ensures $E_{i,t} > 0$ for all observations while preserving the cross-sectional variation in earnings. This transformation allows log earnings $e_{i,t} \equiv \log E_{i,t}$ to be well defined even in periods when reported earnings $E_{i,t}^*$ are negative.

Aggregate level. I aggregate firm-level earnings to the S&P 500 level to obtain a time-series for aggregate earnings:

$$E_t = \Omega_t \sum_{i \in x_t} \frac{E_{i,t}^*}{\text{Divisor}_t},$$

where x_t is the set of S&P 500 firms with IBES data, Ω_t is a scaling factor that adjusts for occasionally incomplete IBES coverage of the S&P 500, and Divisor_t is the S&P 500 divisor.

Cash Flow Expectations (Surveys) *Firm level.* Subjective earnings expectations $\mathbb{F}_t[\Delta e_{i,t+h}]$ are obtained from the Institutional Brokers' Estimate System (IBES) database, which reports the median consensus forecasts of equity research analysts (1983Q4–2023Q4).

I use analyst forecasts as a proxy for managerial expectations. This approach is supported by three considerations. First, analyst and CFO forecasts of earnings growth are highly correlated (approximately 0.60 at the one-year horizon), indicating broadly consistent beliefs across groups (Gennaioli et al., 2016).⁵ Second, prior research shows that analyst forecasts are widely followed by managers and investors and influence corporate decisions (Kothari et al., 2016). Third, analysts have access to similar information sets as managers and often communicate directly with them (Brown et al., 2015). Although analyst forecasts are not produced by firm managers themselves, they provide a market-based measure of expectations that reflects the informational environment in which managers form beliefs. Throughout, I interpret optimism or pessimism in analyst forecasts as indicative of the informational environment and belief distortions surrounding the firm’s decision-making.

IBES analysts provide forecasts of “street” earnings per share (EPS) for each firm’s upcoming fiscal years, typically over horizons of one to four years ahead, as well as a long-term growth (LTG) forecast representing the expected average annual growth in operating earnings over the next three to five years. These forecasts are released monthly and are widely followed by market participants as professional assessments of firms’ expected performance. Because they are tied to specific firms, the IBES forecasts capture firm-level subjective expectations, which can be aggregated to the market level.

For each firm i , I compute expected earnings growth as the forward annual log difference between adjacent horizon level forecasts. Specifically, for $h = 1, 2$, the forecasted annual growth rate $\mathbb{F}_t[\Delta e_{i,t+h}]$ is the log change between the h -year-ahead and $(h-1)$ -year-ahead level forecasts. For horizons $h = 3, 4, 5$, I interpret the LTG forecast as the expected annualized growth rate over the next three to five years, following De La O and Myers (2021).

Aggregate level. Firm-level forecasts are aggregated to the S&P 500 level by value weights based on market capitalization, while long-term growth forecasts are aggregated using value-weighted averages. This aggregation produces an estimate of aggregate expected earnings growth that reflects the beliefs of analysts tracking the firms that constitute the S&P 500. These forecasts therefore serve as proxies for subjective expectations of future corporate cash flows at both the firm and aggregate levels.

⁵ Appendix Table A.5 reports robustness checks using managerial earnings forecasts from the quarterly CFO survey. The correlation between analyst and managerial expectations is approximately 0.60 at the one-year horizon.

Discount Rates (Stock Returns) Subjective expectations of stock returns $\mathbb{F}_t[r_{t+h}]$ are drawn from two survey sources, depending on whether the analysis is at the aggregate or firm level.

Aggregate level. For the S&P 500, I use the quarterly *CFO Global Business Outlook Survey* (2001Q4–2023Q4), which reports the mean expected nominal return on the S&P 500 over horizons of one and ten years. Respondents include chief financial officers, vice presidents of finance, and other senior financial executives from a broad set of U.S. firms ranging from small private companies to large publicly listed corporations (approximately 1,600 members as of 2022). These expectations represent forward-looking assessments of aggregate equity returns held by decision makers directly involved in firms’ investment and financing decisions. For intermediate horizons between one and ten years, I interpolate linearly between the reported forecasts.

Firm level. For individual firms, I use stock price target data from the *IBES* and *Value Line* databases, which report the median forecasted stock price over 12 month and 3 to 5 year horizons, respectively. These forecasts are provided by sell-side equity research analysts who specialize in evaluating firm fundamentals and valuation prospects. I convert these price targets into implied expected total returns as

$$\mathbb{F}_t[r_{i,t+h}] \approx \log\left(\frac{\mathbb{F}_t[P_{i,t+h}]}{P_{i,t}} + \frac{D_{i,t}}{P_{i,t}} \frac{\mathbb{F}_t[D_{i,t+h}]}{D_{i,t}}\right),$$

where $P_{i,t}$ is the firm’s current stock price (CRSP), $D_{i,t}$ is its dividend (Compustat), and the expected dividend growth ratio $\mathbb{F}_t[D_{i,t+h}]/D_{i,t}$ is set to 1.064, the postwar average for U.S. equities (Nagel and Xu, 2022). I interpret Value Line targets as five-year-ahead forecasts and interpolate intermediate horizons linearly between the IBES one-year and Value Line five-year projections.

Price-Earnings Ratio The current log price-earnings ratio is $pe_{i,t} \equiv \log(P_{i,t}/E_{i,t})$. I construct $\mathbb{F}_t[pe_{i,t+h}]$ using the (Campbell and Shiller, 1988) present-value identity:

$$\mathbb{F}_t[pe_{i,t+h}] = \frac{1}{\rho^h} pe_{i,t} - \frac{1}{\rho^h} \sum_{j=1}^h \rho^{j-1} (c_{pe} + \mathbb{F}_t[\Delta e_{i,t+j}] - \mathbb{F}_t[r_{i,t+j}]),$$

where c_{pe} is a constant and $\rho = \frac{\exp(\bar{pe})}{(1+\exp(\bar{pe}))}$ is the discount factor from the log-linearization. I construct time-series data on actual and expected log price-earnings similarly by using the corresponding aggregate time series data at the S&P 500 level.

Machine Learning Forecasts For each survey forecast, I construct the corresponding machine learning forecast using Long Short-Term Memory (LSTM) neural networks following Bianchi et al. (2022, 2024, 2025). The LSTM model predicts stock returns or earnings growth $y \in \{r, \Delta e\}$

at horizons $h = 1, \dots, 5$ years using a data-rich set of real-time predictors:

$$\mathbb{E}_t[y_{t+h}] = G(\mathcal{X}_t, \boldsymbol{\beta}_t^{TS}; \boldsymbol{\lambda}_t^{TS}), \quad \mathbb{E}_t[y_{i,t+h}] = G(\mathcal{X}_{i,t}, \boldsymbol{\beta}_t^{CS}; \boldsymbol{\lambda}_t^{CS}),$$

where $G(\cdot)$ is the nonlinear mapping learned by the LSTM network. The time-series predictor set \mathcal{X}_t includes real-time macroeconomic, financial, and textual variables (LDA-based news sentiment from the *Wall Street Journal*), as well as survey forecasts. Including the survey forecast allows the machine to combine public information with intangible private information embedded in the survey responses.⁶ The cross-sectional set $\mathcal{X}_{i,t} = \mathcal{X}_t \otimes \mathcal{C}_{i,t}$ augments \mathcal{X}_t with firm characteristics $\mathcal{C}_{i,t}$ including valuation, profitability, size, momentum, volatility, and industry dummies.

The parameters $\boldsymbol{\beta}_t^{TS}$ and $\boldsymbol{\beta}_t^{CS}$ are re-estimated dynamically over rolling samples (quarterly for the time-series model and annually for the cross-sectional model) to allow for evolving relationships between predictors and outcomes. Regularization hyperparameters $\boldsymbol{\lambda}_t^{TS}$ and $\boldsymbol{\lambda}_t^{CS}$ control model complexity using L_1 and L_2 penalties, dropout layers, early stopping, and ensemble averaging. These techniques prevent overfitting and ensure smooth updates in the presence of structural change or regime shifts. The model's out-of-sample testing period spans 2005Q1-2023Q4.

I interpret the machine forecast as an information-efficient ex-ante belief for an agent who is rational given a prior that introduces shrinkage. Regularized training methods controlled by hyperparameters $\boldsymbol{\lambda}_t^{TS}$ and $\boldsymbol{\lambda}_t^{CS}$ introduce a prior for smoothness and parsimony. These regularization techniques correspond to Bayesian estimation under a complexity prior, where the forecast represents the posterior mean that minimizes expected squared loss. Importantly, the machine must make its forecast using only real-time information, without look-ahead bias. All inputs are restricted to historical, timestamped data that we verify were accessible to market participants at the time, ensuring the predictions reflect only information a firm manager could have used when deciding whether to hire.

3 Data

This section describes the data used to estimate the time-series and cross-sectional variance decompositions. For each outcome variable, I use survey forecasts to measure subjective expectations $\mathbb{F}_t[\cdot]$ and machine learning forecasts to measure rational expectations $\mathbb{E}_t[\cdot]$. The final estimation sample is quarterly and spans 2005Q1 to 2023Q4. Throughout this section, the t

⁶While the machine uses survey forecasts as one input among many predictive variables, a truly rational agent would efficiently extract signals from all available public information, including potentially biased survey data, and de-bias them optimally. The machine learning model approximates this process by finding the optimal forecast given an information set that includes survey responses alongside other predictive variables.

subscript denotes the quarterly time period, and i subscript denotes the firm.⁷

Vacancy Filling Rate Vacancies V_t are measured using JOLTS job openings starting 2000:12 and the help-wanted index for earlier periods (Barnichon, 2010). Unemployment U_t is measured from the BLS unemployment series (UNEMPLOY). The vacancy filling rate q_t is defined as the rate at which posted vacancies are filled out of unemployment:

$$q_t = \frac{f_t U_t}{V_t}$$

The job finding rate f_t is the share of unemployed workers that find jobs within the period:

$$f_t = 1 - \frac{U_t - U_t^s}{U_{t-1}}$$

where U_t^s is short-term unemployment less than 5 weeks (UEMPLT5). I construct the variables at a monthly frequency, time-aggregate to quarterly averages, and detrend using an HP filter with a smoothing parameter of 10^5 to ensure stationarity (Shimer, 2005). Labor market tightness is defined as the vacancy-to-unemployment ratio, $\theta_t \equiv V_t/U_t$. The job separation rate δ_t uses the corresponding series from JOLTS.

Employment Employment $L_{i,t}$ is measured using annual total employee counts (EMP) of S&P 500 firms, sourced from the CRSP/Compustat Merged Annual Industrial Files. I aggregate the firm-level employment data to construct a total employment series L_t for the S&P 500. I interpolate the annual series to a quarterly frequency by using quarterly averages of the fitted values from regressing annual S&P 500 employment on the monthly BLS nonfarm payrolls series.

Earnings Quarterly earnings for S&P 500 firms $E_{i,t}^*$ are sourced from IBES street earnings per share (EPS) data that starts in 1983Q4. Street earnings, which serve as the forecast target for IBES analysts, differ from standard GAAP earnings by excluding discontinued operations, extraordinary charges, and other non-operating items. This adjustment makes street earnings a cleaner measure of recurring performance and a more relevant proxy for expected cash flows. Street earnings exhibit less transitory volatility and are more informative about firm fundamentals and valuation than standard earnings measures (Hillenbrand and McCarthy, 2024).

To handle instances where firm earnings may be zero or negative, which would make log transformations undefined, I follow the approach of Vuolteenaho (2002) and define a transformed

⁷See Appendix C for more details. Figure A.1 and Table A.1 reports stylized facts about the data.

measure of earnings that is strictly positive. Specifically, each firm is treated as a portfolio consisting of a fraction $(1 - \lambda)$ of equity and a small fraction λ of risk-free assets, such that

$$E_{i,t} = (1 - \lambda)E_{i,t}^* + \lambda r_t^f P_{i,t-1}, \quad \lambda = 0.10,$$

where $E_{i,t}^*$ is the firm's reported earnings, $P_{i,t-1}$ is the lagged market value of equity, and r_t^f is the one-year Treasury bill rate. The risk-free component ensures $E_{i,t} > 0$ for all observations while preserving the cross-sectional variation in earnings. This transformation allows log earnings $e_{i,t} \equiv \log(E_{i,t})$ to be well defined even in periods when reported earnings are negative.

To construct subjective expectations of future cash flows $\mathbb{F}_t[\Delta e_{i,t+h}]$, I use survey forecasts of S&P 500 earnings from the IBES database (De La O and Myers, 2021; Bordalo et al., 2019). IBES provides firm-level forecasts from financial analysts, which I aggregate to form market-wide earnings expectations for the S&P 500. These forecasts reflect the views of professionals who actively track firms for investment research and have strong reputational incentives to report them accurately, as they are not anonymous (Cooper et al., 2001; De La O et al., 2024). Prior research shows that these forecasts are widely followed by market participants and are priced into asset values, supporting their use as proxies for subjective expectations (Kothari et al., 2016).⁸

IBES provides monthly median analyst forecasts for earnings per share (EPS) at one through four year horizons, as well as long-term growth (LTG) forecasts.⁹ One and two-year-ahead forecasts of annual log earnings growth $\mathbb{F}_t[\Delta e_{i,t+h}]$ for $h = 1, 2$ are constructed as log differences between level forecasts from adjacent horizons. For the $h = 3, 4, 5$ year horizons, I interpret the LTG forecast as the expected log growth in earnings from year four to five. The sample spans January 1983 to December 2023 at a monthly frequency, which are time-aggregated to quarterly averages. The forecasts cover approximately 80% of total market capitalization, providing broad coverage of U.S. public firms.

Stock Returns Stock returns $r_{i,t+h}$ are measured using monthly Center for Research in Security Prices (CRSP) value-weighted returns with dividends (VWRETD). Annualized cumulative h -year log stock returns are compounded from monthly returns.

For survey expectations of aggregate stock returns $\mathbb{F}_t[r_{t+h}]$, I use the quarterly CFO survey from 2001Q4 to 2023Q4. The CFO survey asks respondents about their expectations for the

⁸As a robustness check, Appendix Table A.5 considers using earnings forecasts from the CFO survey, which reflect managerial expectations. The two series have a relatively strong correlation of 0.60 at the 1-year horizon, suggesting that analyst and managerial beliefs are broadly aligned.

⁹Long-Term Growth (LTG) is defined in IBES as the “expected annual increase in operating earnings over the company’s next full business cycle. These forecasts refer to a period of between three to five years.”

S&P 500 return over the next 12 months and 10 years ahead. For intermediate horizons between 1 and 10 years, I interpolate linearly between the 1 and 10 year ahead forecasts. The CFO survey panel includes firms ranging from small operations to Fortune 500 companies across all major industries. Respondents include chief financial officers, owner-operators, vice presidents, and directors of finance, and others with financial decision-making roles.

For survey expectations of firm-level stock returns $\mathbb{F}_t[r_{i,t+h}]$, I use survey data on stock price targets (De La O et al., 2024). Specifically, I proxy for stock return expectations by constructing expected price growth from IBES 12-month median price targets and Value Line 3–5 year median price targets.¹⁰ I interpret the Value Line price targets as a five-year-ahead forecast and interpolate linearly to impute expectations for intermediate horizons between 1 and 5 years.

Price-Earnings Ratio The current log price-earnings ratio is defined as $pe_{i,t} \equiv \log(P_{i,t}/E_{i,t})$, where $P_{i,t}$ is the end-of-quarter stock price and $E_{i,t}$ denotes quarterly total earnings for the S&P 500. I construct subjective expectations of log price-earnings $\mathbb{F}_t[pe_{i,t+h}]$ by applying the Campbell and Shiller (1988) approximate present value identity (De La O and Myers, 2021):

$$\mathbb{F}_t[pe_{i,t+h}] = \frac{1}{\rho^h} pe_{i,t} - \frac{1}{\rho^h} \sum_{j=1}^h \rho^{j-1} (c_{pe} + \mathbb{F}_t[\Delta e_{i,t+j}] - \mathbb{F}_t[r_{i,t+j}])$$

where c_{pe} is a linearization constant, $\rho = \exp(\bar{pe})/(1 + \exp(\bar{pe}))$ is the time discount factor from the log-linearization. Expected returns $\mathbb{F}_t[r_{i,t+j}]$ and earnings growth $\mathbb{F}_t[\Delta e_{i,t+j}]$ come from the corresponding survey forecasts listed above.

Machine Learning Forecasts For each survey forecast, I construct the corresponding machine learning forecast using a Long Short-Term Memory (LSTM) neural network:

$$\mathbb{E}_t[y_{t+h}] = G(\mathcal{X}_t, \beta_{h,t})$$

where y_{t+h} denotes the outcome variable (stock returns or earnings growth) to be predicted h periods ahead of time t . \mathcal{X}_t is a large input dataset of macroeconomic, financial, and textual predictors (Appendix D.2). The input dataset also includes the survey forecast of y , allowing the machine to combine public information with intangible private information embedded in the

¹⁰Firm-level forecasts from the CFO survey are not publicly available, which limits their use for cross-sectional analysis. I therefore rely on IBES and Value Line data, which provide firm-specific expectations covering approximately 80% of total market capitalization. At the aggregate level, the IBES and CFO forecasts are highly correlated at the one-year horizon (correlation ≈ 0.6), suggesting that analyst expectations are a reasonable proxy for managerial beliefs.

survey responses.¹¹ $G(\mathcal{X}_t, \boldsymbol{\beta}_{h,t})$ denotes predicted values from Long Short-Term Memory (LSTM) neural networks that can be represented by a potentially high-dimensional set of parameters $\boldsymbol{\beta}_{h,t}$. The parameters are estimated using a dynamic algorithm from Bianchi et al. (2022, 2024, 2025) that takes into account the data-rich environment in which firms operate in (Appendix D.1).

To obtain more granular measures of undistorted expectations with a cross-sectional dimension across firms, I construct analogous machine learning forecasts at the firm level:

$$\mathbb{E}_t[y_{i,t+h}] = G(\mathcal{X}_{i,t}, \boldsymbol{\beta}_{i,h,t})$$

where $y_{i,t+h}$ is the outcome to be predicted for firm i . The predictor set $\mathcal{X}_{i,t} = \mathcal{X}_t \otimes \mathcal{C}_{i,t}$ augments the aggregate predictors \mathcal{X}_t with firm characteristics $\mathcal{C}_{i,t}$ (Gu et al., 2020, Appendix D.3).

I interpret the machine forecast $\mathbb{E}_t[\cdot]$ as an information-efficient ex-ante belief for an agent who is rational given a prior that introduces shrinkage. Regularized training methods such as ℓ_1 and ℓ_2 penalties, weight decay, dropout, and early stopping impose a prior for smoothness and parsimony. These regularization techniques correspond to Bayesian estimation under a complexity prior, where the forecast represents the posterior mean that minimizes expected squared loss. This delivers an information efficient, ex ante belief aligned with the economic question, since vacancy posting is chosen ex ante. It also enables an apples to apples comparison with subjective beliefs: surveys provide $\mathbb{F}_t[\cdot]$, and the machine provides $\mathbb{E}_t[\cdot]$ as the rational counterpart at the same date and horizon.

4 Evidence of Belief Distortions

Predictability of Survey Forecast Errors To assess whether survey expectations deviate from rational expectations, Figure 1 reports the coefficient β_1 from Coibion and Gorodnichenko (2015) regressions of survey forecast errors on survey forecast revisions at the firm level:

$$y_{i,t+h} - \mathbb{F}_t[y_{i,t+h}] = \beta_1 [\mathbb{F}_t[y_{i,t+h}] - \mathbb{F}_{t-1}[y_{i,t+h}]] + \beta_2 \mathbb{F}_{t-1}[y_{i,t+h}] + \alpha_i + \alpha_t + \varepsilon_t \quad (1)$$

where $y_{i,t+h}$ denotes either stock returns $r_{i,t+h}$ (discount rates) or earnings growth $\Delta e_{i,t+h}$ (cash flows) for firm i , as defined in Section 3. These regressions include portfolio α_i and time α_t fixed effects, implying that the identifying variation comes from revisions in expectations that are idiosyncratic to each portfolio.

¹¹While it uses survey forecasts as one input among many predictive variables, a truly rational agent would efficiently extract signals from all available public information, including potentially biased survey data, and de-bias them optimally. The machine learning model approximates this process by finding the optimal forecast given an information set that includes survey responses alongside other predictive variables.

For cash flow expectations, the coefficients on forecast revisions are negative, ranging from -0.433 at the one-year horizon to -0.818 at five years. These results indicate overreaction. Upward revisions in survey forecasts are followed by negative forecast errors, suggesting that survey respondents respond too strongly to positive earnings news and generate overly optimistic forecasts. For discount rate expectations, the coefficients are negative and significant, with a coefficient of -0.191 at the five-year horizon, indicating that respondents overreact to discount rate news.¹² In contrast, the coefficients on machine forecast revisions are small and statistically insignificant at all horizons, with values near zero (0.021 for discount rates and 0.097 for cash flows at the five-year horizon). The absence of a correlation between forecast errors and prior forecast revisions is consistent with the behavior of rational expectations, under which forecast errors should be unpredictable.

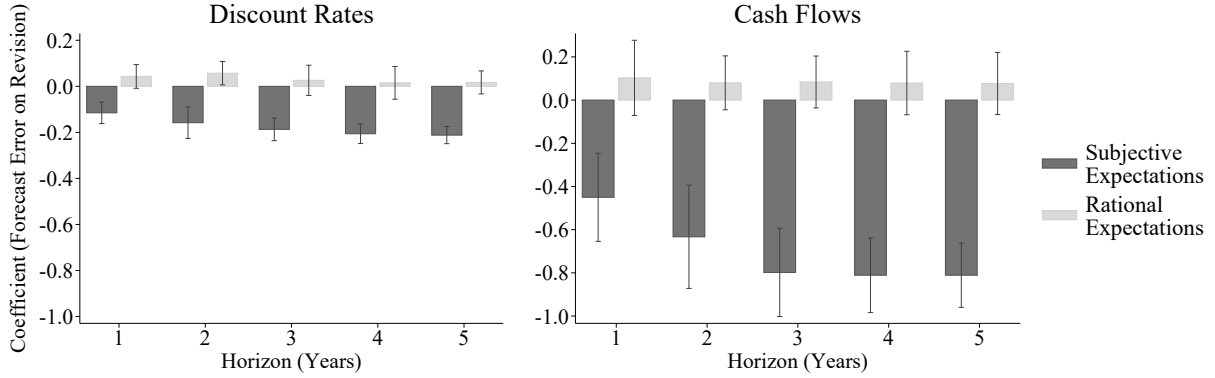
One possible interpretation is that survey forecasts incorporate private information unavailable to the machine learning model, in which case apparent belief distortions might reflect rational responses to superior information. Under this interpretation, forecast revisions reflect analysts updating their beliefs based on new public and private signals. If analysts efficiently incorporated these signals, their revisions should not predict subsequent forecast errors. However, the evidence shows that positive revisions systematically predict negative errors, indicating overreaction rather than efficient information use. Moreover, distortions can arise even when agents possess private information if they overweight the precision of their private signals or inefficiently combine them with public data (Bianchi et al., 2022).

Accuracy of Machine Learning vs. Survey Forecasts To assess whether survey respondents misweight relevant information, Figure 2 evaluates the out-of-sample accuracy of machine learning relative to survey forecasts for discount rates r_{t+h} and cash flows e_{t+h} . These variables are factors that can influence the value of hiring through the firm's optimal hiring decision in the search model. I measure the relative predictive performance using the ratio $MSE_{\mathbb{E}}/MSE_{\mathbb{F}}$ of mean-squared-forecast-error of the machine ($MSE_{\mathbb{E}}$) over that of the survey ($MSE_{\mathbb{F}}$):

$$\text{Machine MSE} = \frac{1}{T} \sum_{t=1}^T (y_{t+h} - \mathbb{E}_t[y_{t+h}])^2, \quad \text{Survey MSE} = \frac{1}{T} \sum_{t=1}^T (y_{t+h} - \mathbb{F}_t[y_{t+h}])^2$$

¹²For future price-earnings expectations, the coefficient is also negative at -0.709 , showing that price-earnings forecasts overreact to news. Through the Campbell-Shiller present-value identity, this suggests cash flow overreaction dominates discount rate overreaction in driving price-earnings forecasts. While both discount rates and cash flow expectations overreact, the cash flow component (which enters positively in the identity) has a stronger influence on price-earnings ratio variation than the discount rate component (which enters negatively), leading to net overreaction in price-earnings forecasts.

Figure 1: Predictability of Survey Forecast Errors



Notes: Table reports regression coefficients β_1 from cross-sectional regressions of forecast errors on forecast revisions and lagged forecast levels for a quarterly panel of listed firms, including firm and time fixed effects. The forecast target is either stock returns r_{t+h} (discount rates) or earnings growth Δe_{t+h} (cash flows). Cross-sectional survey forecasts F_t come from IBES (discount rates and cash flows). Time-series and cross-sectional machine learning expectations E_t are generated using a Long Short-Term Memory (LSTM) model trained in real time on macroeconomic, financial, and textual data. The sample covers quarterly data from 2005Q1 to 2023Q4. All t-statistics are two-way clustering by portfolio and quarter. Significance levels: * $p < 0.10$, ** $p < 0.05$, *** $p < 0.01$.

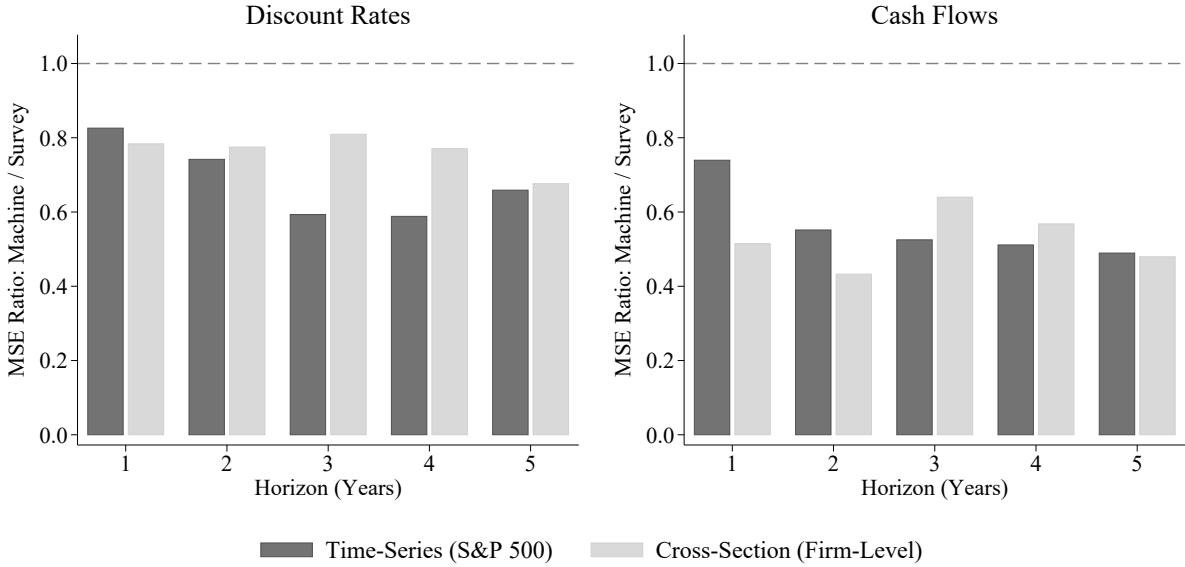
where T is the length of the out-of-sample testing period, which spans 2005Q1 to 2023Q4. The cross-sectional forecasts are evaluated similarly based on the mean-squared-forecast-error across all firms over the testing period.

Figure 2 shows that machine learning forecasts consistently outperform survey forecasts across all variables and horizons, with MSE ratios well below one. The performance gap widens with forecast horizon, indicating that belief distortions are larger at longer horizons. The machine outperforms the survey for both time-series and cross-sectional forecasts, suggesting that belief distortions affect not only aggregate expectations but also the cross-sectional dispersion of beliefs across firms. If survey respondents were rational in forming their beliefs, their forecasts would have performed at least on par with the machine.¹³ The superior performance of the machine also highlights its ability to process a large amount of real-time data efficiently and objectively, supporting its use as a reliable benchmark of undistorted beliefs.

Survey forecasts could in principle contain private information that is not available to the machine. However, the evidence from the Coibion and Gorodnichenko (2015) regressions from Table 1 above show that respondents do not use their information efficiently, since forecast revisions systematically predict future errors. The machine addresses this by conditioning on the survey forecasts as predictors, which allows it to incorporate any information embedded in

¹³The magnitude of the MSE ratio is more consistent with truly subjective beliefs rather than rational but risk-neutral beliefs. Estimates of risk premia typically range 5-10% annually (Adam et al., 2021), which is insufficient to explain the 15-30% deterioration in MSE ratios observed in Figure 2. The magnitude and persistence of forecast errors across horizons instead also point to behavioral biases rather than rational risk compensation.

Figure 2: Accuracy of Machine Learning vs. Survey Forecasts



Notes: Figure plots $MSE_{\mathbb{E}}/MSE_{\mathbb{F}}$, the ratio of mean squared forecast errors between machine learning and survey forecasts. Lower values indicate greater accuracy of the machine learning forecast. $MSE_{\mathbb{E}}$ and $MSE_{\mathbb{F}}$ refer to out-of-sample forecast errors from machine and survey forecasts, respectively. The out-of-sample testing period is 2005Q1–2023Q4. Dark bars correspond to aggregate time-series forecasts for the S&P 500; light bars correspond to cross-sectional forecasts for listed firms. The forecast target y_{t+h} is the present value of discount rates $r_{t,t+h}$ and cash flows $e_{t,t+h}$, as defined in equation (16). Time-series survey forecasts \mathbb{F}_t come from the CFO survey (discount rates) and IBES (cash flows). Cross-sectional survey forecasts \mathbb{F}_t come from IBES (discount rates and cash flows). Time-series and cross-sectional machine learning expectations \mathbb{E}_t are generated using a Long Short-Term Memory (LSTM) model trained in real time on macroeconomic, financial, and textual data.

the surveys while correcting for their inefficient use. The fact that the machine still outperforms indicates that the performance gap reflects systematic biases in belief formation rather than rational use of superior private information.

Hiring Outcomes and Belief Distortions Given the evidence of overreaction in subjective cash flow forecasts, this section examines the relationship between the vacancy filling rate and the belief distortion in subjective 5-year cash flow expectations. In search-and-matching models of the labor market, the vacancy filling rate reflects the marginal value of job creation. Hiring creates a match with expected duration $1/\delta$ years given a job separation rate δ . A 5-year forecast horizon captures the lifetime of a typical match since it aligns with the median job tenure observed in the data, which ranged between 3.4 to 4.6 years over the 1983–2023 sample period Bureau of Labor Statistics, 2024. Using a horizon slightly above the median ensures that the forecast covers the duration of most employment relationships above the median, and the expected duration likely exceeds the median given the right-skewed tenure distribution.

Figure 3 plots the growth rate of the U.S. vacancy filling rate against belief distortions in cash flow growth expectations, measured as the gap between subjective and rational 5-year forecasts of annualized S&P 500 earnings growth ($\mathbb{F}_t[\Delta e_{t+5}] - \mathbb{E}_t[\Delta e_{t+5}]$). The vacancy filling

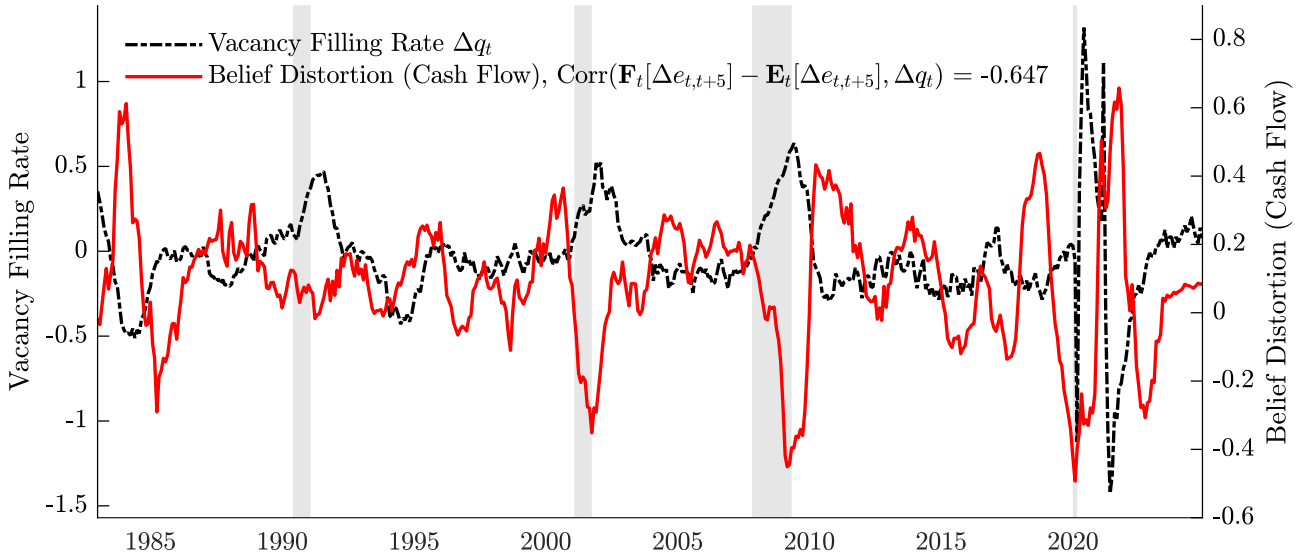
rate, defined as total hires divided by total vacancies, measures the rate at which posted job openings are successfully filled. Total hires are constructed as the job finding rate multiplied by the unemployment level, where the job finding rate captures the probability an unemployed worker finds a job in a given quarter. The subjective forecasts come from survey data, while the rational benchmark uses machine-learning predictions.

The figure shows that belief distortions exhibit strong cyclical patterns that closely track labor market fluctuations, with a negative correlation of -0.647. During expansions, positive belief distortions emerge as subjective forecasts become overly optimistic relative to the rational benchmark. These periods of optimism coincide with declines in the vacancy-filling rate. The negative correlation reflects a congestion effect: when firms become excessively optimistic, they simultaneously surge in vacancy posting, which tightens the labor market and makes it harder for any given vacancy to be filled. Conversely, when belief distortions turn negative and firms scale back vacancy posting, the vacancy-filling rate rises as the market becomes less congested.

This pattern is particularly evident during the large positive belief distortions of the late 1990s and the pre-2008 period, both followed by dramatic reversals to negative distortions that coincided with sharp contractions in vacancy filling rate growth and NBER-dated recessions. The tight co-movement between these expectational errors in cash flow forecasts and vacancy filling rate growth suggests that distortions in firms' earnings expectations are a powerful driver of labor market fluctuations, operating independently of changes in discount rates.

Figure 4 illustrates this key relationship in the cross-section by plotting the cross-sectional correlation between actual hiring rates and belief distortions in cash flow expectations across listed firms. The hiring rate, defined as total hires divided by existing employment, captures firm-level hiring behavior. Unlike the vacancy filling rate, which measures how quickly vacancies are filled, the hiring rate directly measures employment growth at the firm level. The scatter plot reveals a clear positive relationship with a correlation of 0.830 across firms. The figure suggests that firms with equity analyst coverage that is excessively optimistic about future cash flow growth at the 5-year forecast horizon exhibit systematically higher hiring rates. Each point in the binned scatter represents a percentile of the joint distribution in hiring rates and belief distortions across the firms, and the strong positive slope confirms that belief distortions in expected cash flows translate directly into observable differences in hiring behavior across firms. Intuitively, the positive firm-level correlation in the hiring rate complements with the negative aggregate relationship for the vacancy filling rate. When firms become more optimistic, they expand employment and raise hiring rates, but collectively this tightens the labor market and lowers the probability that each vacancy is filled.

Figure 3: Vacancy Filling Rate and Belief Distortions in Subjective Cash Flows



Notes: Figure plots the annual log growth of the U.S. vacancy filling rate Δq_t (left axis) against the belief distortion in cash flows, which is measured as expectational errors $F_t[\Delta e_{t,t+5}] - E_t[\Delta e_{t,t+5}]$ in 5-year forecasts of annualized S&P 500 earnings growth (right axis). Survey expectations $F_t[\Delta e_{t+5}]$: IBES median analyst forecasts for the next four fiscal years and long-term growth (LTG). Rational expectations $E_t[\Delta e_{t+5}]$: Machine learning forecasts from Long Short-Term Memory (LSTM) neural networks. The vacancy filling rate, defined as total hires divided by total vacancies, measures the rate at which posted job openings are filled. Sample is quarterly from 1983Q1 to 2023Q4. Gray shaded areas indicate NBER recessions.

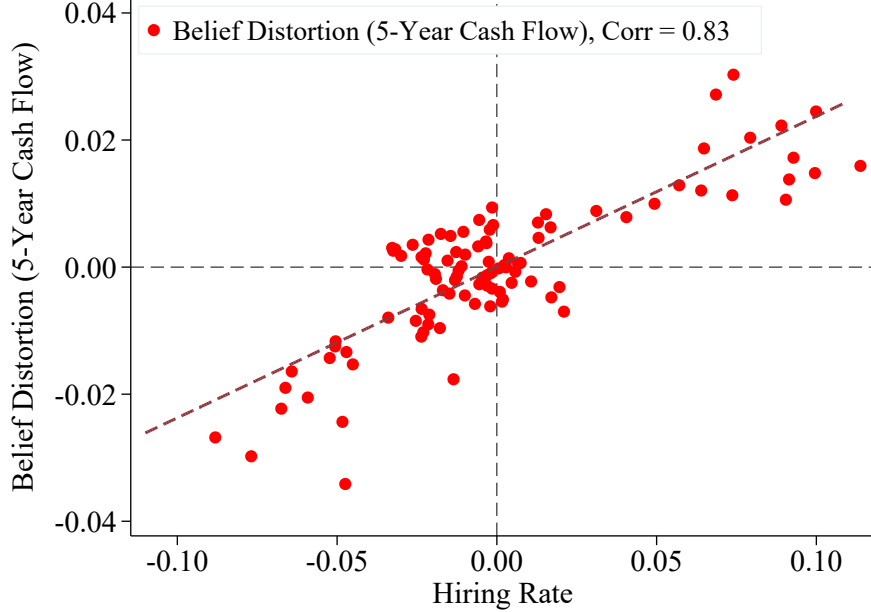
5 Theoretical Framework

The reduced-form link between fluctuations in the vacancy filling rate and belief distortions about cash flows motivate a structural interpretation. This section develops a search and matching model of the labor market in which firms' expectations about future cash flows and discount rates may be distorted, leading to fluctuations in vacancy filling rates and unemployment. The model builds on the Diamond (1982), Mortensen (1982), and Pissarides (2009) framework but departs from the standard rational expectations assumption, allowing firms' hiring decisions to be influenced by biased subjective beliefs.

Environment Consider a discrete time economy populated by a representative household and a mass of firms I , normalized to one, that hires workers in a frictional labor market. The firm uses labor as a single input to production. The household's population is normalized to one and has a continuum of members, where a fraction L_t are employed and the rest are unemployed $U_t = 1 - L_t$. The household's intertemporal consumption decision gives rise to a stochastic discount factor M_{t+1} .

Labor Market Each period, each firm posts job vacancies at a cost $\kappa > 0$ to maximize its cum-dividend value of equity. Employment $L_{i,t}$ reflects the number of workers employed in firm i

Figure 4: Cross-Sectional Hiring Rates and Belief Distortions



Notes: Figure plots the relationship between hiring rates and cash flow expectations across listed firms. y -axis reports the corresponding cross-sectionally demeaned log hiring rate, $\tilde{h}_{i,t}$. x -axis reports the cross-sectionally demeaned belief distortion measured as expectational errors $\mathbb{F}_t[\Delta e_{t,t+5}] - \mathbb{E}_t[\Delta e_{t,t+5}]$ in 5-year forecasts of annualized S&P 500 earnings growth. Subjective expectations \mathbb{F}_t : IBES forecasts. Rational expectations \mathbb{E}_t : Machine learning (LSTM) forecasts. The hiring rate, defined as total hires divided by existing employment, captures firm-level hiring behavior. Each dot is a bin scatter representing one percentile of the pooled distribution across all observations in the sample. A positive slope implies that firms with equity analyst coverage that is excessively optimistic about future cash flow growth exhibit higher hiring rates. The sample is quarterly from 2005Q1 to 2023Q4.

at the beginning of period t before any separations or new hires.¹⁴ During the period, a fraction $\delta_{i,t}$ of employed workers separate, while the firm posts vacancies $V_{i,t}$ to search from a pool of unemployed workers U_t . Let $L_t = \sum_{i \in I} L_{i,t}$ and $V_t = \sum_{i \in I} V_{i,t}$ denote the aggregate number of employed workers and vacancies posted by all firms. Matches are formed at the end of period t according to a Cobb-Douglas matching function $\mathcal{M}(U_t, V_t)$:

$$\mathcal{M}(U_t, V_t) = BU_t^\eta V_t^{1-\eta} \quad (2)$$

where B is the matching efficiency parameter, and $\eta \in (0, 1)$ governs the elasticity of matches with respect to unemployment. The probability that a firm fills a posted vacancy, the vacancy filling rate, is then given by:

$$q_t = \frac{\mathcal{M}(U_t, V_t)}{V_t} = B \left(\frac{U_t}{V_t} \right)^\eta = B\theta_t^{-\eta} \quad (3)$$

and the job finding rate is given by $f_t \equiv \mathcal{M}(U_t, V_t)/U_t$. These new hires enter employment at the start of period $t + 1$, so employment $L_{i,t}$ and unemployment $U_t = 1 - L_t$ evolve according to

¹⁴I adopt an end-of-period matching convention following Petrosky-Nadeau et al. (2018). See Hansen et al. (2005) and Kogan and Papanikolaou (2012) for similar conventions applied for the q theory of investment.

the law of motion:

$$L_{i,t+1} = (1 - \delta_{i,t})L_{i,t} + q_t V_{i,t} \quad (4)$$

Aggregate unemployment $U_t = 1 - L_t$ evolves according to:

$$U_{t+1} = \delta_t(1 - U_t) + (1 - q_t \theta_t)U_t \quad (5)$$

where $\theta_t = V_t/U_t$ denotes labor market tightness, defined as the vacancy-to-unemployment ratio.

Firm's Technology and Cash Flow Each firm i uses labor $L_{i,t}$ to produce output $Y_{i,t}$ via a Cobb-Douglas production function at constant returns to scale:

$$Y_{i,t} = A_{i,t}L_{i,t} \quad (6)$$

where $A_{i,t}$ is firm-level productivity, $L_{i,t}$ is the level of employment. The firm pays wages $W_{i,t}$, incurs hiring costs $\kappa V_{i,t}$, and generates cash flows defined as the firm's period earnings:

$$E_{i,t} = Y_{i,t} - W_t L_{i,t} - \kappa V_{i,t} \quad (7)$$

Earnings represent the net flow profits from operating the firm, which is the output net of the wage bill and vacancy posting costs. I assume that the household owns the equity of the firm and the firm pays out all of its earnings $E_{i,t}$ as dividends (Petrosky-Nadeau et al., 2018). I also assume that the firm's manager has access to complete markets so that the return to hiring equals the stock market return in equilibrium (Cochrane, 1991).

Firm's Problem The firm chooses vacancy postings $V_{i,t}$ to maximize the present discounted value of future cash flows. The firm's value function \mathcal{V} satisfies the Bellman equation:

$$\mathcal{V}(A_{i,t}, L_{i,t}) = \max_{V_{i,t}, L_{i,t+1}} \{E_{i,t} + \mathbb{F}_t[M_{t+1}\mathcal{V}(A_{i,t+1}, L_{i,t+1})]\} \quad (8)$$

subject to the employment accumulation equation (4). $\mathbb{F}_t[\cdot]$ is the firm's subjective expectations conditional on information available at the beginning of period t .¹⁵ These beliefs may depart from rational expectations $\mathbb{E}_t[\cdot]$, where the nature and magnitude of the deviation will be disciplined using survey data. M_{t+1} is the stochastic discount factor that prices the firm's cash flows. The firm does not observe this discount factor directly and needs to form expectations about it by forecasting the household's marginal utility of consumption (Venkateswaran, 2014).

¹⁵I use the term “firm's beliefs” as shorthand to refer to the expectations held by decision makers within firms (Coibion et al., 2018; Caidia et al., 2020).

Hiring Condition Under search frictions, hiring is forward-looking investment. The firm's optimal hiring decision equates the marginal cost of posting a vacancy with the expected discounted marginal value of employment:

$$\underbrace{\frac{\kappa}{q_t}}_{\text{Cost of hiring}} = \underbrace{\mathbb{F}_t \left[M_{t+1} \frac{\partial \mathcal{V}(A_{i,t+1}, L_{i,t+1})}{\partial L_{i,t+1}} \right]}_{\text{Expected discounted value of hiring}} \quad (9)$$

The left side represents the expected cost of hiring an additional worker while accounting for the probability q_t that a posted vacancy will be filled. The right side captures the expected discounted value of the marginal worker, incorporating both the firm's subjective beliefs about the future state and the discount rate for valuing risky cash flows.¹⁶ Subjective distortions in beliefs can thus shift the perceived value of hiring through $\mathbb{F}_t[\cdot]$ and affect equilibrium vacancy filling rates, which in turn affect unemployment through its law of motion in equation (5). Assuming constant returns to scale, the marginal value of hiring equals its average value:

$$\frac{\partial \mathcal{V}(A_{i,t+1}, L_{i,t+1})}{\partial L_{i,t+1}} = \frac{\mathcal{V}(A_{i,t+1}, L_{i,t+1})}{L_{i,t+1}} \quad (10)$$

Define the firm's ex-dividend market value as $P_{i,t} \equiv \mathbb{F}_t[M_{t+1}\mathcal{V}(A_{i,t+1}, L_{i,t+1})]$ to derive a direct link between the vacancy filling rate and the firm's market value per worker:

$$\frac{\kappa}{q_t} = \frac{P_{i,t}}{L_{i,t+1}} \quad (11)$$

where employment $L_{i,t+1}$ is determined at the end of date t under the timing convention from equation (4). Take logarithms, rearrange terms, and expand the price-employment ratio $P_{i,t}/L_{i,t+1}$:

$$\log q_t = \log \kappa - \log \left(\frac{P_{i,t}}{E_{i,t}} \right) - \log \left(\frac{E_{i,t}}{L_{i,t+1}} \right) \quad (12)$$

Define log price-earnings $pe_{i,t} = \log(P_{i,t}/E_{i,t})$ and earnings-employment $el_{i,t} = \log(E_{i,t}/L_{i,t+1})$:

$$\log q_t = \log \kappa - pe_{i,t} - el_{i,t} \quad (13)$$

Log-linear Approximation of Price-Earnings Ratio To decompose the vacancy filling rate into economically meaningful components, I apply the Campbell and Shiller (1988) present value

¹⁶The hiring equation is the labor market analogue of the optimality condition for physical capital in the q theory of investment (Hayashi, 1982), where the upfront cost of hiring κ/q_t is analogous to Tobin's marginal q and the separation rate δ_{t+1} is analogous to the depreciation rate (Borovickova and Borovička, 2017). See Lettau and Ludvigson (2002) and Kogan and Papanikolaou (2012) for a similar log-linearization applied for the q theory of physical capital investment.

identity to the price-earnings ratio. Log-linearize the price-earnings ratio $pe_{i,t} \equiv \log(P_{i,t}/E_{i,t})$ around its long-run mean \bar{pe} to obtain the approximate relationship:

$$pe_{i,t} = c_{pe} - r_{i,t+1} + \Delta e_{i,t+1} + \rho pe_{i,t+1} \quad (14)$$

where c_{pe} is a linearization constant, $\rho = \exp(\bar{pe})/(1 + \exp(\bar{pe}))$ is the time discount factor from the log-linearization, $r_{i,t+1} = \log((P_{i,t+1} + E_{i,t+1})/P_{i,t})$ is the stock return assuming that the firm pays out its earnings as dividends, and $\Delta e_{i,t+1}$ denotes earnings growth.¹⁷ This equation is an accounting identity that links current valuation ratios to future cash flows and discount rates. Substituting recursively for the next h periods yields the present value identity:

$$pe_{i,t} = \sum_{j=1}^h \rho^{j-1} c_{pe} - \sum_{j=1}^h \rho^{j-1} r_{i,t+j} + \sum_{j=1}^h \rho^{j-1} \Delta e_{i,t+j} + \rho^h pe_{i,t+h} \quad (15)$$

Decomposition of Vacancy Filling Rate Substitute log-linearized price-earnings (15) into the hiring equation (13) to obtain a decomposition of the vacancy filling rate q_t :

$$\log q_t = c_q + \underbrace{\sum_{j=1}^h \rho^{j-1} r_{i,t+j}}_{\equiv r_{i,t,t+h}} - \underbrace{\left[el_{i,t} + \sum_{j=1}^h \rho^{j-1} \Delta e_{i,t+j} \right]}_{\equiv e_{i,t,t+h}} - \underbrace{\rho^h pe_{i,t+h}}_{\equiv pe_{i,t,t+h}} \quad (16)$$

where $c_q \equiv \log \kappa - \frac{c_{pe}(1-\rho^h)}{1-\rho}$ is a constant. The vacancy filling rate has been decomposed into three forward-looking components: the present value of future discount rates $r_{i,t,t+h} \equiv \sum_{j=1}^h \rho^{j-1} r_{i,t+j}$, cash flows $e_{i,t,t+h} \equiv el_{i,t} + \sum_{j=1}^h \rho^{j-1} \Delta e_{i,t+j}$, and price-earnings ratio $pe_{i,t,t+h} \equiv \rho^h pe_{i,t+h}$. The cash flow component consists of the current earnings-employment ratio el_t , which captures short-term fluctuations in cash flows, and $j = 1, \dots, h$ period ahead earnings growth Δe_{t+j} , which captures news about future cash flows. To decompose time-series variation in the vacancy filling rate q_t , the right-hand side of equation (16) can be aggregated across firms:

$$\underbrace{\log q_t}_{\text{Vacancy Filling Rate}} = c_q + \underbrace{\mathbb{F}_t[r_{t,t+h}]}_{\text{Discount Rate}} - \underbrace{\mathbb{F}_t[e_{t,t+h}]}_{\text{Cash Flow}} - \underbrace{\mathbb{F}_t[pe_{t,t+h}]}_{\text{Future Price-Earnings}} \quad (17)$$

where $x_t = \sum_{i \in I} w_{i,t} x_{i,t}$ aggregates firm-level variable $x_{i,t}$ using employment weights $w_{i,t} = L_{i,t} / \sum_{j \in I} L_{j,t}$ for $x \in \{r, e, pe\}$.¹⁸ Intuitively, the vacancy filling rate rises when firms expect

¹⁷This identity also holds approximately when dividends differ from earnings. Following Lintner (1956), dividends can be approximated as a stable fraction of earnings (with a long-run payout ratio near 50%). The resulting payout ratio term $(1 - \rho)de_{t+1}$ becomes negligible after log-linearization since $1 - \rho \approx 0.02$, allowing this term to be absorbed into the constant c_{pe} (De La O et al., 2024). See Appendix Section B for a derivation.

¹⁸The aggregate decomposition follows from the firm-level decomposition by summing across individual firms' hiring conditions under two assumptions: (i) vacancy posting costs are linear in the number of vacancies, and (ii)

high future cash flows (making hiring valuable) or low future discount rates (making future profits more valuable today). The Campbell-Shiller formula allows us to separate these two channels by recursively decomposing the price-earnings ratio into expected returns and earnings growth.

Since equation (16) holds both ex-ante and ex-post, it can be evaluated under either subjective or rational expectations. The *subjective decomposition* replaces ex-post realizations of future outcomes with their ex-ante subjective expectation $\mathbb{F}_t[\cdot]$:

$$\log q_t = c_q + \mathbb{F}_t[r_{t,t+h}] - \mathbb{F}_t[e_{t,t+h}] - \mathbb{F}_t[pe_{t,t+h}] \quad (18)$$

The equation implies that the vacancy filling rate is high when firms subjectively expect future returns to be high, expected cash flows to be low, or both. Alternatively, the *rational decomposition* replaces each subjective expectation $\mathbb{F}_t[\cdot]$ with its rational expectation $\mathbb{E}_t[\cdot]$:

$$\log q_t = c_q + \mathbb{E}_t[r_{t,t+h}] - \mathbb{E}_t[e_{t,t+h}] - \mathbb{E}_t[pe_{t,t+h}] \quad (19)$$

Comparing these decompositions can quantify how belief distortions affect the vacancy filling rate. The econometrician can estimate the variance decomposition using predictive regressions of each expected outcome on the current vacancy filling rate. For the subjective decomposition, demean each variable in equation (18), multiply both sides by the current log vacancy filling rate $\log q_t$, and take the sample average:

$$Var[\log q_t] = Cov[\mathbb{F}_t[r_{t,t+h}], \log q_t] - Cov[\mathbb{F}_t[e_{t,t+h}], \log q_t] - Cov[\mathbb{F}_t[pe_{t,t+h}], \log q_t] \quad (20)$$

where $Var[\cdot]$ and $Cov[\cdot]$ are sample variances and covariances based on data observed over a historical sample. Finally, divide both sides by $Var[\log q_t]$ to decompose its variance:

$$1 = \underbrace{\frac{Cov[\mathbb{F}_t[r_{t,t+h}], \log q_t]}{Var[\log q_t]}}_{\text{Discount Rate News}} - \underbrace{\frac{Cov[\mathbb{F}_t[e_{t,t+h}], \log q_t]}{Var[\log q_t]}}_{\text{Cash Flow News}} - \underbrace{\frac{Cov[\mathbb{F}_t[pe_{t,t+h}], \log q_t]}{Var[\log q_t]}}_{\text{Future Price-Earnings News}} \quad (21)$$

The left-hand side represents the full variability in vacancy filling rates, hence is equal to one. Each term on the right reflects the share explained by subjective expectations of discount rates, cash flows, or future price-earnings ratios. Under stationarity, the econometrician can estimate these shares using the OLS coefficients from regressing $\mathbb{F}_t[r_{t,t+h}]$, $\mathbb{F}_t[e_{t,t+h}]$, and $\mathbb{F}_t[pe_{t,t+h}]$ on the current log vacancy filling rate $\log q_t$, respectively. Finally, the decomposition under rational expectations can be estimated similarly based on equation (21) by replacing the subjective expectation $\mathbb{F}_t[\cdot]$ with its rational counterpart $\mathbb{E}_t[\cdot]$.

the labor market for matches is competitive, so that all firms face a common vacancy filling rate q_t . Under these conditions, the aggregate hiring equation is obtained by weighting firm-level equations by employment, which ensures that the decomposition holds exactly at the aggregate level. For the cross-sectional analysis, the same logic applies to portfolios of firms.

Comparing the decompositions implied by subjective and rational expectations can highlight the role of belief distortions, which I define as the gap between the survey and machine forecasts: $F_t - E_t$. This comparison allows us to assess the role of belief distortions in explaining labor market dynamics and determine whether firms systematically mis-perceive economic conditions when making hiring decisions. Although the variance decomposition does not necessarily capture causal relationships, it has the advantage of not requiring the researcher to take a stand on the deep determinants of vacancy filling rates because the evolution of discount rates and cash flows summarize the combined effects of these deep determinants.

6 Time-Series Decomposition of the Vacancy Filling Rate

The evidence of overreaction in survey expectations and the superior forecasting performance of machine learning suggests the presence of distortions in subjective expectations. This section quantifies how those distortions affect hiring behavior by estimating the contributions of discount rate and cash flow expectations to fluctuations in the aggregate vacancy filling rate.

Rational Expectations Figure 5 presents the variance decomposition of the vacancy filling rate. The figure shows that, under rational beliefs, discount rate news is the dominant driver of variation in vacancy filling rates. At the five-year horizon, rational discount rates explain 69.1% of the variation in vacancy filling rates, while rational cash flow news accounts for 6.6%.¹⁹ Consistent with the predictions of the search and matching model, higher vacancy filling rates are associated with higher discount rates and lower expected cash flows because a lower value of hiring leads firms to post fewer vacancies, reducing tightness and raising q_t . The contribution from terminal price-earnings ratios still remains sizable at the five-year horizon, accounting for 20.1%. The combined contribution from the three components sums to 95.8% at the five-year horizon, a value reasonably close to 100.0% suggesting that the decomposition is empirically accurate despite being estimated freely without imposing this constraint.

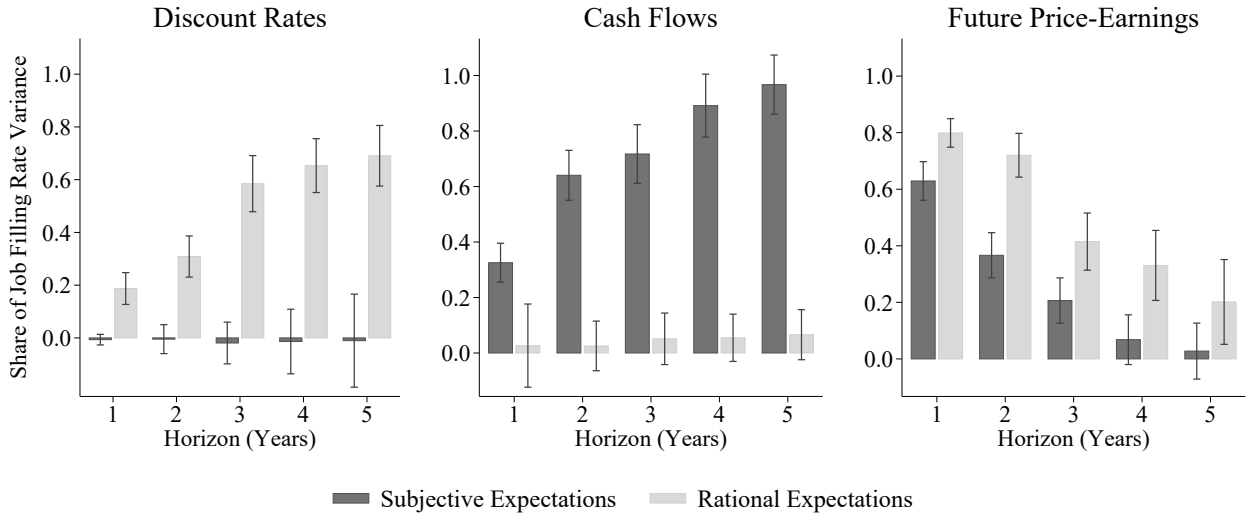
These findings are consistent with predictions from search-and-matching models that emphasize time-varying risk premia while maintaining rational expectations. The large contribution from discount rate news is consistent with models that introduce rational time-varying discount rates to explain unemployment fluctuations (Hall, 2017).²⁰ The increasing importance of discount

¹⁹Table A.2 reports more detailed statistics on the variance decomposition. First-differenced estimates in Figure A.2 show similar patterns, with rational discount rates explaining 58.7% and cash flows explaining only 10.0% of vacancy filling rate variation. Figure A.3 uses a VAR to extend the decomposition to the infinite horizon where rational discount rates explain 78.1% of vacancy filling rate variation.

²⁰On the relative importance of risk-free rates and risk premia, which are two components of discount rates,

rate news at longer horizons is consistent with rational models that match observed fluctuations in unemployment by modeling hiring as a risky investment with long-duration returns (Kehoe et al., 2023). Finally, the small rational cash flow component aligns with the unemployment volatility puzzle, as Shimer (2005) showed that, without time-varying discount rates, standard search models cannot generate enough unemployment volatility from productivity shocks, which would mainly be reflected in the cash flow component.

Figure 5: Time-Series Decomposition of the Vacancy Filling Rate



Notes: Figure illustrates the discount rate, cash flow, and future price-earnings components from the time-series decomposition of the U.S. aggregate vacancy filling rate. Light bars show contributions under rational expectations; dark bars show contributions under subjective expectations. Subjective expectations \mathbb{F}_t are constructed from CFO survey forecasts (discount rates) and IBES analyst forecasts (cash flows). Rational expectations \mathbb{E}_t are based on machine learning forecasts from Long Short-Term Memory (LSTM) neural networks. x -axis denotes the forecast horizon h . The sample is quarterly from 2005Q1 to 2023Q4. Each bar shows Newey-West 95% confidence intervals with lags = 4.

Subjective Expectations On the other hand, Figure 5 reveals a strikingly different result under subjective expectations. At the five-year horizon, subjective cash flow news explains 96.7% of the variation in vacancy filling rates, while subjective discount rate news accounts for only -1.0%.²¹ These results suggest that firms systematically believe distortions drive excess sensitivity to cash flow news when hiring workers. Since vacancy filling rates are countercyclical (declining during expansions as labor markets tighten), the positive cash flow coefficient indicates that firms expect high cash flows during periods when q_t is low, consistent with excessive optimism during

Figure A.7 shows that rational risk-free rate expectations explain less than 5% of the variation in the vacancy filling rate. This implies that the explanatory power of discount rate news is driven primarily by risk premia, consistent with rational models of labor markets that introduce time-varying risk premia (Borovickova and Borovička, 2017).

²¹First-differenced estimates in Figure A.2 show similar results, with subjective cash flows explaining 90.6% and discount rates explaining only -1.3% of the vacancy filling rate. Figure A.3 uses a VAR to extend the decomposition to the infinite horizon where subjective cash flows explain 95.4% of vacancy filling rate variation.

economic booms. The negative contribution on the discount rate component indicates that survey respondents predict lower future returns during recessions, contrary to what a rational forecast would imply.

The contribution from the terminal price-earnings ratio falls with horizon and is negligible by year five (2.8%), compared with 20.1% under rational expectations. This implies that subjective beliefs place excessive weight on near-term cash flows relative to long-run fundamentals. Finally, the three components sum to 98.5% at the five-year horizon, showing that survey expectations are internally consistent and the model’s approximation is reasonably accurate, with any remaining gap likely attributable to measurement error in the survey data (e.g., Ma et al., 2020).²²

Compared to the rational benchmark, the implied overreaction to cash flow news is substantial. Low vacancy filling rates during expansions are associated with a significant disappointment in future cash flows. Defining the belief distortion as the difference between subjective and rational expectations $\mathbb{F}_t - \mathbb{E}_t$, the estimates imply that, at the five-year horizon, $96.7\% - 6.6\% = 90.1\%$ of variation in vacancy filling rates can be attributed to the fact that the vacancy filling rate predicts distortions in cash flow expectations with a significant positive relationship (Table A.4). These distortions capture inefficiencies or behavioral biases in survey respondents’ subjective beliefs that the machine learning model could have identified ex-ante.

Sources of Vacancy Filling Rate Variation While Table 1 has shown subjective discount rate forecasts to exhibit overreaction, their contribution to the variance decomposition of vacancy filling rates remains small in Figure 5. This can be reconciled by the fact that subjective discount rate expectations display relatively little time-series variation, so even overreactive revisions have limited impact on hiring decisions. In contrast, subjective cash flow expectations vary much more over time, making them the primary driver of belief-driven fluctuations in hiring.²³

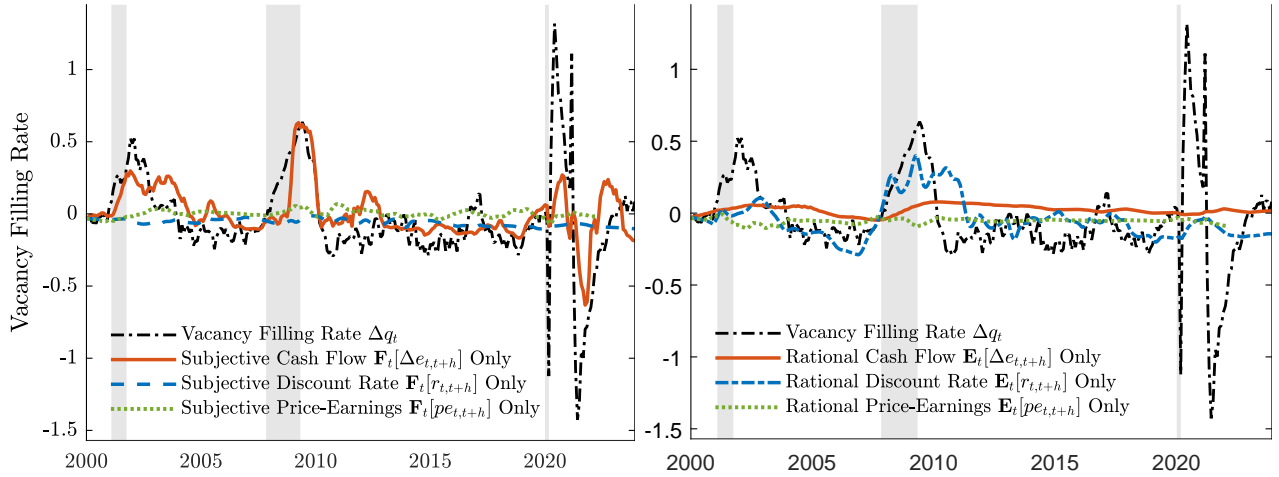
To visualize the relative importance of each component in the decomposition, Figure 6 constructs counterfactual time series for the annual growth in the vacancy filling rate. These series represent the component of vacancy filling rate growth explained by a single driver, based on the fitted values from the variance decomposition from Figure 5. As shown in the figures, each counterfactual series is initialized to match the actual vacancy filling rate in 2005Q1 to provide a common baseline for comparison. The results are consistent with the variance decomposition.

²²This residual term captures any model misspecification or approximation errors in the decomposition, including potential misspecification of the stochastic discount factor or approximation errors in the Campbell-Shiller decomposition under subjective beliefs. As shown in Section A.2.2, the residual is quantitatively negligible and approximately orthogonal to the model’s main components of discount rates and cash flow expectations.

²³Figure A.1 illustrates this point visually by showing that subjective expectations exhibit excessive cyclicalities in cash flow forecasts and muted responses in discount rate forecasts compared to their machine-based counterparts.

Under subjective beliefs, the counterfactual based on cash flow expectations tracks the realized path of vacancy filling rate growth remarkably well, explaining a substantial portion of its cyclical fluctuations. In contrast, while the discount rate component under rational beliefs accounts for a significant share of fluctuations, its explanatory power is visibly less pronounced than that of subjective cash flows.

Figure 6: Role of Components in the Vacancy Filling Rate



Notes: Figure presents counterfactual time series showing the evolution of vacancy filling rate growth if driven solely by each expectation component. Left panel shows subjective expectations; right panel shows rational expectations. Counterfactual series are constructed by accumulating fitted values from regressions of vacancy filling rate growth on individual expectation measures, with all series initialized to the actual vacancy filling rate growth in 2005Q1. Black line shows actual vacancy filling rate growth for comparison. Subjective expectations F_t are based on CFO survey forecasts (discount rates) and IBES analyst forecasts (cash flows, price-earnings). Rational expectations E_t are based on machine learning forecasts from Long Short-Term Memory (LSTM) neural networks. Gray shaded areas indicate NBER recessions. Sample period: 2000Q4 to 2023Q4.

Discussion Although the decomposition does not necessarily estimate causal relationships, it can account for possible sources of variation in the vacancy filling rate. A large estimate for subjective cash flow news means that, whatever shocks drive the vacancy filling rate, they must have a larger impact on subjective cash flow expectations than subjective discount rates. Under rational expectations, by contrast, firms correctly interpret those same shocks as signals about future risk compensation embedded in discount rates. This divergence points to belief distortions as a key source of vacancy filling rate fluctuations. By overreacting to perceived changes in future cash flows, firms may cut hiring and vacancies too sharply during downturns, amplifying unemployment volatility beyond what rational models predict.

Several robustness checks confirm this interpretation. The patterns persist when comparing subjective expectations against risk-neutral benchmarks extracted from futures prices (Figure A.8). This confirms that the observed distortions reflect genuine departures from rational belief formation. They are not simply the result of respondents reporting forecasts under a

rational risk-neutral measure. At the five-year horizon, cash flow expectations explain 96.7% of the variation in vacancy filling rates under subjective beliefs, compared to just 59.6% under risk-neutral expectations, with the gap between the two capturing the extent of overreaction in subjective beliefs. Additionally, extending the baseline model to introduce financial constraints does not alter the overreaction in subjective cash flow expectations, suggesting that hiring patterns are driven more by belief distortions than by financial frictions (Figure A.11).

The large contribution of subjective cash flows in shaping hiring decisions is consistent with models that introduce nonrational expectations about earnings growth to account for fluctuations in asset prices (Bordalo et al., 2024a; Bianchi et al., 2024) and the business cycle (Bordalo et al., 2024b). This parallel implies that the belief distortions known to influence asset valuations can also extend to real economic behavior through the labor market.

On the other hand, the small and negative contribution of subjective discount rates (although not statistically different from zero) is consistent with existing survey evidence showing that subjective return expectations are acyclical (Nagel and Xu, 2022) or even procyclical (Greenwood and Shleifer, 2014; Adam et al., 2016), contrary to the countercyclical discount rate variation implied by rational models (Cochrane, 2017). In standard asset pricing models, discount rates reflect the firm's market-based cost of capital, such as the weighted average cost of debt and cost of equity (WACC). In contrast, survey evidence suggests that CFOs likely rely on internal discount rates that are persistent and often unresponsive to market conditions, even when firms are not financially constrained (Gormsen and Huber, 2025). My findings extend this evidence to labor markets, where hiring decisions appear similarly detached from subjective beliefs about risk premia or financial constraints.

7 Cross-Sectional Decomposition of the Hiring Rate

To analyze the sources of dispersion in hiring across firms, I implement a cross-sectional decomposition of the log hiring rate based on the same theoretical framework developed for the time-series decomposition. The log hiring rate for each firm can be constructed using the employment accumulation equation:

$$hl_{i,t} = \log \left(\frac{q_t V_{i,t}}{L_{i,t}} \right) = \log \left(\frac{L_{i,t+1}}{L_{i,t}} - (1 - \delta_{i,t}) \right) \quad (22)$$

where $L_{i,t}$ uses data from Compustat number of employees (EMP) and $\delta_{i,t}$ uses JOLTS industry-level job separation rate. The hiring rate captures the fraction of new hires per existing employee, conditional on vacancies being filled at rate q_t . This demeaned hiring rate is then decomposed

into three components:²⁴

$$\tilde{hl}_{i,t} = - \underbrace{\sum_{j=1}^h \rho^{j-1} \mathbb{F}_t[\tilde{r}_{i,t+j}]}_{\text{Discount Rate} \equiv \mathbb{F}_t[\tilde{r}_{i,t+h}]} + \underbrace{\left[\tilde{el}_{i,t} + \sum_{j=1}^h \rho^{j-1} \mathbb{F}_t[\Delta \tilde{e}_{i,t+j}] \right]}_{\text{Cash Flow} \equiv \mathbb{F}_t[\tilde{e}_{i,t+h}]} + \underbrace{\rho^h \mathbb{F}_t[\tilde{pe}_{i,t+h}]}_{\text{Future Price-Earnings} \equiv \mathbb{F}_t[\tilde{pe}_{i,t+h}]} \quad (23)$$

where $\rho = \exp(\bar{pe})/(1 + \exp(\bar{pe}))$ is the time discount factor from the log-linearization. The first term represents cross-sectional dispersion in expected returns, which affect the discount rate at which future expected cash flows are converted to present value. The second term captures dispersion in the current earnings per worker, $\tilde{el}_{i,t}$, and the sum of expected earnings growth over the forecast horizon h . The third term is the dispersion in expected future price-earnings ratios, which is a terminal value that captures longer-run influences not already captured in discount rates and expected cash flows by horizon h . All expectations are formed using either survey (subjective expectation) or machine learning forecasts (rational expectation benchmark). To isolate cross-sectional variation, I demean each variable across firms indexed by I , defining $\tilde{hl}_{i,t} = hl_{i,t} - \frac{1}{I} \sum_{j \in I} hl_{j,t}$, so that the decomposition isolates the extent to which deviations from the average hiring rate can be traced to each component.

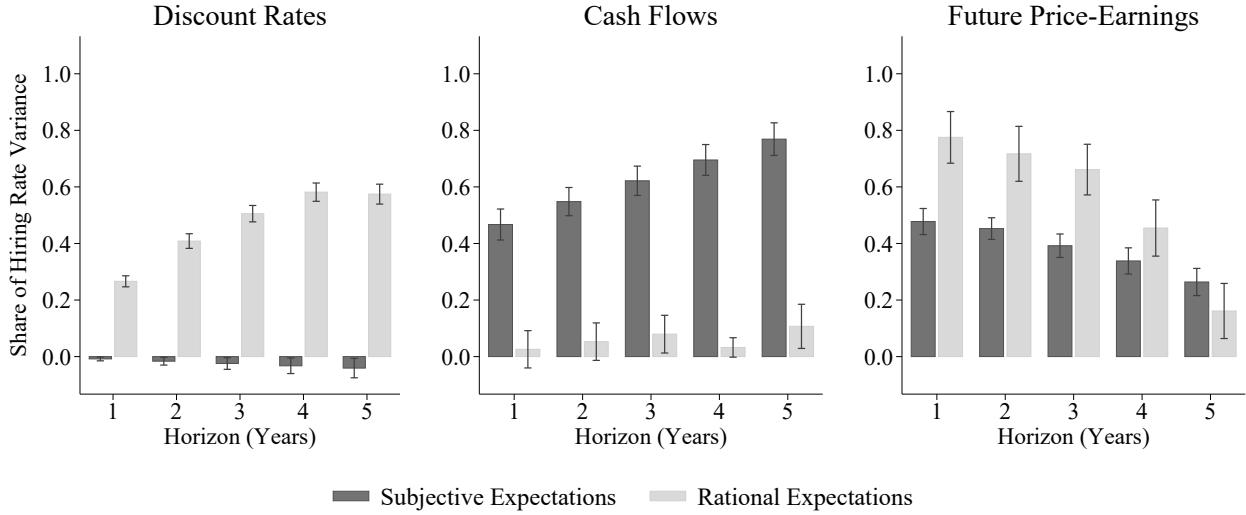
Under stationarity, the econometrician can estimate these shares using OLS coefficients from regressing $\mathbb{F}_t[\tilde{r}_{i,t+h}]$, $\mathbb{F}_t[\tilde{e}_{i,t+h}]$, and $\mathbb{F}_t[\tilde{pe}_{i,t+h}]$ on the current log hiring rate $\tilde{hl}_{i,t}$, respectively. The sample covers all common stocks (share code 10 and 11) listed on NYSE, AMEX, and NASDAQ, restricted to firms that have sufficient data to construct total employee counts (EMP) from Compustat and the median analyst stock return and earnings growth forecasts at the five-year horizon from IBES, as described in Section 3.

Figure 7 shows that under subjective expectations, cross-sectional dispersion in the hiring rate is dominated by differences in expected cash flows. At the five-year horizon, 79.2% of the cross-sectional variance is explained by the expected cash flows. In contrast, only -5.2% of the variation is explained by discount rates, and 29.8% is attributed to differences in the terminal future price-earnings expectation. Under subjective beliefs, a higher discount rate is associated with a higher hiring rate, a direction that is not consistent with the predictions of the search model. These results indicate that firms sorted into different idiosyncratic shock deciles have sharply different expectations about future cash flows when expectations are subjective, and these differences in beliefs translate into differences in perceived hiring incentives. The combined

²⁴See Appendix Section B.2 for a derivation. Note that the signs on each component are reversed compared to the vacancy filling rate decomposition in equation (21). The flipped sign reflects the distinction between how easy it is to fill vacancies (vacancy filling rate) versus how much hiring actually occurs (hiring rate). Good economic conditions make vacancies harder to fill but increase overall hiring activity.

contribution of the three components sums to 103.8% at the five-year horizon, a value close to 100.0% suggesting that the approximations used in the decomposition are reasonably accurate despite being freely estimated without imposing this constraint.

Figure 7: Cross-Sectional Decomposition of the Hiring Rate



Notes: Figure illustrates the discount rate, cash flow, and future price-earnings components from the cross-sectional decomposition of the hiring rate. Light bars show contributions under rational expectations; dark bars show contributions under subjective expectations. Subjective expectations \mathbb{F}_t are constructed from IBES analyst forecasts (discount rates and cash flows). Rational expectations \mathbb{E}_t are based on machine learning forecasts from Long Short-Term Memory (LSTM) neural networks. x -axis denotes the forecast horizon h . The sample is quarterly from 2005Q1 to 2023Q4. Each bar shows 95% confidence intervals under two-way clustering by portfolio and quarter.

Under rational expectations, 60.2% of cross-sectional variation in hiring is explained by differences in expected discount rates at horizon five, while only 13.1% is explained by expected cash flows. This pattern is consistent with existing estimates showing that, under rational expectations, much of the variation across firms in asset valuations comes from dispersion in risk premia rather than expected cash flows (De La O et al., 2024). Finally, the contribution of the terminal price-earnings component is 17.8%, which is sizeable and is larger than the same component estimated under subjective beliefs.

Taken together, the results reveal that under subjective beliefs, cross-sectional variation in hiring is driven primarily by firms overreacting to news about their future cash flows. This provides a micro-foundation for the aggregate results by showing that the same type of belief distortion that drives fluctuations in aggregate unemployment also operates at the firm level, where hiring decisions are actually made.²⁵

²⁵The cross-sectional results suggest that much of the dispersion in hiring rates reflects belief-driven forecast errors. Such distorted expectations can act as a wedge that misallocates labor by inducing over-hiring at optimistic firms and under-hiring at pessimistic firms (Ma et al., 2020; David et al., 2022; Ropele et al., 2024).

Profits per Worker Response to Idiosyncratic Shocks Figure 8 examines how profits per worker respond to idiosyncratic shocks to distinguish between subjective belief formation and existing rational risk-based explanations, as these two mechanisms generate qualitatively different predictions for firm-level profitability dynamics. For the response under subjective beliefs, I use survey forecast revisions to estimate local projections of the following form:

$$y_{i,t+h} = \alpha_i + \tau_t + \beta_h(\mathbb{F}_t[\Delta e_{i,t+1}] - \mathbb{F}_{t-1}[\Delta e_{i,t+1}]) + \boldsymbol{\gamma}'_h \mathbf{X}_{i,t} + \varepsilon_{i,t+h} \quad (24)$$

The dependent variable $y_{i,t} \equiv \log E_{i,t} - \log L_{i,t}$ measures profits per worker for firm i at time t . The regressor captures forecast revisions $\mathbb{F}_t[\Delta e_{i,t+1}] - \mathbb{F}_{t-1}[\Delta e_{i,t+1}]$ representing the change in expected idiosyncratic cash flow growth between periods $t-1$ and t . As shown in the Coibion and Gorodnichenko (2015) regression of Table 1, these forecast revisions capture belief over- or under-reaction to idiosyncratic shocks. The specification includes firm fixed effects α_i and time fixed effects τ_t to control for systematic differences across firms and common time trends. The control vector $\mathbf{X}_{i,t}$ includes lags of profits per worker and the forecast revision variable. For the response under rational beliefs, I use machine forecast revisions in discount rates to estimate local projections of the following form:

$$y_{i,t+h} = \alpha_i + \tau_t + \beta_h(\mathbb{E}_t[r_{i,t+1}] - \mathbb{E}_{t-1}[r_{i,t+1}]) + \boldsymbol{\gamma}'_h \mathbf{X}_{i,t} + \varepsilon_{i,t+h} \quad (25)$$

The coefficient β_h provides a direct test of expectation formation mechanisms. Under rational expectations with hiring frictions, positive idiosyncratic shocks should lead to temporary increases in profits per worker as firms face time costs in adjusting employment. This predicts $\beta_h \geq 0$. Conversely, under subjective expectations where firms systematically overreact to good idiosyncratic news, we expect overhiring relative to the optimal level. This behavior would generate a decline in profits per worker following positive forecast revisions, implying $\beta_h < 0$.

Figure 8 presents the impulse response functions comparing our data to model predictions under both rational and subjective expectations. The blue dashed line shows the data impulse response function under rational expectations (proxied by machine forecasts), while the red solid line displays results under subjective expectations (proxied by survey forecasts). The results show that, consistent with the predictions, profits per worker do not decline under rational expectations, while under subjective expectations they drop significantly. This pattern is consistent with firms over-hiring in response to overly optimistic cash flow beliefs, generating predictable declines in profits per worker.²⁶

²⁶As shown in Figure A.12, employment rises sharply while total profits increase only modestly, so the average profit per worker falls.

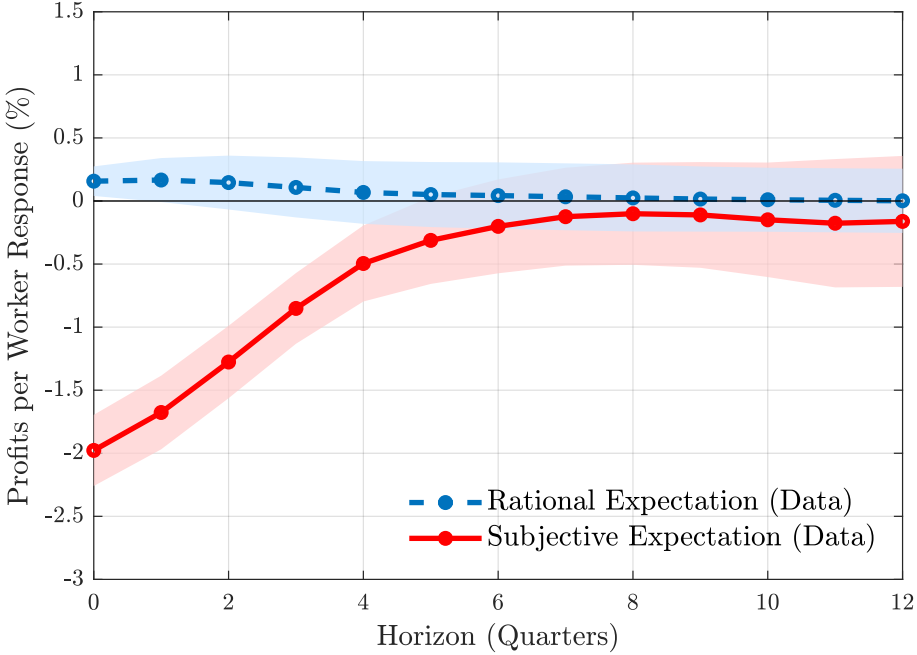


Figure 8: Profits per Worker Response to Forecast Revision

Notes: Figure displays impulse responses of log profits per worker $\log(E_{i,t+h}/L_{i,t+h})$ to forecast revisions, estimated via local projections: $\log(E_{i,t+h}/L_{i,t+h}) = \beta_h \text{ForecastRevision}_{i,t} + \alpha_i + \tau_t + \varepsilon_{i,t+h}$, where α_i and τ_t denote firm and time fixed effects. Blue dashed line: IRF under rational expectations, where forecast revision is the machine learning discount rate revision $\mathbb{E}_t[r_{i,t+1}] - \mathbb{E}_{t-1}[r_{i,t+1}]$. Red solid line: IRF under subjective expectations, where forecast revision is the survey cash flow revision $\mathbb{F}_t[\Delta e_{i,t+1}] - \mathbb{F}_{t-1}[\Delta e_{i,t+1}]$. Blue dash (red solid) line: data IRF under rational (subjective) expectations proxied by machine (survey) forecasts. Observations weighted by each firm's market value. Shaded area: two-way clustered 90% confidence intervals by firm and time (data IRF). Data sample: 1999Q1–2023Q4.

The decline in profits per worker under subjective beliefs primarily reflects excessive hiring relative to earnings. Following a positive idiosyncratic shock, firms become overly optimistic, post more vacancies, and expand employment aggressively. Although profits increase, the rise is insufficient to offset the higher wage bill and larger workforce, leading to a decline in profits per worker. Because idiosyncratic shocks are transitory, the underlying productivity improvement fades quickly, while subjective beliefs remain persistently optimistic. Labor market frictions amplify this persistence: once workers are hired, adjustment takes time due to vacancy posting costs and frictions in separations. Consequently, employment remains elevated even after profitability normalizes, producing a prolonged decline in profits per worker.

The profit measure used in the analysis is IBES “street earnings,” which correspond to adjusted net income that excludes one-off charges but still includes depreciation. Since capital expenditures are capitalized rather than expensed, they only affect earnings gradually through depreciation. Hence, in the short run, investment does not directly depress IBES earnings, and

the observed decline in profits per worker is best interpreted as reflecting excessive hiring relative to underlying cash flows, rather than an artifact of capital investment.

8 Model of Constant-Gain Learning

In this section, I introduce a model of hiring in which firms form subjective beliefs about cash flows and prices using a constant-gain learning rule.²⁷ The model embeds belief distortions in a search-and-matching framework from Section 5. The distortions shape firms' vacancy posting decisions and drive variation in hiring and vacancy filling rates. Simulations from the model generate decompositions that can match those estimated from the data in Sections 6 and 7.

Cash Flow Process Firms do not have full knowledge of the stochastic processes governing their cash flows. Instead, they form beliefs about their long-run mean using constant-gain learning. Assume that the firm's cash flow process consists of aggregate and idiosyncratic components. Firm i 's earnings at time t are given by:

$$E_{i,t} = E_t \cdot \tilde{E}_{i,t} = \exp(e_t + \tilde{e}_{i,t}) \quad (26)$$

The aggregate component follows an AR(1) process:

$$e_t = \mu + \phi e_{t-1} + u_t, \quad u_t \sim \mathcal{N}(0, \sigma_u^2) \quad (27)$$

where μ is the unknown long-run mean, $\phi < 1$ is the known persistence parameter, and u_t is an i.i.d. Gaussian innovation. This specification captures both persistent variation in aggregate earnings and stochastic fluctuations. The idiosyncratic component also follows an AR(1) process:

$$\tilde{e}_{i,t} = \tilde{\mu}_i + \tilde{\phi} \tilde{e}_{i,t-1} + v_{i,t}, \quad v_{i,t} \sim \mathcal{N}(0, \sigma_v^2) \quad (28)$$

where $\tilde{\mu}_i$ is a firm-specific long-run mean in earnings (unknown to the firm), $\tilde{\phi} < 1$ is a known persistence parameter, and $v_{i,t}$ is an i.i.d. idiosyncratic shock.

Subjective Expectations Under Learning Objectively, mean growth is identical across firms: $\mu = \tilde{\mu}_i = 0$. Under subjective beliefs, however, agents do not observe the true long-run mean μ and $\tilde{\mu}_i$. Instead, they form beliefs and update these beliefs recursively as new

²⁷For applications of constant-gain learning in macroeconomics, see Evans and Honkapohja (2001) and Marcet and Sargent (1989). For applications in asset pricing, see Adam et al. (2016), Nagel and Xu (2021), and De La O et al. (2024).

information arrives. I assume firms employ constant-gain learning, which places greater weight on recent forecast errors. The updating rules are:

$$\mathbb{F}_t[\mu] = \mathbb{F}_{t-1}[\mu] + \nu (\Delta e_t - \mathbb{F}_{t-1}[\Delta e_t]) \quad (29)$$

$$\mathbb{F}_t[\tilde{\mu}_i] = \mathbb{F}_{t-1}[\tilde{\mu}_i] + \nu (\Delta \tilde{e}_{i,t} - \mathbb{F}_{t-1}[\Delta \tilde{e}_{i,t}]) \quad (30)$$

where ν is the constant gain parameter and governs the speed of learning.²⁸ A higher ν implies greater responsiveness to new data. The term $\mathbb{F}_t[\mu]$ denotes the firm's time- t belief about the aggregate long-run mean, and $\Delta e_t \equiv e_t - e_{t-1}$ is the realized growth in aggregate earnings, which the firm observes at time t . Both updating rules use the same learning rate ν for parsimony. Existing estimates of the learning rate are deliberately small, ensuring slow learning that allows subjective beliefs to remain persistently distorted even after large forecast errors (Malmendier and Nagel, 2015; Adam et al., 2016).²⁹ This persistence can generate the sustained belief distortions needed to explain fluctuations in hiring.

Constant-gain learning assigns exponentially decreasing weights to past observations, causing memory to fade over time. Beliefs never fully converge to rational expectations, even in stationary environments. This avoids the unrealistic declining volatility implied by other learning schemes such as OLS learning, while allowing for beliefs to adapt to potential regime shifts.³⁰ The mechanism generates overreaction to economic news because agents cannot distinguish temporary shocks ($u_t, v_{i,t}$) from permanent changes to the long-run mean ($\mu, \tilde{\mu}_i$). They misattribute recent surprises to persistent shifts in underlying growth rates, over-extrapolating short-run fluctuations and creating persistent belief distortions that amplify valuation and hiring responses. Given these beliefs, firms forecast future aggregate earnings growth using:

$$\mathbb{F}_t[\Delta e_{t+h}] = \phi^{h-1}(\mathbb{F}_t[\mu] + (\phi - 1)e_t) \quad (31)$$

$$\mathbb{F}_t[\Delta \tilde{e}_{i,t+h}] = \tilde{\phi}^{h-1}(\mathbb{F}_t[\tilde{\mu}_i] + (\tilde{\phi} - 1)\tilde{e}_{i,t}) \quad (32)$$

This reflects the fact that agents know the process is AR(1) with known persistence ϕ and $\tilde{\phi}$ but uncertain μ and $\tilde{\mu}_i$, and project the process forward using current levels of earnings and the

²⁸To isolate the importance of expected cash flows, the baseline model assumes agents learn only about cash flows. One can obtain qualitatively similar results when agents employ constant-gain learning to update beliefs about both earnings growth and stock price growth (e.g., Adam et al., 2016).

²⁹This constant-gain learning specification is supported by empirical evidence presented in Appendix A.6, which shows that survey respondents update their long-run earnings expectations only gradually following short-term earnings surprises. Specifically, the response of 5-year-ahead forecasts to earnings news is small and often statistically insignificant, consistent with the slow, partial updating implied by constant-gain learning.

³⁰Constant-gain learning can be micro-founded using an overlapping generations model where agents learn from recent experience across generations, where the average expectation closely approximates a constant-gain learning rule (Nagel and Xu, 2021).

estimated perceived long-run mean. The forecast of firm-level earnings growth is then:

$$\mathbb{F}_t[\Delta e_{i,t+h}] = \mathbb{F}_t[\Delta e_{t+h}] + \mathbb{F}_t[\Delta \tilde{e}_{i,t+h}] \quad (33)$$

These expectations will feed directly into the firm's market value, which in turn influences their vacancy posting decisions through the hiring equation (9).

Aggregate Stock Price and Returns Firms use their beliefs about future earnings to form expectations about asset returns and valuations. I assume that the economy is governed by a representative household such that the log stochastic discount factor (SDF) is:

$$m_{t+1} = -r_f - \frac{1}{2}\gamma^2\sigma_u^2 - \gamma u_{t+1} \quad (34)$$

where r_f is the risk-free rate, γ is the coefficient of relative risk aversion, and u_{t+1} is the aggregate earnings shock from the earnings process. With constant relative risk aversion and log-normal shocks, this SDF implies a constant risk premia under rational beliefs. The exercise here is to ask how far we can explain asset prices and labor market fluctuations by relying only on distortions in subjective beliefs, without relying on rational time-varying risk premia.

The stochastic discount factor determines how firms value future cash flows. $-r_f$ reflects time discounting, where future payoffs are worth less than current payoffs because investors can always earn the risk-free rate. $-\frac{1}{2}\gamma^2\sigma_u^2$ is the price of uncertainty, where uncertainty about the future aggregate shock u_{t+1} lowers the discounted value of risky payoffs. $-\gamma u_{t+1}$ is the price of risk, making the SDF high in bad times and low in good times depending on the aggregate shock u_{t+1} . During bad economic shocks ($u_{t+1} < 0$), the SDF is high because an extra dollar is highly valued. Risk aversion γ amplifies these effects, making the SDF more sensitive to aggregate shocks.

Let $P_t^{(h)}$ denote the time t price for an aggregate strip of a one-dollar payoff received h periods in the future. The strip price reflects the discounted value of a dollar paid at horizon h , with beliefs about long-run growth embedded in the recursive coefficients. I guess and verify a log-linear solution:³¹

$$P_t^{(h)} = \mathbb{F}_t[M_{t+1}P_{t+1}^{(h-1)}] = \exp \{ A^{(h)} + B^{(h)}\mathbb{F}_t[\mu] + \phi^h e_t \} \quad (35)$$

³¹In constant-gain learning models, fading memory breaks the law of iterated expectations, making the buy-and-hold and resale valuation methods non-equivalent. While the former values long-run payoffs using only today's beliefs, the resale method prices assets iteratively using updated, one-period-ahead expectations. Following Nagel and Xu (2021), I adopt the resale method because it is time-consistent and better reflects trading among agents with evolving beliefs. For consistency between firm decisions and asset pricing, I assume both the manager and the representative investor share the same beliefs and use this valuation approach.

This expression implies that strip prices depend on current earnings e_t , beliefs about the aggregate long-run mean $\mathbb{F}_t[\mu]$, and constants $A^{(h)}$, $B^{(h)}$ that evolve recursively. These recursive coefficients are computed using the method of undetermined coefficients:

$$A^{(h)} = A^{(h-1)} - r_f + \frac{1}{2}C^{(h)} [C^{(h)} - 2\gamma] \sigma_u^2 \quad (36)$$

$$B^{(h)} = B^{(h-1)} + \phi^{h-1} = \frac{1 - \phi^h}{1 - \phi} \quad (37)$$

$$C^{(h)} = \nu B^{(h-1)} + \phi^{h-1} \quad (38)$$

where $A^{(0)} = B^{(0)} = C^{(0)} = 0$. $A^{(h)}$ captures discounting and risk premia, pushing down long-horizon strip prices. $B^{(h)}$ measures sensitivity to beliefs about long-run cash flow growth μ , with its influence rising in the horizon. $C^{(h)}$ reflects the effect of constant-gain learning, where recent forecast errors are overweighted, distorting valuations relative to rational expectations. The aggregate strip price implies the realized return on the strip:

$$R_{t+1}^{(h)} = \frac{P_{t+1}^{(h-1)}}{P_t^{(h)}} = \exp\{[A^{(h-1)} - A^{(h)}] + C^{(h)}(\mu - \mathbb{F}_t[\mu] + u_{t+1})\} \quad (39)$$

The expected return on a strip of horizon h is then:

$$\mathbb{F}_t[R_{t+1}^{(h)}] = \exp\{r_f + C^{(h)}\gamma\sigma_u^2\} \quad (40)$$

which shows that expected returns decline with horizon h when agents believe earnings growth is persistent ($\phi < 1$) and learning slows perceived mean reversion. Since $C^{(h)} = \nu B^{(h-1)} + \phi^{h-1}$, a smaller learning rate ν makes $C^{(h)}$ decline more quickly, muting the influence of long-horizon strip returns. The aggregate stock price is the sum of strip prices across all future periods:

$$P_t = \sum_{h=1}^{\infty} P_t^{(h)} \quad (41)$$

The aggregate stock return realized between t and $t + 1$ is defined as the value-weighted average return across all strips maturing from $h = 1$ onwards:

$$R_{t+1} = \frac{\sum_{h=1}^{\infty} P_{t+1}^{(h-1)}}{\sum_{h=1}^{\infty} P_t^{(h)}} = \sum_{h=1}^{\infty} w_{t,h} R_{t+1}^{(h)}, \quad w_{t,h} = \frac{P_t^{(h)}}{\sum_{k=1}^{\infty} P_t^{(k)}} \quad (42)$$

where $R_{t+1}^{(h)} = P_{t+1}^{(h-1)}/P_t^{(h)}$ is the return on the h -period strip, and $w_{t,h}$ is the share of total market value accounted for by strip h . I assume that, under subjective beliefs, the expected strip weights are approximately constant: $w_{t+j-1,h} \approx w_{t,h}$. This assumption reflects the idea that

subjective beliefs simplify their expectations by projecting a constant term structure of asset values forward.³² Then the expected aggregate return at time t for horizon $j \geq 1$ is:

$$\mathbb{F}_t[R_{t+j}] \approx \sum_{h=1}^{\infty} w_{t,h} \mathbb{F}_t[\mathbb{F}_{t+1}[\dots \mathbb{F}_{t+j-1}[R_{t+j}^{(h)}]]] = \sum_{h=1}^{\infty} w_{t,h} \exp \{r_f + C^{(h)} \gamma \sigma_u^2\} \quad (43)$$

To obtain the expected log return, I apply the log approximation: $\mathbb{F}_t[r_{t+j}] \approx \log(\mathbb{F}_t[R_{t+j}])$.

Firm Stock Price and Returns Each firm's total value is the sum of expected discounted future cash flows. Let $P_{i,t}$ be the ex-dividend value of firm i , which is the sum of strip prices across all future periods:

$$P_{i,t} = \sum_{h=1}^{\infty} P_{i,t}^{(h)}, \quad P_{i,t}^{(h)} = \mathbb{F}_t[M_{t+1} P_{i,t+1}^{(h-1)}] = \mathbb{F}_t[M_{t+1} \dots \mathbb{F}_{t+h-1}[M_{t+h} E_{t+h} \tilde{E}_{i,t+h}]] \quad (44)$$

Assuming independence between aggregate discounting and idiosyncratic earnings:

$$P_{i,t}^{(h)} = P_t^{(h)} \cdot \mathbb{F}_t[\dots \mathbb{F}_{t+h-1}[\tilde{E}_{i,t+h}]] \quad (45)$$

Firm-level strip price implies realized next-period return on the strip:

$$R_{i,t+1}^{(h)} = \frac{P_{i,t+1}^{(h-1)}}{P_{i,t}^{(h)}} = \frac{P_{t+1}^{(h-1)} \mathbb{F}_{t+1}[\dots \mathbb{F}_{t+h-1}[\tilde{E}_{i,t+h}]]}{P_t^{(h)} \mathbb{F}_t[\dots \mathbb{F}_{t+h-1}[\tilde{E}_{i,t+h}]]} \quad (46)$$

$$= R_{t+1}^{(h)} \exp \left\{ \tilde{C}^{(h)} (\tilde{\mu}_i - \mathbb{F}_t[\tilde{\mu}_i] + v_{i,t+1}) - \frac{1}{2} \tilde{\phi}^{2(h-1)} \sigma_v^2 \right\} \quad (47)$$

where $\tilde{C}^{(h)} \equiv \tilde{\phi}^{h-1} + \nu \frac{1-\tilde{\phi}^{h-1}}{1-\tilde{\phi}}$. Then the expected return on the firm-level strip is:

$$\mathbb{F}_t[R_{i,t+1}^{(h)}] = \mathbb{F}_t[R_{t+1}^{(h)}] \exp \left\{ \frac{1}{2} ((\tilde{C}^{(h)})^2 - \tilde{\phi}^{2(h-1)}) \sigma_v^2 \right\} \quad (48)$$

$$= \exp \left\{ r_f + C^{(h)} \gamma \sigma_u^2 + \frac{1}{2} ((\tilde{C}^{(h)})^2 - \tilde{\phi}^{2(h-1)}) \sigma_v^2 \right\} \quad (49)$$

The firm-level stock return realized between t and $t+1$ is defined as the value-weighted average return across all strips maturing from $h=1$ onwards:

$$R_{i,t+1} = \frac{\sum_{h=1}^{\infty} P_{i,t+1}^{(h-1)}}{\sum_{h=1}^{\infty} P_{i,t}^{(h)}} = \sum_{h=1}^{\infty} w_{i,t,h} R_{i,t+1}^{(h)}, \quad w_{i,t,h} = \frac{P_{i,t}^{(h)}}{\sum_{k=1}^{\infty} P_{i,t}^{(k)}} \quad (50)$$

³²It can be shown that the assumption holds approximately in the small-gain limit. As $\nu \rightarrow 0$, strip prices move proportionally to changes in cash flows: $P_{t+1}^{(h)}/P_t^{(h)} \approx \exp\{\phi^h(e_{t+1} - e_t)\}$. Since the strip price of all maturities shift by the same factor raised to different powers ϕ^h , relative strip weights $w_{t,h} = P_t^{(h)}/\sum_k P_t^{(k)}$ remain approximately constant over time.

where $R_{i,t+1}^{(h)} = P_{i,t+1}^{(h-1)}/P_{i,t}^{(h)}$ is the return on the h -period strip, and $w_{i,t,h}$ is the share of total market value accounted for by strip h . Assuming that expected strip weights are approximately constant under subjective beliefs $w_{i,t+j-1,h} \approx w_{i,t,h}$, the expected firm-level return is:

$$\mathbb{F}_t[R_{i,t+j}] \approx \sum_{h=1}^{\infty} w_{i,t,h} \mathbb{F}_t[\mathbb{F}_{t+1}[\dots \mathbb{F}_{t+j-1}[R_{i,t+j}^{(h)}]]] \quad (51)$$

$$= \sum_{h=1}^{\infty} w_{i,t,h} \exp \left\{ r_f + C^{(h)} \gamma \sigma_u^2 + \frac{1}{2} ((\tilde{C}^{(h)})^2 - \tilde{\phi}^{2(h-1)}) \sigma_v^2 \right\} \quad (52)$$

Subjective Firm Valuation The firm's equilibrium stock price under subjective beliefs is the sum of its strip prices:

$$P_{i,t} = \sum_{h=1}^{\infty} P_{i,t}^{(h)} = \sum_{h=1}^{\infty} \exp \left\{ A_i^{(h)} + B^{(h)} \mathbb{F}_t[\mu] + \tilde{B}^{(h)} \mathbb{F}_t[\tilde{\mu}_i] + \phi^h e_t + \tilde{\phi}^h \tilde{e}_{i,t} \right\} \quad (53)$$

where the coefficients are defined as $A_i^{(h)} = A^{(h)} + \frac{1}{2} \sigma_v^2 \frac{1-\tilde{\phi}^{2h}}{1-\tilde{\phi}^2}$ and $\tilde{B}^{(h)} = \frac{1-\tilde{\phi}^h}{1-\tilde{\phi}}$. The equation shows that the firm's value rises with expected cash flow intercepts $\mathbb{F}_t[\mu]$ and $\mathbb{F}_t[\tilde{\mu}_i]$. The belief distortions captured in these expectation terms will affect the firm's hiring decisions through its valuation.

Hiring Condition I close the model by connecting asset valuations to firm hiring behavior. The connection to labor markets operates through the hiring condition. As shown in Section 5, firms post vacancies until the marginal cost of hiring equals its marginal value:

$$\underbrace{\frac{\kappa}{q_t}}_{\text{Cost of Hiring}} = \underbrace{\frac{P_{i,t}}{L_{i,t+1}}}_{\text{Value of Hiring}} \quad (54)$$

where κ is the cost per vacancy posting, q_t is the vacancy filling rate, and $L_{i,t+1}$ denotes employment. Overly pessimistic beliefs about expected cash flows (low $\mathbb{F}_t[\mu_i]$) lower the firm value $P_{i,t}$, which reduces the value of hiring and leads to fewer job postings. The resulting decrease in vacancy creation drives up the vacancy filling rate q_t and unemployment U_t .

Given values for $\kappa, \delta, B, \eta, P_{i,t}$ and initial values for employment $L_{i,0}$, one can construct the sequence of vacancies $V_{i,t}$, employment $L_{i,t+1}$, labor market tightness θ_t , vacancy filling rates q_t , and unemployment rate U_t by solving for the employment accumulation (4), firm valuation (53), and optimal hiring (54) equations under a Cobb-Douglas matching function (3).

1. Initialize labor market tightness: $\theta_t^{(0)} = 1$

2. At iteration s , use labor market tightness $\theta_t^{(s)}$ to construct vacancy filling rate by using the Cobb-Douglas matching function in equation (3):

$$q_t^{(s)} = B(\theta_t^{(s)})^{-\eta} \quad (55)$$

3. Update each firm's employment policy using the hiring equation (54):

$$L_{i,t+1}^{(s)} = \frac{P_{i,t} q_t^{(s)}}{\kappa} \quad (56)$$

where $P_{i,t}$ is determined by the firm valuation equation (53) under the constant-gain learning rules in equations (29) and (30).

4. Update each firm's vacancy posting using the employment accumulation equation (4):

$$V_{i,t}^{(s)} = \frac{1}{q_t^{(s)}} (L_{i,t+1}^{(s)} - (1 - \delta)L_{i,t}) \quad (57)$$

5. Aggregate firm-level variables over the set of firms I :

$$V_t^{(s)} = \sum_{i \in I} V_{i,t}^{(s)}, \quad L_{t+1}^{(s)} = \sum_{i \in I} L_{i,t+1}^{(s)}, \quad U_t^{(s)} = 1 - \sum_{i \in I} L_{i,t} \quad (58)$$

6. Update labor market tightness: $\theta_t^{(s+1)} = \frac{V_t^{(s)}}{U_t^{(s)}}$. Check convergence: $|\theta_t^{(s+1)} - \theta_t^{(s)}| < \varepsilon$ for some small tolerance $\varepsilon > 0$. If not, return to step 2 with the updated values.

Model-Implied Decompositions I use simulated data implied by the model to decompose the vacancy filling rate at the aggregate level (Section 6) and hiring rates at the firm level (Section 7). The time-series decomposition of the aggregate vacancy filling rate q_t is given by:

$$\log q_t = \underbrace{\sum_{j=1}^h \rho^{j-1} \mathbb{F}_t[r_{t+j}]}_{\text{Discount Rate}} - \underbrace{\left[el_t + \sum_{j=1}^h \rho^{j-1} \mathbb{F}_t[\Delta e_{t+j}] \right]}_{\text{Cash Flow}} - \underbrace{\rho^h \mathbb{F}_t [pe_{t+h}]}_{\text{Future Price-Earnings}} \quad (59)$$

where $x_t = \sum_{i \in I} x_{i,t}$ aggregates firm-level variable $x_{i,t}$. $el_t \equiv e_{i,t} - l_{i,t+1} = \log E_{i,t} - \log L_{i,t+1}$ denotes log earnings per worker. To analyze heterogeneity across firms, I estimate a cross-sectional decomposition of hiring rates using simulated firm-level data:

$$\tilde{hl}_{i,t} = - \underbrace{\sum_{j=1}^h \rho^{j-1} \mathbb{F}_t[\tilde{r}_{i,t+j}]}_{\text{Discount Rate}} + \underbrace{\left[\tilde{el}_{i,t} + \sum_{j=1}^h \rho^{j-1} \mathbb{F}_t[\Delta \tilde{e}_{i,t+j}] \right]}_{\text{Cash Flow}} + \underbrace{\rho^h \mathbb{F}_t [\tilde{pe}_{i,t+h}]}_{\text{Future Price-Earnings}} \quad (60)$$

where $\tilde{x}_{i,t} = x_{i,t} - \frac{1}{I} \sum_i x_{i,t}$ denotes a cross-sectional deviation from the mean at time t .³³

Subjective expectations will over-weight the role of the cash flow channel relative to the discount rate channel, in contrast to the pattern observed under rational expectations. Under rational expectations, agents know the true long-run mean, making these belief distortions zero. Any distortions in beliefs about the intercept terms $\mu - \mathbb{F}_t[\mu]$ (aggregate) and $\tilde{\mu}_i - \mathbb{F}_t[\tilde{\mu}_i]$ (idiosyncratic) could serve as a common driving force behind the cash flow component and the vacancy filling rate q_t . The distortion then drives fluctuations in expected cash flow growth $\mathbb{F}_t[\Delta e_{t+j}]$ and $\mathbb{F}_t[\Delta \tilde{e}_{i,t+j}]$ through equations (31) and (32), respectively, with persistent effects on hiring decisions over time through the firm's hiring condition in equation (54).

The expected return at both the aggregate (43) and firm level (52) is driven by the term $C(h)\gamma\sigma_u^2$. This component is constant over time for fixed parameters and horizon h , so the implied risk premium is effectively time-invariant. Hence the subjective discount rate exhibits only minor variation, arising only through changes in portfolio weights $w_{t,h}$ if those are not treated as constant. This supports the conclusion that belief distortions primarily affect the cash flow channel rather than the discount-rate channel.

Simulation Details To evaluate the model's quantitative performance, I simulate a panel of 300 firms over 500 periods, where the first 150 periods are discarded as a burn-in to eliminate the influence of initial conditions. Each firm updates its beliefs using constant-gain learning based on the updating rules in equations (29) and (30). All expectations, returns, and decompositions are computed at an annual frequency using the model equations derived above. At each horizon h , I compute the model-implied time-series decomposition of the aggregate vacancy filling rate based on equation (17) and the cross-sectional decomposition of the firm-level hiring rates (60). I then compare these model-implied decompositions to those estimated from the observed data from Figures 5 and 7.

Model Estimation Table 1 reports the parameter values used in the quantitative model along with the empirical moments they are calibrated to or sourced from. The model is calibrated at an annual frequency. The persistence ϕ and volatility σ_u of aggregate earnings growth is set to match the autocorrelation and standard deviation of aggregate S&P 500 earnings growth for the period

³³Note that the decomposition consists of expectations of the future values of the three components, not the contemporaneous values. The free-entry condition of the search model pins down the current value of $pe_{i,t} + el_{i,t}$, but it does not necessarily eliminate cross-sectional variation in forward-looking expectations. These subjective beliefs can differ across firms even when the current sum is identical.

between 1983 to 2022 (De La O et al., 2024).³⁴ The persistence $\tilde{\phi}$ and volatility σ_v of idiosyncratic earnings growth is set to match the autocorrelation and standard deviation of earnings growth across publicly listed firms over the same period, after cross-sectionally demeaning the variable. The risk-free rate r_f and risk aversion γ match the average level and volatility of aggregate S&P 500 stock returns (De La O et al., 2024). The time discount rate $\rho = \exp(\bar{pe})/(1+\exp(\bar{pe})) = 0.98$ is chosen to be consistent with a steady-state price-earnings ratio from the Campbell and Shiller (1988) present value identity, where \bar{pe} is the long-run average of the log price-earnings ratio.

Table 1: Model Parameters

Parameter	Value	Moments
ν	0.018	Constant-gain learning (Malmendier and Nagel (2015))
ϕ	0.856	Autocorrelation aggregate earnings growth
$\tilde{\sigma}_u$	0.268	S.D. aggregate earnings growth
$\tilde{\phi}$	0.698	Autocorrelation firm-level earnings growth
σ_v	0.194	S.D. firm-level earnings growth
r_f	0.046	Average risk-free rate
γ	1.586	Average and S.D. aggregate return
ρ	0.980	Average price-earnings ratio
B	0.562	Matching function efficiency (Kehoe et al. (2023))
η	0.500	Matching function elasticity (Kehoe et al. (2023))
δ	0.286	Separation rate (Kehoe et al. (2023))
κ	0.314	Per worker hiring cost (Elsby and Michaels (2013))

Notes: Table reports the parameter values used in the quantitative model along with the empirical moments they are calibrated to or sourced from. The model is calibrated at an annual frequency.

The speed at which agents discount past observations of realized cash flow growth depends on the constant gain parameter ν in the learning rule. This parameter shapes the persistence and volatility of the price-earnings ratio and the extent of return predictability. I take the value directly from survey-based estimates in Malmendier and Nagel (2015), setting it to $\nu = 0.018$ at the quarterly frequency.³⁵ This implies that in forming expectations, agents assign a weight of 0.018 to the most recent growth surprise and $1 - \nu = 0.982$ to their previous estimate, making the perceived growth rate evolve slowly over time.³⁶

³⁴See Section A.7 for a mapping from the AR(1) level parameters to the implied moments of earnings growth.

³⁵Malmendier and Nagel (2015) estimate $\nu = 0.018$ at the quarterly frequency, while the model is simulated annually. Using this value unchanged does not materially alter the implied speed of learning: for small gains, the difference between quarterly and annual updating is second order (De La O et al., 2024). Thus, applying the quarterly estimate at the annual frequency still yields an effective half-life of roughly a decade, consistent with the survey evidence.

³⁶Appendix A.7 describes an alternative estimation using the Method of Simulated Moments (MSM), where ν is disciplined jointly with other structural parameters by matching model-implied and empirical moments. The MSM results yield learning rate estimates that are close in magnitude to the calibrated survey-based value ($\hat{\nu}^{MSM} = 0.13$), providing independent support for the baseline choice of ν .

Labor market parameters are mainly from Kehoe et al. (2023). Following Shimer (2005), I normalize the value of labor market tightness θ to one in the deterministic steady state, which implies an efficiency of the matching function $B = 0.562$ by noting from the matching function that $q = B\theta^{-\eta}$. I set the elasticity of the matching function to $\eta = 0.5$ following Ljungqvist and Sargent (2017). I use an annual job separation rate of $\delta = 0.286$, which is the annualized value of the Abowd-Zellner corrected estimate by Krusell et al. (2017) based on data from the Current Population Survey (CPS). Following Elsby and Michaels (2013), per-worker vacancy posting cost 0.314 is targeted to match a per-worker hiring cost κ/q equal to 14 percent of the quarterly worker compensation. In the context of the annual calibration of this model, this implies a value approximately equal $\kappa = 4 \times 0.14 \times q = 0.314$, where 4×0.14 is the annualized percent of worker compensation, while $q = 0.562$ is the long-run average of the vacancy filling rate in the historical sample from 1983 to 2023.

Model vs. Data: Variance Decompositions The model successfully replicates the empirical variance decompositions from the data. Figure 9 shows that the model can reproduce the finding that belief distortions drive excess sensitivity to cash flow news in explaining labor market fluctuations, both in the time series and the cross section.

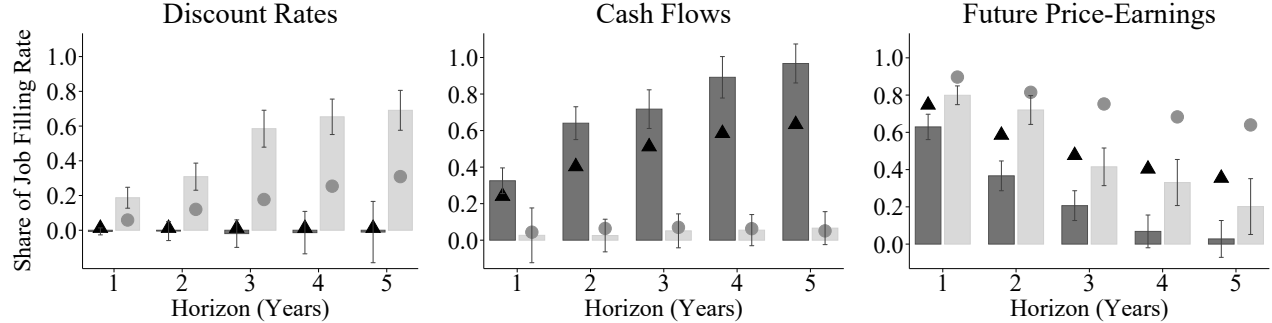
Panel (a) presents the time-series decomposition of the vacancy filling rate, comparing contributions under subjective and rational expectations. The model captures the empirical pattern where subjective expectations (dark bars) assign a larger role to cash flows compared to rational expectations (light bars). The model-implied values (circles and triangles) align closely with the empirical estimates, demonstrating the model's ability to match the data. The large estimated discount rate component under rational beliefs is consistent with existing search models formulated under rational expectations, which have emphasized time-varying discount rates to match the volatility of unemployment fluctuations.

Panel (b) shows the cross-sectional decomposition of hiring rates across firms. Again, the model captures the empirical pattern that subjective belief distortions drive excess sensitivity to cash flow news. This cross-sectional fit is particularly important as it shows that the model can explain not just aggregate patterns but also the heterogeneity in hiring behavior across different firms.

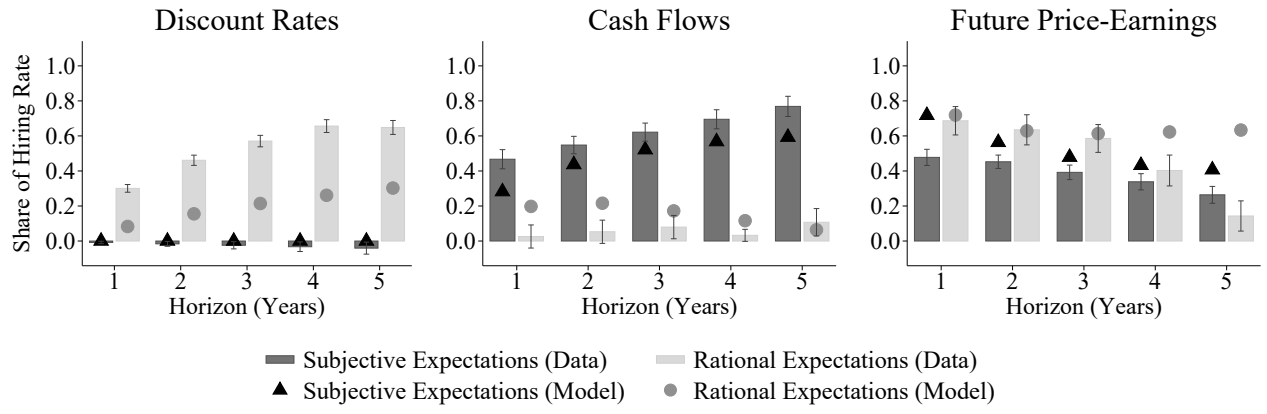
Model vs. Data: Moments Table 2 demonstrates that the constant-gain learning model successfully matches both asset market and labor market moments. The table compares moments generated by the learning model against those generated from a rational model under no learning,

Figure 9: Model vs. Data: Variance Decompositions

(a) Time-Series Decomposition of the Vacancy Filling Rate



(b) Cross-Sectional Decomposition of the Hiring Rate



Notes: Figure illustrates the discount rate, cash flow, and future price-earnings components of the time-series decomposition of the aggregate vacancy filling rate (panel (a)) and cross-sectional decomposition of the hiring rate (panel (b)). Light bars show contributions under rational expectations; dark bars show contributions under subjective expectations. The sample is quarterly from 2005Q1 to 2023Q4. Each bar shows Newey-West 95% confidence intervals with lags = 4. Circle and triangle dots show the values of rational and subjective expectations implied by the model, respectively.

where all agents have full information rational expectations. To generate simulations under the rational model, I employ the same sequence of shocks as in the baseline learning specification but set the learning rate parameter to zero. This eliminates belief updating and, conditional on the true initial values, reduces the model exactly to its rational expectations counterpart.

Panel (a) reports time-series and cross-sectional moments for asset prices. The learning model broadly matches the mean and volatility of price-earnings ratios, the persistence in valuations, and the volatility of returns and expected returns. In contrast, the rational expectations model severely understates price-earnings volatility and generates virtually no variation in expected returns, confirming that belief distortions are essential for matching observed financial market behavior (Adam et al., 2016). For the cross-sectional moments, the learning model captures the dispersion in price-earnings ratios, expected earnings growth, and returns. These moments

Table 2: Model vs. Data: Asset Market and Labor Market Moments

Moment	Data	Learning Model	Rational Model
(a) Asset Market			
$SD(pe_t) \times 100$	47.0	43.5	13.0
$AC(pe_t)$	0.75	0.84	0.92
$SD(r_t) \times 100$	16.0	12.3	3.0
$SD(\mathbb{F}_t[r_{t+1}]) \times 100$	1.1	1.4	0.5
$SD(\mathbb{F}_t[\Delta e_{t+1}]) \times 100$	26.8	24.3	7.2
$SD_i(pe_{i,t}) \times 100$	22.6	21.1	4.2
$SD_i(r_{i,t}) \times 100$	5.7	3.1	1.2
$SD_i(\mathbb{F}_t[r_{i,t+1}]) \times 100$	2.6	0.2	0.2
$SD_i(\mathbb{F}_t[\Delta e_{i,t+1}]) \times 100$	14.0	16.6	3.9
(b) Labor Market			
$SD(u_t) \times 100$	2.10	1.28	0.34
$AC(u_t)$	0.91	0.95	0.99
$SD(q_t) \times 100$	8.70	6.16	0.91
$AC(q_t)$	0.94	0.83	0.99
$Corr(u_t, q_t)$	-0.82	-0.86	-0.99
$SD_i(hl_{i,t}) \times 100$	15.70	10.39	4.65

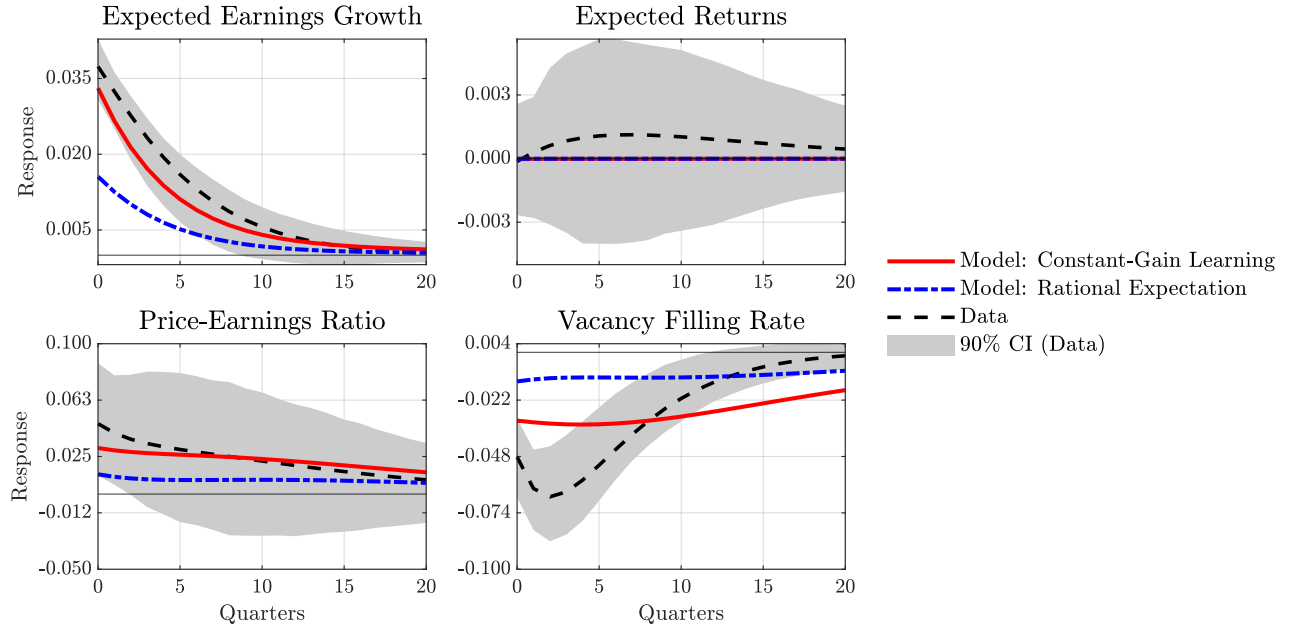
Notes: This table compares empirical moments with model-generated moments with and without constant-gain learning. $SD(\cdot)$ denotes the time-series standard deviation of aggregate variables. $SD_i(\cdot)$ denotes the cross-sectional standard deviation across firms at each point in time, averaged over time. $AC(\cdot)$ denotes the first-order autocorrelation coefficient. $Corr(\cdot)$ denotes the correlation between two time series. pe_t is the log price-earnings ratio, r_t is the log stock return, Δe_t is log earnings growth, q_t is the job-filling rate, u_t is the unemployment rate, and $hl_{i,t}$ is the firm-level hiring rate. $\mathbb{F}_t[\cdot]$ denotes subjective expectations formed at time t . Data column reports empirical moments estimated from historical data. Learning model reports moments from simulations of the constant-gain learning model. Rational model reports moments from the rational expectations benchmark where agents have perfect knowledge of the earnings process.

confirm that the firm-specific beliefs $\mathbb{F}_t[\tilde{\mu}_i]$ can generate realistic heterogeneity in firm valuations and expectations. The rational expectations model, by construction, produces substantially smaller cross-sectional variation in expectations.

Panel (b) reports moments related to the labor market. The constant-gain learning model matches the volatility and persistence of the vacancy filling rate q_t and the unemployment rate u_t better than the rational benchmark. The model explains about 60% of observed U.S. unemployment volatility and cross-sectional hiring dispersion, compared with less than 30% explained by the standard rational search model without time-varying discount rates (Shimer, 2005).³⁷ The learning model's ability to match these moments demonstrates that the constant-gain learning mechanism provides an explanation for both asset market and labor market fluctuations.

³⁷This improvement isolates the contribution of belief distortions in expected cash flows while abstracting from variation in discount rates. Models that incorporate rational expectations of time-varying discount rates, such as Kehoe et al. (2023), can explain up to 95% of unemployment volatility once longer-duration cash flows are introduced, indicating that belief distortions and discount-rate fluctuations are complementary channels in explaining observed labor market dynamics.

Figure 10: Impulse responses to a one standard deviation innovation in expected cash flow growth



Notes: Red solid line: model-based IRFs from simulated series under constant-gain learning. Blue solid line: model-based IRFs from simulated series under rational expectations. Black dashed line: data-based IRFs. Shaded area: 90% bootstrap confidence interval for the data VAR. Sample: 1984Q1-2023Q4.

Response to 1 Std. Dev. Shock to Cash Flow Growth Expectation To examine the dynamic implications of the model and compare them with the data, Figure 10 estimates a four-variable VAR where the observation vector includes expected cash flow growth, expected returns, expected price-earnings, and the job-filling rate. The VAR is estimated using both the actual survey data and the simulated series generated from the model. For identification, I apply a recursive (Cholesky) scheme in which expected cash flow growth is ordered first, so that the estimated impulse responses trace out the effect of a one standard deviation shock to cash flow growth expectations.

The impulse response functions in Figure 10 reveal several notable patterns. Expectations of cash flow growth jump immediately on impact and then gradually decay back toward zero. Subjective expected returns exhibit a flat response consistent with a near constant subjective discount rate. The subjective price-earnings ratio rises initially before decaying back to zero. Finally, the job-filling rate falls immediately after the shock and then slowly converges back to its baseline level.

9 Robustness Checks and Extensions

This section presents additional results that reinforce the main finding. Across multiple robustness checks, the evidence consistently shows that firms overweight expected cash flows and underweight discount rates under subjective expectations.

Predictability of Unemployment and Hiring Section A.5 extends the baseline analysis to the unemployment rate and to firm-level employment growth. Starting from the unemployment accumulation equations, I derive predictive regressions linking future unemployment directly to subjective and rational expectations of discount rates and cash flows. I derive similar predictive firm-level regressions using the employment accumulation equation. Distortions in subjective cash flow expectations emerge as the strongest single predictor both in the time series and the cross section, improving both in-sample fit and out-of-sample performance. In the cross-section, employment growth across firms also loads heavily on cash flow distortions: firms with overly optimistic beliefs hire more aggressively, while those with pessimistic beliefs retrench. These results are not consistent with subjective beliefs being observationally equivalent to rational expectations, and instead point to heterogeneous, distorted forecasts that crowd out rational discount rate variation as the main driver of hiring fluctuations

Decomposition of Price-Earnings Ratios The decomposition of price-earnings ratios developed by De La O and Myers (2021) and De La O et al. (2024) provides a natural benchmark for thinking about distorted beliefs in financial markets. Their analysis applies the Campbell and Shiller (1988) identity to the aggregate price-earnings ratio and shows that subjective expectations systematically underestimate the role of discount rates while overstating the importance of cash flows. In Section A.4, I replicate this exercise using my data and learning model. The resulting decompositions parallel findings for the vacancy filling rate: under rational expectations, most variation in the price-earnings ratio is attributed to discount rate news, while under subjective expectations the weight shifts strongly toward cash flows. The similarity in magnitudes across the two decompositions underscores that they are consistent views of the same underlying belief distortions. The main difference lies in interpretation. The price-earnings decomposition highlights how distorted beliefs manifest in asset valuations, whereas the vacancy filling rate and hiring rate decompositions show how those same distorted beliefs translate into hiring decisions and unemployment fluctuations.

Subjective vs. Risk-Neutral Expectations A natural question is whether subjective beliefs implied by survey expectations reflect a risk-neutral measure rather than genuine belief distortions (Cochrane, 2017). While one might argue that these survey forecasts reflect a risk premium, this interpretation is inconsistent with several lines of evidence.

First, decompositions using risk-neutral expectations implied by futures prices show that subjective expectations overweight long-horizon cash flows even relative to risk-neutral counterparts (Figure A.8). Under rational expectations, any indirect effect of cash flow news on hiring that operates through discount-rate news is allocated to the discount-rate term, while the direct effect appears in the cash flow term. Under subjective beliefs, the cash flow term absorbs much of the variation that, under rational beliefs, would have been attributed to this indirect channel. Importantly, subjective beliefs are not simply a reallocation of the same indirect effect. Comparing survey-based cash flow expectations to a risk-neutral benchmark from futures prices shows that subjective cash flow expectations exert a much stronger influence on hiring than implied by the risk-neutral measure. Risk-neutral expectations from market prices already embed any indirect effect of cash flows on discount rates in asset valuations. The persistent over-weighting of cash flows in survey data therefore points to genuine belief distortions, not just another measure of the same underlying relationships.

Second, survey forecasts of stock returns consistently exceed risk-free rates, and the expected excess returns they imply vary predictably over time (Adam et al., 2021). Moreover, rather than being systematically pessimistic, these forecasts are often predictably optimistic, contradicting the idea that they reflect ambiguity aversion or robustness-driven pessimism. These findings are inconsistent with rational or risk-neutral pricing and suggest that subjective beliefs reflect genuine behavioral distortions rather than a rational risk-neutral measure.

Financial Constraints To assess whether financial frictions confound the decomposition of hiring variation, Figure A.11 controls for five firm-level financial constraint proxies, firm size, payout ratio, the SA index, expected free cash flow, and the Whited-Wu index. Controlling for these measures modestly reduces the contribution of expected earnings to hiring under subjective expectations, but leaves most of the decomposition intact. In contrast, under rational expectations, the contribution of discount rates drops substantially once financial constraints are accounted for, consistent with constraint-induced variation in internal discount rates. These results suggest that while financial frictions matter, distortions in subjective beliefs continue to play an independent role in shaping hiring.

Capital Investment Appendix Section A.9 extends the baseline framework to include firm investment decisions, distinguishing between tangible and intangible capital. Firms choose investment and hiring jointly to maximize value, facing convex adjustment costs and forming expectations over future productivity, returns, and earnings. A decomposition of investment rates in Figures A.15 (time-series) and A.16 (cross-section) reveals that distortions in subjective beliefs play a central role in driving capital allocation, mirroring results for hiring. Using IBES and Compustat data, the decomposition shows that subjective expectations substantially overstate the role of expected earnings and underestimate the importance of discount rates.

Regional Model using Shift-Share Instrument Appendix Section A.8 strengthens the causal interpretation of belief distortions by using a Bartik shift-share instrument to isolate exogenous variation in subjective expectations. Specifically, I interact national industry-level beliefs about future cash flows (and discount rates) with historical state-industry level employment shares. This instrument affects local vacancy filling rates only through its impact on perceived expectations. State-level regressions reveal that subjective forecasts of earnings growth respond strongly to these local shocks, even after controlling for state and time fixed effects, while discount rates respond less (Table A.10). The results confirm that belief distortions, especially overreaction to perceived cash flow opportunities, are not merely correlated with labor demand, but can causally influence hiring decisions across regions.

10 Conclusion

This paper develops a unified framework linking asset valuations and hiring behavior to distortions in firms' beliefs about future cash flows. The framework explains both aggregate fluctuations and cross-sectional dispersion across firms. Using machine learning forecasts as an objective benchmark for rational and efficient belief formation, I document that survey forecasts systematically overreact to cash flow news, while machine forecasts do not. These belief distortions make hiring excessively sensitive to perceived cash flow news, explaining over 60% of variation in both aggregate and firm-level hiring. Firms with distorted beliefs overhire following positive idiosyncratic shocks, reducing realized profits per worker, while rational firms do not.

A search-and-matching model in which firms learn about the long-run mean of their cash flows with fading memory can reproduce these empirical patterns. The learning process generates persistent overreaction to transitory shocks, producing fluctuations in hiring and unemployment that rational models cannot explain. The model accounts for about 60% of observed U.S. unemployment volatility and matches the cross-sectional dispersion in hiring rates across firms.

By overreacting to recent news, firms interpret temporary improvements in cash flows as lasting booms and downturns as protracted slumps, leading to excessive swings in vacancy posting. These findings suggest that the same belief distortions that drive asset price fluctuations also drive volatility in labor demand.

Belief distortions offer a common framework for understanding business cycle fluctuations by linking asset valuations and real activity. Because hiring is a forward-looking decision valued like any other asset, the same behavioral biases that drive asset valuations can also drive fluctuations in hiring, capital investment, R&D spending, and broader business cycle dynamics. Incorporating belief formation into macroeconomic models can therefore improve our understanding of how expectations shape both asset valuations and real economic activity. Exploring these connections across different types of investment decisions remains an important avenue for future research.

These findings have implications for macroeconomic stabilization policy, as firms overhire during booms and underhire during recessions. Because firms overreact to economic conditions, monetary policy can lean against the wind more forcefully to temper excessive optimism, but this same overreaction also calls for cautious state-contingent calibration of interest rate changes to avoid amplifying volatility. Fiscal policy through unemployment insurance may need to be more generous during recessions, as firms' pessimistic overreaction can prolong unemployment spells beyond what true fundamentals justify. Forward guidance and policy communication can help correct distorted beliefs by providing relevant information in a clear and accessible format, anchoring expectations when uncertainty is high. Finally, belief distortions themselves can serve as a practical early-warning indicator for shifts in unemployment and labor demand.

References

- Acharya, Sushant and Shu Lin Wee**, "Rational Inattention in Hiring Decisions," *American Economic Journal: Macroeconomics*, January 2020, 12 (1), 1–40.
- Adam, Klaus, Albert Marcet, and Juan Pablo Nicolini**, "Stock Market Volatility and Learning," *The Journal of Finance*, 2016, 71 (1), 33–82.
- and Stefan Nagel, "Expectations data in asset pricing," in Rüdiger Bachmann, Giorgio Topa, and Wilbert van der Klaauw, eds., *Handbook of Economic Expectations*, Academic Press, 2023, pp. 477–506.
- , Dmitry Matveev, and Stefan Nagel, "Do survey expectations of stock returns reflect risk adjustments?," *Journal of Monetary Economics*, 2021, 117, 723–740.
- Ait-Sahalia, Yacine, Yubo Wang, and Francis Yared**, "Do option markets correctly price the probabilities of movement of the underlying asset?," *Journal of Econometrics*, 2001, 102 (1), 67–110.
- Andreou, Elena, Eric Ghysels, and Andros Kourtellos**, "Should macroeconomic forecasters use daily financial data and how?," *Journal of Business & Economic Statistics*, 2013, 31 (2), 240–251.
- Baker, Scott, Nicholas Bloom, Steven J Davis, and Marco Sammon**, "What triggers stock market jumps?," 2019. Unpublished manuscript, Stanford University.

- Barberis, Nicholas, Andrei Shleifer, and Robert Vishny**, "A model of investor sentiment," *Journal of Financial Economics*, 1998, 49 (3), 307–343.
- Barnichon, Regis**, "Building a composite Help-Wanted Index," *Economics Letters*, 2010, 109 (3), 175–178.
- Bastianello, Francesca, Paul H. Décaire, and Marius Guenzel**, "Mental Models and Financial Forecasts," October 2024. SSRN Working Paper No. 5004839.
- Bauer, Michael D. and Eric T. Swanson**, "An Alternative Explanation for the "Fed Information Effect"," *American Economic Review*, March 2023, 113 (3), 664–700.
- Belo, Frederico, Andres Donangelo, Xiaoji Lin, and Ding Luo**, "What Drives Firms' Hiring Decisions? An Asset Pricing Perspective," *The Review of Financial Studies*, 02 2023. hhad012.
- , **Xiaoji Lin, and Santiago Bazardresch**, "Labor Hiring, Investment, and Stock Return Predictability in the Cross Section," *Journal of Political Economy*, 2014, 122 (1), 129–177.
- Ben-David, Itzhak, John R. Graham, and Campbell R. Harvey**, "Managerial Miscalibration," *The Quarterly Journal of Economics*, 09 2013, 128 (4), 1547–1584.
- Beraja, Martin, Erik Hurst, and Juan Ospina**, "The Aggregate Implications of Regional Business Cycles," *Econometrica*, 2019, 87 (6), 1789–1833.
- Bhandari, Anmol, Jaroslav Borovička, and Paul Ho**, "Survey Data and Subjective Beliefs in Business Cycle Models," *The Review of Economic Studies*, 05 2024, p. rdae054.
- Bianchi, Francesco, Do Lee, Sydney C. Ludvigson, and Sai Ma**, "The Prestakes of Stock Market Investing," 2025. Unpublished manuscript.
- , **Sydney C. Ludvigson, and Sai Ma**, "Belief Distortions and Macroeconomic Fluctuations," *American Economic Review*, July 2022, 112 (7), 2269–2315.
- , **Sydney C Ludvigson, and Sai Ma**, "What Hundreds of Economic News Events Say About Belief Overreaction in the Stock Market," Working Paper 32301, National Bureau of Economic Research April 2024.
- Blei, David M, Andrew Y Ng, and Michael I Jordan**, "Latent dirichlet allocation," *Journal of machine Learning research*, 2003, 3 (Jan), 993–1022.
- Bordalo, Pedro, Nicola Gennaioli, Rafael La Porta, and Andrei Shleifer**, "Diagnostic Expectations and Stock Returns," *The Journal of Finance*, 2019, 74 (6), 2839–2874.
- , — , **Rafael La Porta, and Andrei Shleifer**, "Belief Overreaction and Stock Market Puzzles," *Journal of Political Economy*, 2024, 132 (5), 1450–1484.
- , — , **Matthew OBrien, and Andrei Shleifer**, "Long-Term Expectations and Aggregate Fluctuations," *NBER Macroeconomics Annual*, 2024, 38, 311–347.
- , — , **Yueran Ma, and Andrei Shleifer**, "Overreaction in Macroeconomic Expectations," *American Economic Review*, September 2020, 110 (9), 2748–82.
- Borovickova, Katarina and Jaroslav Borovička**, "Discount Rates and Employment Fluctuations," 2017 Meeting Papers 1428, Society for Economic Dynamics 2017.
- Borusyak, Kirill, Peter Hull, and Xavier Jaravel**, "A Practical Guide to Shift-Share Instruments," *Journal of Economic Perspectives*, February 2025, 39 (1), 181–204.
- Brown, Lawrence D., Andrew C. Call, Michael B. Clement, and Nathan Y. Sharp**, "Inside the "Black Box" of Sell-Side Financial Analysts," *Journal of Accounting Research*, 2015, 53 (1), 1–47.

Bureau of Labor Statistics, “Median tenure with current employer was 3.9 years in January 2024,” *The Economics Daily* 2024.

Bybee, Leland, Bryan T Kelly, Asaf Manela, and Dacheng Xiu, “Business news and business cycles,” Technical Report, National Bureau of Economic Research 2021.

—, —, —, and —, “Business News and Business Cycles,” *The Journal of Finance*, 2024, 79 (5), 3105–3147.

Campbell, John Y. and Robert J. Shiller, “The Dividend-Price Ratio and Expectations of Future Dividends and Discount Factors,” *The Review of Financial Studies*, 1988, 1 (3), 195–228.

Candia, Bernardo, Olivier Coibion, and Yuriy Gorodnichenko, “Communication and the Beliefs of Economic Agents,” Working Paper 27800, National Bureau of Economic Research September 2020.

Chen, Long, Zhi Da, and Xinlei Zhao, “What Drives Stock Price Movements?,” *The Review of Financial Studies*, 02 2013, 26 (4), 841–876.

Chodorow-Reich, Gabriel and Johannes Wieland, “Secular Labor Reallocation and Business Cycles,” *Journal of Political Economy*, 2020, 128 (6), 2245–2287.

— and Loukas Karabarbounis, “The Cyclicalities of the Opportunity Cost of Employment,” *Journal of Political Economy*, 2016, 124 (6), 1563–1618.

Cochrane, John H., “Production-Based Asset Pricing and the Link Between Stock Returns and Economic Fluctuations,” *The Journal of Finance*, 1991, 46 (1), 209–237.

—, “The Dog That Did Not Bark: A Defense of Return Predictability,” *The Review of Financial Studies*, 09 2007, 21 (4), 1533–1575.

Cochrane, John H., “Macro-Finance,” *Review of Finance*, 03 2017, 21 (3), 945–985.

Coibion, Olivier and Yuriy Gorodnichenko, “Information rigidity and the expectations formation process: A simple framework and new facts,” *American Economic Review*, 2015, 105 (8), 2644–78.

—, —, and Saten Kumar, “How Do Firms Form Their Expectations? New Survey Evidence,” *American Economic Review*, September 2018, 108 (9), 2671–2713.

Collin-Dufresne, Pierre, Michael Johannes, and Lars A. Lochstoer, “Parameter Learning in General Equilibrium: The Asset Pricing Implications,” *American Economic Review*, March 2016, 106 (3), 664–98.

Cong, Lin William, Ke Tang, Jingyuan Wang, and Yang Zhang, “Deep Sequence Modeling: Development and Applications in Asset Pricing,” *The Journal of Financial Data Science*, December 2020, 3 (1), 28–42.

Cooper, Rick A., Theodore E. Day, and Craig M. Lewis, “Following the leader: a study of individual analysts’ earnings forecasts,” *Journal of Financial Economics*, 2001, 61 (3), 383–416.

David, Joel M., Lukas Schmid, and David Zeke, “Risk-adjusted capital allocation and misallocation,” *Journal of Financial Economics*, 2022, 145 (3), 684–705.

Décaire, Paul H and John R Graham, “Valuation fundamentals,” Available at SSRN 4951338, 2024.

Dennis, William, “Small Business Credit In a Deep Recession,” Report, NFIB Research Foundation, United States February 2010. Financial Crisis Inquiry Commission (FCIC) Case Series.

Diamond, Peter A., “Wage Determination and Efficiency in Search Equilibrium,” *The Review of Economic Studies*, 04 1982, 49 (2), 217–227.

Donangelo, Andres, “Labor Mobility: Implications for Asset Pricing,” *The Journal of Finance*, 2014, 69 (3), 1321–1346.

- , **François Gourio, Matthias Kehrig, and Miguel Palacios**, “The cross-section of labor leverage and equity returns,” *Journal of Financial Economics*, 2019, 132 (2), 497–518.
- Du, William, Adrian Monninger, Xincheng Qiu, and Tao Wang**, “Perceived Unemployment Risks over Business Cycles,” Staff Working Papers 2025-23, Bank of Canada Aug 2025.
- Elsby, Michael W. L. and Ryan Michaels**, “Marginal Jobs, Heterogeneous Firms, and Unemployment Flows,” *American Economic Journal: Macroeconomics*, January 2013, 5 (1), 1–48.
- Erickson, Timothy and Toni M. Whited**, “Measurement Error and the Relationship between Investment and q ,” *Journal of Political Economy*, 2000, 108 (5), 1027–1057.
- Evans, George W. and Seppo Honkapohja**, *Learning and Expectations in Macroeconomics*, Princeton University Press, 2001.
- Faberman, R. Jason, Andreas I. Mueller, Ayşegül Şahin, and Giorgio Topa**, “Job Search Behavior Among the Employed and Non-Employed,” *Econometrica*, 2022, 90 (4), 1743–1779.
- Fama, Eugene F. and Kenneth R. French**, “A five-factor asset pricing model,” *Journal of Financial Economics*, 2015, 116 (1), 1–22.
- Favilukis, Jack and Xiaoji Lin**, “Wage Rigidity: A Quantitative Solution to Several Asset Pricing Puzzles,” *The Review of Financial Studies*, 08 2015, 29 (1), 148–192.
- Fazzari, Steven, R. Glenn Hubbard, and Bruce Petersen**, “Financing Constraints and Corporate Investment,” *Brookings Papers on Economic Activity*, 1988, 19 (1), 141–206.
- Gaur, Meghana, John R Grigsby, Jonathon Hazell, and Abdoulaye Ndiaye**, “Bonus Question: How Does Flexible Incentive Pay Affect Wage Rigidity?,” Working Paper 31722, National Bureau of Economic Research September 2023.
- Gennaioli, Nicola, Yueran Ma, and Andrei Shleifer**, “Expectations and Investment,” *NBER Macroeconomics Annual*, 2016, 30, 379–431.
- Gertler, Mark and Antonella Trigari**, “Unemployment Fluctuations with Staggered Nash Wage Bargaining,” *Journal of Political Economy*, 2009, 117 (1), 38–86.
- Giglio, Stefano, Matteo Maggiori, Johannes Stroebel, and Stephen Utkus**, “Five Facts about Beliefs and Portfolios,” *American Economic Review*, May 2021, 111 (5), 1481–1522.
- Gormsen, Niels Joachim and Kilian Huber**, “Corporate Discount Rates,” Working Paper 31329, National Bureau of Economic Research 06 2023.
- and —, “Corporate Discount Rates,” *American Economic Review*, June 2025, 115 (6), 2001–49.
- Green, Jeremiah, John R.M. Hand, and X. Frank Zhang**, “The supraview of return predictive signals,” *Review of Accounting Studies*, September 2013, 18 (3), 692–730.
- Greenwood, Robin and Andrei Shleifer**, “Expectations of returns and expected returns,” *The Review of Financial Studies*, 2014, 27 (3), 714–746.
- Gu, Shihao, Bryan Kelly, and Dacheng Xiu**, “Empirical Asset Pricing via Machine Learning,” *The Review of Financial Studies*, 02 2020, 33 (5), 2223–2273.
- Hadlock, Charles J. and Joshua R. Pierce**, “New Evidence on Measuring Financial Constraints: Moving Beyond the KZ Index,” *The Review of Financial Studies*, 03 2010, 23 (5), 1909–1940.
- Hagedorn, Marcus and Iourii Manovskii**, “The Cyclical Behavior of Equilibrium Unemployment and Vacancies Revisited,” *American Economic Review*, September 2008, 98 (4), 1692–1706.

- Hall, Robert E.**, "The Stock Market and Capital Accumulation," *American Economic Review*, December 2001, 91 (5), 1185–1202.
- , "Employment Fluctuations with Equilibrium Wage Stickiness," *American Economic Review*, March 2005, 95 (1), 50–65.
- , "High Discounts and High Unemployment," *American Economic Review*, 2 2017, 107 (2), 305–30.
- and **Paul R. Milgrom**, "The Limited Influence of Unemployment on the Wage Bargain," *American Economic Review*, September 2008, 98 (4), 1653–74.
- Hansen, Lars Peter, John C. Heaton, and Nan Li**, "Intangible Risk," in "Measuring Capital in the New Economy," University of Chicago Press, October 2005.
- Hayashi, Fumio**, "Tobin's Marginal q and Average q: A Neoclassical Interpretation," *Econometrica*, 1982, 50 (1), 213–224.
- Hillenbrand, Sebastian and Odhrain McCarthy**, "Street Earnings: Implications for Asset Pricing," August 2024. Available at SSRN: <https://ssrn.com/abstract=4892475>.
- Jin, Lawrence J. and Pengfei Sui**, "Asset pricing with return extrapolation," *Journal of Financial Economics*, 2022, 145 (2, Part A), 273–295.
- Jäger, Simon, Christopher Roth, Nina Roussille, and Benjamin Schoefer**, "Worker Beliefs About Outside Options*," *The Quarterly Journal of Economics*, 01 2024, 139 (3), 1505–1556.
- Kaas, Leo and Philipp Kircher**, "Efficient Firm Dynamics in a Frictional Labor Market," *American Economic Review*, October 2015, 105 (10), 3030–60.
- Kehoe, Patrick J, Pierlauro Lopez, Virgiliu Midrigan, and Elena Pastorino**, "Asset Prices and Unemployment Fluctuations: A Resolution of the Unemployment Volatility Puzzle," *The Review of Economic Studies*, 08 2023, 90 (3), 1304–1357.
- Kehoe, Patrick J., Virgiliu Midrigan, and Elena Pastorino**, "Debt Constraints and Employment," *Journal of Political Economy*, 2019, 127 (4), 1926–1991.
- Kilic, Mete and Jessica A Wachter**, "Risk, Unemployment, and the Stock Market: A Rare-Event-Based Explanation of Labor Market Volatility," *The Review of Financial Studies*, 01 2018, 31 (12), 4762–4814.
- Kogan, Leonid and Dimitris Papanikolaou**, "Economic Activity of Firms and Asset Prices," *Annual Review of Financial Economics*, 2012, 4 (Volume 4, 2012), 361–384.
- Korniotis, George M.**, "Habit Formation, Incomplete Markets, and the Significance of Regional Risk for Expected Returns," *The Review of Financial Studies*, 08 2008, 21 (5), 2139–2172.
- Kothari, S.P., Eric So, and Rodrigo Verdi**, "Analysts' Forecasts and Asset Pricing: A Survey," *Annual Review of Financial Economics*, 2016, 8 (Volume 8, 2016), 197–219.
- Krusell, Per, Toshihiko Mukoyama, Richard Rogerson, and Aysegül Sahin**, "Gross Worker Flows over the Business Cycle," *American Economic Review*, November 2017, 107 (11), 3447–76.
- Kudlyak, Marianna**, "The cyclicalities of the user cost of labor," *Journal of Monetary Economics*, 2014, 68, 53–67.
- Kuehn, Lars-Alexander, Mikhail Simutin, and Jessie Jiaxu Wang**, "A Labor Capital Asset Pricing Model," *The Journal of Finance*, 2017, 72 (5), 2131–2178.
- Kuhn, Moritz, Iourii Manovskii, and Xincheng Qiu**, "The Geography of Job Creation and Job Destruction," Working Paper 29399, National Bureau of Economic Research October 2021.

- Lettau, Martin and Sydney Ludvigson**, “Time-varying risk premia and the cost of capital: An alternative implication of the Q theory of investment,” *Journal of Monetary Economics*, 2002, 49 (1), 31–66.
- Lewellen, Jonathan and Katharina Lewellen**, “Investment and Cash Flow: New Evidence,” *The Journal of Financial and Quantitative Analysis*, 2016, 51 (4), 1135–1164.
- Lintner, John**, “Distribution of Incomes of Corporations Among Dividends, Retained Earnings, and Taxes,” *The American Economic Review*, 1956, 46 (2), 97–113.
- Liu, Yukun**, “Labor-based asset pricing,” *SSRN*, 2021.
- Ljungqvist, Lars and Thomas J. Sargent**, “The Fundamental Surplus,” *American Economic Review*, September 2017, 107 (9), 2630–65.
- Ludvigson, Sydney C. and Serena Ng**, “The empirical risk-return relation: A factor analysis approach,” *Journal of Financial Economics*, January 2007, 83 (1), 171–222.
- Ma, Yueran, Tiziano Ropele, David Sraer, and David Thesmar**, “A Quantitative Analysis of Distortions in Managerial Forecasts,” Working Paper 26830, National Bureau of Economic Research March 2020.
- Malmendier, Ulrike and Stefan Nagel**, “Learning from Inflation Experiences,” *The Quarterly Journal of Economics*, 10 2015, 131 (1), 53–87.
- Manning, Alan and Barbara Petrongolo**, “How Local Are Labor Markets? Evidence from a Spatial Job Search Model,” *American Economic Review*, October 2017, 107 (10), 2877–2907.
- Marcat, Albert and Thomas J Sargent**, “Convergence of least squares learning mechanisms in self-referential linear stochastic models,” *Journal of Economic Theory*, 1989, 48 (2), 337–368.
- Meeuwis, Maarten, Dimitris Papanikolaou, Jonathan L Rothbaum, and Lawrence D.W. Schmidt**, “Time-Varying Risk Premia, Labor Market Dynamics, and Income Risk,” Working Paper 31968, National Bureau of Economic Research December 2023.
- Menzio, Guido**, “Stubborn Beliefs in Search Equilibrium,” *NBER Macroeconomics Annual*, 2023, 37, 239–297.
- Merz, Monika and Eran Yashiv**, “Labor and the Market Value of the Firm,” *American Economic Review*, September 2007, 97 (4), 1419–1431.
- Mitra, Indrajit and Yu Xu**, “Time-Varying Risk Premium and Unemployment Risk across Age Groups,” *The Review of Financial Studies*, 10 2019, 33 (8), 3624–3673.
- Mortensen, Dale T.**, “The Matching Process as a Noncooperative Bargaining Game,” in “The Economics of Information and Uncertainty” NBER Chapters, National Bureau of Economic Research, Inc, May 1982, pp. 233–258.
- Mueller, Andreas I., Johannes Spinnewijn, and Giorgio Topa**, “Job Seekers’ Perceptions and Employment Prospects: Heterogeneity, Duration Dependence, and Bias,” *American Economic Review*, January 2021, 111 (1), 324–63.
- Nagel, Stefan**, *Machine Learning in Asset Pricing*, Vol. 8, Princeton University Press, 2021.
- and **Zhengyang Xu**, “Asset Pricing with Fading Memory,” *The Review of Financial Studies*, 08 2021, 35 (5), 2190–2245.
- and —, “Dynamics of Subjective Risk Premia,” Working Paper 29803, National Bureau of Economic Research 2 2022.
- O, Ricardo De La and Sean Myers**, “Subjective Cash Flow and Discount Rate Expectations,” *The Journal of Finance*, 2021, 76 (3), 1339–1387.

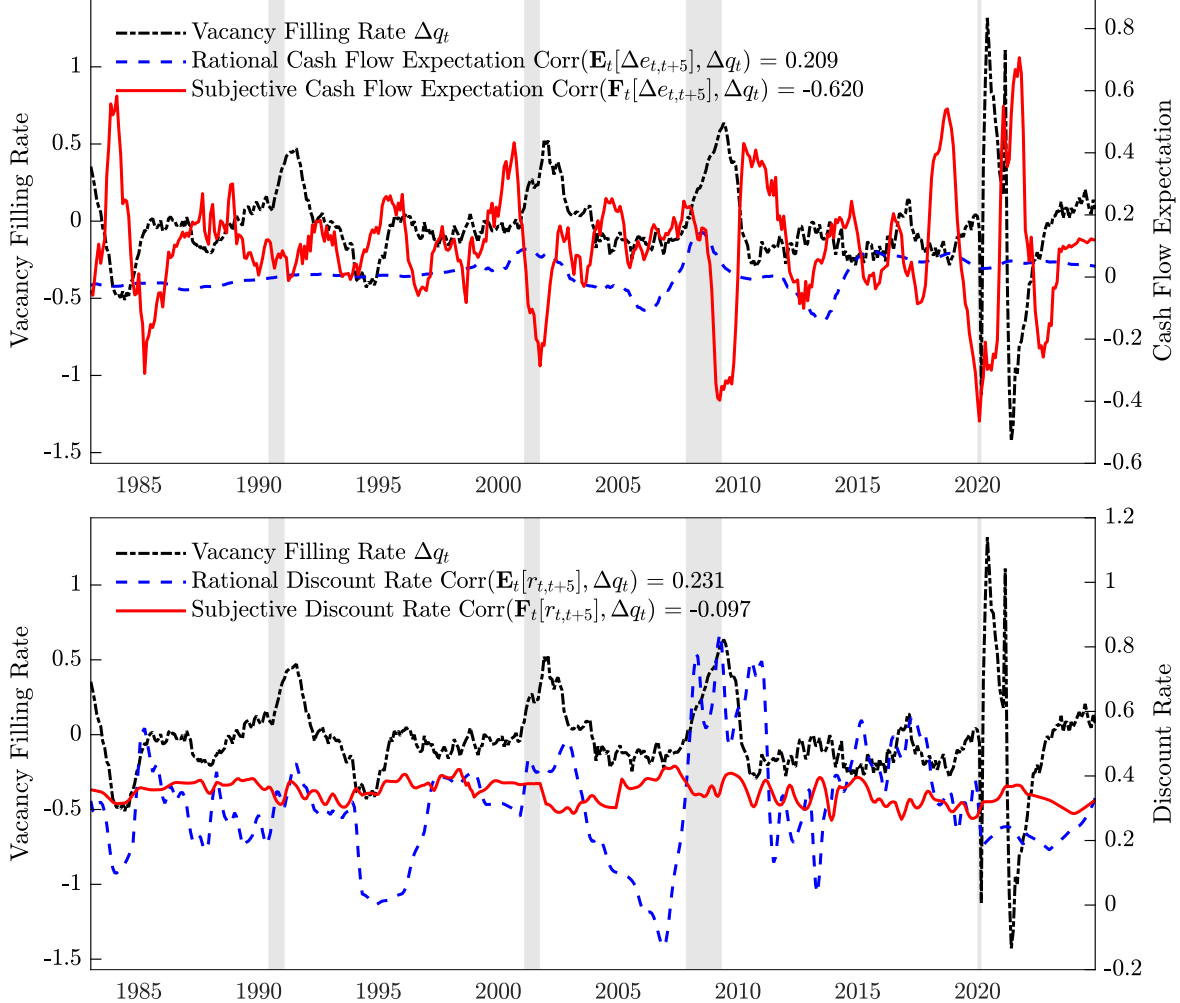
- , **Xiao Han, and Sean Myers**, “The Cross-section of Subjective Expectations: Understanding Prices and Anomalies,” *SSRN*, 2024.
- Petrosky-Nadeau, Nicolas, Lu Zhang, and Lars-Alexander Kuehn**, “Endogenous Disasters,” *American Economic Review*, 8 2018, 108 (8), 2212–45.
- Pissarides, Christopher A.**, “The Unemployment Volatility Puzzle: Is Wage Stickiness the Answer?,” *Econometrica*, 2009, 77 (5), 1339–1369.
- Ropele, Tiziano, Yuriy Gorodnichenko, and Olivier Coibion**, “Inflation Expectations and Misallocation of Resources: Evidence from Italy,” *American Economic Review: Insights*, June 2024, 6 (2), 246–61.
- Shimer, Robert**, “The Cyclical Behavior of Equilibrium Unemployment and Vacancies,” *American Economic Review*, 3 2005, 95 (1), 25–49.
- , “Reassessing the ins and outs of unemployment,” *Review of Economic Dynamics*, 2012, 15 (2), 127–148.
- Solon, Gary, Robert Barsky, and Jonathan A. Parker**, “Measuring the Cyclicity of Real Wages: How Important is Composition Bias,” *The Quarterly Journal of Economics*, 1994, 109 (1), 1–25.
- Timmermann, Allan G.**, “How Learning in Financial Markets Generates Excess Volatility and Predictability in Stock Prices,” *The Quarterly Journal of Economics*, 1993, 108 (4), 1135–1145.
- Venkateswaran, Venky**, “Heterogeneous information and labor market fluctuations,” Available at SSRN 2687561, 2014.
- Vuolteenaho, Tuomo**, “What Drives Firm-Level Stock Returns?,” *The Journal of Finance*, 2002, 57 (1), 233–264.
- Whited, Toni M. and Guojun Wu**, “Financial Constraints Risk,” *The Review of Financial Studies*, 01 2006, 19 (2), 531–559.

A Appendix: Additional Results

A.1 Stylized Facts

Vacancy filling rate, discount rate, and expected cash flows Figure A.1 compares subjective and machine expectations for discount rates and cash flows, plotted against the vacancy filling rate. These series represent the specific theoretical components that drive hiring decisions in the search model.

Figure A.1: Vacancy Filling Rates, Discount Rates, and Expected Cash Flows



Notes: Figure plots $h = 5$ year ahead survey forecasts $\mathbb{F}_t[\cdot]$ and machine learning forecasts $\mathbb{E}_t[\cdot]$ of discount rates $r_{t,t+h}$ and annual cash flow growth $\Delta e_{t,t+h}$ (left axis) against the annual log growth in the vacancy filling rate q_t (right axis). x axis denotes the date on which each forecast has been made and the vacancy filling rate was realized. Subjective expectations \mathbb{F}_t are based on survey forecasts from the CFO survey for stock returns, and IBES for earnings growth. Machine expectations are based on machine learning forecasts \mathbb{E}_t from Long Short-Term Memory (LSTM) neural networks $G(\mathcal{X}_t, \beta_{h,t})$, whose parameters $\beta_{h,t}$ are estimated in real time using \mathcal{X}_t , a large scale dataset of macroeconomic, financial, and textual data. The out-of-sample forecast testing period is quarterly and spans 2005Q1 to 2023Q4. NBER recessions are shown with gray shaded bars.

Machine expectations of discount rates exhibit a strong positive relationship with vacancy filling rates, particularly around the Global Financial Crisis. This pattern aligns with the theoretical prediction that higher discount rates (reflecting greater compensation for risk) should coincide with lower hiring as firms perceive a lower present discounted value of employment. Survey expectations of discount rates, by contrast, are relatively flat and display little sensitivity to the business cycle, consistent with studies that find acyclical subjective risk premia (Nagel and Xu, 2022).

For cash flows, the pattern reverses. Survey expectations show exaggerated cyclical variation, becoming sharply pessimistic during downturns, such as the Global Financial Crisis, when vacancy filling rates are high. Machine forecasts also vary cyclically but to a much lesser extent, indicating that survey respondents tend to overreact to macroeconomic conditions when forming cash flow expectations. This overreaction manifests in the decomposition as an outsized role for

subjective cash flow news in explaining vacancy filling rate variation, even when a model under rational beliefs suggests that discount rate changes should be the primary driver of hiring fluctuations.

Summary Statistics Appendix Table A.1 summarizes the distributions of survey-based and machine learning forecasts for the key components of the variance decomposition. The most notable pattern is the contrast in time-series volatility and cross-sectional dispersion between the two sources of expectations. In the time series, 5-year survey-based discount rate expectations $\mathbb{F}_t[r_{t,t+5}]$ are substantially less volatile than machine forecasts, with standard deviations of 0.037 and 0.118, respectively. In contrast, 5-year survey-based cash flow expectations $\mathbb{F}_t[e_{t,t+5}]$ exhibit much higher volatility than machine forecasts, with standard deviations of 0.299 and 0.058, respectively.

Table A.1: Summary statistics

	Obs	Mean	St. Dev.	Min	p25	Median	p75	Max
$r_{t,t+5}$	72	0.284	0.283	-0.279	0.131	0.330	0.464	0.789
$\mathbb{F}_t[r_{t,t+5}]$	72	0.226	0.037	0.147	0.195	0.229	0.251	0.327
$\mathbb{E}_t[r_{t,t+5}]$	72	0.287	0.118	0.036	0.209	0.284	0.362	0.572
$e_{t,t+5}$	72	3.739	0.300	2.353	3.741	3.777	3.905	4.288
$\mathbb{F}_t[e_{t,t+5}]$	72	3.908	0.299	3.264	3.768	3.892	4.101	4.423
$\mathbb{E}_t[e_{t,t+5}]$	72	3.801	0.058	3.704	3.763	3.793	3.823	3.936
pe_{t+5}	72	3.553	0.294	3.084	3.332	3.527	3.642	4.594
$\mathbb{F}_t[pe_{t,t+5}]$	72	3.654	0.146	3.321	3.537	3.686	3.761	3.925
$\mathbb{E}_t[pe_{t,t+5}]$	72	3.603	0.284	2.864	3.408	3.590	3.803	4.208
q_t	72	0.596	0.236	0.211	0.408	0.587	0.731	1.202
U_t	72	0.061	0.021	0.036	0.046	0.054	0.078	0.130
θ_t	72	0.598	0.315	0.160	0.339	0.558	0.747	1.438
δ_t	72	0.350	0.058	0.265	0.316	0.354	0.370	0.689

Notes: This table reports summary statistics for ex-post realized outcomes (Actual), subjective expectations (Survey), and machine expectations (Machine) of key variables used in the variance decomposition. The forecasted variables are $h = 5$ year present discounted values of discount rates $r_{t,t+h}$, cash flows $e_{t,t+h}$, and price-earnings ratios $pe_{t,t+h}$, as defined in equation (16). Aggregate labor market variables include the vacancy filling rate q_t , unemployment rate U_t , vacancy-to-unemployment ratio θ_t , and job separation rate δ_t . Portfolio-level variables are constructed by aggregating employment and forecast data across firms within each book-to-market group, holding portfolio assignment fixed at the time of portfolio formation. Subjective expectations at the aggregate level \mathbb{F}_t are based on survey forecasts from the CFO survey for stock returns and from IBES for earnings growth. Subjective expectations at the portfolio level \mathbb{F}_t are based on survey forecasts from the IBES survey for both stock returns and earnings growth. Machine expectations \mathbb{E}_t are based on forecasts from Long Short-Term Memory (LSTM) neural networks $G(\mathcal{X}_t, \beta_{h,t})$, where parameters $\beta_{h,t}$ are estimated in real time using \mathcal{X}_t , a large-scale dataset of macroeconomic, financial, and textual data. The sample is quarterly and spans 2005Q1 to 2023Q4.

A.2 Variance Decomposition of Vacancy Filling Rate

A.2.1 Baseline Specification

Table A.2 reports a variance decomposition of the aggregate vacancy filling rate based on equation (21). Under rational expectations, discount rate fluctuations explain the largest share of variation, accounting for 69.1% at the five-year horizon. Under subjective expectations, cash flow beliefs dominate at all horizons, accounting for 96.7% in the five-year horizon.

Table A.2: Time-Series Decomposition of the Vacancy Filling Rate

Horizon h (Years)	1	2	3	4	5
(a) Rational Expectations: $\log q_t = c_q + \mathbb{E}_t[r_{t,t+h}] - \mathbb{E}_t[e_{t,t+h}] - \mathbb{E}_t[pe_{t,t+h}]$					
Discount Rate	0.187***	0.309***	0.585***	0.653***	0.691***
t -stat	(3.310)	(4.708)	(5.977)	(6.974)	(6.659)
(-) Cash Flow	0.027	0.026	0.051	0.055	0.066
t -stat	(0.090)	(0.181)	(0.364)	(0.459)	(0.472)
(-) Price-Earnings	0.799***	0.720***	0.415***	0.331***	0.201**
t -stat	(5.620)	(4.322)	(3.332)	(2.845)	(1.716)
Residual	-0.013	-0.054	-0.051	-0.039	0.042
t -stat	(-0.030)	(-0.141)	(-0.076)	(-0.046)	(0.049)
N	76	76	76	76	76
(b) Subjective Expectations: $\log q_t = c_q + \mathbb{F}_t[r_{t,t+h}] - \mathbb{F}_t[e_{t,t+h}] - \mathbb{F}_t[pe_{t,t+h}]$					
Discount Rate	-0.007	-0.005	-0.019	-0.014	-0.010
t -stat	(-0.457)	(-0.130)	(-0.400)	(-0.157)	(-0.091)
(-) Cash Flow	0.325***	0.641***	0.717***	0.892***	0.967***
t -stat	(3.939)	(4.500)	(4.661)	(5.572)	(7.097)
(-) Price-Earnings	0.629***	0.366***	0.206***	0.068	0.028
t -stat	(8.383)	(4.231)	(2.896)	(0.701)	(0.313)
Residual	0.052	-0.002	0.096	0.054	0.015
t -stat	(0.186)	(-0.008)	(0.292)	(0.126)	(0.039)
N	76	76	76	76	76

Notes: This table reports variance decompositions of the aggregate vacancy filling rate under rational expectations (panel (a)) or subjective expectations (panel (b)). Each row reports the share of the variation in vacancy filling rates that can be explained by h -year expected present discounted values of discount rates $r_{t,t+h}$, (negative) cash flows $e_{t,t+h}$, and (negative) price-earnings ratios $pe_{t,t+h}$, as defined in equation (16). Residual term represents the variation in vacancy filling rates that are not captured by the other components. Positive numbers in the Cash Flow and Price-Earnings rows represent the negative of the regression coefficients, ensuring that all variance shares are positive and sum to unity. Subjective expectations \mathbb{F}_t are based on survey forecasts of CFOs and IBES financial analysts. Rational expectations \mathbb{E}_t are based on machine learning forecasts from Long Short-Term Memory (LSTM) neural networks. The sample is quarterly from 2005Q1 to 2023Q4. Newey-West corrected t -statistics with lags = 4 are reported in parentheses: *sig. at 10%. **sig. at 5%. ***sig. at 1%.

A.2.2 Role of Model Misspecification and Approximation Errors

This section extends the variance decompositions by allowing for two residual sources: (i) approximation errors arising from the Campbell and Shiller (1988) log-linearization, and (ii) misspecification errors that stem from simplifying assumptions in the search model, such as ignoring firing costs or endogenous separations.

Campbell-Shiller residual For any horizon $h \geq 1$,

$$pe_t = \sum_{j=1}^h \rho^{j-1} (c_{pe} + \mathbb{F}_t[\Delta e_{t+j}] - \mathbb{F}_t[r_{t+j}]) + \rho^h \mathbb{F}_t[pe_{t+h}] + v_{t,h}^{CS}, \quad (\text{A.1})$$

where $\rho \in (0, 1)$ is the log-linearization constant. $v_{t,h}^{CS}$ captures any approximation errors from the log-linearization and allows for the possibility that the Campbell-Shiller present value identity may be misspecified under subjective beliefs.

Search-model residual To allow for model misspecification in the hiring condition, such as layoff frictions or deviations from constant returns in production and matching, I add a separate residual $v_{t,h}^M$:

$$\log q_t = c_q + \mathbb{F}_t[r_{t,t+h}] - \mathbb{F}_t[e_{t,t+h}] - \mathbb{F}_t[pe_{t,t+h}] - \underbrace{v_{t,h}^{CS}}_{\substack{\text{Campbell-Shiller} \\ \text{Residual}}} - \underbrace{v_{t,h}^M}_{\substack{\text{Search Model} \\ \text{Residual}}}, \quad (\text{A.2})$$

where $v_{t,h}^M$ captures deviations between the observed vacancy-filling rate and the theoretical expression implied by the baseline search model. For instance, if firing frictions create an option value of waiting to hire, firms may be more reluctant to fill vacancies than the baseline model suggests, an effect that would be captured by $v_{t,h}^M$.

Variance decomposition with residuals With both residuals included, the variance decomposition becomes

$$1 = \underbrace{\frac{\text{Cov}(\mathbb{F}_t[r_{t,t+h}], \log q_t)}{\text{Var}(\log q_t)}}_{\text{Discount Rate News}} - \underbrace{\frac{\text{Cov}(\mathbb{F}_t[e_{t,t+h}], \log q_t)}{\text{Var}(\log q_t)}}_{\text{Cash Flow News}} - \underbrace{\frac{\text{Cov}(\mathbb{F}_t[pe_{t,t+h}], \log q_t)}{\text{Var}(\log q_t)}}_{\text{Future Price-Earnings News}} - \underbrace{\frac{\text{Cov}(v_{t,h}^{CS}, \log q_t)}{\text{Var}(\log q_t)}}_{\substack{\text{Campbell-Shiller Residual}}} - \underbrace{\frac{\text{Cov}(v_{t,h}^M, \log q_t)}{\text{Var}(\log q_t)}}_{\substack{\text{Search Model Residual}}}.$$

The cross-sectional decomposition for $\tilde{hl}_{i,t}$ from equation (7) includes analogous residuals $\tilde{v}_{i,t,h}^{CS}$ and $\tilde{v}_{i,t,h}^M$. In all figures and tables, we report the two residual components separately: the Campbell-Shiller residual reflects approximation noise from the log-linearization, while the model residual captures specification errors in the underlying search model.

Table A.3 shows that both residual components are approximately orthogonal to the main decomposition terms, indicating that neither materially distorts the attribution. Time-series and cross-sectional correlations remain small, confirming that approximation and misspecification errors do not drive the main results.

Table A.3: Correlation with Residual Terms from Regression Coefficients

Component	Campbell–Shiller Residual		Search Model Residual	
	Rational	Subjective	Rational	Subjective
(a) Time-Series				
Current Price–Earnings pe_t	0.001	0.007	0.010	0.170
Vacancy Filling Rate $\log q_t$	-0.003	0.010	-0.018	0.051
Discount Rate $\mathbb{F}_t[r_{t,t+5}]$	-0.002	0.009	-0.074	-0.155
Cash Flow $\mathbb{F}_t[e_{t,t+5}]$	-0.013	-0.002	0.046	0.048
Future Price–Earnings $\mathbb{F}_t[pe_{t,t+5}]$	-0.002	0.031	-0.024	-0.127
(b) Cross-Section				
Current Price–Earnings $pe_{i,t}$	-0.001	-0.000	0.005	0.001
Vacancy Filling Rate $\log q_{i,t}$	0.000	-0.002	-0.036	-0.128
Discount Rate $\mathbb{F}_t[r_{i,t,t+5}]$	-0.002	0.014	-0.079	-0.112
Cash Flow $\mathbb{F}_t[e_{i,t,t+5}]$	-0.022	-0.002	-0.033	0.034
Future Price–Earnings $\mathbb{F}_t[pe_{i,t,t+5}]$	0.002	0.053	0.014	0.130

Notes: This table reports correlations between residuals and decomposition components under both rational and subjective beliefs. The Campbell–Shiller residual ($v_{t,h}^{CS}$) captures log-linearization and measurement errors in the price–earnings decomposition. The search-model residual ($v_{t,h}^M$) captures deviations from the baseline search model, such as omitted firing costs or endogenous separations. Time-series correlations use aggregate data; cross-sectional correlations use firm-level deviations from time- t means.

A.2.3 Belief Distortions and Vacancy Filling Rate

To directly quantify the importance of belief distortions in subjective beliefs, I consider predictive regressions of belief distortions in subjective expectations of discount rates, cash flows, and price-earnings ratios on the vacancy filling rate. I define the belief distortion as the difference between subjective and machine expectations. Table A.4 reports estimates $\beta_{1,B}$ from regressing belief distortions in subjective discount rate, cash flow, and log price-earnings expectations on the vacancy filling rate:

$$\mathbb{F}_t[y_{t+h}] - \mathbb{E}_t[y_{t+h}] = \beta_{0,B} + \beta_{1,B} \log q_t + \varepsilon_{t,B}, \quad y = r, e, pe$$

The results indicate that distortions in survey forecasts are important contributors to fluctuations in vacancy filling rates, especially at longer horizons. At the five-year horizon, distortions in cash flow expectations lead survey respondents to over-weight 90.1% of the variation in vacancy filling rates to the cash flow component. This mis-perception is counteracted by distortions in subjective discount rate expectations, which leads survey respondents to under-weight 70.1% of the variation in the vacancy filling rate. These findings emphasize the importance of belief distortions in driving labor market fluctuations. The profile of the response across forecast horizons is broadly consistent with the profile of the MSE ratios across horizons in Figure 2. For discount rate and cash flow expectations, the machine outperformed the survey by a wider margin over longer horizons, suggesting that the belief distortions in survey responses likely play a bigger role over these longer horizons.

Table A.4: Belief Distortions in Subjective Beliefs and the Vacancy Filling Rate

Horizon h (Years)	1	2	3	4	5
Belief Distortions: $\mathbb{F}_t[y_{t+h}] - \mathbb{E}_t[y_{t+h}] = \beta_{0,B} + \beta_{1,B} \log q_t + \varepsilon_{t,B}$, $y = r, e, pe$					
Discount Rate	-0.194	-0.313**	-0.604***	-0.667***	-0.701***
t -stat	(-1.574)	(-2.167)	(-2.896)	(-2.918)	(-2.740)
(-) Cash Flow	0.299	0.615***	0.666***	0.837***	0.901***
t -stat	(1.421)	(5.476)	(5.703)	(7.365)	(6.665)
(-) Price-Earnings	-0.170	-0.354**	-0.209	-0.262	-0.174
t -stat	(-0.464)	(-2.373)	(-0.503)	(-0.479)	(-0.292)
Residual	-0.065	-0.052	-0.147	-0.093	0.026
t -stat	(-0.148)	(-0.219)	(-0.306)	(-0.154)	(0.040)
N	76	76	76	76	76

Notes: This table reports estimates $\beta_{1,B}$ from regressing the survey belief distortion $\mathbb{F}_t[y_{t+h}] - \mathbb{E}_t[y_{t+h}]$ on the vacancy filling rate q_t . y_{t+h} denotes the dependent variable of type j to be predicted h years ahead of time t . The components of the decomposition are h -year present discounted values of discount rates $r_{t,t+h}$, (negative) cash flows $e_{t,t+h}$, and (negative) price-earnings ratios $pe_{t,t+h}$. The residual term captures variation in the vacancy filling rate that cannot be explained by the three components. Subjective expectations \mathbb{F}_t are based on survey forecasts from the CFO survey for stock returns, and IBES for earnings growth. Machine expectations are based on machine learning forecasts \mathbb{E}_t from Long Short-Term Memory (LSTM) neural networks $G(\mathcal{X}_t, \beta_{h,t})$, whose parameters $\beta_{h,t}$ are estimated in real time using \mathcal{X}_t , a large scale dataset of macroeconomic, financial, and textual data. The belief distortion is defined as the difference between subjective and machine expectations: $\mathbb{F}_t - \mathbb{E}_t$. The sample is quarterly from 2005Q1 to 2023Q4. Newey-West corrected t -statistics with lags = 4 are reported in parentheses: *sig. at 10%. **sig. at 5%. ***sig. at 1%.

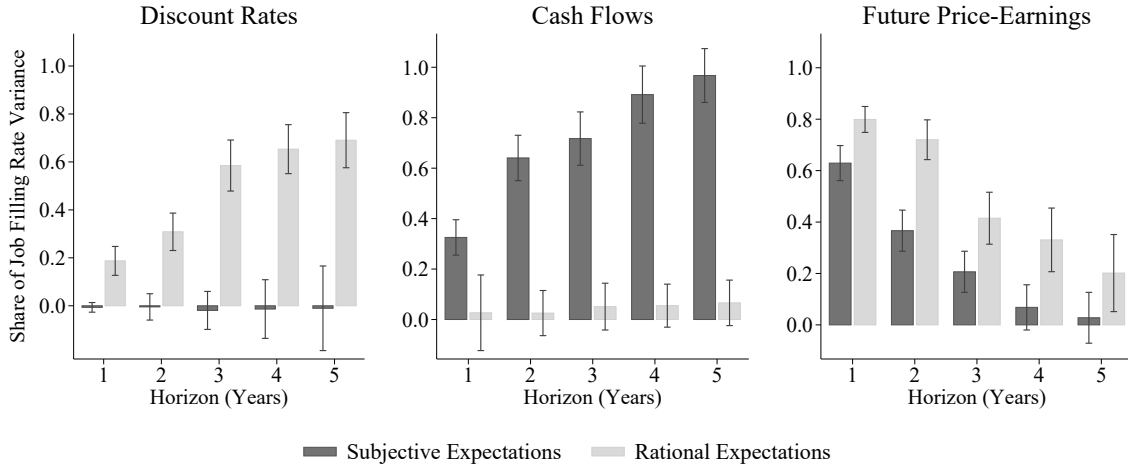
A.2.4 First Differences

The decomposition in equation (21) may be more accurate in first differences than in levels, as low-frequency variation in the vacancy filling rate or subjective expectations can introduce measurement error. This concern is similar to the argument in Cochrane (1991), who points to low-frequency changes in fundamentals as a potential source of measurement error in the context of the q -theory of investment. Figure A.2 estimates the variance decomposition of the vacancy filling rate from equation (21) in first differences:

$$\begin{aligned}\Delta \log q_t &= \Delta \mathbb{E}_t[r_{t,t+h}] - \Delta \mathbb{E}_t[e_{t,t+h}] - \Delta \mathbb{E}_t[pe_{t,t+h}] \\ \Delta \log q_t &= \Delta \mathbb{F}_t[r_{t,t+h}] - \Delta \mathbb{F}_t[e_{t,t+h}] - \Delta \mathbb{F}_t[pe_{t,t+h}]\end{aligned}$$

Under rational expectations, discount rate fluctuations explain the largest share of variation, accounting for 58.7% at the five-year horizon. Under subjective expectations, cash flow beliefs dominate, accounting for 90.6% at the five-year horizon.

Figure A.2: Variance Decomposition of Vacancy Filling Rate: First Differences



Notes: Figure reports variance decompositions of the aggregate vacancy filling rate in first differences. Each panel reports the share of the variation in vacancy filling rates that can be explained by h -year expected present discounted values of discount rates $r_{t,t+h}$, (negative) cash flows $e_{t,t+h}$, and (negative) price-earnings ratios $pe_{t,t+h}$, as defined in equation (16). Light (dark) bars show the contribution under rational (subjective) expectations. Subjective expectations \mathbb{F}_t are based on survey forecasts of CFOs and IBES financial analysts. Rational expectations \mathbb{E}_t are based on machine learning forecasts from Long Short-Term Memory (LSTM) neural networks. The sample is quarterly from 2005Q1 to 2023Q4. Each bar shows Newey-West 95% confidence intervals with lags = 4 quarters.

A.2.5 VAR Estimates

To validate the robustness of the variance decompositions, I estimate a Vector Autoregression (VAR) for the log vacancy filling rate $\log q_t$ and its forward-looking components under subjective or rational expectations. For the case of subjective beliefs, the VAR is estimated using survey expectations for future returns, earnings growth, and price-earnings ratios:

$$X_{t+1} = AX_t + \varepsilon_{t+1}, \quad X_t = [\mathbb{F}_t[r_{t,t+1}] \quad \mathbb{F}_t[e_{t,t+1}] \quad \mathbb{F}_t[pe_{t,t+1}] \quad \log q_t]'$$

From the theoretical framework in Section 5, the log vacancy filling rate can be decomposed as:

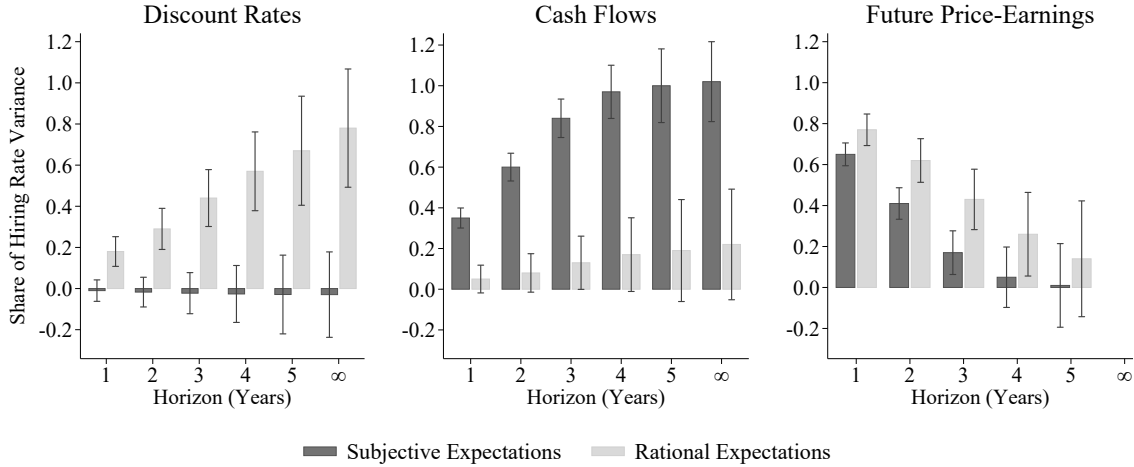
$$\log q_t = c_q + \mathbb{F}_t[r_{t,t+h}] - \mathbb{F}_t[e_{t,t+h}] - \rho^h \mathbb{F}_t[pe_{t+h}]$$

where the expected present values $\mathbb{F}_t[r_{t,t+h}]$ and $\mathbb{F}_t[e_{t,t+h}]$ are constructed recursively using the VAR forecast. As $h \rightarrow \infty$, the terminal value $\rho^h \mathbb{F}_t[pe_{t+h}]$ converges to zero under a transversality condition, yielding the long-run decomposition:

$$\log q_t = c_q + \mathbb{F}_t[r_{t,t+\infty}] - \mathbb{F}_t[e_{t,t+\infty}].$$

The same procedure is repeated using machine learning forecasts $\mathbb{E}_t[\cdot]$ to obtain the decomposition under rational expectations. Figure A.3 reports variance shares across horizons $h = 1$ to $h = 5$, as well as the full-horizon case $h = \infty$. Under rational expectations, discount rate fluctuations explain an increasing share of variation, rising to 78.1% at long horizons. Under subjective expectations, cash flow beliefs dominate at all horizons, accounting for 102.0% in the long run.

Figure A.3: Variance Decomposition of Vacancy Filling Rate: VAR Estimates



Notes: Figure reports variance decompositions of the aggregate vacancy filling rate based on a Vector Autoregression (VAR). Each panel reports the share of the variation in vacancy filling rates that can be explained by h -year expected present discounted values of discount rates $r_{t,t+h}$, (negative) cash flows $e_{t,t+h}$, and (negative) price-earnings ratios $pe_{t,t+h}$, as defined in equation (16). Light (dark) bars show the contribution under rational (subjective) expectations. Subjective expectations \mathbb{F}_t are based on survey forecasts of CFOs and IBES financial analysts. Rational expectations \mathbb{E}_t are based on machine learning forecasts from Long Short-Term Memory (LSTM) neural networks. The sample is quarterly from 2005Q1 to 2023Q4. Each bar shows bootstrapped 95% confidence intervals.

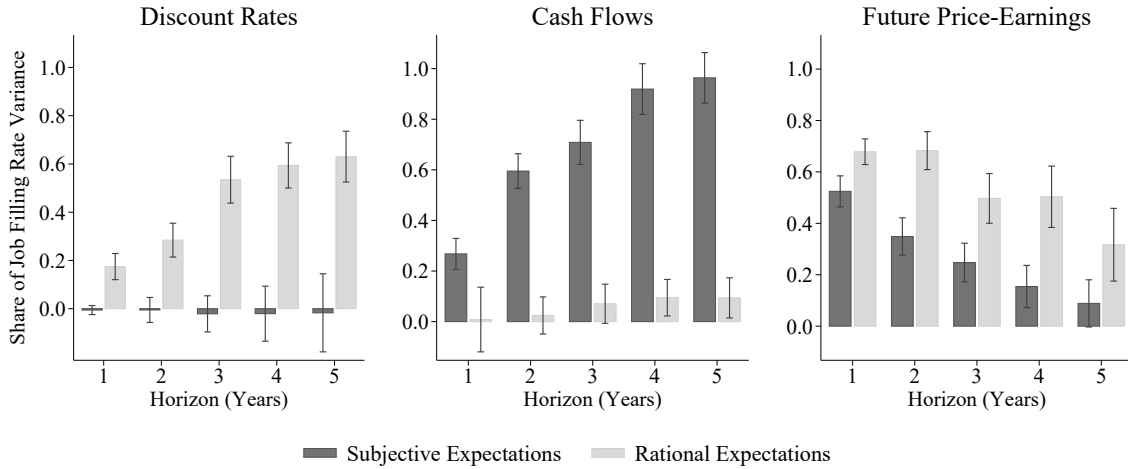
A.2.6 All Listed Firms

Figure A.4 reports the variance decomposition of the vacancy filling rate from equation (21) using an expanded definition of subjective expectations that includes all publicly listed firms with IBES analyst coverage, rather than restricting to the S&P 500. Subjective cash flow expectations are computed as value-weighted aggregates of IBES median forecasts of long-horizon earnings growth across all covered firms. Subjective discount rate expectations are constructed analogously, using the same survey-based measures as in the baseline but applying the expanded firm universe for consistency in coverage.

The results are similar to the baseline. Under rational expectations, discount rate fluctuations explain 63.0% of the variation in vacancy filling rates at the five-year horizon, while under subjective expectations, distorted cash flow beliefs remain dominant, accounting for 96.3%. The similarity in results suggests that the dominance of cash flow distortions under subjective beliefs is not specific to large-cap firms in the S&P 500 but holds more broadly across publicly listed firms with analyst coverage.

While this paper focuses on publicly listed firms due to data limitations, preliminary evidence suggest that similar patterns likely emerge among smaller private businesses. A 2010 report from the National Federation of Independent Business (NFIB) on small business credit during the recession shows that hiring decisions were primarily driven by pessimism about future sales rather than financing constraints. At the time, 51% of small employers cited weak sales expectations as their top concern, compared to just 8% who cited access to credit (Dennis, 2010). To the extent that access to credit capture financial frictions that would show up in discount rates, this survey suggests that subjective beliefs about future cash flows also shape employment decisions in the small business sector.

Figure A.4: Variance Decomposition of Vacancy Filling Rate: All Listed Firms

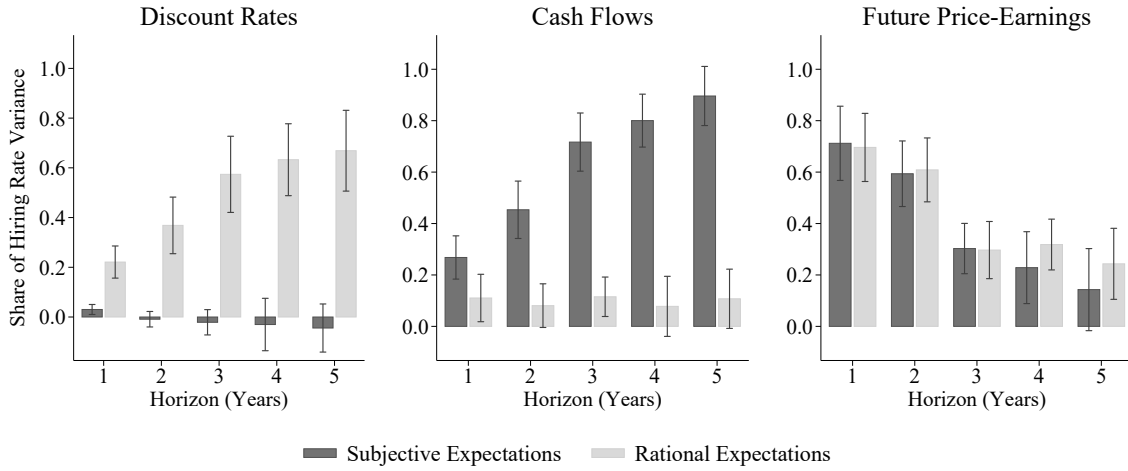


Notes: Figure reports variance decompositions of the aggregate vacancy filling rate using forecasts aggregated over all publicly listed firms with IBES analyst coverage. Each panel reports the share of the variation in vacancy filling rates that can be explained by h -year expected present discounted values of discount rates $r_{t,t+h}$, (negative) cash flows $e_{t,t+h}$, and (negative) price-earnings ratios $p_{t,t+h}$, as defined in equation (16). Light (dark) bars show the contribution under rational (subjective) expectations. Subjective expectations \mathbb{F}_t are based on IBES survey forecasts of financial analysts aggregated over all covered firms. Rational expectations \mathbb{E}_t are based on machine learning forecasts from Long Short-Term Memory (LSTM) neural networks. The sample is quarterly from 2005Q1 to 2023Q4. Each bar shows Newey-West 95% confidence intervals with lags = 4 quarters.

A.2.7 Extended Historical Sample

Figure A.5 reports the variance decomposition of the vacancy filling rate from equation (21) using an extended quarterly sample from 1983Q4 to 2023Q4. Subjective cash flow expectations are measured using IBES survey forecasts of earnings growth, available from 1983Q4. Subjective discount rate expectations are extended by extracting a common latent component from multiple historical survey sources from Table A.6 using a state-space model estimated via the Kalman filter. The latent state S_t is interpreted as the one-year-ahead expected stock return, $\mathbb{F}_t[r_{t+1}]$. To construct the five annual forecasts needed for the present-value sum $r_{t,t+h}$, I impose a flat term-structure assumption and set $\mathbb{F}_t[r_{t+j}] = S_t$ for $j = 1, \dots, 5$. This approach ensures that all horizons are anchored by the common latent factor while remaining consistent with the information set of the historical surveys. The extended sample results are consistent with the baseline. Under rational expectations, discount rate fluctuations explain 66.9% of vacancy filling rate variation at the five-year horizon. Under subjective expectations, distorted cash flow beliefs dominate, accounting for 89.6%.

Figure A.5: Variance Decomposition of Vacancy Filling Rate: Extended Sample 1983Q4–2023Q4



Notes: Figure reports variance decompositions of the aggregate vacancy filling rate using an extended sample from 1983Q4 to 2023Q4. Each panel reports the share of the variation in vacancy filling rates that can be explained by h -year expected present discounted values of discount rates $r_{t,t+h}$, (negative) cash flows $e_{t,t+h}$, and (negative) price-earnings ratios $pe_{t,t+h}$, as defined in equation (16). Light (dark) bars show the contribution under rational (subjective) expectations. Subjective expectations \mathbb{F}_t are based on survey forecasts of CFOs and IBES financial analysts. Rational expectations \mathbb{E}_t are based on machine learning forecasts from Long Short-Term Memory (LSTM) neural networks. Each bar shows Newey-West 95% confidence intervals with lags = 4 quarters.

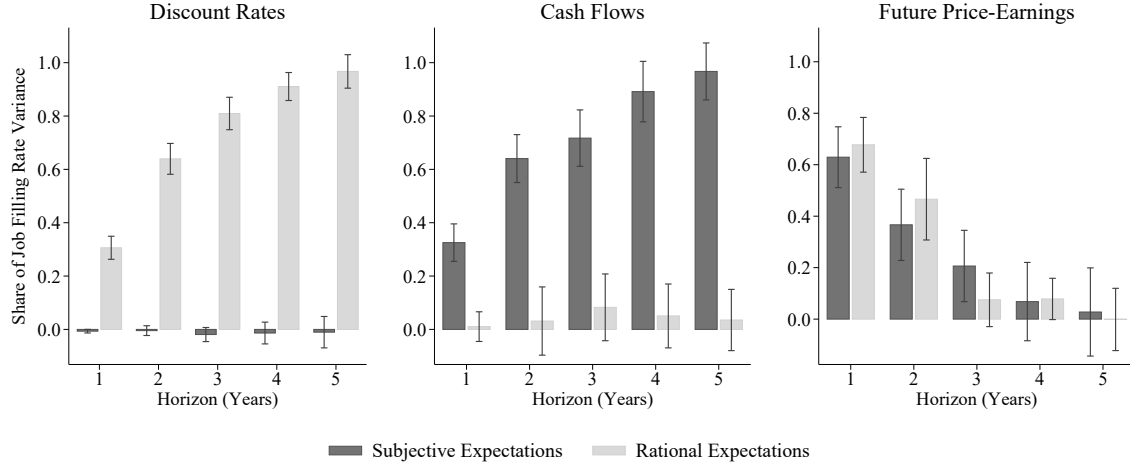
A.2.8 Ex-post Decomposition

Since the log-linear decomposition of the vacancy filling rate holds both ex-ante and ex-post, a variance decomposition of the vacancy filling rate can also be estimated using ex-post realized data, under the assumption of the firm's perfect foresight:

$$1 \approx \underbrace{\frac{Cov[r_{t,t+h}, \log q_t]}{Var[\log q_t]}}_{\text{Discount Rate news}} - \underbrace{\frac{Cov[e_{t,t+h}, \log q_t]}{Var[\log q_t]}}_{\text{Cash Flow News}} - \underbrace{\frac{Cov[pe_{t,t+h}, \log q_t]}{Var[\log q_t]}}_{\text{Future Price-Earnings News}}$$

Table A.6 reports the estimates. For the main sample covering 2005Q1 to 2023Q4, at the 5 year horizon, 79.4% of the variation in the vacancy filling rate is driven by discount rate news. In contrast, cash flow news has a smaller effect, contributing only 10.3% over the same period. For the full sample covering 1965Q1 to 2023Q4, at the 5 year horizon, 78.6% of the variation in the vacancy filling rate is driven by discount rate news. In contrast, cash flow news has a smaller effect, contributing only 9.5% over the same period.

Figure A.6: Variance Decomposition of Vacancy Filling Rate: Ex-Post Measure 1965Q1–2023Q4

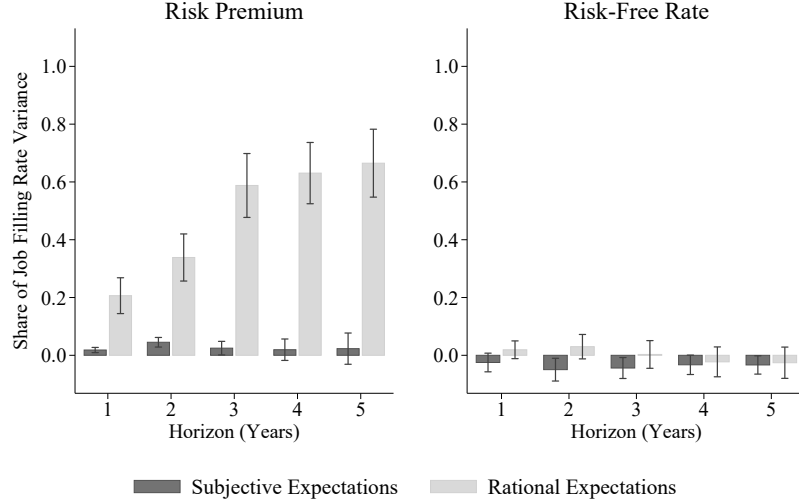


Notes: Figure reports variance decompositions of the vacancy filling rate from equation using ex-post realized outcomes. Each panel reports the share of the variation in vacancy filling rates that can be explained by h -year expected present discounted values of discount rates $r_{t,t+h}$, (negative) cash flows $e_{t,t+h}$, and (negative) price-earnings ratios $pe_{t,t+h}$, as defined in equation (16). Light bars show the contribution under rational expectations. The sample is quarterly from 1965Q1 to 2023Q4. Each bar shows Newey-West 95% confidence intervals with lags = 4 quarters.

A.2.9 Risk Premia vs. Risk-Free Rate

Risk-free rates play only a small role in explaining fluctuations in vacancy filling rates. Figure A.7 plots estimates from regressing subjective expectations implied by forecasts from the Survey of Professional Forecasters (SPF), and machine expectations of h year ahead annualized log 3-month Treasury bill rates on the vacancy filling rate. Under all measures of beliefs and all horizons considered, the contribution from risk-free rates explain less than 5% of the variation in vacancy filling rates. The result suggests that the significant contribution of rational discount rates in Table A.2 is driven by fluctuations in risk premia instead of risk-free rates.

Figure A.7: Variance Decomposition of Vacancy Filling Rate: Risk Premia vs. Risk-Free Rate



Notes: Figure plots estimates from regressing h year present discounted value of annualized log 3-month Treasury bill rates $\sum_{j=1}^h \rho^{j-1} r_{t+j}^f$ on the vacancy filling rate under alternative assumptions about the firm's beliefs. Subjective expectations \mathbb{F}_t of risk-free rates are based on survey forecasts from the Survey of Professional Forecasters. Subjective expectations of the equity risk premium is defined as the difference between CFO survey S&P 500 stock return forecast and the SPF risk-free rate forecast. Machine expectations are based on machine learning forecasts \mathbb{E}_t from Long Short-Term Memory (LSTM) neural networks $G(\mathcal{X}_t, \beta_{h,t})$, whose parameters $\beta_{h,t}$ are estimated in real time using \mathcal{X}_t , a large scale dataset of macroeconomic, financial, and textual data. The sample is quarterly from 2005Q1 to 2023Q4. Each bar shows Newey-West 95% confidence intervals with lags = 4.

A.2.10 Risk-Neutral Measure Implied by Futures Prices

To address whether forecast errors simply reflect risk compensation rather than belief distortions, I re-evaluate the decomposition using risk-neutral expectations extracted from futures prices. Under risk-neutral pricing, forecast errors should equal risk premia plus noise, with no patterns beyond those explained by time-varying risk compensation. In contrast to subjective survey forecasts, which may reflect belief distortions, risk-neutral expectations are extracted directly from financial market prices and reflect the valuations of marginal investors in the economy. The decomposition parallels the earlier analysis based on subjective beliefs but replaces the expectations operator $\mathbb{E}_t[\cdot]$ with the risk-neutral operator $\mathbb{E}_t^Q[\cdot]$, where Q denotes the risk-neutral probability measure. I begin with the ex-post decomposition of the vacancy filling rate $\log q_t$, which can be expressed as:

$$\log q_t = c_q + \sum_{j=1}^h \rho^{j-1} r_{t+j} - \left(d_{lt} + \sum_{j=1}^h \rho^{j-1} \Delta d_{t+j} \right) - \rho^h p d_{t+h}$$

where r_{t+j} denotes the return on the S&P 500 index, Δd_{t+j} denotes the change in log dividends, and $p d_{t+h}$ is the terminal log price-dividend ratio. Since market-based risk-neutral expectations are available for dividends but not for earnings, I re-write the decomposition in terms of dividend growth. To evaluate this decomposition under the risk-neutral measure, I replace each future variable with its risk-neutral expectation. Using the standard no-arbitrage pricing result that the futures price equals the risk-neutral expectation of the future spot price (Ait-Sahalia et al., 2001), I compute the expected return over horizon h using log differences of S&P 500 futures prices:

$$\mathbb{E}_t^Q[r_{t,t+h}] = \sum_{j=1}^h \rho^{j-1} (f_{t,t+j}^{sp500} - f_{t,t+j-1}^{sp500})$$

where $f_{t,t+j}^{sp500}$ denotes the log futures price of the S&P 500 at time t for delivery at $t+j$, and $f_{t,t}^{sp500} \equiv p_t$ is the log spot price. This expression captures the risk-neutral expectation of the capital-gain component of returns. In principle, total returns also include the dividend yield. However, since dividends represent only a small fraction of S&P 500 total returns over this sample period, and reliable dividend futures are limited in maturity and liquidity, I abstract from this component and focus on the capital gain for tractability. Similarly, I measure expected dividend growth using dividend futures:

$$\mathbb{E}_t^Q[d_{t,t+h}] = d_{lt} + \sum_{j=1}^h \rho^{j-1} (f_{t,t+j}^{div} - f_{t,t+j-1}^{div})$$

where $f_{t,t+j}^{div}$ is the log price of the dividend future for maturity $t+j$, and $f_{t,t}^{div} \equiv d_t$ is the log of current dividends. To compute the terminal price-dividend ratio $\mathbb{E}_t^Q[p d_{t+h}]$, I apply a forward iteration of the log-linear price-dividend identity:

$$\mathbb{E}_t^Q[p d_{t+h}] = \frac{1}{\rho^h} p d_t - \frac{1}{\rho^h} \sum_{j=1}^h \rho^{j-1} (c_{pd} + \mathbb{E}_t^Q[\Delta d_{t+j}] - \mathbb{E}_t^Q[r_{t+j}])$$

where c_{pd} is a constant from the log-linearization. Since market data on futures prices is typically limited to near-term maturities (e.g., 1-year ahead), I extrapolate longer-horizon expectations using fitted values from autoregressive models. Specifically, I estimate first-order predictive regressions of the 1-year forward S&P 500 return and dividend growth on the lagged spot value:

$$\begin{aligned} f_{t,t+1}^{sp500} - p_t &= \mu_{sp500} + \rho_{sp500}(p_t - p_{t-1}) + \varepsilon_t \\ f_{t,t+1}^{div} - d_t &= \mu_{div} + \rho_{div}(d_t - d_{t-1}) + \varepsilon_t \end{aligned}$$

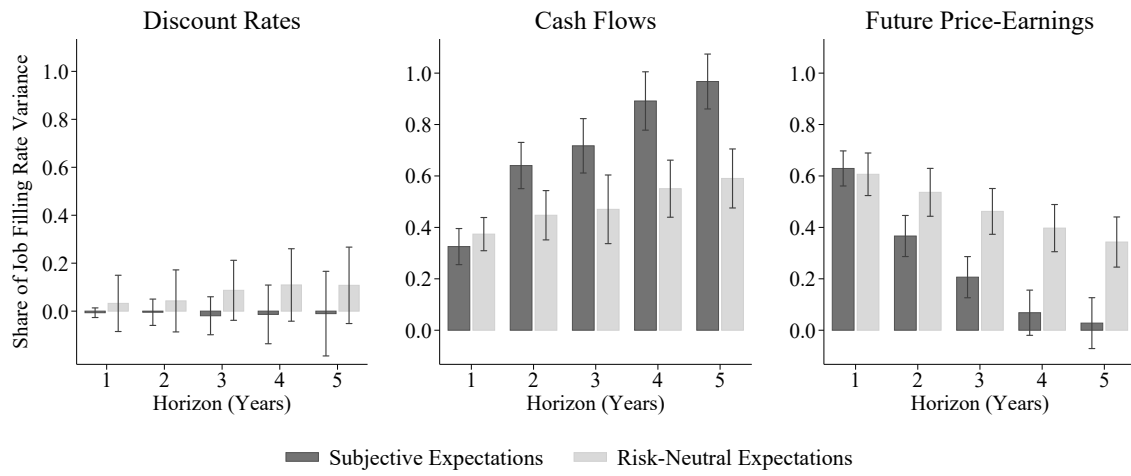
and then forecast growth at horizons $j > 1$ recursively using the standard multi-step formula for an AR(1) process:

$$\begin{aligned} f_{t,t+j}^{sp500} - f_{t,t+j-1}^{sp500} &= \frac{\mu_{sp500}(1 - \rho_{sp500}^{j-1})}{1 - \rho_{sp500}} + \rho_{sp500}^{j-1} (f_{t,t+1}^{sp500} - p_t) \\ f_{t,t+j}^{div} - f_{t,t+j-1}^{div} &= \frac{\mu_{div}(1 - \rho_{div}^{j-1})}{1 - \rho_{div}} + \rho_{div}^{j-1} (f_{t,t+1}^{div} - d_t) \end{aligned}$$

Using these forward-imputed values, I compute the full set of risk-neutral expectations required for the decomposition.

The results of this exercise are shown in Figure A.8. Compared to subjective expectations, risk-neutral expectations attribute a smaller role to future cash flows and a greater role to discount rates in explaining the variation in the vacancy filling rate. This contrast suggests that belief distortions in survey forecasts may overweight the informational content of short-term earnings outlooks and underweight changes in risk premia, leading to distorted hiring incentives.

Figure A.8: Variance Decomposition of Vacancy Filling Rate: Risk-Neutral Expectations

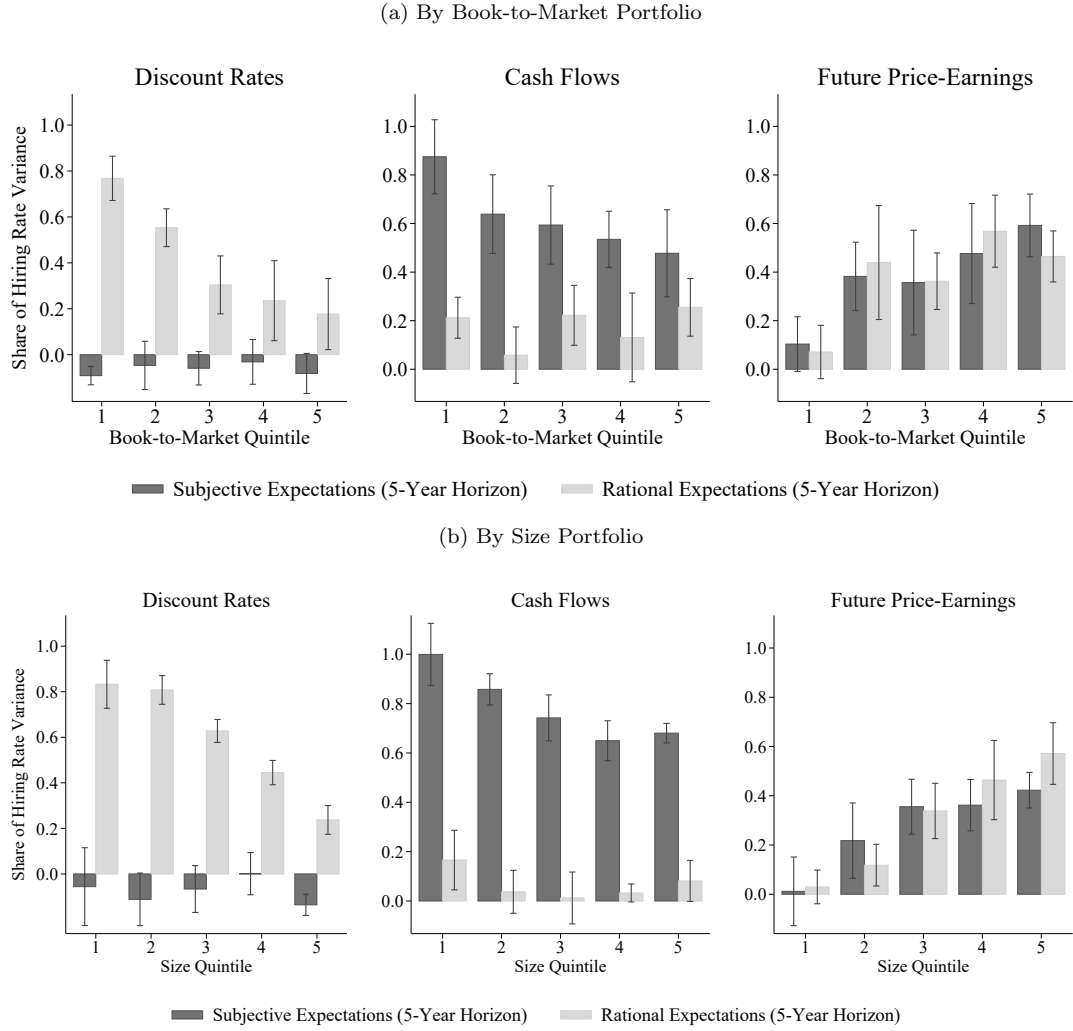


Notes: Figure illustrates the discount rate, cash flow, and future price-earnings components of the time-series decomposition of the aggregate vacancy filling rate. Light bars show the contribution under risk-neutral expectations implied by S&P 500 and dividend futures. Dark bars show the contribution under subjective expectations. The sample is quarterly from 2005Q1 to 2023Q4. Each bar shows Newey-West 95% confidence intervals with lags = 4.

A.2.11 Time-Series Decomposition of Hiring Rate by Book-to-Market and Size Portfolios

Figure A.9 shows that belief distortions play a significant role in explaining the cross-sectional variation in hiring across book-to-market portfolios (panel (a)) and size portfolios (panel (b)). I run the time-series decomposition of the hiring rate separately for each of the portfolios. The decomposition reveals that under subjective expectations, distorted beliefs about future cash flows account for a larger share of hiring rate variation, particularly among low book-to-market (growth) firms and small firms. This pattern is consistent with the idea that growth firms and small firms are more sensitive to subjective beliefs about long-term fundamentals, amplifying the role of distorted expectations in their hiring decisions. In contrast, for high book-to-market (value) firms and large firms, the contribution of cash flow expectations remains relatively stable across subjective and rational benchmarks, suggesting their hiring is less exposed to belief distortions.

Figure A.9: Time-Series Decomposition of Hiring Rate by Portfolio

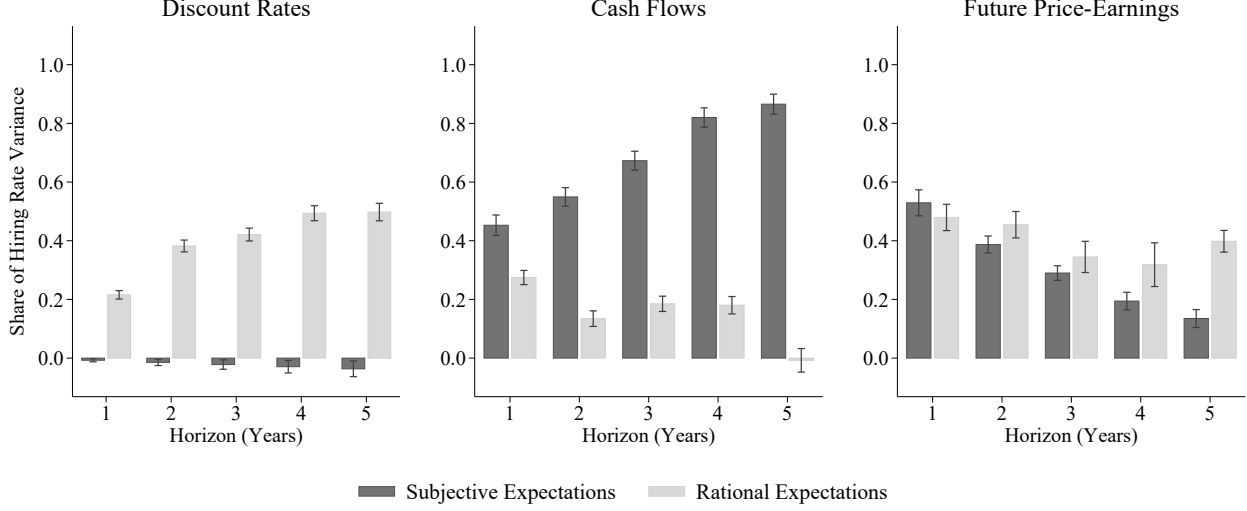


Notes: Figure estimates time-series decomposition of hiring rate separately for each of the five book-to-market (panel (a)) and size (panel (b)) portfolios. Firms have been sorted into five value-weighted portfolios by book-to-market ratio or size (market capitalization). Light bars show contributions under rational expectations; dark bars show contributions under subjective expectations. The sample is quarterly from 2005Q1 to 2023Q4. Each bar shows Newey-West 95% confidence intervals with lags = 4.

A.2.12 Cross-Sectional Decomposition of Hiring Rate: By Industry

Figure A.10 shows that belief distortions play a significant role in explaining the cross-sectional variation in hiring across Fama-French 49 industry portfolios.

Figure A.10: Cross-Sectional Decomposition of Hiring Rate: By Industry



Notes: Figure estimates a cross-sectional decomposition of the hiring rate across Fama-French 49 industry portfolios. Light bars show contributions under rational expectations; dark bars show contributions under subjective expectations. The sample is quarterly from 2005Q1 to 2023Q4. Each bar shows Newey-West 95% confidence intervals with lags = 4.

A.2.13 Financial Constraints

A natural concern is that variation in hiring may reflect differences in financial constraints rather than distortions in beliefs. In a rational expectations model, financial constraints appear as a Lagrange multiplier that tightens the firm's stochastic discount factor (SDF), raising internal hurdle rates and suppressing hiring (Kehoe et al., 2019). In this setting, constraint-induced fluctuations in hiring would be rationally attributed to higher discount rates. By contrast, under subjective expectations, survey respondents may misattribute the effect of constraints to lower future cash flows, especially if internal hurdle rates are persistent, upward-biased, and unresponsive to market conditions (Gormsen and Huber, 2025). Financial constraints could also allow the effects of belief distortions to persist by limiting arbitrage that would otherwise correct them (De La O et al., 2024).

Measures of Financial Constraints To test these hypotheses, I incorporate firm-level financial constraint measures into the decomposition framework:

- Firm Size (Total Assets): Firms in the bottom tertile of the asset size distribution are classified as financially constrained, while those in the top tertile are unconstrained (Erickson and Whited, 2000).
- Payout Ratio: Defined as dividends plus stock repurchases scaled by total assets. Firms with the lowest (highest) payout ratios are classified as constrained (unconstrained), consistent with the idea that constrained firms conserve internal funds (Fazzari et al., 1988).
- SA Index: The size-age index developed by Hadlock and Pierce (2010), constructed as $SA = -0.737 \cdot \text{Size} + 0.043 \cdot \text{Size}^2 - 0.040 \cdot \text{Age}$, where Size is log real assets and Age is years since listing. Higher SA values indicate tighter constraints.
- Expected Free Cash Flow: Based on Lewellen and Lewellen (2016), firms are sorted into constraint groups using predicted free cash flow, estimated from cross-sectional regressions on lagged characteristics. Low expected FCF implies tighter constraints.
- WW Index: The Whited-Wu index (Whited and Wu, 2006), a linear combination of cash flow, dividend status, leverage, size, and sales growth, where higher index values imply greater constraints.

Each measure is updated annually and firms are classified based on terciles or continuous index values. Each measure is aggregated to the portfolio level and standardized before entering the regression as controls.

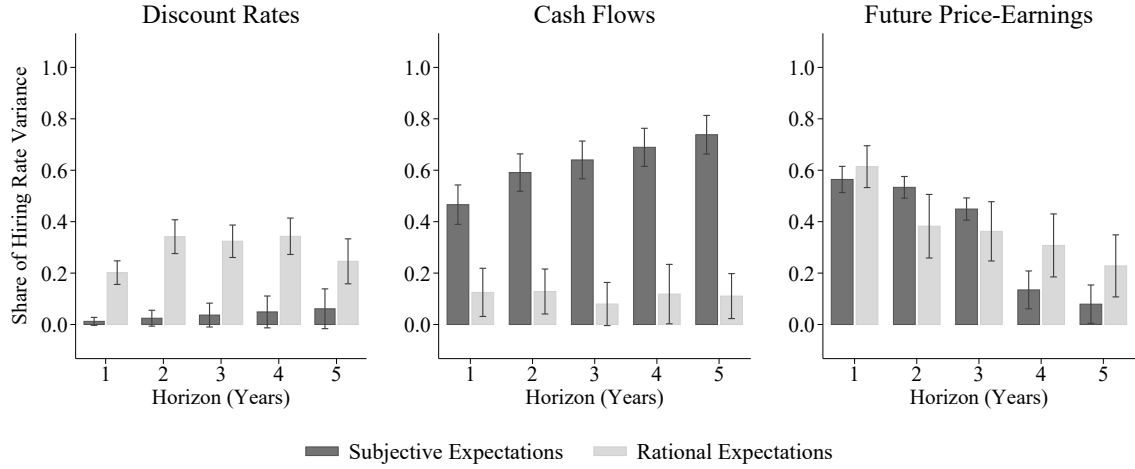
Decomposition with Financial Constraints I modify the baseline decomposition regression as follows:

$$\mathbb{E}_t[e_{i,t,t+h}] = \beta \cdot h l_{i,t} + \Gamma \cdot FC_{i,t} + \alpha_i + \alpha_t + \varepsilon_{i,t}$$

where $FC_{i,t}$ is a vector of standardized financial constraint measures for firm i at time t . As before, the parameter of interest is β , which captures the share of variation in the hiring rate $hl_{i,t}$ explained by subjective expectations, but this time conditional on financial constraints. I run analogous regressions to estimate the contributions of discount rate expectations and future price-earnings ratios. I also replace survey forecasts with machine learning forecasts to estimate the decomposition under rational expectations, again controlling for financial constraints using the same specification.

Results Figure A.11 presents the decomposition estimates with and without financial constraint controls, under both subjective and rational expectations. Under subjective expectations, the contribution of expected earnings to hiring variation remains large and significant, with only a modest reduction in explanatory power after controlling for financial constraints. This suggests that distorted beliefs about cash flows persist even after adjusting for observable constraint-related fundamentals. These findings are consistent with the view that constrained firms overreact to cash flow news or internalize persistent pessimism about earnings. Under rational expectations, however, the contribution of discount rate expectations drops substantially once constraint controls are included. This is consistent with a rational model in which financial constraints tighten the SDF and raise internal hurdle rates. When this variation is accounted for, the rational model assigns less importance to discount rate news in explaining hiring variation. The results supports the interpretation that financial constraints can explain a nontrivial share, but do not fully explain, variation in hiring. While rational forecasts attribute constraint effects to discount rates, subjective expectations appear to reflect persistent pessimism about cash flows.

Figure A.11: Cross-Sectional Decomposition of Hiring Rate: Control for Financial Constraints



Notes: Figure estimates cross-sectional decomposition of hiring rate, controlling for measures of financial constraints. Light bars show contributions under rational expectations; dark bars show contributions under subjective expectations. Financial constraint controls include firm size, payout ratio, SA index, expected free cash flow, and the Whited-Wu index. The sample is quarterly from 2005Q1 to 2023Q4. Each bar shows Newey-West 95% confidence intervals with lags = 4.

A.2.14 Alternative Survey Measures of Subjective Cash Flow Expectations

The large role played by subjective cash flow expectations in explaining the vacancy filling rate holds more generally across alternative survey forecasts of earnings growth. Table A.5 re-estimates the subjective variance decomposition while replacing IBES survey forecasts of earnings growth with the corresponding forecast from the Bloomberg (BBG) and CFO surveys. The forecast horizon for the CFO survey has been limited to $h = 1$ year ahead and the sample covers a shorter period over 2002Q1 to 2019Q3 due to missing earnings growth forecasts in the CFO survey.

To summarize the alternative survey measures into a single series, I construct Filtered Investor (FI) expectations by extracting the common component of subjective cash flow beliefs using a Kalman filter. The latent state variable is defined as the h -month-ahead expected earnings growth, $S_t \equiv \mathbb{F}_t[\Delta e_{t+h}]$, which captures investors' subjective beliefs about future cash flows. The observation vector X_t contains survey measures of expected earnings growth over the next h periods from IBES, Bloomberg, and CFO surveys. The Kalman filter then estimates the latent S_t as the optimal linear combination of these noisy survey indicators $S_t = C(\Theta) + T(\Theta)S_{t-1} + R(\Theta)\varepsilon_t$, where C, T, R are matrices of the model's primitive parameters $\Theta = (\alpha, \rho, \sigma_\varepsilon)'$. ε_t is an innovation to the latent expectation that was unpredictable from the point of view of the forecaster. α is the intercept, ρ is the persistence, and σ_ε is the standard deviation of the latent innovation error. The Observation equation takes the form $X_t = D + ZS_t + Uv_t$, where h is a fixed forecast horizon. The observation vector X_t contains measures of survey expected cash flows from IBES, BBG, and CFO surveys over the next h periods. v_t is a vector of observation errors with standard deviations in the diagonal matrix U . Z and D are parameters that have been set to 1s and 0s, respectively. I use the Kalman filter to estimate the remaining parameters $\alpha, \rho, \sigma_\varepsilon, U$. Since some of our observable series are not available at all frequencies and/or over the full sample, the state-space estimation fills in missing values using the Kalman filter.

Table A.5: Variance Decomposition of Vacancy Filling Rate: Alternative Subjective Cash Flow Expectations

Horizon h (Years)	1	2	3	4	5
Subjective Expectations: $\log q_t = c_q + \mathbb{F}_t[r_{t,t+h}] - \mathbb{F}_t[e_{t,t+h}] - \mathbb{F}_t[pe_{t,t+h}]$					
(-) Cash Flow	0.578***	0.625***	0.684***	0.887***	0.933***
t -stat	(3.046)	(4.275)	(4.894)	(6.019)	(7.612)
N	76	76	76	76	76
(a) Filtered Investor (FI) Expectations					
(-) Cash Flow	0.586***	0.830***	0.851***	0.896***	0.949***
t -stat	(8.476)	(8.317)	(7.213)	(5.288)	(4.541)
N	76	76	76	76	76
(b) Bloomberg (BBG) Survey					
(-) Cash Flow	0.637*	0.830***	0.851***	0.896***	0.949***
t -stat	(1.934)	(8.317)	(7.213)	(5.288)	(4.541)
N	71	76	76	76	76
(c) CFO Survey					
(-) Cash Flow	0.637*	0.830***	0.851***	0.896***	0.949***
t -stat	(1.934)	(8.317)	(7.213)	(5.288)	(4.541)
N	71	76	76	76	76

Notes: Table reports variance decompositions of the vacancy filling rate while replacing IBES earnings growth forecast with alternative surveys as measures of subjective cash flows. FI summarizes the alternative survey measures into a single series using a Kalman filter. The sample for BBG and FI is quarterly from 2005Q1 to 2023Q4. The sample for CFO is quarterly from 2002Q1 to 2019Q3. Newey-West corrected t -statistics with lags = 4 are reported in parentheses: *sig. at 10%. **sig. at 5%. ***sig. at 1%.

A.2.15 Alternative Survey Measures of Subjective Discount Rates

The small role played by subjective discount rate expectations in explaining the vacancy filling rate holds more generally across alternative survey forecasts of stock returns. Table A.6 reports estimates from regressing 1 year ahead survey expectations of stock returns $\mathbb{F}_t[r_{t,t+h}]$ on the log vacancy filling rate q_t under alternative survey forecasts of stock returns. In all survey measures, the estimates suggest a weak relationship between subjective stock return expectations $\mathbb{F}_t^s[r_{t,t+h}]$ and the vacancy filling rate q_t .

$r_{t,t+h}$ denotes h year CRSP stock returns (with dividends) or S&P 500 price growth from time t to $t+h$, depending on the concept that survey respondents are asked to predict: log stock returns for CB, SOC, Gallup/UBS, and CFO; log price growth for Livingston. $\mathbb{F}_t^s[r_{t,t+h}]$ denotes subjective expectations of stock returns or price growth from survey s . CoC and Hurdle denotes corporate cost of capital and hurdle rates constructed in Gormsen and Huber (2023). The forecast horizon has been limited to 1 year ahead due to limited data availability in the alternative surveys. The sample is quarterly over 2005Q1 to 2023Q4 when considering the NX, CB, SOC, and CFO surveys, 2005Q1 to 2008Q4 for Gallup/UBS, and semi-annual over 2005Q1 to 2023Q4 from Q2 and Q4 of each calendar year for Livingston.

To summarize the alternative survey measures into a single series, the Filtered Invesotr (FI) series extracts the common component of subjective discount rates using a Kalman filter. The state variable is a latent h -month ahead expected stock return capturing investors' subjective beliefs $S_t \equiv \mathbb{F}_t[r_{t+h}]$, which evolves according to an AR(1) state equation $S_t = C(\Theta) + T(\Theta)S_{t-1} + R(\Theta)\varepsilon_t$, where C, T, R are matrices of the model's primitive parameters $\Theta = (\alpha, \rho, \sigma_\varepsilon)'$. ε_t is an innovation to the latent expectation that was unpredictable from the point of view of the forecaster. α is the intercept, ρ is the persistence, and σ_ε is the standard deviation of the latent innovation error. The Observation equation takes the form $X_t = D + ZS_t + Uv_t$, where $h = 12$ months is a fixed forecast horizon. The observation vector X_t contains measures of survey expected returns listed above over the next h periods. v_t is a vector of observation errors with standard deviations in the diagonal matrix U . Z and D are parameters that have been set to 1s and 0s, respectively. I use the Kalman filter to estimate the remaining parameters $\alpha, \rho, \sigma_\varepsilon, U$. Since some of our observable series are not available at all frequencies and/or over the full sample, the state-space estimation fills in missing values using the Kalman filter.

Table A.6: Variance Decomposition of Vacancy Filling Rate: Alternative Discount Rates

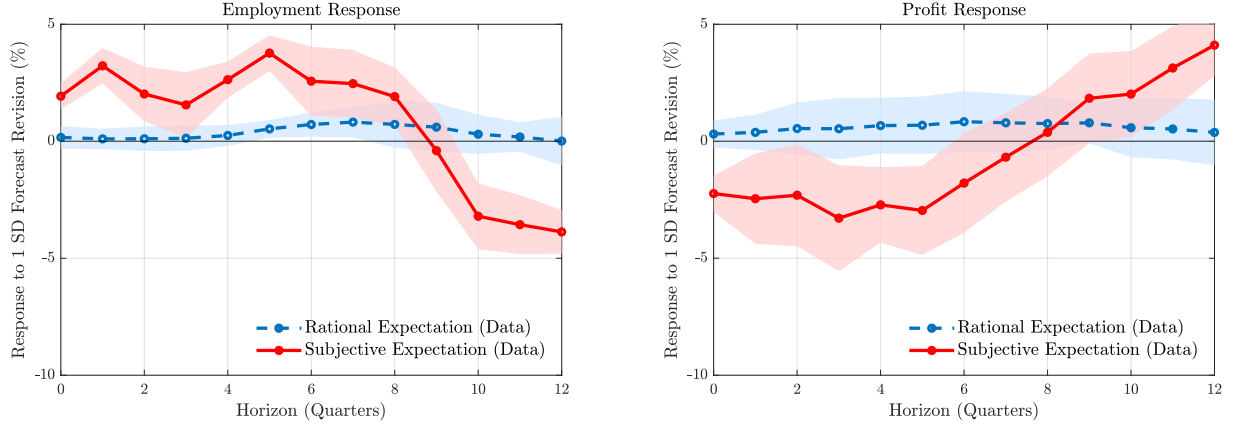
Horizon h (Years)	1	1	1	1	1	1	1	1
Subjective Expectations: $\log q_t = c_q + \mathbb{F}_t^s[r_{t,t+h}] - \mathbb{F}_t[e_{t,t+h}] - \mathbb{F}_t[pe_{t,t+h}]$								
Survey s	FI	NX	CB	SOC	Gallup	Liv	CoC	Hurdle
Discount Rate	0.013 (0.614)	-0.011 (-0.249)	0.026 (0.504)	0.002 (0.103)	-0.065 (-0.922)	0.067 (0.181)	0.024 (0.734)	0.013 (0.522)
t -stat								
Adj. R^2	0.070	0.012	0.069	0.009	0.216	0.045	0.232	0.154
N	76	76	76	76	16	40	76	76

Notes: Table reports slope (β_1) estimates from regressing $h = 1$ year ahead survey expectations of stock returns $\mathbb{F}_t[r_{t,t+h}]$ on the log vacancy filling rate q_t . $r_{t,t+h}$ denotes h year CRSP stock returns (with dividends) or S&P 500 price growth from time t to $t+h$, depending on the concept that survey respondents are asked to predict: log stock returns for CB, SOC, Gallup/UBS, and CFO; log price growth for Livingston. $\mathbb{F}_t^s[r_{t,t+h}]$ denotes subjective expectations of stock returns or price growth from survey s . CoC and Hurdle denotes corporate cost of capital and hurdle rates constructed in Gormsen and Huber (2023). Filtered Investor (FI) expectations summarize the alternative survey measures into a single series using a Kalman filter. The sample is quarterly over 2005Q1 to 2023Q4 when considering the NX, CB, SOC, and CFO surveys, 2005Q1 to 2008Q4 for Gallup/UBS, and semi-annual over 2005Q1 to 2023Q4 from Q2 and Q4 of each calendar year for Livingston. Newey-West corrected t -statistics with lags = 4 are reported in parentheses: *sig. at 10%. **sig. at 5%. ***sig. at 1%.

A.3 Profits and Employment Response to Forecast Revisions

Figure A.12 decomposes the profits per worker response into profits and employment. Under rational expectations (blue dashed lines), both profits and employment remain stable after positive forecast revisions. Under subjective expectations (red solid lines), employment increases while profits decrease to a less extend, leading to a decline in profits per worker. This pattern indicates that the fall in profits per worker reflects excessive employment expansion relative to profit growth, consistent with firms over-hiring under optimistic beliefs.

Figure A.12: Profits and Worker Response to Forecast Revision



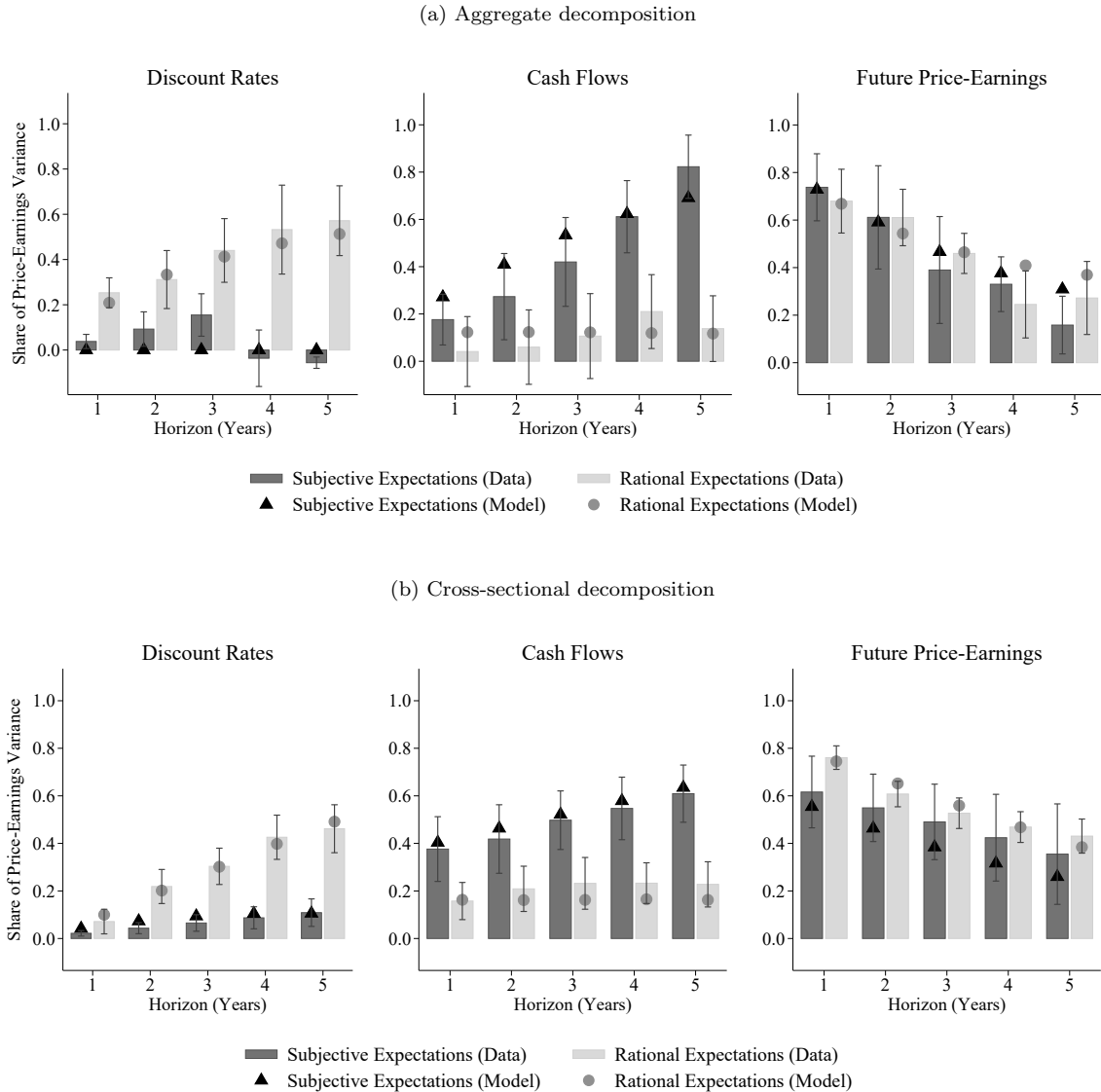
Notes: Figure displays impulse responses of $\log(E_{i,t+h})$ (left) and $\log(L_{i,t+h})$ (right) to forecast revisions, estimated via local projections: $\log(Y_{i,t+h}) = \beta_h \text{ForecastRevision}_{i,t} + \alpha_i + \tau_t + \varepsilon_{i,t+h}$ where $Y = E, L$. α_i and τ_t denote firm and time fixed effects. Blue dashed line: IRF under rational expectations, where forecast revision is the machine learning discount rate revision $\mathbb{E}_t[r_{i,t+1}] - \mathbb{E}_{t-1}[r_{i,t+1}]$. Red solid line: IRF under subjective expectations, where forecast revision is the survey cash flow revision $\mathbb{F}_t[\Delta e_{i,t+1}] - \mathbb{F}_{t-1}[\Delta e_{i,t+1}]$. Blue dash (red solid) line: data IRF under rational (subjective) expectations proxied by machine (survey) forecasts. Observations weighted by each firm's market value. Shaded area: two-way clustered 90% confidence intervals by firm and time (data IRF). Data sample: 1999Q1–2023Q4.

A.4 Decomposition of Price-Earnings Ratios

The decomposition of the price-earnings ratio developed by De La O and Myers (2021) and De La O et al. (2024) provide a useful benchmark for thinking about the role of distorted beliefs in financial markets. Their analysis applies the Campbell and Shiller (1988) identity to the aggregate price-earnings ratio and shows that subjective expectations systematically underestimate the role of discount rates while overstating the importance of cash flows.

Figure A.13 shows that the decompositions for price-earnings ratios and vacancy filling rates yield broadly similar magnitudes. In both cases, rational expectations attribute most variation to discount-rate news, while subjective expectations shift the weight strongly toward cash flows. The parallel magnitudes underscore that the two decompositions are consistent, but the economic implications differ. Whereas the price-earnings decomposition highlights distortions in asset valuations, the vacancy filling rate decomposition shows how these same distortions translate into fluctuations in job creation and unemployment.

Figure A.13: Variance Decomposition of the Price-Earnings Ratio



Notes: Panels (a) and (b) illustrate the discount rate, cash flow, and future price-earnings components of the time-series and cross-sectional decompositions of the price-earnings ratio. Firms are sorted into five value-weighted portfolios by book-to-market ratio in the cross-sectional case. Light bars show contributions under rational expectations; dark bars show contributions under subjective expectations. The sample is 2005Q1–2023Q4. Each bar shows Newey-West 95% confidence intervals with lags = 4. Circle and triangle dots show the values of rational and subjective expectations implied by the model, respectively.

A.5 Predictability of Unemployment and Hiring Rates

Time-Series Predictability of Aggregate Unemployment Rate To complement the decomposition of the vacancy filling rate, this section analyzes the unemployment rate directly. While the vacancy filling rate captures the main driver of unemployment dynamics in search models, the unemployment rate is the key macroeconomic outcome of interest and the direct target of policy. Start from the unemployment accumulation equation of the search model in Section 5:

$$U_{t+1} = \delta_t(1 - U_t) + (1 - q_t\theta_t)U_t \quad (\text{A.3})$$

which states that the number of unemployed workers at the beginning of next period U_{t+1} equals the number of unemployed worker who fail to find a job in the current period $(1 - q_t\theta_t)U_t$ plus the number of employed workers who lose their jobs due to separations $\delta_t(1 - U_t)$. Log-linearize around the steady state and substitute in equation (16), which is a decomposition of the vacancy filling rate q_t into discount rate, cash flow, and future price-earnings components. As shown in Section B.3, the log unemployment rate u_{t+1} satisfies the following predictive relationship:

$$u_{t+1} = \alpha + \beta_r \mathbb{F}_t[r_{t,t+h}] + \beta_e \mathbb{F}_t[e_{t,t+h}] + \gamma' X_t + \varepsilon_{s,t+1} \quad (\text{A.4})$$

where $X_t \equiv [u_t, \log \theta_t, \log \delta_t]'$ collects labor market factors including the lagged log unemployment rate u_t , vacancy-to-unemployment ratio $\log \theta_t$, and job separation rate $\log \delta_t$. The coefficients of interest, β_r and β_e , quantify the effect of subjective expectations about discount rates and cash flows, respectively, on future unemployment.

To isolate the contribution of belief distortions, I further decompose each subjective expectation \mathbb{F}_t into its rational expectation \mathbb{E}_t and its distortion $\mathbb{F}_t - \mathbb{E}_t$:

$$\begin{aligned} u_{t+1} = & \alpha + \beta_{r,\mathbb{E}} \mathbb{E}_t[r_{t,t+h}] + \beta_{r,\mathbb{F}} (\mathbb{F}_t[r_{t,t+h}] - \mathbb{E}_t[r_{t,t+h}]) \\ & + \beta_{e,\mathbb{E}} \mathbb{E}_t[e_{t,t+h}] + \beta_{e,\mathbb{F}} (\mathbb{F}_t[e_{t,t+h}] - \mathbb{E}_t[e_{t,t+h}]) + \gamma' X_t + \varepsilon_{s,t+1} \end{aligned} \quad (\text{A.5})$$

I estimate equation (A.5) using multivariate OLS regressions, allowing the data to inform the relative importance of each component. The future price-earnings ratio term $\mathbb{F}_t[p_{e_{t,t+h}}]$ has been omitted in the multivariate regression because it is nearly collinear with future discount rates $\mathbb{F}_t[r_{t,t+h}]$ and cash flows $\mathbb{F}_t[e_{t,t+h}]$ as long as the Campbell and Shiller (1988) present value identity holds in equation (15). To ensure stationarity and remove seasonal effects, I estimate the regression in log growth rates relative to the same quarter of the previous year. The regression is designed to test whether perceived shocks to discount rates or earnings forecasts help predict fluctuations in unemployment rates. If firms form distorted beliefs about future returns or earnings, they should manifest in hiring behavior and thus influence unemployment.

Table A.7 reports the results. Column (1) predicts the unemployment rate based on a benchmark model using only machine-based forecasts of discount rates and cash flows. Rational discount rates $\mathbb{E}_t[r_{t,t+h}]$ significantly predict unemployment (coefficient 0.551), consistent with rational models that introduce time-varying discount rates to generate realistic fluctuations in unemployment. The rational cash flow expectation $\mathbb{E}_t[e_{t,t+h}]$ is not a significant predictor (-0.041), consistent with the unemployment volatility puzzle where productivity shocks on its own struggle to generate sufficient unemployment fluctuations. Overall, the sign of the estimated coefficients are consistent with the implications of the search model, since higher discount rates or low expected cash flows depress the expected discounted value of job creation, leading to reduced hiring and higher future unemployment.

Column (2) extends the baseline model by incorporating belief distortions in subjective discount rate and cash flow expectations. The distortion in subjective cash flow expectation $\mathbb{F}_t[e_{t,t+h}] - \mathbb{E}_t[e_{t,t+h}]$ emerges as the strongest predictor of future unemployment, with a large statistically significant coefficient of -0.701. The inclusion of belief distortions improves model performance substantially. The adjusted R^2 increases from 0.528 to 0.745 in-sample and the out-of-sample R^2 increases from 0.149 to 0.254, where the out-of-sample R^2 implies an improvement in the MSE ratio relative to the Survey of Professional Forecasters (SPF) by $0.254 - 0.149 = 0.105$. Traditional labor market factors including lagged unemployment, labor market tightness, and separations explain only a modest portion of unemployment fluctuations, with an in-sample adjusted R^2 of 0.260. In terms of out-of-sample performance, a model that excludes expectations entirely performs worse than the Survey of Professional Forecasters (SPF) benchmark with a negative OOS R^2 of -0.094. These results suggest that the distortions embedded in survey expectations contain valuable information not captured by other rational forecasts and pre-existing labor market factors.

Strikingly, distortions in subjective cash flow expectations drive out the predictive power of the machine-based discount rate forecast, whose coefficient has been reduced to 0.236 and is no longer statistically significant. This result suggests that behavioral factors can crowd out rational forces in driving labor market fluctuations, consistent with models of behavioral overreaction where salient signals can dominate decision making (Bordalo et al., 2020). Since machine forecasts already incorporate a high-dimensional set of real-time predictors, this displacement likely reflect misperceptions of underlying economic shocks rather than statistical bias due to omitted variables.

Figure A.14 illustrates the result by plotting the actual annual change in unemployment against its model-implied decomposition using both rational expectations and belief distortions based on equation (A.5). Fluctuations in unemployment closely track the component attributed to the distortion in expected cash flows. In particular, the cash flow distortion component captures the sharp rise and fall in unemployment during the global financial crisis and COVID-19 recessions with considerable precision.

Table A.7: Time-Series and Cross-Sectional Predictability

Forecast Target: Unemployment Growth Δu_{t+1}		Forecast Target: Employment Growth $\Delta \tilde{l}_{i,t+1}$		
	(1)	(2)	(3)	
$\mathbb{E}_t[r_{t,t+h}]$	0.551***	0.236	$\mathbb{E}_t[\tilde{r}_{i,t,t+h}]$	-0.498***
<i>t</i> -stat	(5.046)	(0.893)	<i>t</i> -stat	(-3.058)
$\mathbb{E}_t[e_{t,t+h}]$	-0.041	-0.018	$\mathbb{E}_t[\tilde{e}_{i,t,t+h}]$	0.154
<i>t</i> -stat	(-0.108)	(-0.050)	<i>t</i> -stat	(1.304)
$\mathbb{F}_t[r_{t,t+h}] - \mathbb{E}_t[r_{t,t+h}]$	-0.006		$\mathbb{F}_t[\tilde{r}_{i,t,t+h}] - \mathbb{E}_t[\tilde{r}_{i,t,t+h}]$	-0.043
<i>t</i> -stat	(-0.033)		<i>t</i> -stat	(-0.410)
$\mathbb{F}_t[e_{t,t+h}] - \mathbb{E}_t[e_{t,t+h}]$	-0.701***		$\mathbb{F}_t[\tilde{e}_{i,t,t+h}] - \mathbb{E}_t[\tilde{e}_{i,t,t+h}]$	0.759***
<i>t</i> -stat	(-5.584)		<i>t</i> -stat	(6.412)
Labor Market Factors	Yes	Yes	Labor Market Factors	Yes
<i>N</i>	76	76	<i>N</i>	380
Adj. R^2	0.528	0.745	Adj. R^2	0.135
OOS R^2	0.149	0.254	OOS R^2	0.207
				0.447

Notes: This table reports predictive regressions of log annual growth in the unemployment rate (time-series) and employment growth (cross-section) from equation (A.5), under subjective or rational expectations. Labor market factors in the time-series regression X_t include the log annual growth of lagged log unemployment rate u_t , log labor market tightness $\log \theta_t$ and log job separation rate $\log \delta_t$; cross-sectional regressions include the same set of controls at the portfolio level. The sample is quarterly from 2005Q1 to 2023Q4. OOS R^2 is defined as $1 - MSE_{Model}/MSE_{Benchmark}$. Out-of-sample forecasts are constructed as 1-year-ahead predictions using model parameters estimated over a rolling 10-year window. $MSE_{Model}/MSE_{Benchmark}$ denotes the ratio of each model's out-of-sample mean squared forecast error to that of a benchmark, which is the Survey of Professional Forecasters (SPF) consensus for time-series predictions and an AR(1) model for cross-sectional predictions. Newey-West corrected (time-series) and two-way clustering by portfolio and quarter (cross-sectional) *t*-statistics with lags = 4 are reported in parentheses: *sig. at 10%. **sig. at 5%. ***sig. at 1%.

Cross-Sectional Predictability of Employment Growth To complement the aggregate analysis, I examine whether belief distortions also explain cross-sectional differences in hiring behavior across firms. Start from the employment accumulation equation:

$$L_{i,t+1} = (1 - \delta_{i,t})L_{i,t} + H_{i,t} \quad (\text{A.6})$$

for firm i , where $\delta_{i,t}$ is the job separation rate and $H_{i,t}$ denotes hires. Then we can approximate employment growth $\Delta L_{i,t+1} \equiv \Delta \log L_{i,t+1}$ as:

$$\Delta L_{i,t+1} \approx h_{i,t} - \delta_{i,t} \quad (\text{A.7})$$

where $h_{i,t} = H_{i,t}/L_{i,t}$ is the hiring rate. As shown in Section 5, the hiring rate reflects the firm's valuation of a job match and embeds forward-looking expectations of return, cash flow, and terminal value:

$$h_{i,t} = -\mathbb{F}_t[r_{i,t,t+j}] + \mathbb{F}_t[e_{i,t,t+j}] + \mathbb{F}_t[pe_{i,t,t+j}], \quad (\text{A.8})$$

where expectations are formed under the firm's subjective belief measure \mathbb{F}_t . Substituting into the employment growth approximation yields a predictive regression:

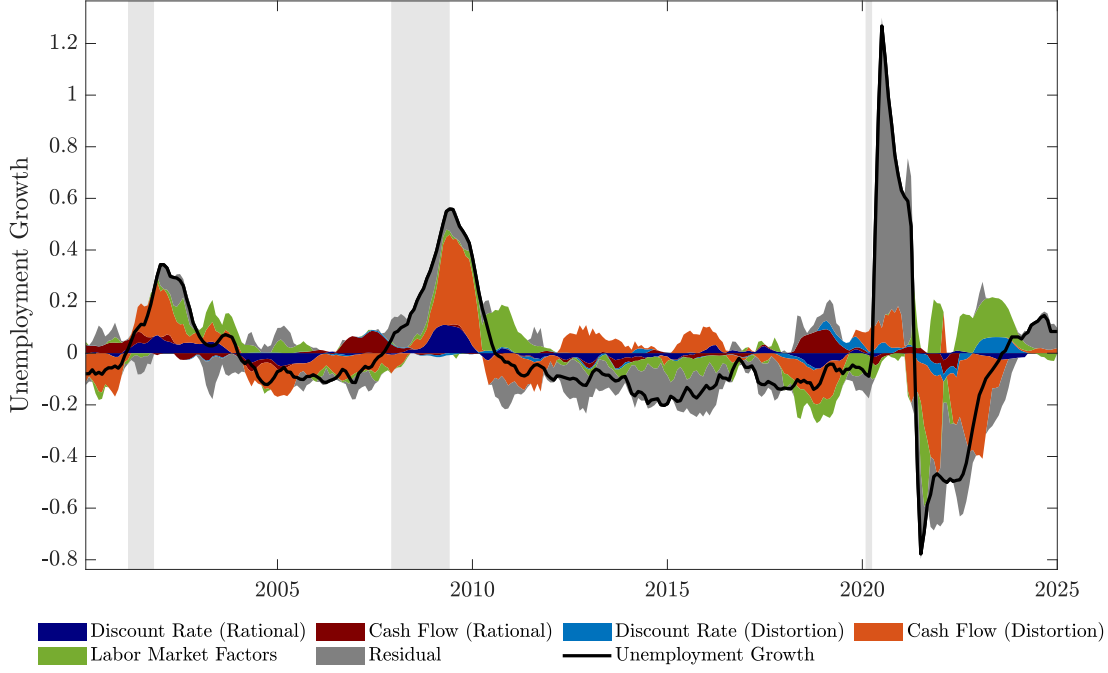
$$\Delta \tilde{l}_{i,t+1} = \alpha_i - \beta_1 \mathbb{F}_t[\tilde{r}_{i,t,t+j}] + \beta_2 \mathbb{F}_t[\tilde{e}_{i,t,t+j}] + \beta_3 \tilde{\delta}_{i,t} + \varepsilon_{i,t+1}, \quad (\text{A.9})$$

where α_i denotes a firm fixed effect, and $\delta_{i,t}$ is included directly as a control for firm-level separations. The terminal price-earnings term $\mathbb{F}_t[\tilde{pe}_{i,t,t+j}]$ has been dropped due to its near collinearity with expected returns and expected earnings growth under the Campbell and Shiller (1988) present value identity. To isolate cross-sectional variation, I demean each variable across the firms, defining $\tilde{x}_{i,t} = x_{i,t} - \frac{1}{5} \sum_{j=1}^5 x_{j,t}$ for variable x . This specification can be estimated using panel methods with firm and time fixed effects. To isolate the contribution of belief distortions, I further decompose each subjective expectation \mathbb{F}_t into its rational expectation \mathbb{E}_t and its distortion $\mathbb{F}_t - \mathbb{E}_t$:

$$\begin{aligned} \Delta \tilde{l}_{i,t+1} = & \alpha_i - \beta_{1,\mathbb{E}} \mathbb{E}_t[\tilde{r}_{i,t,t+j}] - \beta_{1,\mathbb{F}} (\mathbb{F}_t[\tilde{r}_{i,t,t+j}] - \mathbb{E}_t[\tilde{r}_{i,t,t+j}]) \\ & + \beta_{2,\mathbb{E}} \mathbb{E}_t[\tilde{e}_{i,t,t+j}] + \beta_{2,\mathbb{F}} (\mathbb{F}_t[\tilde{e}_{i,t,t+j}] - \mathbb{E}_t[\tilde{e}_{i,t,t+j}]) + \beta_3 \tilde{\delta}_{i,t} + \varepsilon_{i,t+1}. \end{aligned} \quad (\text{A.10})$$

If firms overreact to news about cash flows, we expect significant positive coefficients on $\beta_{2,\mathbb{F}}$, reflecting inflated expectations of future cash flows that induce excessive hiring. Similarly, if firms overreact to news about discount rates, we may observe large distortions in $\beta_{1,\mathbb{F}}$.

Figure A.14: Time-Series Decomposition of the U.S. Unemployment Rate



Notes: Figure plots decompositions of log annual growth in the unemployment rate from equation (A.80), using rational expectations \mathbb{E}_t and belief distortions $\mathbb{F}_t - \mathbb{E}_t$ of expected cash flows and discount rates. Labor market factors include the log annual growth of lagged unemployment Δu_t , labor market tightness $\Delta\theta_t$ and job separations $\Delta\delta_t$. Residual (dark gray) represents the variation in vacancy filling rates that are not captured by the other components. Subjective expectations \mathbb{F}_t are based on survey forecasts from CFOs and IBES financial analysts. Rational expectations \mathbb{E}_t are based on machine learning forecasts from Long Short-Term Memory (LSTM) neural networks. NBER recessions are shown with light gray shaded bars.

Table A.7 column (3) predicts portfolio-level employment growth using only machine forecasts of future returns and earnings growth. Rational return expectations $\mathbb{E}_t[\tilde{r}_{i,t,t+j}]$ predict future employment growth (coefficient -0.498), consistent with the search model's implication that firms hire more when the expected value of a match rises due to lower discounting. In contrast, the rational cash flow expectation $\mathbb{E}_t[\tilde{e}_{i,t,t+j}]$ is not a significant predictor, although the size of the estimate remains nontrivial (coefficient 0.154).

Column (4) extends the baseline model by incorporating belief distortions in subjective return and cash flow expectations. Strikingly, distortions in subjective cash flow expectations $\mathbb{F}_t[\tilde{e}_{i,t,t+j}] - \mathbb{E}_t[\tilde{e}_{i,t,t+j}]$ emerge as the dominant predictor of future employment growth, with a large and statistically significant coefficient of 0.759. At the same time, the coefficient on the machine return forecast falls to -0.119 and becomes statistically insignificant. The inclusion of belief distortions substantially improves the model's predictive accuracy. The adjusted R^2 rises from 0.135 to 0.253 in-sample, and the out-of-sample R^2 rises from 0.207 to 0.443, indicating that distorted expectations provide explanatory power beyond what is captured by rational benchmarks. These cross-sectional findings reinforce the aggregate evidence that survey expectations embed economically meaningful belief distortions driven by boom-bust cycles that help explain differences in hiring across firms.

Discussion The results can be informative about whether the survey-based subjective expectation is observationally equivalent to rational expectations. If subjective beliefs differ from rational beliefs only through a change of measure based on a Radon–Nikodym derivative that preserves its pricing implications, then subjective and rational forecasts should have equal predictive power for unemployment and hiring. While the gap $\mathbb{F}_t - \mathbb{E}_t$ might initially appear to represent a risk premium that should affect hiring, the crucial constraint is that pricing implications are preserved. This requires both return and cash flow expectations to move in perfect lock-step, canceling out their individual effects on the hiring decision. In that case, the difference between the two expectations should be pure noise and should not improve predictions.

However, the predictive regressions show that the belief distortion component $\mathbb{F}_t - \mathbb{E}_t$ has a highly significant explanatory power for both aggregate unemployment and cross-sectional employment growth. These results reject the null of observational equivalence and suggest that the implied stochastic discount factor under subjective beliefs is distinct from the one used under rational expectations. This difference implies that deviations from rational expectations can

meaningfully influence real decisions.

In particular, the cross-sectional predictability results point to a meaningful departure from standard search models that assume a common, rational stochastic discount factor across firms. Rather than rational variation in discount rates, the evidence indicates that distorted beliefs about future cash flows are the main driver of both aggregate unemployment fluctuations and cross-sectional differences in hiring. If subjective and rational beliefs differed only by a change of measure, they would have similar predictive power. The result that belief distortions in cash flows predict cross-sectional differences in hiring better than rational discount rate forecasts suggests that the distortion term varies substantially across firms. Firm-specific differences in the distortion term implies that subjective beliefs influence the perceived value of job creation in firm-specific ways, possibly reflecting differences in perceived patience or risk even when fundamentals are held constant. These findings suggest the need for models that allow for heterogeneous and biased beliefs, rather than relying on a uniform stochastic discount factor with no distortions.

A.6 Gradual Adjustment of Expectations

To provide evidence on the dynamics of belief formation, this section examines how survey respondents revise their expectations about future earnings following an earnings surprise. The following regression estimates the responsiveness of long-horizon forecasts to short-term earnings news:

$$\mathbb{F}_{t+j}[\tilde{x}_{i,t+h}] - \mathbb{F}_{t+j-1}[\tilde{x}_{i,t+h}] = \alpha_{h,j} + \gamma_{h,j}(\tilde{x}_{i,t+1} - \mathbb{F}_t[\tilde{x}_{i,t+1}]) + \eta_{h,t+j},$$

where $\mathbb{F}_{t+j}[\tilde{x}_{i,t+h}]$ denotes the expectation formed at time $t+j$ for earnings-related variable \tilde{x} at horizon h , and $\tilde{x}_{i,t+1} - \mathbb{F}_t[\tilde{x}_{i,t+1}]$ captures the earnings surprise. The coefficient $\gamma_{h,j}$ measures how much of the surprise is incorporated into expectations for long-run outcomes.

Table A.8 reports estimates for two forward-looking variables: (a) long-run earnings growth, and (b) the long-run ratio of earnings to employment. The target horizon is fixed at $h = 5$ years, while the revision horizon j ranges from 1 to 4 years. The estimated $\gamma_{h,j}$ coefficients are uniformly small and often statistically insignificant, indicating that respondents only partially incorporate short-term earnings news into their long-run expectations. This pattern is consistent with models of belief formation under constant-gain learning, in which agents update expectations gradually and exhibit fading memory. In such models, a fixed updating gain leads to persistent deviations from rational expectations and a breakdown of the law of iterated expectations.

Table A.8: Gradual adjustment of expectations

Target Horizon h (Years)	5	5	5	5
Revision Horizon j (Years)	1	2	3	4
Survey Forecast Revisions: $\mathbb{F}_{t+j}[\tilde{x}_{i,t+h}] - \mathbb{F}_{t+j-1}[\tilde{x}_{i,t+h}] = \alpha_{h,j} + \gamma_{h,j}(\tilde{x}_{i,t+1} - \mathbb{F}_t[\tilde{x}_{i,t+1}]) + \eta_{h,t+j}$				
(a) Earnings Growth	0.0929 (0.0734)	0.0934 (0.0455)	0.1121 (0.0776)	0.1245 (0.0743)
(b) Earnings to Employment	0.0600 (0.1281)	0.0508 (0.0725)	0.0697 (0.0321)	0.0745 (0.0419)

Notes: Table shows the gradual adjustment of expectations about future earnings $\tilde{x}_{i,t+h}$ after an earnings surprise at $t+1$. Sample: 2005Q1 to 2023Q4. Newey-West t -statistics with lags = 4 reported in parentheses: *sig. at 10%. **sig. at 5%. ***sig. at 1%.

A.7 Method of Simulated Moments Estimation

This section describes the Method of Simulated Moments (MSM) implementation for the constant-gain learning model. The estimation proceeds in three steps: (i) define the parameters to be estimated, (ii) specify the empirical statistics S_N to be matched, and (iii) derive the model-implied counterparts $S(\theta)$ that map parameters into moments.

Parameters estimated. The MSM estimation targets a parameter vector

$$\theta \equiv (\nu, \phi, \sigma_u, r_f, \gamma, \phi_e, \sigma_v),$$

where ν is the constant-gain learning rate, (ϕ, σ_u) govern the aggregate earnings process, r_f is the risk-free rate, γ is relative risk aversion, and (ϕ_e, σ_v) govern the idiosyncratic earnings process. Other parameters (e.g., separation rate, matching-function elasticity) are calibrated externally as described in Table 1.

Empirical statistics. The set of empirical statistics S_N used in the objective function consists of twelve moments: the volatility and autocorrelation of aggregate price–earnings ratios, the volatility of aggregate stock returns, the volatility of aggregate earnings growth, the volatility of the vacancy filling rate, three statistics for idiosyncratic earnings growth (variance, autocorrelation, and cross-sectional dispersion), the volatility of idiosyncratic stock returns, the volatility of idiosyncratic price–earnings ratios, the mean price–earnings ratio, and the Coibion–Gorodnichenko regression slopes at horizons $h = 4$ and $h = 8$. The degrees of freedom for the over-identification test therefore correspond to twelve matched moments and seven free parameters.

Model mappings. The model delivers simulated analogs $S(\theta)$ for each of the nine empirical statistics. These mappings tie the data moments directly to the estimated parameters. For the earnings growth block, aggregate earnings follow the process

$$e_t = \mu + \phi e_{t-1} + u_t, \quad u_t \sim \mathcal{N}(0, \sigma_u^2),$$

so that $\Delta e_t = (\phi - 1)e_{t-1} + u_t$. In the stationary distribution, the variance of earnings is $\text{Var}(e_t) = \sigma_u^2 / (1 - \phi^2)$. This leads to exact mappings for the variance and autocorrelation of growth:

$$\text{Var}(\Delta e_t) = \frac{(\phi - 1)^2}{1 - \phi^2} \sigma_u^2 + \sigma_u^2, \quad (\text{A.11})$$

$$\rho_{\Delta e}(1) = \frac{(\phi - 1)^2 \frac{\phi}{1 - \phi^2} \sigma_u^2 + (\phi - 1) \sigma_u^2}{\frac{(\phi - 1)^2}{1 - \phi^2} \sigma_u^2 + \sigma_u^2}. \quad (\text{A.12})$$

These moments provide direct information about the persistence and volatility parameters (ϕ, σ_u) . For expected returns, strip prices are given by

$$P_t^{(h)} = \exp\{A(h) + B(h)\mathbb{F}_t[\mu] + \phi^h e_t\},$$

where the coefficients are defined recursively as

$$A(h) = A(h-1) - r_f + \frac{1}{2}C(h)(C(h) - 2\gamma)\sigma_u^2, \quad (\text{A.13})$$

$$B(h) = \frac{1 - \phi^h}{1 - \phi}, \quad (\text{A.14})$$

$$C(h) = \nu B(h-1) + \phi^{h-1}. \quad (\text{A.15})$$

The expected return on a strip of maturity h is then

$$\mathbb{F}_t[R_{t+1}^{(h)}] = \exp\{r_f + C(h)\gamma\sigma_u^2\}. \quad (\text{A.16})$$

The aggregate stock return is constructed as the value-weighted average of strip returns,

$$R_{t+1} = \sum_{h \geq 1} w_{t,h} R_{t+1}^{(h)}, \quad w_{t,h} = \frac{P_t^{(h)}}{\sum_{k \geq 1} P_t^{(k)}}. \quad (\text{A.17})$$

Simulation of (A.16)-(A.17) yields the model-implied mean and volatility of returns, and thereby helps to identify γ jointly with (ϕ, σ_u) . For the price-earnings ratio, the Campbell-Shiller log-linearization implies

$$pe_t = c_{pe} - r_{t+1} + \Delta e_{t+1} + \rho pe_{t+1}, \quad (\text{A.18})$$

Simulating (A.18) provides the model-implied volatility and persistence of pe_t , which are jointly informative about ν, ϕ , and γ . For the Coibion and Gorodnichenko (2015) regression coefficient, start by noting that earnings follow an AR(1) process

$$e_t = \mu + \phi e_{t-1} + u_t, \quad u_t \sim \mathcal{N}(0, \sigma_u^2),$$

so that

$$\Delta e_t = (\phi - 1)e_{t-1} + u_t.$$

Beliefs update with constant gain ν according to

$$\mathbb{F}_t[\mu] - \mathbb{F}_{t-1}[\mu] = \nu(\Delta e_t - \mathbb{F}_{t-1}[\Delta e_t]).$$

The one-step forecast error is

$$\text{FE}_{t,1} = \Delta e_t - \mathbb{F}_{t-1}[\Delta e_t] = u_t - \mathbb{F}_{t-1}[\mu],$$

and the h -step forecast revision is

$$\text{Rev}_{t,h} = \mathbb{F}_t[\Delta e_{t+h}] - \mathbb{F}_{t-1}[\Delta e_{t+h}] = \phi^{h-1}\nu \text{FE}_{t,1} + \phi^{h-1}(\phi - 1)\Delta e_t.$$

Iterating the updating recursion gives

$$\mathbb{F}_t[\mu] = \nu \sum_{j=0}^{\infty} (1 - \nu)^j u_{t-j},$$

which implies

$$\text{Var}(\mathbb{F}_t[\mu]) = \frac{\nu}{2-\nu} \sigma_u^2, \quad \text{Var}(\text{FE}_{t,1}) = \frac{2}{2-\nu} \sigma_u^2.$$

The covariance between earnings growth and the forecast error is

$$\text{Cov}(\Delta e_t, \text{FE}_{t,1}) = \sigma_u^2 - (\phi - 1) \frac{\nu}{1 - \phi(1 - \nu)} \sigma_u^2,$$

so that

$$\frac{\text{Cov}(\Delta e_t, \text{FE}_{t,1})}{\text{Var}(\text{FE}_{t,1})} = \frac{2 - \nu}{2} \cdot \frac{1 - \phi + \nu}{1 - \phi + \phi\nu}.$$

Therefore the CG slope is

$$\beta^{CG}(h) = \frac{\text{Cov}(\text{Rev}_{t,h}, \text{FE}_{t,1})}{\text{Var}(\text{FE}_{t,1})} = \phi^{h-1} \left[\nu + (\phi - 1) \frac{2 - \nu}{2} \cdot \frac{1 - \phi + \nu}{1 - \phi + \phi\nu} \right].$$

These statistics discipline the constant-gain parameter ν .

MSM criterion. The estimator minimizes the distance between empirical and model-implied moments:

$$\hat{\theta}_N = \arg \min_{\theta} (S_N - S(\theta))' W_N^{-1} (S_N - S(\theta)).$$

In the first step, the weighting matrix W_N is set to the identity. In the second step, it is replaced by a heteroskedasticity and autocorrelation robust covariance matrix of the empirical moments, with regression-based moments adjusted by the delta method. The minimized criterion also yields a test of overidentifying restrictions with degrees of freedom equal to the number of moments minus the number of estimated parameters.

Estimation results. Table A.9 reports the results of the MSM estimation. Panel A compares each data moment to its model counterpart and reports the t -statistic of the difference based on the step two weighting matrix. Panel B lists the estimated values of the parameters ν , ϕ , σ_u , r_f , and γ . Panel C reports the parameters that are held fixed during estimation, such as the time discount factor ρ , matching efficiency B , matching elasticity η , separation rate δ , and vacancy posting cost κ . The final rows of Panel B report the minimized value of the MSM criterion and the associated p -value of the overidentification test. These results summarize how the model parameters map into the observed dynamics of earnings, returns, price-earnings ratios, and learning coefficients, providing a joint test of the model's ability to replicate the empirical moments.

Table A.9: Model Estimation Outcome

Moment or parameter	Data	Model	<i>t</i> statistic
Panel A: Moments			
Mean log stock return	0.072	0.088	-0.510
SD log stock return	0.160	0.118	0.568
Mean log risk free rate	0.046	0.045	0.144
Mean of log price earnings	2.980	2.392	0.424
SD of log price earnings	0.285	0.293	-0.084
AC of log price earnings	0.750	0.798	-0.457
SD of aggregate earnings growth	0.268	0.294	-0.455
AC of aggregate earnings growth	-0.144	-0.142	-0.045
SD of idiosyncratic earnings growth	0.112	0.091	0.388
AC of idiosyncratic earnings growth	-0.027	-0.023	-0.304
CG slope $h = 4$ aggregate	-0.263	-0.266	0.063
CG slope $h = 8$ aggregate	-0.463	-0.454	-0.040
Panel B: Estimated Parameters			
Gain coefficient ν	0.013		
AR coefficient aggregate ϕ	0.854		
AR coefficient idiosyncratic ϕ_e	0.936		
Aggregate shock standard deviation σ_u	0.271		
Idiosyncratic shock standard deviation σ_v	0.086		
Risk free rate r_f	0.045		
Risk aversion γ	1.647		
Test statistic W_N	728.457		
p value of W_N	0.000		
Panel C: Assigned Parameters			
Time discount factor ρ (Campbell and Shiller (1988))	0.980		
Matching function efficiency B (Kehoe et al. (2023))	0.562		
Matching function elasticity η (Kehoe et al. (2023))	0.500		
Separation rate δ (Kehoe et al. (2023))	0.286		
Per worker hiring cost κ (Elsby and Michaels (2013))	0.314		

Notes: This table reports data moments, moments from the estimated model, parameter estimates, and test statistics. The model is calibrated at an annual frequency.

A.8 Regional Model and Shift-Share Instrument

The aggregate analysis in Section 6 shows that belief distortions in subjective expectations play an important role in explaining hiring fluctuations. This section extends that analysis by exploiting cross-sectional variation in state-level data to strengthen identification and test whether the theoretical mechanism generalizes beyond aggregate dynamics.

Overview While the aggregate-level variance decompositions are informative, they cannot establish causality. The limited number of business cycles in the time series also restricts inference. This section addresses these challenges by extending the aggregate model to a regional framework. In estimating the regional model, I introduce a Bartik shift-share instrument for survey expectations to address endogeneity challenges in identifying the relative importance of subjective discount rate and cash flow expectations. Specifically, I investigate whether regional labor markets characterized by more distorted subjective cash flow expectations experience larger swings in vacancy filling rates. This analysis is motivated by empirical evidence of substantial geographic variation in unemployment dynamics, especially during crises (Beraja et al., 2019, Kehoe et al., 2019; Chodorow-Reich and Wieland, 2020). While existing work studies these regional differences under a rational expectations framework, differences in subjective beliefs may also be an important explanatory factor.

Regional Model To guide the empirical strategy, I extend the baseline search model to a multi-region, multi-sector environment, building from the models in Kehoe et al. (2019) and Chodorow-Reich and Wieland (2020). The economy consists of a continuum of islands indexed by s . Each island produces a differentiated variety of tradable goods that is consumed everywhere and a nontradable good. Both of these goods are produced using intermediate goods. Each consumer is endowed with one of two types of skills which are used in different intensities in the nontradable and tradable goods sectors. Labor is immobile across islands but can switch sectors. This assumption aligns with empirical evidence indicating that labor markets are predominantly local in nature (Manning and Petrongolo, 2017). Consumers receive utility from a composite consumption good that is either purchased in the market or produced at home. Consumers and firms are ex-ante homogeneous and share the same subjective belief measure $\mathbb{F}_t[\cdot]$. The islands only differ in the shocks that hit them.

Predictability of Regional Unemployment Rates In this environment, the log unemployment rate $u_{s,t+1}$ in region s approximately satisfies the following predictive relationship:

$$u_{s,t+1} = \beta_r \mathbb{F}_t[r_{s,t,t+h}] + \beta_e \mathbb{F}_t[e_{s,t,t+h}] + \gamma' X_{s,t} + \alpha_s + \alpha_t + \varepsilon_{s,t+1} \quad (\text{A.19})$$

where $X_{s,t} \equiv [u_{s,t}, \log \theta_{s,t}, \log \delta_{s,t}]'$ collects standard labor market controls: the lagged unemployment rate $u_{s,t}$, the log vacancy-to-unemployment ratio $\log \theta_{s,t}$, and the log separation rate $\log \delta_{s,t}$. The cross-sectional unit s corresponds to U.S. states, and time t is measured at the monthly frequency. Following Korniotis (2008), each firm is assigned to the state in which it is headquartered. The regression includes state fixed effects α_s to absorb time-invariant regional heterogeneity and time fixed effects α_t to capture national shocks. The coefficients of interest, β_r and β_e , quantify the effect of subjective expectations about discount rates and cash flows, respectively, on future unemployment.

This regional equation extends the aggregate specification in equation (A.5), and is designed to test whether perceived shocks to discount rates or earnings forecasts help explain variation in unemployment across local labor markets. If firms form biased beliefs about future returns or earnings, those belief distortions should manifest in regional hiring behavior and thus influence unemployment at the state level. A counterpart regression can be estimated under rational expectations by replacing $\mathbb{F}_t[\cdot]$ with machine learning-based forecasts $\mathbb{E}_t[\cdot]$.

Empirical Specification: OLS As a baseline, I estimate the regression above using multivariate OLS applied to a panel of state-level data. This allows for a direct assessment of whether variation in firm-level beliefs, aggregated to the state level, predicts changes in unemployment. The future price-earnings ratio term $\mathbb{F}_t[pe_{s,t,t+h}]$ is omitted from the regression due to its near collinearity with forecasted discount rates and cash flows via the present-value identity of Campbell and Shiller (1988). State-level forecasts of discount rates $\mathbb{F}_t[r_{s,t,t+h}]$ are constructed from IBES price target forecasts. These targets are used to infer expected returns by back-solving from analysts' price projections. Forecasts are assigned to states based on firm headquarters and then aggregated using value-weighted averages. Expected cash flows $\mathbb{F}_t[e_{s,t,t+h}]$ are constructed analogously from IBES analyst forecasts of earnings per share.

Regional labor market variables are constructed from publicly available BLS datasets. Unemployment rates $u_{s,t}$ are sourced from the Local Area Unemployment Statistics (LAUS). The vacancy-to-unemployment ratio $\theta_{s,t}$ is computed using job openings from the state-level Job Openings and Labor Turnover Survey (JOLTS) combined with unemployment counts from LAUS. Separation rates $\delta_{s,t}$ are also taken from JOLTS. Monthly series are time-aggregated to the quarterly frequency by averaging values within each quarter.

Empirical Specification: Bartik Shift-Share Instrument A key challenge in estimating the regional decomposition is that regional labor market conditions and subjective expectations may be jointly determined, potentially leading to biased estimates. For example, firms might revise their beliefs in response to local shocks in unemployment or hiring,

making it difficult to separate cause from effect. Additionally, state-level aggregates of firm-level forecasts may suffer from measurement error if the geographic scope of a firm's operations does not align with the location of its headquarters.

To address these concerns, I construct a leave-one-out Bartik-style shift-share instrument $\widehat{\mathbb{F}}_t[y_{s,t,t+h}]$ that isolates plausibly exogenous variation in subjective expectations at the regional level, while avoiding mechanical feedback between local shocks and the national forecast component:

$$\widehat{\mathbb{F}}_t[y_{s,t,t+h}] = \sum_{i \in I} \phi_{s,i,t-1} \cdot \mathbb{F}_t^{-s}[y_{i,t+h}], \quad \phi_{s,i,t} = \frac{L_{s,i,t}}{\sum_{i' \in I} L_{s,i',t}}, \quad y \in \{r, e\} \quad (\text{A.20})$$

Here, $\phi_{s,i,t}$ denotes the lagged employment share of industry i in state s , sourced from the Quarterly Census of Employment and Wages (QCEW). $\mathbb{F}_t^{-s}[y_{i,t+h}]$ is the national IBES forecast for industry i constructed by excluding all firms headquartered in state s . The leave-one-out structure ensures that local shocks in state s do not mechanically influence the national industry-level forecasts used to construct the instrument, strengthening the validity of the exogeneity assumption. Using the leave-one-out Bartik instrument, I estimate the following predictive regression:

$$u_{s,t+1} = \beta_r \widehat{\mathbb{F}}_t[r_{s,t,t+h}] + \beta_e \widehat{\mathbb{F}}_t[e_{s,t,t+h}] + \gamma' X_{s,t} + \alpha_s + \alpha_t + \varepsilon_{s,t+1} \quad (\text{A.21})$$

The coefficients β_r and β_e now reflect the causal effect of variation in subjective discount rate and earnings expectations that is exogenous to state-specific labor market conditions.

Identification Assumptions Compared to the OLS specification, the Bartik approach offers stronger identification by addressing both measurement error and endogeneity concerns. First, it reduces measurement error by replacing noisy state-level aggregates of firm-level forecasts with industry-level forecasts weighted by predetermined employment shares. Second, it mitigates endogeneity by exploiting the fact that national industry trends in expectations are unlikely to respond to contemporaneous state-level labor market shocks.

For example, consider a scenario where national energy sector earnings expectations surge due to geopolitical developments. The shift-share instrument would assign Texas (with high energy employment shares) a much larger increase in instrumented expectations than Vermont (with minimal energy exposure). Crucially, this variation stems from predetermined industrial composition interacted with national sectoral trends, rather than from endogenous responses to Texas-specific labor market conditions or measurement error in aggregating individual firm forecasts within Texas.

The identifying assumption is that, conditional on fixed effects and controls, there are no omitted factors that simultaneously affect both national industry-level expectations and local hiring behavior in states more exposed to those industries. While many shift-share designs rely on the exogenous shocks assumption, in our setting the exogenous shares assumption is likely more appropriate. In sectors where specific regions have large exposures to (e.g., Texas in oil energy), national energy industry-level expectations $\mathbb{F}_t[e_{i,t,t+h}]$ may be influenced by news from firms headquartered in those regions. Even with the leave-one-out construction, regional developments can create spillover effects that contaminate the national industry shock. For example, a slowdown in hiring or disappointing earnings guidance from large Texas energy firms could cause IBES analysts to revise downward their national energy sector earnings forecasts. If so, the national shock would be endogenous to Texas-specific developments, violating the exogenous shock assumption. In contrast, the state-level industry shares $\phi_{s,i,t-1}$, measured using lagged QCEW employment data, reflect slow-moving industrial structure and are plausibly predetermined. We therefore treat industry shares as conditionally exogenous and interpret our identification through the lens of the exogenous shares assumption following Borusyak et al. (2025).

This assumption would be violated, for example, if pre-existing trends in local demand systematically coincided with national shocks. To mitigate this concern, I include a rich set of controls and fixed effects. Specifically, state fixed effects α_s absorb time-invariant differences in labor market characteristics across states. Time fixed effects α_t account for common national shocks such as business cycles or federal policy changes. By leveraging only the cross-sectional variation in state exposure to national shocks, the Bartik specification helps isolate the exogenous component of belief-driven hiring fluctuations.

Cross-Sectional Decomposition of the State-Level Unemployment Rate Table A.10 reports regression estimates that evaluate the predictive power of state-level expectations for future unemployment. Each column adds different combinations of rational or subjective forecasts for discount rates and cash flows, with all specifications controlling for standard labor market factors and including both state and time fixed effects.

The estimates demonstrate that subjective earnings expectations are not only informative about regional unemployment but crowd out the predictive power of rational components. Column (1) shows that rational discount rate expectations $\mathbb{E}_t[r_{s,t,t+5}]$ significantly predict unemployment, with a coefficient of 0.725 and R^2 of 0.414. This implies that a one standard deviation increase in rational discount rate expectations predicts a 0.240 percentage point increase in the unemployment rate. Column (2) shows that among subjective forecasts, only expected earnings $\mathbb{F}_t[e_{s,t,t+5}]$ matter, with a large negative coefficient (-0.817) and higher explanatory power ($R^2 = 0.558$). A one standard deviation increase in

expected earnings predicts a 0.129 percentage point decrease in the unemployment rate. Column (3) includes both sets of expectations. Subjective earnings dominate: their coefficient remains significant (-0.791), while rational expectations become insignificant.

Column (4) repeats the rational-only regression using Bartik instruments; the discount rate remains significant (0.572), implying a 0.181 percentage point increase in unemployment per standard deviation increase in instrumented discount rate expectations. In Column (5), only instrumented subjective earnings are significant (-0.690), with a standard deviation of 0.168 implying a 0.116 percentage point decrease in unemployment. Column (6) confirms that instrumented subjective earnings expectations (-0.708) continue to drive out all other predictors, implying a 0.119 percentage point decline in unemployment for a one standard deviation increase.

The shift-share estimates are generally smaller in magnitude than their OLS counterparts, as expected, since the shift-share instrument isolates only variation that is plausibly exogenous to regional labor market conditions. The attenuation suggests that some of the OLS signal reflects endogenous responses to regional shocks, such as changes in local labor supply, that amplify belief-driven dynamics. Nevertheless, the fact that the earnings coefficient remains large and significant under instrumentation supports a causal interpretation: belief distortions about cash flows play a central role in driving unemployment fluctuations across regions.

Taken together, the results provide robust evidence that distorted beliefs about future earnings are a key driver of regional labor market volatility. The strong and consistent link between subjective earnings expectations and unemployment, even when instrumented, suggests that firms' hiring decisions are shaped not only by fundamentals but also by biased beliefs. Regions where firms overreact to cash flow news experience deeper hiring cuts during downturns and more aggressive expansions during booms, thereby driving business cycle volatility. These findings indicate that persistent regional differences in unemployment may arise not only from structural characteristics such as industry mix or demographics, but also from variation in how firms perceive and respond to economic signals.

Table A.10: Predictability of the State-Level Unemployment Rate

	Dependent Variable: Log Unemployment Rate u_{t+1}					
	OLS			Shift-Share Instrument		
	(1)	(2)	(3)	(4)	(5)	(6)
$\mathbb{E}_t[r_{s,t,t+h}]$	0.725*** (0.235)		0.470 (0.780)	0.572*** (0.222)		0.207 (0.240)
$\mathbb{E}_t[e_{s,t,t+h}]$	-0.247 (0.499)		-0.065 (0.182)	-0.064 (0.075)		0.005 (0.168)
$\mathbb{F}_t[r_{s,t,t+h}]$		0.248 (0.297)	0.233 (0.300)		0.052 (0.228)	0.052 (0.228)
$\mathbb{F}_t[e_{s,t,t+h}]$		-0.817*** (0.236)	-0.791*** (0.242)		-0.690*** (0.160)	-0.708*** (0.200)
R^2	0.414	0.558	0.558	0.414	0.549	0.549
State FE	Yes	Yes	Yes	Yes	Yes	Yes
Time FE	Yes	Yes	Yes	Yes	Yes	Yes
Labor Market Factors	Yes	Yes	Yes	Yes	Yes	Yes
N	4,358	4,358	4,358	4,358	4,358	4,358

Notes: Labor market factors include the log annual growth of lagged log unemployment rate $u_{s,t}$, log labor market tightness $\log \theta_{s,t}$ and log job separation rate $\log \delta_{s,t}$. The sample is quarterly from 2005Q1 to 2023Q4. Newey-West corrected t -statistics with lags = 4 are reported in parentheses: *sig. at 10%. **sig. at 5%. ***sig. at 1%.

A.9 Capital Investment

This section extends the baseline model by incorporating firm investment decisions and distinguishing between tangible and intangible capital. I show how belief distortions about future returns and earnings influence not only hiring decisions, but also capital investment behavior. I then decompose the investment rate into components associated with discount rates and cash flows.

Model Setup I assume firms produce output using a Cobb-Douglas production function that depends on both capital and labor inputs:

$$Y_{i,t} = A_{i,t} K_{i,t}^\alpha L_{i,t}^{1-\alpha}$$

where $A_{i,t}$ denotes total factor productivity, $K_{i,t} = K_{i,t}^{\text{phy}} + K_{i,t}^{\text{int}}$ is total capital input composed of tangible and intangible capital, and $L_{i,t}$ is labor input. Following Hall (2001) and Hansen et al. (2005), I treat tangible and intangible capital as perfect substitutes. Earnings are defined as:

$$E_{i,t} = Y_{i,t} - W_{i,t} L_{i,t} - \kappa V_{i,t} - I_{i,t} - \phi\left(\frac{I_{i,t}}{K_{i,t}}\right) K_{i,t}$$

where $W_{i,t}$ is the wage rate, $\kappa V_{i,t}$ is the vacancy posting cost, $I_{i,t} = I_{i,t}^{\text{phy}} + I_{i,t}^{\text{int}}$ is total investment, and $\phi(\cdot)$ denotes convex adjustment costs. I adopt a piecewise-quadratic specification for $\phi(\cdot)$ with different coefficients for expansion and contraction:

$$\phi\left(\frac{I_{i,t}}{K_{i,t}}\right) = \begin{cases} \frac{c_k^+}{2} \left(\frac{I_{i,t}}{K_{i,t}}\right)^2 & \text{if } I_{i,t} \geq 0 \\ \frac{c_k^-}{2} \left(\frac{I_{i,t}}{K_{i,t}}\right)^2 & \text{if } I_{i,t} < 0 \end{cases}$$

Firms choose investment $I_{i,t}$ and vacancies $V_{i,t}$ to maximize firm value:

$$V(A_{i,t}, K_{i,t}, L_{i,t}) = \max_{I_{i,t}, V_{i,t}} \{E_{i,t} + \mathbb{F}_t [M_{t+1} V(A_{i,t+1}, K_{i,t+1}, L_{i,t+1})]\}$$

subject to both capital and employment accumulation equations:

$$\begin{aligned} K_{i,t+1} &= (1 - \delta_{i,t}^k) K_{i,t} + I_{i,t} \\ L_{i,t+1} &= (1 - \delta_{i,t}^l) L_{i,t} + q_t V_{i,t} \end{aligned}$$

The first order condition with respect to investment implies:

$$1 + \phi' \left(\frac{K_{i,t+1} - (1 - \delta_{i,t}^k) K_{i,t}}{K_{i,t}} \right) = \frac{P_{i,t}}{K_{i,t+1}}$$

where $P_{i,t} = \mathbb{F}_t [M_{t+1} V(A_{i,t+1}, K_{i,t+1})]$ is the ex-dividend firm value.

Recovering Intangible Capital For each firm, I measure realized data on physical capital $K_{i,t}^{\text{phy}}$, tangible investment $I_{i,t}^{\text{phy}}$, depreciation rates $\delta_{i,t}^k$, and market value $P_{i,t}$. The physical capital stock $K_{i,t}^{\text{phy}}$ is measured using Compustat's PPEGT item, and tangible investment $I_{i,t}^{\text{phy}}$ is measured using capital expenditures (CAPX). The depreciation rate $\delta_{i,t}^k$ is calculated as depreciations (DP) as a share of physical capital stock (PPEGT), and applied to both tangible and intangible capital (Hall, 2001). I construct the firm's total market value $P_{i,t}$ as the sum of the market value of equity, the book value of debt, minus current assets. Starting from an initial value $K_{i,1970Q1} = P_{i,1970Q1}$, I recursively solve the first order condition for $K_{i,t+1}$, using observed investment, depreciation, and market value. Intangible capital is then recovered as the residual:

$$K_{i,t}^{\text{int}} = K_{i,t} - K_{i,t}^{\text{phy}}$$

Decomposition of Investment Rates Taking logs and linearizing the first order condition:

$$\log \left(1 + c_k \frac{I_{i,t}}{K_{i,t}} \right) \approx \log c_k + \log \left(\frac{I_{i,t}}{K_{i,t}} \right) = \log \left(\frac{P_{i,t}}{K_{i,t+1}} \right)$$

I decompose the right-hand side into price-to-earnings and earnings-to-capital terms:

$$\underbrace{\log \left(\frac{I_{i,t}}{K_{i,t}} \right)}_{ik_{i,t}} = -\log c_k + \underbrace{\log \left(\frac{P_{i,t}}{E_{i,t}} \right)}_{pe_{i,t}} + \underbrace{\log \left(\frac{E_{i,t}}{K_{i,t+1}} \right)}_{ek_{i,t}}$$

Using a Campbell and Shiller (1988) log-linear approximation for the price-earnings ratio:

$$pe_{i,t} = \sum_{j=1}^h \rho^{j-1} (c_{pe} + \Delta e_{i,t+j} - r_{i,t+j}) + \rho^h pe_{i,t+h}$$

Substituting yields the final decomposition:

$$ik_{i,t} = c_{ik} - \sum_{j=1}^h \rho^{j-1} r_{i,t+j} + \left(ek_{i,t} + \sum_{j=1}^h \rho^{j-1} \Delta e_{i,t+j} \right) + \rho^h pe_{i,t+h}$$

where $c_{ik} \equiv \frac{c_{pe}(1-\rho^h)}{1-\rho} - \log c_k$. To separately analyze tangible and intangible investment, I define $ik_{i,t}^m \equiv \log(\frac{I_{i,t}^m}{K_{i,t}})$ and $s_{i,t}^m \equiv \log(\frac{I_{i,t}^m}{I_{i,t}})$ so that:

$$ik_{i,t}^m = s_{i,t}^m + ik_{i,t}, \quad m = phy, int$$

implying the decomposition structure remains unchanged up to an additive shift $s_{i,t}^m$. I estimate the decomposition separately for tangible and intangible investment. The time-series decomposition of the aggregate investment rate is:

$$ik_t^m \approx - \sum_{j=1}^h \rho^{j-1} \mathbb{F}_t[r_{t+j}] + \left(ek_t + \sum_{j=1}^h \rho^{j-1} \mathbb{F}_t[\Delta e_{t+j}] \right) + \rho^h \mathbb{F}_t[pe_{t+h}]$$

where $x_t = \sum_{i \in I} x_{i,t}$ aggregates firm-level variable $x_{i,t}$. For the cross-section, demeaned variables yield:

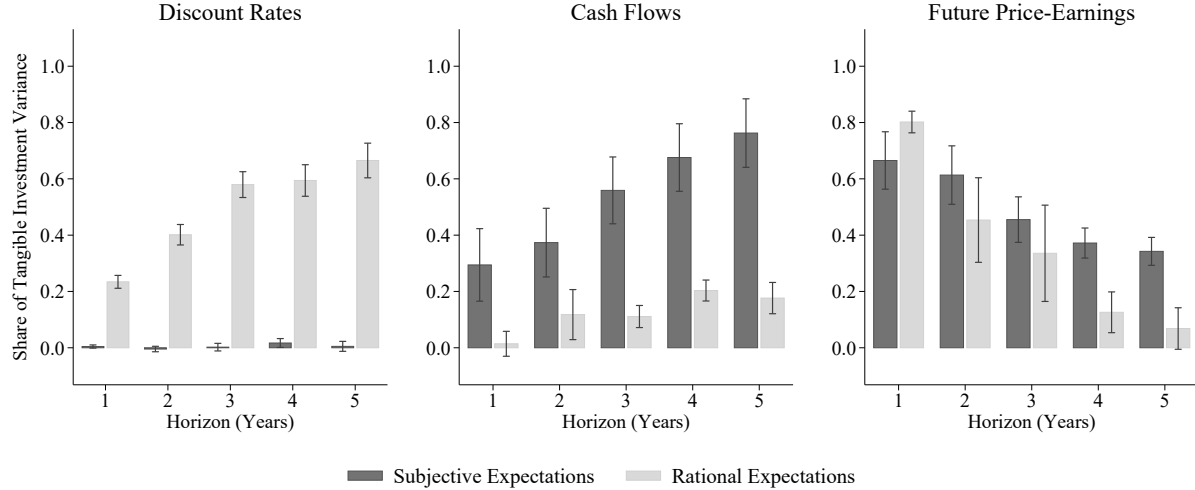
$$\tilde{ik}_{i,t}^m \approx - \sum_{j=1}^h \rho^{j-1} \mathbb{F}_t[\tilde{r}_{i,t+j}] + \left(\tilde{ek}_{i,t} + \sum_{j=1}^h \rho^{j-1} \mathbb{F}_t[\Delta \tilde{e}_{i,t+j}] \right) + \rho^h \mathbb{F}_t[\tilde{pe}_{i,t+h}]$$

where $\tilde{x}_{i,t} = x_{i,t} - \sum_{i \in I} x_{i,t}$ cross-sectionally demeans variable $x_{i,t}$.

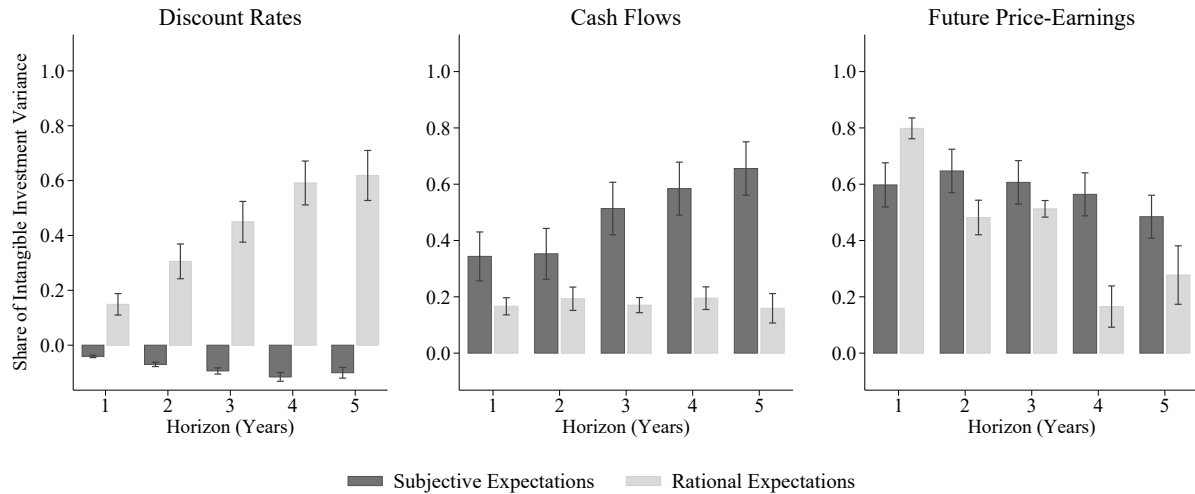
Results The empirical results mirror those for hiring rates, both in the time series (Figure A.15) and the cross-section (Figure A.16). Subjective expectations substantially overstate the contribution of cash flows and understate that of discount rates, both for tangible and intangible investment. Notably, the distortions are stronger for intangible investment, consistent with greater uncertainty and measurement error in expectations about intangible value creation. These findings highlight how belief distortions affect not only labor demand but also capital allocation decisions across asset types.

Figure A.15: Time-Series Decomposition of Capital Investment

(a) Tangible Capital Investment Rate



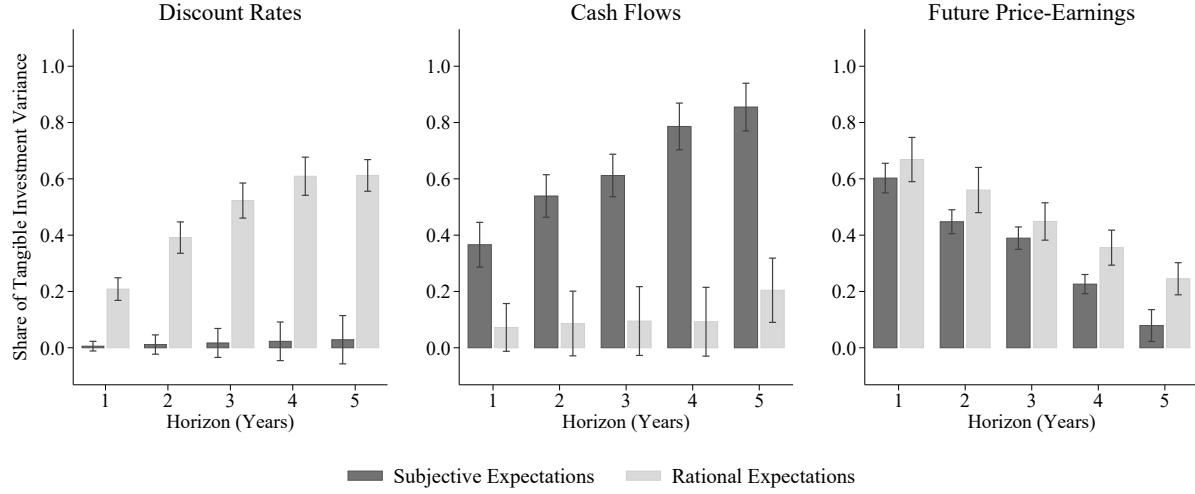
(b) Intangible Capital Investment



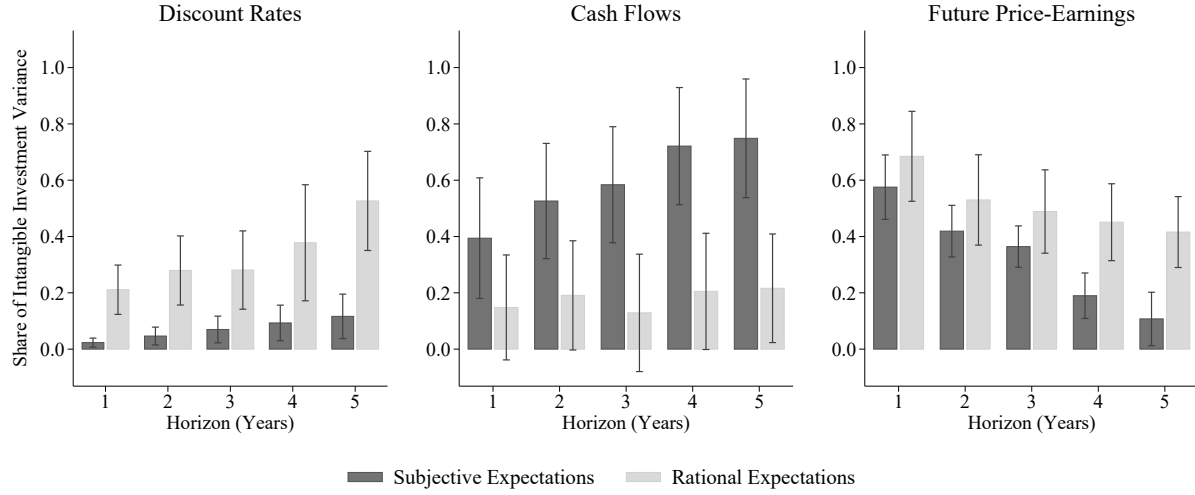
Notes: Figure illustrates the discount rate, cash flow, and future price-earnings components of the time-series decomposition of the aggregate tangible and intangible capital investment rate. Light bars show contributions under rational expectations; dark bars show contributions under subjective expectations. The sample is quarterly from 2005Q1 to 2023Q4. Each bar shows Newey-West 95% confidence intervals with lags = 4.

Figure A.16: Cross-Sectional Decomposition of Capital Investment

(a) Tangible Capital Investment Rate



(b) Intangible Capital Investment



Notes: Figure illustrates the discount rate, cash flow, and future price-earnings components of the cross-sectional decomposition to the dispersion of the current tangible and intangible capital investment rate. Light bars show contributions under rational expectations; dark bars show contributions under subjective expectations. The sample is quarterly from 2005Q1 to 2023Q4. Each bar shows Newey-West 95% confidence intervals with lags = 4.

A.10 Decreasing Returns to Scale and Composition Effects

Stock market valuations reflect average profits, while hiring decisions depend on marginal profits (Borovickova and Borovička, 2017). Decreasing returns to scale can amplify unemployment fluctuations even under a rational framework by making the marginal value of hiring more sensitive to productivity shocks, prompting firms to adjust vacancies more aggressively in response (Elsby and Michaels, 2013; Kaas and Kircher, 2015). Allowing for decreasing returns to scale introduces the notion of firm size. Changes in the equilibrium firm size distribution can thus introduce a composition effect that also contributes to fluctuations in the vacancy filling rate (Solon et al. (1994)).

This section relaxes the constant returns to scale (CRS) assumption by allowing for decreasing returns to scale (DRS) in the production function. Assume that firm i 's output is $Y_{i,t} = F(L_{i,t}) = A_{i,t}L_{i,t}^\alpha$, where $A_{i,t}$ is an exogenous productivity process and $0 < \alpha < 1$. This introduces a “DRS wedge” between marginal and average profits:

$$\pi_{i,t}L_{i,t} - \kappa V_{i,t} = \alpha A_{i,t}L_{i,t}^\alpha - W_{i,t}L_{i,t} - \kappa V_{i,t} = E_{i,t} - (1 - \alpha)Y_{i,t}$$

where $E_{i,t} \equiv \Pi_{i,t} - \kappa V_{i,t}$ is the firm's earnings, $\Pi_{i,t} \equiv Y_{i,t} - W_{i,t}L_{i,t} = A_{i,t}L_{i,t}^\alpha - W_{i,t}L_{i,t}$ is the total profit before wages $W_{i,t}L_{i,t}$ and vacancy posting costs $\kappa V_{i,t}$, and $\pi_{i,t} = \frac{\partial \Pi_{i,t}}{\partial L_{i,t}}$ is the marginal profit from hiring. The second term $(1 - \alpha)Y_{i,t}$ is a “DRS wedge” that captures the gap between the average profit and marginal profit. Under DRS, the firm's hiring condition becomes:

$$\frac{\kappa}{q_t} = \mathbb{F}_t \left[\sum_{j=1}^{\infty} \frac{1}{R_{i,t,t+j}} \left(\frac{E_{i,t+j}}{L_{i,t+1}} - (1 - \alpha) \frac{Y_{i,t+j}}{L_{i,t+1}} \right) \right]$$

where firm i takes the aggregate vacancy filling rate q_t as given. Express aggregate earning-employment and output-employment ratios as the employment-weighted average of firm-level ratios:

$$\frac{\kappa}{q_t} = \mathbb{F}_t \left[\sum_i \sum_{j=1}^{\infty} \frac{1}{R_{i,t,t+j}} \left(\frac{E_{i,t+j}}{L_{i,t+1}} - (1 - \alpha) \frac{Y_{i,t+j}}{L_{i,t+1}} \right) \frac{L_{i,t+1}}{L_{t+1}} \right]$$

Define $S_{i,t+1} \equiv \frac{L_{i,t+1}}{L_{t+1}}$ as the employment share, $EL_{i,t+j} \equiv E_{i,t+j}/L_{i,t+1}$ the earnings-employment ratio, and $YL_{i,t+j} \equiv Y_{i,t+j}/L_{i,t+1}$ the output-employment ratio of firm i . Log linearize the expression around the steady state:

$$\log q_t = \sum_{j=1}^{\infty} \sum_i \left[\underbrace{\mathbb{F}_t [w_{r,i,j} r_{i,t,t+j}]}_{\text{Discount Rate}} - \underbrace{\mathbb{F}_t [w_{el,i,j} el_{i,t,t+j}]}_{\substack{\text{Cash Flow} \\ (\text{Earnings-Employment})}} + \underbrace{\mathbb{F}_t [w_{yl,i,j} yl_{i,t,t+j}]}_{\substack{\text{Cash Flow} \\ (\text{Output-Employment})}} - \underbrace{\mathbb{F}_t [w_{s,i,j} s_{i,t+1}]}_{\text{Employment Share}} \right] \quad (\text{A.22})$$

where $r_{i,t,t+j}$, $el_{i,t,t+j}$, $yl_{i,t,t+j}$, and $s_{i,t+1}$ denote log deviations of $R_{i,t,t+j}$, $EL_{i,t,t+j}$, $YL_{i,t,t+j}$, and $S_{i,t+1}$ from the steady state state, respectively. The coefficients $w_{r,i,j} = w_{s,i,j} \equiv \frac{\bar{q}}{\kappa} \frac{(\bar{E}L_i + (1-\alpha)\bar{Y}L_i) \cdot \bar{S}_i}{\bar{R}_i^j}$, $w_{el,i,j} \equiv \frac{\bar{q}}{\kappa} \frac{\bar{E}L_i \cdot \bar{S}_i}{\bar{R}_i^j}$, and $w_{yl,i,j} \equiv (1 - \alpha) \frac{\bar{q}}{\kappa} \frac{\bar{Y}L_i \cdot \bar{S}_i}{\bar{R}_i^j}$ are functions of steady-state values and linearization constants. Note that $s_{i,t+1}$ is constant in j and that the effective weight is the sum of the $w_{s,i,j}$'s. $\alpha = 0.72$ comes from the labor share, $\kappa = 0.133$ comes from the flow vacancy cost (Elsby and Michaels, 2013). $\bar{q} = 0.631$, $\bar{R}_i = 1.04$, $\bar{E}L = 0.014$, $\bar{Y}L = 0.074$ are long-run sample averages. Finally, approximate the infinite sum by truncating up to h periods.

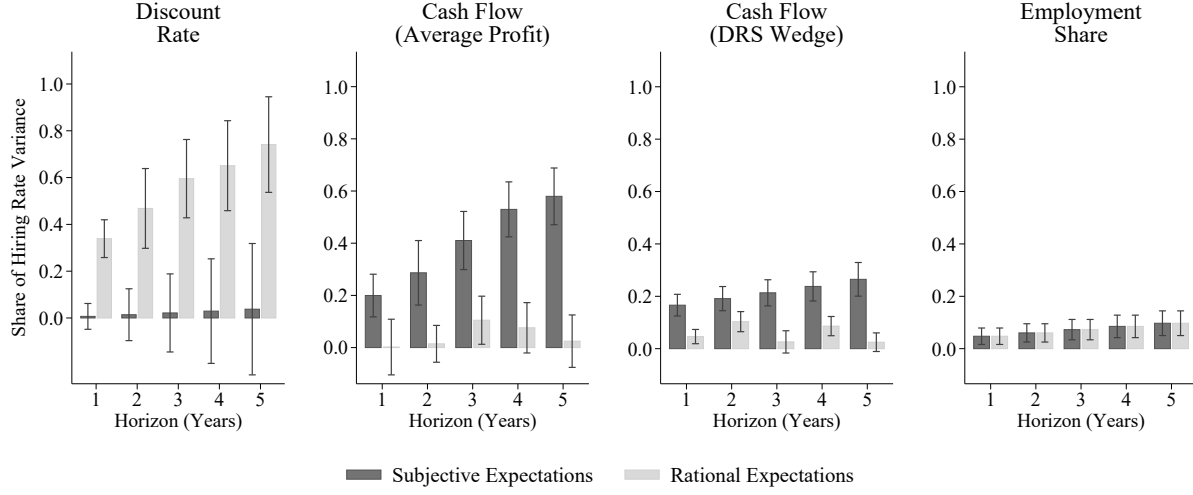
The expected output-employment ratio $\mathbb{F}_t[y_{l,i,t+j}]$ captures the DRS wedge, and the employment share $s_{i,t+1}$ captures composition effects of changes in the firm size distribution. I measure the expected output-employment ratio $\mathbb{F}_t[y_{l,i,t+j}]$ by using IBES sales forecasts. Figure A.17 shows that under subjective expectations, the output-employment term accounts for roughly 30% of the variation in the vacancy filling rate, while the earnings-employment term explains slightly less than 60%. The compositional term is small. These results confirm that even under DRS, subjective cash flow expectations, whether expressed in average or marginal terms, remain the dominant driver of hiring fluctuations.

A.11 On-the-Job Search

The baseline model assumes that all hires come from the pool of unemployed workers. However, measured earnings and hiring flows reflect contributions from both unemployed-to-employed (UE) and job-to-job (J2J) transitions. To better capture the sources of observed hiring, this section extends the baseline model to allow for on-the-job search. This modification draws on recent work modeling labor market flows with job-to-job transitions (Kuhn et al., 2021; Faberman et al., 2022). Let a fraction ϕ of employed workers search for jobs each period, in addition to the unemployed. The total number of searchers is:

$$S_t = U_t + \phi L_t = U_t + \phi(1 - U_t), \quad (\text{A.23})$$

Figure A.17: Time-Series Decomposition of the Vacancy Filling Rate: Decreasing Returns to Scale



Notes: This figure illustrates the components of the time-series decomposition of aggregate vacancy filling rate under decreasing returns to scale, based on equation (A.22). The components of the decomposition are expected present discounted values of discount rate, earnings-employment ratio, output-employment ratio, and the employment share. The light bars show the contributions to the vacancy filling rate obtained under rational expectations. The dark bars show the contributions to the time-series variation in the vacancy filling rate obtained in subjective expectations. Subjective expectations \mathbb{F}_t are based on survey forecasts of CFOs and IBES financial analysts. Rational expectations \mathbb{E}_t are based on machine learning forecasts from Long Short-Term Memory (LSTM) neural networks. The sample is quarterly from 2005Q1 to 2023Q4. Each bar shows Newey-West 95% confidence intervals with lags = 4.

where U_t is the unemployment rate and $L_t = 1 - U_t$ is the employment rate. Vacant firms post V_t vacancies, and matches form via a constant returns to scale matching function $\mathcal{M}(S_t, V_t)$. Not all on-the-job searchers who receive an offer accept it. Let $\chi \in (0, 1)$ denote the fraction of employed searchers who accept a job offer. The effective hiring efficiency from the firm's perspective is:

$$\varphi_t = \frac{U_t + \chi\phi(1 - U_t)}{U_t + \phi(1 - U_t)}. \quad (\text{A.24})$$

The law of motion for employment becomes:

$$L_{t+1} = (1 - \delta_t)L_t + q_t\varphi_t V_t, \quad (\text{A.25})$$

where δ_t is the separation rate and $q_t = \frac{\mathcal{M}(S_t, V_t)}{V_t}$ is the vacancy filling rate. The Bellman equation for the firm's value is updated to reflect turnover due to J2J transitions:

$$\mathcal{V}(A_t, L_t) = \max_{V_t, L_{t+1}} \{E_t + (1 - \phi\chi f_t)\mathbb{F}_t [M_{t+1}\mathcal{V}(A_{t+1}, L_{t+1})]\}, \quad (\text{A.26})$$

subject to the employment accumulation equation above. The term $1 - \phi\chi f_t$ reflects the retention rate, accounting for voluntary separations from employed workers who successfully switch jobs. Under constant returns to scale, the firm's optimal vacancy posting condition implies:

$$\frac{\kappa}{q_t\varphi_t} = (1 - \phi\chi f_t) \cdot \frac{P_t}{L_{t+1}}, \quad (\text{A.27})$$

where $P_t = \mathbb{F}_t [M_{t+1}\mathcal{V}(A_{t+1}, L_{t+1})]$ is the ex-dividend firm value and κ is the flow cost of posting a vacancy. Taking logs and rearranging, the log vacancy filling rate can be written as:

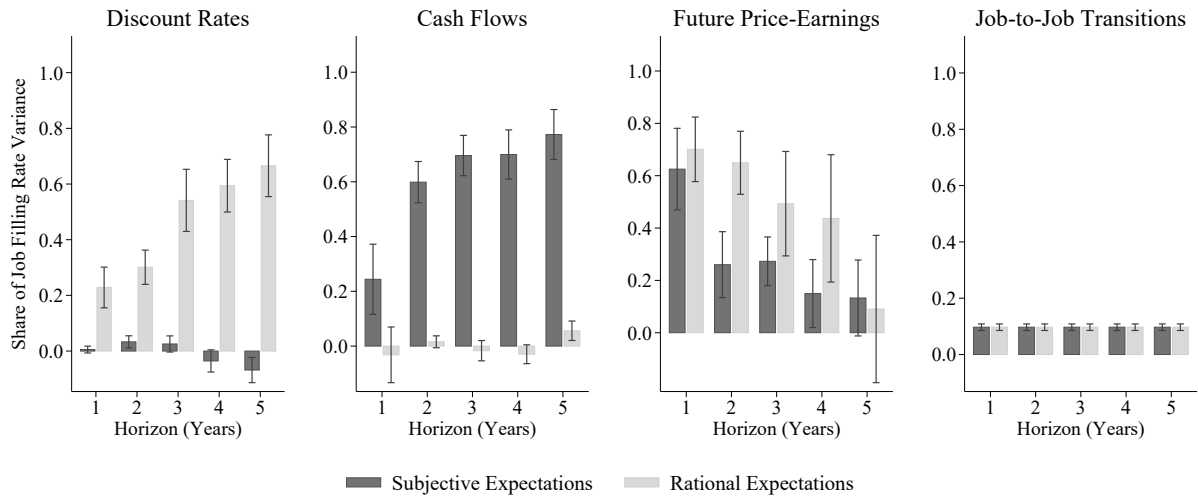
$$\log q_t = c_q - \log(1 - \phi\chi f_t) + \mathbb{F}_t[r_{t,t+h}] - \mathbb{F}_t[e_{t,t+h}] - \mathbb{F}_t[p e_{t,t+h}], \quad (\text{A.28})$$

where $c_q = \log \kappa - \log \varphi_t - \frac{c p e^{(1-\rho^h)}}{1-\rho}$ is a constant, $r_{t,t+h}$ is the present value of expected discount rates, $e_{t,t+h}$ is expected cumulative earnings growth, and $p e_{t,t+h}$ is the expected terminal price-earnings ratio. This decomposition extends the Campbell and Shiller (1988) present value identity to account for hiring frictions due to job-to-job transitions. The vacancy

filling rate q_t is computed as the ratio of total hires to vacancies $q_t = \frac{H_t}{V_t}$ using JOLTS data for hires and job openings. The total search pool S_t includes both unemployed and a fraction $\phi = 0.12$ of employed workers, based on estimates from Kuhn et al. (2021) and Faberman et al. (2022). The job finding rate is then inferred from the matching function as $f_t = q_t \cdot \theta_t$, where labor market tightness is defined as $\theta_t = \frac{V_t}{S_t} = \frac{V_t}{U_t + \phi(1 - U_t)}$. I assume that $\chi = 0.75$ of employed job seekers accept offers. These parameter values imply an endogenous efficiency term φ_t and a retention rate $1 - \phi\chi f_t$, which are used to adjust the firm's hiring incentives and derive the decomposition. Subjective expectations of earnings growth are from IBES, which aggregates analyst forecasts of total firm earnings and therefore reflect both UE and J2J hires.

Figure A.18 presents the decomposition of the vacancy filling rate under this extended model with on-the-job search. Consistent with the baseline analysis, the cash flow component remains the dominant driver of variation in the vacancy filling rate under subjective expectations. However, accounting for job-to-job transitions modestly shifts the decomposition: the log retention rate term $\log(1 - \phi\chi f_t)$ explains 8.9% of the variation in $\log q_t$. This adjustment reflects the influence of selective separations on firms' incentives to post vacancies. Overall, the results reinforce the finding that distorted cash flow expectations are the primary driver of hiring fluctuations. The extension confirms that even when allowing for endogenous separations due to on-the-job search, subjective belief distortions about firm-level earnings continue to dominate the variation in hiring behavior.

Figure A.18: Time-Series Decomposition of the Vacancy Filling Rate: On-the-Job Search



Notes: Figure illustrates the discount rate, cash flow, and future price-earnings components of the time-series decomposition of the aggregate vacancy filling rate. Light bars show contributions under rational expectations; dark bars show contributions under subjective expectations. The sample is quarterly from 2005Q1 to 2023Q4. Each bar shows Newey-West 95% confidence intervals with lags = 4.

B Model Details

B.1 Representative Agent Model

In this section, I present a search and matching model based on Diamond (1982), Mortensen (1982), and Pissarides (2009). The model introduces subjective beliefs that may depart from rational expectations, thereby capturing the impact of belief distortions on labor market dynamics. See Petrosky-Nadeau et al. (2018) for a standard search and matching model formulated under rational expectations. I begin with a representative firm setup to develop intuition for the aggregate dynamics, then extend the model in Section B.2 to include firm heterogeneity to support the cross-sectional analysis. Consider a discrete time economy populated by a representative household and a representative firm that uses labor as a single input to production.

Representative Household The household has a continuum of mass 1 members who are either employed L_t or unemployed U_t at any point in time. The population is normalized to 1, i.e., $L_t + U_t = 1$, meaning that L_t and U_t are also the rates of employment and unemployment, respectively. The household's consumption decision implies a stochastic discount factor M_{t+1} . The household pools the income of all members before making its consumption decision. Assume that the household has perfect consumption insurance and its members have access to complete contingent claims against aggregate risk. Risk sharing implies each member consumes the same amount regardless of idiosyncratic shocks.

Search and Matching At the start of period t , the employment stock L_t reflects the total number of workers carried over from the previous period before any separations or new hires in period t . A fraction δ_t of these workers separate during the period, so the number of continuing employees becomes $(1 - \delta_t)L_t$. The representative firm posts job vacancies V_t and engages in search over the course of the period to attract unemployed workers U_t . Matches are formed at the end of period t according to a matching function $m(U_t, V_t)$, where $q_t \equiv m(U_t, V_t)/V_t$ is the *vacancy filling rate*, and $f_t \equiv m(U_t, V_t)/U_t$ is the *job finding rate*. These new matches become part of the workforce starting in period $t + 1$, so employment evolves according to the employment accumulation equation:

$$L_{t+1} = (1 - \delta_t)L_t + q_t V_t \quad (\text{A.29})$$

The vacancy filling rate q_t maps vacancy posting decisions made during period t into employment outcomes observed at the beginning of period $t + 1$. The variance decomposition does not require us to fully specify the matching function m . Posting a vacancy costs the firm $\kappa > 0$ per period, reflecting fixed hiring costs such as training and administrative setup. Jobs are destroyed at a time-varying job separation rate δ_t . Unemployment $U_t = 1 - L_t$ evolves according to:

$$U_{t+1} = \delta_t(1 - U_t) + (1 - q_t\theta_t)U_t \quad (\text{A.30})$$

where $\theta_t = V_t/U_t$ denotes labor market tightness, defined as the vacancy-to-unemployment ratio.

Representative Firm The firm has access to a production function F which uses labor L_t as an input to produce output $Y_t = F(L_t)$. Dividends to the firm's shareholders E_t are defined as $E_t \equiv \Pi_t - \kappa V_t$, where $\Pi_t \equiv Y_t - W_t L_t$ is the total profit before vacancy posting costs κV_t and W_t is the wage rate. As in Petrosky-Nadeau et al. (2018), I assume that the representative household owns the equity of the firm, and that the firm pays out all of its earnings as dividends. I also assume that firms have the same unconstrained access to financing as investors in the financial market. The firm posts the optimal number of vacancies to maximize the cum-dividend market value of equity S_t :

$$S_t = \max_{\{V_{t+j}, L_{t+j}\}_{j=0}^{\infty}} \mathbb{F}_t \left[\sum_{j=0}^{\infty} M_{t,t+j} E_{t+j} \right] \quad (\text{A.31})$$

subject to the employment accumulation equation (A.29). The firm takes the wage rate W_t , household's stochastic discount factor $M_{t,t+j} = \prod_{s=1}^j M_{t+s}$, and vacancy filling rate q_t as given. $\mathbb{F}_t[\cdot]$ denotes expectations conditional on information available at period t , computed based on the firm's possibly distorted beliefs. These beliefs may depart from rational expectations $\mathbb{E}_t[\cdot]$, with the nature and magnitude of the deviation disciplined using survey data.

Hiring Equation The firm's optimal hiring decision equates the expected discounted value of hiring a marginal worker with its marginal cost. Rewrite the firm's problem in equation (A.31) from infinite-horizon to recursive form:

$$S_t = \max_{V_t, L_{t+1}} \Pi_t - \kappa V_t + \mathbb{F}_t [M_{t+1} S_{t+1}] \quad (\text{A.32})$$

$$\text{s.t. } L_{t+1} = (1 - \delta_t)L_t + q_t V_t \quad (\text{A.33})$$

The first-order condition with respect to V_t is:

$$\frac{\partial S_t}{\partial V_t} = -\kappa + \mathbb{F}_t \left[M_{t+1} \frac{\partial S_{t+1}}{\partial L_{t+1}} \frac{\partial L_{t+1}}{\partial V_t} \right] = 0 \quad (\text{A.34})$$

Substitute $\frac{\partial L_{t+1}}{\partial V_t} = q_t$ and $\frac{\partial L_{t+1}}{\partial L_t} = (1 - \delta_t)$ from the employment accumulation equation (A.33), and rearrange (A.34) in terms of the marginal cost of hiring κ/q_t :

$$\frac{\kappa}{q_t} = \mathbb{F}_t \left[M_{t+1} \frac{\partial S_{t+1}}{\partial L_{t+1}} \right] \quad (\text{A.35})$$

Next, differentiate S_t with respect to L_t :

$$\frac{\partial S_t}{\partial L_t} = \frac{\partial \Pi_t}{\partial L_t} + \mathbb{F}_t \left[M_{t+1} \frac{\partial S_{t+1}}{\partial L_{t+1}} \frac{\partial L_{t+1}}{\partial L_t} \right] \quad (\text{A.36})$$

Substitute $\frac{\partial L_{t+1}}{\partial L_t} = (1 - \delta_t)$ from the employment accumulation equation (A.33):

$$\frac{\partial S_t}{\partial L_t} = \frac{\partial \Pi_t}{\partial L_t} + (1 - \delta_t) \mathbb{F}_t \left[M_{t+1} \frac{\partial S_{t+1}}{\partial L_{t+1}} \right] \quad (\text{A.37})$$

Substitute equation (A.37) for period $t + 1$ into equation (A.35):

$$\frac{\kappa}{q_t} = \mathbb{F}_t \left[M_{t+1} \left(\frac{\partial \Pi_{t+1}}{\partial L_{t+1}} + (1 - \delta_{t+1}) \mathbb{F}_{t+1} \left[M_{t+2} \frac{\partial S_{t+2}}{\partial L_{t+2}} \right] \right) \right] \quad (\text{A.38})$$

Finally, substitute in (A.35) for period $t + 1$ to arrive at the *hiring equation*:

$$\underbrace{\frac{\kappa}{q_t}}_{\text{Cost of hiring}} = \underbrace{\mathbb{F}_t \left[M_{t+1} \left(\pi_{t+1} + (1 - \delta_{t+1}) \frac{\kappa}{q_{t+1}} \right) \right]}_{\text{Expected discounted value of hiring}} \quad (\text{A.39})$$

where $\pi_t \equiv \frac{\partial \Pi_t}{\partial L_t}$ is the profit flow from the marginal hired worker. The hiring equation relates the marginal cost of hiring $\frac{\kappa}{q_t}$ with the expected marginal value of hiring to the firm, which equals the future expected marginal benefits of hiring discounted to present value with the stochastic discount factor M_{t+1} . The future marginal benefits of hiring include π_{t+1} , the future marginal product of labor net of the wage rate, plus the future marginal value of hiring, which equals the future marginal cost of hiring $\frac{\kappa}{q_{t+1}}$ net of separation $(1 - \delta_{t+1})$. During recessions, vacancy filling rates q_t are high, which makes the cost of hiring κ/q_t low. The low cost of hiring must be rationalized by either low expected discounted profit flows $\mathbb{F}_t[M_{t+1}\pi_{t+1}]$ or low future value of hiring $(1 - \delta_{t+1})\frac{\kappa}{q_{t+1}}$. The hiring equation is the labor market analogue of the optimality condition for physical capital in the q theory of investment (Hayashi, 1982), where κ/q_t is the upfront cost of investment analogous to Tobin's marginal q and δ_{t+1} is the depreciation rate.

Constant Returns to Scale (CRS) Next, I derive the firm's stock price implied by the optimal hiring decision. Assume a constant returns to scale (CRS) production function so that marginal profits equal average profits:

$$\pi_{t+1} L_{t+1} = \frac{\partial \Pi_{t+1}}{\partial L_{t+1}} L_{t+1} = \Pi_{t+1} \quad (\text{A.40})$$

Multiply both sides of the hiring equation by the number of employees L_{t+1} :

$$\frac{\kappa}{q_t} L_{t+1} = \mathbb{F}_t \left[M_{t+1} \left(\pi_{t+1} L_{t+1} + (1 - \delta_{t+1}) \frac{\kappa}{q_{t+1}} L_{t+1} \right) \right] \quad (\text{A.41})$$

Substitute in the employment accumulation equation (A.33) and rearrange terms:

$$\frac{\kappa}{q_t} L_{t+1} = \mathbb{F}_t \left[M_{t+1} \left(\pi_{t+1} L_{t+1} + \frac{\kappa}{q_{t+1}} (L_{t+2} - q_{t+1} V_{t+1}) \right) \right] \quad (\text{A.42})$$

$$= \mathbb{F}_t \left[M_{t+1} \left(\pi_{t+1} L_{t+1} - \kappa V_{t+1} + \frac{\kappa}{q_{t+1}} L_{t+2} \right) \right] \quad (\text{A.43})$$

Use the constant returns to scale assumption to simplify $\pi_{t+1} L_{t+1} - \kappa V_{t+1} = \Pi_{t+1} - \kappa V_{t+1} = E_{t+1}$:

$$\frac{\kappa}{q_t} L_{t+1} = \mathbb{F}_t \left[M_{t+1} \left(E_{t+1} + \frac{\kappa}{q_{t+1}} L_{t+2} \right) \right] \quad (\text{A.44})$$

Substitute the equation recursively:

$$\frac{\kappa}{q_t} L_{t+1} = \mathbb{F}_t \left[\sum_{j=1}^{\infty} M_{t,t+j} E_{t+j} \right] + \lim_{T \rightarrow \infty} \mathbb{F}_t \left[M_{t,t+T} \frac{\kappa}{q_{t+T}} L_{t+T+1} \right] \quad (\text{A.45})$$

The first term on the right-hand side is the firm's stock price $P_t \equiv S_t - E_t$, which is the firm's ex-dividend equity value. Take the second term to zero by applying a transversality condition to arrive at an equation that relates the total cost of hiring with the firm's stock price:

$$\frac{\kappa}{q_t} L_{t+1} = P_t \quad (\text{A.46})$$

where employment L_{t+1} is determined at the end of date t under the timing convention from equation (A.29). Take logarithms of both sides of the firm's stock price equation (A.46) and rearrange terms:

$$\log \kappa - \log q_t = \log \frac{P_t}{L_{t+1}} = \log \frac{P_t}{E_t} - \log \frac{E_t}{L_{t+1}} \equiv pe_t - el_t \quad (\text{A.47})$$

where I define $pe_t \equiv \log \frac{P_t}{E_t}$ and $el_t \equiv \log \frac{E_t}{L_{t+1}}$ for notational convenience.

Log-linear Approximation of Price-Earnings Ratio To express the price-earnings ratio pe_t in terms of forward-looking variables, start by log-linearizing the price-dividend ratio $pd_t = \log(P_t/D_t)$ around its long-term average \bar{pd} (Campbell and Shiller, 1988):

$$pd_t = c_{pd} + \Delta d_{t+1} - r_{t+1} + \rho pd_{t+1} \quad (\text{A.48})$$

where c_{pd} is a linearization constant, $r_{t+1} \equiv \log(\frac{P_{t+1}+D_{t+1}}{P_t})$ is the log stock return (with dividends), and $\rho \equiv \exp(\bar{pd})/(1+\exp(\bar{pd})) = 0.98$ is a persistence parameter that arises from the log linearization. Rewrite the equation in terms of log price-earnings instead of log price-dividends by using the identity $pe_t = pd_t + de_t$, where de_t log payout ratio:

$$pe_t = c_{pd} + \Delta e_{t+1} - r_{t+1} + \rho pe_{t+1} + (1-\rho)de_{t+1} \quad (\text{A.49})$$

Since $1-\rho \approx 0$ and the payout ratio de_t is bounded, $(1-\rho)de_{t+1}$ can be approximated as a constant, i.e., $c_{pe} \approx c_{pd} + (1-\rho)de_{t+1}$ (De La O et al., 2024):

$$pe_t \approx c_{pe} + \Delta e_{t+1} - r_{t+1} + \rho pe_{t+1} \quad (\text{A.50})$$

Recursively substitute for the next h periods

$$pe_t = \sum_{j=1}^h \rho^{j-1} (c_{pe} + \Delta e_{t+j} - r_{t+j}) + \rho^h pe_{t+h} \quad (\text{A.51})$$

Decomposition of Vacancy Filling Rate Substitute the log-linearized price-earnings ratio in equation (A.51) into the hiring equation in equation (A.47):

$$\log q_t = \log \kappa - pe_t - el_t = \log \kappa - \left[\sum_{j=1}^h \rho^{j-1} (c_{pe} + \Delta e_{t+j} - r_{t+j}) + \rho^h pe_{t+h} \right] - el_t \quad (\text{A.52})$$

Rearrange and collect terms to obtain an ex-post decomposition of the vacancy filling rate:

$$\log q_t = c_q + \underbrace{\sum_{j=1}^h \rho^{j-1} r_{t+j}}_{r_{t,t+h}} - \underbrace{\left[el_t + \sum_{j=1}^h \rho^{j-1} \Delta e_{t+j} \right]}_{e_{t,t+h}} - \underbrace{\rho^h pe_{t+h}}_{pe_{t,t+h}} \quad (\text{A.53})$$

where $c_q \equiv \log \kappa - \frac{c_{pe}(1-\rho^h)}{1-\rho}$ is a constant. The equation decomposes the vacancy filling rate into future discount rates $r_{t,t+h} \equiv \sum_{j=1}^h \rho^{j-1} r_{t+j}$, cash flows $e_{t,t+h} \equiv el_t + \sum_{j=1}^h \rho^{j-1} \Delta e_{t+j}$, and price-earnings $pe_{t,t+h} \equiv \rho^h pe_{t+h}$. The cash flow component consists of one period ahead log earnings-employment el_t , which captures news about current cash flow fluctuations, and $j = 1, \dots, h$ period ahead log earnings growth Δe_{t+j} , which captures news about future cash flows. The earnings-employment ratio can be interpreted as a measure of the marginal product of labor under constant returns to scale (David et al., 2022). $pe_{t,t+h}$ is a terminal value that captures other long-term influences beyond h periods into the future not already captured in discount rates and cash flows. Since equation (A.53) holds both ex-ante and ex-post, it can be evaluated under either subjective or rational expectations. The *subjective decomposition* replaces ex-post realizations of future outcomes with their subjective expectations:

$$\log q_t = c_q + \underbrace{\sum_{j=1}^h \rho^{j-1} \mathbb{F}_t[r_{t+j}]}_{\mathbb{F}_t[r_{t,t+h}]} - \underbrace{\left[el_t + \sum_{j=1}^h \rho^{j-1} \mathbb{F}_t[\Delta e_{t+j}] \right]}_{\mathbb{F}_t[e_{t,t+h}]} - \underbrace{\rho^h \mathbb{F}_t[pe_{t+h}]}_{\mathbb{F}_t[pe_{t,t+h}]} \quad (\text{A.54})$$

Alternatively, the *rational decomposition* replaces ex-post realizations of future outcomes with their rational expectations:

$$\log q_t = c_q + \underbrace{\sum_{j=1}^h \rho^{j-1} \mathbb{E}_t[r_{t+j}]}_{\mathbb{E}_t[r_{t,t+h}]} - \underbrace{\left[el_t + \sum_{j=1}^h \rho^{j-1} \mathbb{E}_t[\Delta e_{t+j}] \right]}_{\mathbb{E}_t[e_{t,t+h}]} - \underbrace{\rho^h \mathbb{E}_t[pe_{t+h}]}_{\mathbb{E}_t[pe_{t,t+h}]} \quad (\text{A.55})$$

Comparing these decompositions can quantify how belief distortions affect the vacancy filling rate.

Estimation The econometrician can estimate the variance decomposition using predictive regressions of each expected outcome on the current vacancy filling rate. For the subjective decomposition, demean each variable in equation (A.54), multiply both sides by the current log vacancy filling rate $\log q_t$, and take the sample average:

$$\text{Var}[\log q_t] = \text{Cov}[\mathbb{F}_t[r_{t,t+h}], \log q_t] - \text{Cov}[\mathbb{F}_t[e_{t,t+h}], \log q_t] - \text{Cov}[\mathbb{F}_t[pe_{t,t+h}], \log q_t] \quad (\text{A.56})$$

where $\text{Var}[\cdot]$ and $\text{Cov}[\cdot]$ are sample variances and covariances based on data observed over a historical sample. Finally, divide both sides by $\text{Var}[\log q_t]$ to decompose its variance:

$$1 = \underbrace{\frac{\text{Cov}[\mathbb{F}_t[r_{t,t+h}], \log q_t]}{\text{Var}[\log q_t]}}_{\text{Discount Rate News}} - \underbrace{\frac{\text{Cov}[\mathbb{F}_t[e_{t,t+h}], \log q_t]}{\text{Var}[\log q_t]}}_{\text{Cash Flow News}} - \underbrace{\frac{\text{Cov}[\mathbb{F}_t[pe_{t,t+h}], \log q_t]}{\text{Var}[\log q_t]}}_{\text{Future Price-Earnings News}} \quad (\text{A.57})$$

The left-hand side represents the full variability in vacancy filling rates, hence is equal to one. Each term on the right reflects the share explained by subjective expectations of discount rates, cash flows, or price-earnings ratios. Under stationarity, the econometrician can estimate these shares using the OLS coefficients from regressing $\mathbb{F}_t[r_{t,t+h}]$, $\mathbb{F}_t[e_{t,t+h}]$, and $\mathbb{F}_t[pe_{t,t+h}]$ on the current log vacancy filling rate $\log q_t$, respectively. Finally, the decomposition under rational expectations can be estimated similarly based on equation (A.55) by replacing the subjective expectation $\mathbb{F}_t[\cdot]$ with its rational counterpart $\mathbb{E}_t[\cdot]$:

$$1 = \underbrace{\frac{\text{Cov}[\mathbb{E}_t[r_{t,t+h}], \log q_t]}{\text{Var}[\log q_t]}}_{\text{Discount Rate News}} - \underbrace{\frac{\text{Cov}[\mathbb{E}_t[e_{t,t+h}], \log q_t]}{\text{Var}[\log q_t]}}_{\text{Cash Flow News}} - \underbrace{\frac{\text{Cov}[\mathbb{E}_t[pe_{t,t+h}], \log q_t]}{\text{Var}[\log q_t]}}_{\text{Future Price-Earnings News}} \quad (\text{A.58})$$

Under stationarity, the econometrician can estimate these shares using the OLS coefficients from regressing $\mathbb{E}_t[r_{t,t+h}]$, $\mathbb{E}_t[e_{t,t+h}]$, and $\mathbb{E}_t[pe_{t,t+h}]$ on the current log vacancy filling rate $\log q_t$, respectively.

B.2 Details on Cross-Sectional Decomposition of Hiring Rate

The cross-sectional analysis employs a firm-level hiring framework that is the direct analogue of the aggregate representative firm search model. Both approaches derive from the same fundamental principle: firms hire until the marginal cost of hiring equals the marginal value of an additional worker. The key difference lies in the level of aggregation and the specific frictions that generate hiring costs. In the aggregate search model, linear vacancy posting costs (κ per vacancy) combined with constant returns to scale imply that marginal value equals average value, leading to the simplified hiring condition $\frac{\kappa}{q_t} = \frac{P_t}{L_{t+1}}$. For cross-sectional analysis, I retain firm-level heterogeneity and introduce convex adjustment costs that generate dispersion in hiring rates while preserving the core economic mechanism linking firm valuations to hiring decisions.

Consider firm i with production function:

$$Y_{i,t} = A_{i,t} L_{i,t}^\alpha \quad (\text{A.59})$$

where $A_{i,t}$ represents productivity and $L_{i,t}$ is labor input. The firm's earnings, net of hiring costs and wages, are:

$$E_{i,t} = Y_{i,t} - \phi\left(\frac{H_{i,t}}{L_{i,t}}\right) L_{i,t} - W_{i,t} L_{i,t} \quad (\text{A.60})$$

where $\phi(\cdot)$ captures convex adjustment costs for hiring at rate $H_{i,t}/L_{i,t}$, and $W_{i,t}$ is the equilibrium wage. The adjustment cost function $\phi(\cdot)$ represents the firm-level analogue of the aggregate matching friction. While the search model features linear vacancy costs that aggregate to determine the market-wide vacancy filling rate, individual firms face convex costs when rapidly adjusting their workforce due to capacity constraints in recruitment, training bottlenecks, and organizational frictions. Firm value satisfies the Bellman equation:

$$V(A_{i,t}, L_{i,t}) = \max_{H_{i,t}} \left\{ E_{i,t} + \mathbb{F}_t \left[\frac{M_{t+1}}{M_t} V(A_{i,t+1}, L_{i,t+1}) \right] \right\} \quad (\text{A.61})$$

subject to the employment accumulation equation:

$$L_{i,t+1} = (1 - \delta_{i,t}) L_{i,t} + H_{i,t} \quad (\text{A.62})$$

where M_t is the stochastic discount factor and $\delta_{i,t}$ is the job separation rate. The first-order condition with respect to hiring equates marginal cost to marginal benefit:

$$\phi' \left(\frac{H_{i,t}}{L_{i,t}} \right) = \mathbb{F}_t \left[\frac{M_{t+1}}{M_t} \frac{\partial V(A_{i,t+1}, L_{i,t+1})}{\partial L_{i,t+1}} \right] \quad (\text{A.63})$$

Under constant returns to scale, the envelope theorem yields $\frac{\partial V}{\partial L} = \frac{V}{L}$, allowing us to express the marginal value in terms of observable quantities:

$$\phi' \left(\frac{H_{i,t}}{L_{i,t}} \right) = \mathbb{F}_t \left[\frac{M_{t+1}}{M_t} \frac{V(A_{i,t+1}, L_{i,t+1})}{L_{i,t+1}} \right] = \frac{P_{i,t}}{L_{i,t+1}} \quad (\text{A.64})$$

where $P_{i,t}$ is the ex-dividend firm value (stock price). This hiring condition is the firm-level equivalent of the aggregate search model's condition $\frac{\kappa}{q_t} = \frac{P_t}{L_{t+1}}$. Both express the fundamental insight that hiring depends on the ratio of firm value to employment, but the cross-sectional version allows for firm-specific variation in both the adjustment cost parameters and the value-to-employment ratios. Assuming quadratic adjustment costs $\phi \left(\frac{H_{i,t}}{L_{i,t}} \right) = \frac{c_l}{2} \left(\frac{H_{i,t}}{L_{i,t}} \right)^2$, the marginal cost becomes $\phi' \left(\frac{H_{i,t}}{L_{i,t}} \right) = c_l \frac{H_{i,t}}{L_{i,t}}$, yielding:

$$c_l \frac{H_{i,t}}{L_{i,t}} = \frac{P_{i,t}}{L_{i,t+1}} \quad (\text{A.65})$$

Taking logs and decomposing the price-to-employment ratio:

$$\ln(c_l) + \ln \left(\frac{H_{i,t}}{L_{i,t}} \right) = \ln \left(\frac{P_{i,t}}{E_{i,t}} \right) - \ln \left(\frac{E_{i,t+1}}{E_{i,t}} \right) + \ln \left(\frac{E_{i,t+1}}{L_{i,t+1}} \right) \quad (\text{A.66})$$

Using lowercase letters to denote log variables, this becomes:

$$\ln(c_l) + hl_{i,t} = pe_{i,t} - \Delta e_{i,t+1} + el_{i,t+1} \quad (\text{A.67})$$

Substituting the Campbell-Shiller decomposition of the log price-earnings ratio:

$$pe_{i,t} \approx c + \sum_{j=1}^h \rho^{j-1} \Delta e_{i,t+j} - \sum_{j=1}^h \rho^{j-1} r_{i,t+j} + \rho^h pe_{i,t+h} \quad (\text{A.68})$$

Taking subjective expectations and cross-sectionally demeaning to eliminate common terms yields the final decomposition:

$$\tilde{hl}_{i,t} \approx \underbrace{\mathbb{F}_t[\tilde{el}_{i,t+1}]}_{\text{Cash Flow}} + \underbrace{\sum_{j=2}^h \rho^{j-1} \mathbb{F}_t[\Delta \tilde{e}_{i,t+j}]}_{\text{Discount Rate}} - \underbrace{\sum_{j=1}^h \rho^{j-1} \mathbb{F}_t[\tilde{r}_{i,t+j}]}_{\text{Future Price-Earnings}} + \rho^h \mathbb{F}_t[\tilde{pe}_{i,t+h}] \quad (\text{A.69})$$

where $\tilde{x}_{i,t}$ denotes the cross-sectionally demeaned variable. The variance decomposition follows directly from the hiring rate decomposition:

$$1 \approx \underbrace{\frac{\text{Cov}(\mathbb{F}_t[\tilde{el}_{i,t,t+h}], \tilde{hl}_{i,t})}{\text{Var}(\tilde{hl}_{i,t})}}_{\text{CF}_h} + \underbrace{\frac{\text{Cov}(-\mathbb{F}_t[\tilde{r}_{i,t,t+h}], \tilde{hl}_{i,t})}{\text{Var}(\tilde{hl}_{i,t})}}_{\text{DR}_h} + \underbrace{\frac{\text{Cov}(\mathbb{F}_t[\tilde{pe}_{i,t,t+h}], \tilde{hl}_{i,t})}{\text{Var}(\tilde{hl}_{i,t})}}_{\text{PE}_h} \quad (\text{A.70})$$

where $\tilde{el}_{i,t,t+h} \equiv el_{i,t+1} + \sum_{j=2}^h \rho^{j-1} \Delta \tilde{e}_{i,t+j}$, $\tilde{r}_{i,t,t+h} \equiv \sum_{j=1}^h \rho^{j-1} \tilde{r}_{i,t+j}$, and $\tilde{pe}_{i,t,t+h} \equiv \rho^h \tilde{pe}_{i,t+h}$. These covariance terms are estimated as coefficients from univariate regressions with time fixed effects, allowing us to isolate the cross-sectional variation attributable to each component while controlling for aggregate time-series effects.

The data uses Compustat annual employment data ($L_{i,t}$, variable EMP) from 2000 to 2023. The firm-level hiring rate is constructed from the employment accumulation equation:

$$\frac{H_{i,t}}{L_{i,t}} = \frac{L_{i,t+1}}{L_{i,t}} - (1 - \delta_{i,t}) \quad (\text{A.71})$$

where the job separation rate $\delta_{i,t}$ uses industry-level data from JOLTS.

B.3 Decomposition of Unemployment Rates

The unemployment rate can be decomposed into components similar to the decomposition for vacancy filling rates from equation (A.54). Log linearize the unemployment accumulation equation from equation (5):

$$U_{t+1} = \delta_t(1 - U_t) + (1 - q_t \theta_t)U_t \quad (\text{A.72})$$

Denote the steady state values without time subscripts: U , δ , q , and θ . Define log deviations from steady state as $\hat{x}_t = \log(X_t) - \log(X)$ for some variable X . Log-linearizing the accumulation equation around the steady state involves taking a first-order Taylor approximation:

$$U e^{\hat{u}_{t+1}} \approx \delta e^{\hat{\delta}_t} (1 - U e^{\hat{u}_t}) + (1 - q\theta e^{\hat{q}_t + \hat{\theta}_t}) U e^{\hat{u}_t} \quad (\text{A.73})$$

Use the approximation $X e^{x_t} \approx X(1 + x_t)$, expand, and simplify:

$$U(1 + \hat{u}_{t+1}) \approx \delta(1 + \hat{\delta}_t)(1 - U(1 + \hat{u}_t)) + (1 - q\theta(1 + \hat{q}_t + \hat{\theta}_t))U(1 + \hat{u}_t) \quad (\text{A.74})$$

Use the steady state equation and collect terms with log deviations:

$$U \hat{u}_{t+1} \approx \delta(1 - U)\hat{\delta}_t - \delta U \hat{u}_t - q\theta U \hat{q}_t - q\theta U \hat{\theta}_t + U(1 - q\theta)\hat{u}_t \quad (\text{A.75})$$

Divide both sides by U :

$$\hat{u}_{t+1} \approx \frac{\delta(1 - U)}{U}\hat{\delta}_t - \delta \hat{u}_t - q\theta \hat{q}_t - q\theta \hat{\theta}_t + (1 - q\theta)\hat{u}_t \quad (\text{A.76})$$

The steady state relationship $\delta(1 - U) = q\theta U$ implies: $\frac{\delta(1 - U)}{U} = q\theta$. Substitute this back into our equation:

$$\hat{u}_{t+1} \approx -q\theta \hat{q}_t + (1 - \delta - q\theta)\hat{u}_t - q\theta \hat{\theta}_t + q\theta \hat{\delta}_t \quad (\text{A.77})$$

Finally, substitute in equation (A.54), which is a decomposition of the vacancy filling rate \hat{q}_t into discount rate, cash flow, and future price-earnings under subjective expectations:

$$\hat{u}_{t+1} \approx -\underbrace{q\theta \cdot \mathbb{F}_t[\hat{r}_{t,t+h}]}_{\text{Discount Rate}} + \underbrace{q\theta \cdot \mathbb{F}_t[\hat{e}_{t,t+h}]}_{\text{Cash Flow}} + \underbrace{q\theta \cdot \mathbb{F}_t[\hat{p}e_{t,t+h}]}_{\text{Future Price-Earning}} + \underbrace{(1 - \delta - q\theta) \cdot \hat{u}_t - q\theta \cdot \hat{\theta}_t + q\theta \cdot \hat{\delta}_t}_{\text{Lag Unemployment, Tightness, Separations}} \quad (\text{A.78})$$

The equation holds both ex-ante and ex-post. Therefore, I compare results from evaluating the equation under subjective $\mathbb{F}_t[\cdot]$ or rational $\mathbb{E}_t[\cdot]$ expectations. The decomposition can be estimated using regressions of the log unemployment rate on each of the components shown in the equation:

$$u_{t+1} = \beta_0 + \beta_1 u_t + \beta_2 \log \theta_t + \beta_3 \log \delta_t + \beta_4 \mathbb{F}_t[r_{t,t+h}] + \beta_5 \mathbb{F}_t[e_{t,t+h}] + \varepsilon_{t+1} \quad (\text{A.79})$$

where lowercase variables denote log deviations from steady state. I estimate the decomposition using multivariate OLS regressions to jointly identify the relative contributions of each component to observed unemployment fluctuations. To ensure stationarity and remove seasonal effects, I estimate the regression in log annual growth rates relative to the same quarter of the previous year.

$$\Delta u_{t+1} = \beta_1 \Delta u_t + \beta_2 \Delta \log \theta_t + \beta_3 \Delta \log \delta_t + \beta_4 \Delta \mathbb{F}_t[r_{t,t+h}] + \beta_5 \Delta \mathbb{F}_t[e_{t,t+h}] + v_{t+1} \quad (\text{A.80})$$

The future price-earnings ratio term $\Delta \mathbb{F}_t[p e_{t,t+h}]$ has been omitted in the multivariate regression because it is nearly collinear with future discount rates $\Delta \mathbb{F}_t[r_{t,t+h}]$ and cash flows $\Delta \mathbb{F}_t[e_{t,t+h}]$ through the Campbell and Shiller (1988) present value identity in equation (15). Similarly, the equation can also be estimated under rational expectations by replacing $\mathbb{F}_t[\cdot]$ with its rational expectations counterpart $\mathbb{E}_t[\cdot]$ based on machine learning forecasts.

C Data Details

This section describes the time-series and cross-sectional data sources used in the estimation. I use quarterly data on the variables represented in the decomposition from equations (A.54) and (A.55): employment L_t , unemployment U_t , vacancy filling rates q_t , stock returns $r_{t,t+h}$, earnings growth $\Delta e_{t,t+h}$, price-earnings ratio $p e_{t,t+h}$, and earnings-employment ratio $e l_{t,t+h}$. For each dependent variable of the decomposition, I also construct their corresponding survey expectations \mathbb{F}_t and machine expectations \mathbb{E}_t .

C.1 Employment

For realized values of employment, I first construct an annual series for the aggregate number of employees (EMP) of the S&P 500 constituents by using accounting information from the CRSP and Compustat Merged Annual Industrial Files. The data spans 1970 to 2023 and was downloaded from WRDS on May 15, 2024. I aggregate the firm-level employment data to construct a total employment series for the S&P 500. I interpolate this series to a monthly frequency by using the fitted values from real-time regressions of log annual Compustat employment series on the log monthly BLS series for total nonfarm payrolls (PAYEMS). The regressions are estimated over recursively expanding samples from an initial monthly sample that begins on 1970:01 and ends on the month of the data release for each month's total nonfarm payrolls. To ensure that the fitted values do not use future information not available on each data release, I align each monthly BLS nonfarm payroll release with the annual Compustat S&P 500 employment series from the previous calendar year. To obtain a measure of employment L_{t+1} at the beginning of period $t+1$, I convert the monthly interpolated values to a quarterly frequency by taking the value of the series as of the last month of each calendar quarter. This timing assumption ensures that the measures are consistent with the timing conventions from Section B while still remaining known to firms by the end of period t . Data on nonfarm payrolls was downloaded through FRED on May 15, 2024.

C.2 Vacancy Filling Rate

I construct a monthly series for the number of vacancies V_t following Barnichon (2010), by using JOLTS job openings starting 2000:12 (JTS00000000JOL) and extending the series back in time using the help-wanted index before 2000:12. The vacancies data has been downloaded from available on the author's website on May 19, 2024. For realized values of unemployment U_t , I use the BLS monthly series for the unemployment level (UNEMPLOY), downloaded through FRED on May 15, 2024. Labor market tightness $\theta_t = V_t/U_t$ is the ratio between vacancies and unemployment. The job separation rate δ_t uses the corresponding series from JOLTS.

I follow Shimer (2012) in constructing the job separation rate δ_t , job finding rate f_t , and vacancy filling rate q_t . Job separation rate is the share of short-term unemployed out of total employment $\delta_t = U_t^s/L_t$, where U_t^s is the BLS series for the number of unemployed less than 5 weeks (UEMPLT5) that was downloaded through FRED on May 15, 2024. The job finding rate is:

$$f_t = 1 - \frac{U_t - U_t^s}{U_{t-1}}$$

The expression for the job finding rate follows from the unemployment accumulation equation:

$$U_t = (1 - f_t)U_{t-1} + U_t^s$$

which states that unemployment U_t consists of either the previously unemployed U_{t-1} who did not find a job $(1 - f_t)$, or the short-term unemployed U_t^s that lost a job during the current period. The vacancy filling rate is defined as the share of filled vacancies $f_t V_t$ out of unemployment U_t :

$$q_t = \frac{f_t}{\theta_t} = \frac{f_t U_t}{V_t}$$

I first construct the vacancy filling rate q_t at the monthly frequency. To remove high-frequency fluctuations that likely reflect measurement errors, I time-aggregate the monthly series to a quarterly frequency by taking a 3-month trailing average that ends on the first month of each calendar quarter. This timing assumption ensures that the survey and machine expectations in the variance decomposition do not use advance information about vacancy filling rates that were not published at the time of each forecast. To ensure that all variables used in the variance decomposition are stationary, I follow Shimer (2012) by detrending the quarterly vacancy filling rate q_t using an HP filter with a smoothing parameter of 10^5 .

C.3 Stock Returns

C.3.1 Realized Stock Returns

Stock market returns use monthly data on CRSP value-weighted returns including dividends (VWRETD) from the Center for Research in Security Prices (CRSP). I compute annualized log stock returns by compounding the monthly returns using $r_{t+h} \equiv \frac{1}{h} \sum_{j=1}^{12h} \log(1 + VWRETD_{t+j/12})$. The data was downloaded from WRDS on May 15, 2024. When evaluating the MSE ratios of the machine relative to that of a benchmark survey, I compute machine forecasts for either annual CRSP returns or S&P 500 price growth depending on which value most closely aligns with the concept that survey respondents are asked to predict. To measure one-year stock market price growth, I use the one-year log cumulative growth rate of the S&P 500 index, $\Delta p_{t+1} \equiv \log(P_{t+1}/P_t)$. The monthly S&P index series spans the period 1957:03 to 2022:12 and was downloaded from WRDS on May 15, 2024 from the Annual Update data of the Index File on the S&P 500.

C.3.2 Survey Expectations of Stock Returns

CFO Survey I use survey forecasts of S&P 500 stock returns from the CFO survey to measure subjective return expectations. The CFO survey is a quarterly survey that asks respondents about their expectations for the S&P 500 return over the next 12 months and 10 years ahead, obtained from https://www.richmondfed.org/-/media/RichmondFedOrg/research/national_economy/cfo_survey/current_historical_cfo_data.xlsx. I use the mean point forecast for the value of the “most likely” future stock return in the estimation. More specifically, the survey asks the respondent “over the next 12 months, I expect the average annual S&P 500 return will be: Most Likely: I expect the return to be: ___%”. The survey question for stock return expectations 10 years ahead is “over the next 10 years, I expect the average annual S&P 500 return will be: Most Likely: I expect the return to be: ___%”. The CFO survey panel includes firms that range from small operations to Fortune 500 companies across all major industries. Respondents include chief financial officers, owner-operators, vice presidents, and directors of finance, and others with financial decision-making roles. The CFO panel has 1,600 members as of December 2022.

I take a stand on the information set of respondents when each forecast was made, and I assume that respondents could have used all data released before they completed the survey. Because the CFO survey releases quarterly forecasts at the end of each quarter, I conservatively set the response deadline for the machine forecast to be the first day of the last month of each quarter (e.g., March 1st). The data spans the periods 2001Q4 to 2023Q4 and were downloaded on March 20th, 2024. Mean point forecasts before 2020Q3 are available in column `sp_1_exp` of sheet `through_Q1_2020`; mean point forecasts from 2020Q3 and onwards are available in column `sp_12moexp_2` of sheet `CFO_SP500`. The forecast is not

available in 2019Q1, 2019Q4, 2020Q1, and 2020Q2. I impute the missing forecast for 2019Q1 by linearly interpolating between the available forecasts from 2018Q4 and 2019Q2. I impute the missing forecasts for 2019Q4, 2020Q1, and 2020Q2 by interpolating with the nearest available forecast between 2019Q3 and 2020Q3. Following Nagel and Xu (2022), I assume that the forecasted S&P 500 return includes dividends and capture expectations about annualized cumulative simple net returns compounded from time t to $t + h$, i.e., $\mathbb{F}_t[R_{t,t+h}]$. To obtain survey expectations of log returns $\mathbb{F}_t[\log(1 + r_{t,t+h})]$ from a survey expectation of net simple returns $\mathbb{F}_t[R_{t,t+h}]$, I use the approximation $\mathbb{F}_t[\log(1 + r_{t,t+h})] \approx \log(1 + \mathbb{F}_t[R_{t,t+h}])$.

To obtain long-horizon survey expectations of annualized cumulative log S&P 500 returns over the next $1 < h < 10$ years, I interpolate the forecasts across annualized 1 year and 10 year cumulative log return expectations:

$$\mathbb{F}_t[r_{t,t+h}] = \frac{10 - h}{10 - 1} \mathbb{F}_t[r_{t,t+1}] + \frac{h - 1}{10 - 1} \mathbb{F}_t[r_{t,t+10}], \quad h = 1, 2, \dots, 10$$

Finally, I use the difference between cumulative long-horizon log return expectations between adjacent years (i.e., $\mathbb{F}_t[r_{t,t+h-1}]$ and $\mathbb{F}_t[r_{t,t+h}]$) to obtain $\mathbb{F}_t[r_{t+h}]$, the survey expectation of forward one-year log stock returns h years ahead:

$$\mathbb{F}_t[r_{t+h}] = h \times \mathbb{F}_t[r_{t,t+h}] - (h - 1) \times \mathbb{F}_t[r_{t,t+h-1}], \quad h = 1, 2, \dots, 10$$

IBES and Value Line I proxy expected firm-level stock returns using price growth expectations following De La O et al. (2024). Specifically, I construct expected price growth from IBES 12-month median price targets and Value Line 3–5 year median price targets, interpolating linearly for intermediate horizons.

To construct expected price growth, I combine short- and long-term price targets from two sources. For the short horizon, I use the 12-month median price targets from the Institutional Brokers Estimate System (IBES) database. For longer horizons, I use the median price targets from Value Line, which provide the expected stock price level approximately 3–5 years into the future for each firm. These targets reflect analysts' consensus expectations for each firm's stock price. I interpret the Value Line price target as the expected price level five years ahead and interpolate linearly between the IBES 12-month price target and the Value Line five-year price target to construct expected price growth for intermediate horizons between one and five years. For each firm i , expected annualized price growth over horizon h is given by:

$$\mathbb{F}_t[r_{i,t+h}] \approx \frac{1}{h} \log \left(\frac{\mathbb{F}_t[P_{i,t+h}]}{P_{i,t}} \right)$$

where $\mathbb{F}_t[P_{i,t+h}]$ is the forecasted price at horizon h , constructed through linear interpolation of IBES and Value Line targets, and $P_{i,t}$ is the observed stock price at time t . As shown in De La O et al. (2024), using price growth expectations to approximate expected firm-level stock returns is reasonably accurate, as dividends represent a relatively small component of total returns for most firms.

Gallup/UBS Survey The UBS/Gallup is a monthly survey of one-year-ahead stock market return expectations. I use the mean point forecast in our estimation and compare these to machine forecasts of the annual CRSP return. Gallup conducted 1,000 interviews of investors during the first two weeks of every month and results were reported on the last Monday of the month. The first survey was conducted on 1998:05. Until 1992:02, the survey was conducted quarterly on 1998:05, 1998:09, and 1998:11. The data on 1998:06, 1998:07, 1998:08, 1998:10, 1998:12, 1999:01, and 2006:01 are missing because the survey was not conducted on these months. I follow Adam et al. (2021) in starting the sample after 1999:02 due to missing values at the beginning of the sample.

For each month when the survey was conducted, respondents are asked about the return they expect on their own portfolio. The survey question is “*What overall rate of return do you expect to get on your portfolio in the next twelve months?*” Before 2003:05, respondents are also asked about the return they expect from an investment in the stock market during the next 12 months. The survey question is “*Thinking about the stock market more generally, what overall rate of return do you think the stock market will provide investors during the coming twelve months?*” For each month, I calculate the average expectations of returns on their own portfolio and returns on the market index. When calculating the average, survey respondents are weighted by the weight factor provided in the survey. I exclude extreme observations where a respondent reported expected returns higher than 95% or lower than -95%.

In order to construct a consistent measure of stock market return expectations over the entire sample period, I impute missing market return expectations using the fitted values from two regressions. First, I impute missing values during 1999:02–2005:12 and 2006:02–2007:10 with the fitted value from regressing expected market returns on own portfolio expectations contemporaneously, where the regression is estimated using the part of the sample where both are available. Second, I impute the one missing observation in both market and own portfolio return expectations for 2006:01 with the fitted value from regressing the market return expectations on the lagged own portfolio return expectations, where the coefficients are estimated using part of the sample where both are available, and the fitted value combines the estimated coefficients with lagged own portfolio expectations data from 2005:12. Following Nagel and Xu (2022), I assume that the forecasted stock market return includes dividends and capture expectations about annual simple net stock returns $\mathbb{F}_t[R_{t+1}]$. To obtain survey expectations of annual log returns $\mathbb{F}_t[\log(1 + r_{t+1})]$ from a survey expectation of annual net

simple returns $\mathbb{F}_t[R_{t+1}]$, I use the approximation $\mathbb{F}_t[\log(1 + r_{t+1})] \approx \log(1 + \mathbb{F}_t[R_{t+1}])$. After applying all the procedures, the Gallup market return expectations series spans the periods 1999:02 to 2007:10. The data were downloaded on August 1st, 2024 from Roper iPoll: <http://ropercenter.cornell.edu/ubs-index-investor-optimism/>.

I take a stand on the information set of respondents when each forecast was made, and I assume that respondents could have used all data released before they completed the survey. Since interviews are in the first two weeks of a month (e.g., February), I conservatively set the response deadline for the machine forecast to be the first day of the survey month (e.g., February 1st), implying that I allow the machine to use information only up through the end of the previous month (e.g., through January 31st). This ensures that the machine only sees information that would have been available to all UBS/Gallup respondents for that survey month (February). This approach is conservative in the sense that it handicaps the machine, since all survey respondents who are being interviewed during the next month would have access to more timely information than the machine. Since the survey asks about the “one-year-ahead” I interpret the question to be asking about the forecast period spanning from the current survey month to the same month one year ahead.

Michigan Survey of Consumers (SOC) The SOC contains approximately 50 core questions, and a minimum of 500 interviews are conducted by telephone over the course of the entire month, each month. Table 20 of the SOC reports the probability of an increase in stock market in next year. The survey question was *“The next question is about investing in the stock market. Please think about the type of mutual fund known as a diversified stock fund. This type of mutual fund holds stock in many different companies engaged in a wide variety of business activities. Suppose that tomorrow someone were to invest one thousand dollars in such a mutual fund. Please think about how much money this investment would be worth one year from now. What do you think the percent chance that this one thousand dollar investment will increase in value in the year ahead, so that it is worth more than one thousand dollars one year from now?”* When using this survey forecast to compare to machine forecasts, I impute a point forecast for stock market returns using the method described in Section C.3.2 below. I compare the imputed point forecast to machine forecasts of CRSP returns.

For the SOC, interviews are conducted monthly typically over the course of an entire month. (In rare cases, interviews may commence at the end of the previous month, as in February 2018 when interviews began on January 31st 2018.) I take a stand on the information set of respondents when each forecast was made, and I assume that respondents could have used all data released before they completed the survey. Since interviews are almost always conducted over the course of an entire month (e.g., February), I conservatively set the response deadline for the machine forecast to be the first day of the survey month (e.g., February 1st), implying that I allow the machine to use information only up through the end of the previous month (e.g., through January 31st). This ensures that the machine only sees information that would have been available to all respondents for that survey month (February). This approach is conservative in the sense that it handicaps the machine, since all survey respondents who are being interviewed during the next month would have access to more timely information than the machine. Since the survey asks about the “year ahead” I interpret the question to be asking about the forecast period spanning the period running from the current survey month to the same month one year ahead. The data spans 2002:06 to 2023:12. The SOC responses were obtained from <https://data.sca.isr.umich.edu/data-archive/mine.php> and downloaded on May 15, 2024.

Livingston Survey Stock Price Forecast I obtain the Livingston Survey S&P 500 index forecast (SPIF) from the Federal Reserve Bank of Philadelphia, and use the mean values in our structural and forecasting models. I compare the one-year growth in these forecasts to machine forecasts of S&P 500 price growth. Our sample spans 1947:06 to 2023:06. The forecast series were downloaded on January 24, 2024.

The survey provides semi-annual forecasts on the level of the S&P 500 index. Participants are asked to provide forecasts for the level of the S&P 500 index for the end of the current survey month, 6 months ahead, and 12 months ahead. I use the mean of the respondents’ forecasts each period, where the sample is based on about 50 observations. Most of the survey participants are professional forecasters with “formal and advanced training in economic theory and forecasting and use econometric models to generate their forecasts.” Participants receive questionnaires for the survey in May and November, after the Consumer Price Index (CPI) data release for the previous month. All forecasts are typically submitted by the end of the respective month of May and November. The results of the survey are released near the end of the following month, on June and December of each calendar year. The exact release dates are available on the Philadelphia Fed website, at the header of each news release. I take a stand on the information set of the respondents when each forecast was made by assuming that respondents could have used all data released before they completed the survey. Since all forecasts are typically submitted by the end of May and November of each calendar year, I set the response deadline for the machine forecast to be the first day of the last month of June and December, implying that I allow the machine to use information only up through the end of the May and November.

I follow Nagel and Xu (2021) in constructing one-year stock price growth expectations from the level forecasts. Starting from June 1992, I use the ratio between the 12-month level forecast ($SPIF_12M_t$) and 0-month level nowcasts ($SPIF_ZM_t$) of the S&P 500 index. Before June 1992, the 0-month nowcast is not available. Therefore I use the annualized ratio between

the 12-month (spi12_t) and 6-month (spi6_t) level forecast of the S&P 500 index

$$\mathbb{F}_t^{(Liv)} \left[\frac{P_{t+1}}{P_t} \right] \approx \begin{cases} \frac{\mathbb{F}_t^{(Liv)}[P_{t+1}]}{\mathbb{F}_t^{(Liv)}[P_t]} = \frac{\text{SPIF_12M}_t}{\text{SPIF_ZM}_t} & \text{if } t \geq 1992M6 \\ \left(\frac{\mathbb{F}_t^{(Liv)}[P_{t+1}]}{\mathbb{F}_t^{(Liv)}[P_{t+6}]} \right)^2 = \left(\frac{\text{spi12}_t}{\text{spi6}_t} \right)^2 & \text{if } t < 1992M6 \end{cases}$$

where P_t is the S&P 500 index and t indexes the survey's response deadline. To obtain a survey expectation of the log change in price growth I use the approximation $\mathbb{F}_t(\Delta p_{t+1}) \approx \log(\mathbb{F}_t[P_{t+1}]) - \log(P_t)$.

Conference Board (CB) Survey Respondents provide the categorical belief of whether they expect stock prices to “increase,” “decrease,” or stay the “same” over the next year. Since the survey asks respondents about stock prices in the “year ahead,” I interpret the question to be asking about the forecast period from the end of the current survey month to the end of the same month one year ahead. When we use this qualitative survey forecast to compare to machine forecasts, we impute a point forecast for stock market returns using the method described in Section C.3.2 below. I compare the imputed point forecast to machine forecasts of CRSP returns.

The survey is conducted monthly and I use the survey responses over 1987:04 to 2022:08. The data was downloaded on September 26, 2022. The survey uses an address-based mail sample design. Questionnaires are mailed to households on or about the first of each month. Survey responses flow in throughout the collection period, with the sample close-out for preliminary estimates occurring around the 18th of the month. Any responses received after then are used to produce final estimates for the month, which are published with the following month’s data. Conversations with those knowledgeable about the survey suggested that most panelists respond early. Any responses received after around the 20th of the month—regardless of when they are filled out—are included in the final (but not preliminary) numbers.

I take a stand on the information set of the respondents when each forecast was made by assuming that respondents could have used all data released before they completed the survey. Since questionnaires reach households on or about the first of each month (e.g., February 1st) and most respondents respond early, I conservatively set the response deadline for the machine forecast to be the first day of the survey month (e.g., February 1st), implying that I allow the machine to use information only up through the end of the previous month (e.g., January 31st).

Converting Qualitative Forecasts to Point Forecasts (SOC and CB) I use the SOC probability to impute a quantitative point forecast of stock returns using a linear regression of CFO point forecasts for returns onto the SOC probability of a price increase. The SOC asks respondents about the percent chance that an investment will “increase in value in the year ahead.” I interpret this as asking about the ex dividend value, i.e., about price price growth. The CFO survey is conducted quarterly, where the survey quarters span 2001Q4 to 2021Q1. The SOC survey is conducted monthly, where survey months span 2002:06 to 2021:12. Since the CFO is a quarterly survey, the regression is estimated in real-time over a quarterly overlapping sample. Since the CFO survey is conducted during the last month of the quarter while the SOC is conducted monthly, I align the survey months between CFO and SOC by regressing the quarterly CFO survey point forecast with the qualitative SOC survey response during the last month of the quarter.

Since the SOC survey question is interpreted as asking about S&P 500 price growth while the CFO survey question asks about stock returns including dividends, I follow Nagel and Xu (2021) in subtracting the current dividend yield of the CRSP value weighted index from the CFO variable before running the regression. After estimating the regression, I then add back the dividend yield to the fitted value to obtain an imputed SOC point forecast of stock returns including dividends. Specifically, at time t , I assume that the CFO forecast of stock returns, $\mathbb{F}_t^{\text{CFO}}[r_{t,t+1}]$, minus the current dividend yield, D_t/P_t , is related to the contemporaneous SOC probability of an increase in the stock market next year, $P_{t,t+1}^{\text{SOC}}$, by:

$$\mathbb{F}_t^{\text{CFO}}[r_{t,t+1}] - D_t/P_t = \beta_0 + \beta_1 P_{t,t+1}^{\text{SOC}} + \epsilon_t.$$

The final imputed SOC point forecast is constructed as $\mathbb{F}_t^{\text{SOC}}[r_{t,t+1}] = \hat{\beta}_0 + \hat{\beta}_1 P_{t,t+1}^{\text{SOC}} + D_t/P_t$. I first estimate the coefficients of the above regression over an initial overlapping sample of 2002Q2 to 2004Q4, where the quarterly observations from the CFO survey is regressed on the SOC survey responses from the last month of each calendar quarter. Using the estimated coefficients and the SOC probability from 2005:03 gives us the point forecast of the one-year stock return from 2005Q1 to 2006Q1. I then re-estimate this equation, recursively, adding one quarterly observation to the end of the sample at a time, and storing the fitted values. This results in a time series of SOC point forecasts $\mathbb{F}_t^{\text{SOC}}[r_{t,t+1}]$ spanning 2005Q1 to 2021Q1.

The same procedure is done for the Conference Board Survey, except I replace $P_{t,t+1}^{\text{SOC}}$ by $P_{t,t+1}^{\text{CB}}$, a ratio of the proportion of those who respond with “increase” to the sum of “decrease” and “same.” The CB survey asks respondents to provide the categorical belief of whether they expect stock prices to “increase,” “decrease,” or stay the “same” over the next year. I interpret this as asking about price price growth. Since the CB survey question is interpreted as asking about S&P 500 price growth while the CFO survey question asks about stock returns including dividends, I follow Nagel and Xu (2021) in subtracting the current dividend yield of the CRSP value weighted index from the CFO variable before running the regression. After estimating the regression, I then add back the dividend yield to the fitted value to obtain an imputed CB point forecast of stock returns including dividends.

The CFO survey is conducted quarterly, where the survey quarters span 2001Q4 to 2021Q1. The CB survey is conducted monthly, where survey months span 1987:04 to 2022:08. The regression is first estimated over an initial overlapping sample of 2001Q4 to 2004Q4, where the quarterly observations from the CFO survey is regressed on the CB survey responses from the last month of each calendar quarter. Using the estimated coefficients and the CB survey response $P_{t,t+1}^{\text{CB}}$ from 2005:03 gives us the point forecast of the stock return from 2005Q1 to 2006Q1. I then re-estimate this equation, recursively, adding one observation to the end of the sample at a time, and storing the fitted values. This results in a time series of CB point forecasts $\mathbb{F}_t^{\text{CB}}[r_{t,t+1}]$ over 2005Q1 to 2021Q1.

Nagel and Xu Individual Investor Expectations Nagel and Xu (2021)'s individual investor expectations series for returns covers 1972-1977 (Annual) and 1987Q2-2023Q4 (Quarterly) and combine data from the following surveys:

1. UBS/Gallup: 1998:06-2007:10; Survey captures respondents' expected stock market returns, in percent, over a 1-year horizon.
2. Michigan Survey of Consumers (SOC): 2002:04-2023:12; Respondents provide the probability of a rise in the stock market over a 1-year horizon.
3. Conference Board (CB): 1987:04-2022:08; Respondents provide the categorial opinion whether they expect stock prices to rise, or stay about where they are, or decline over the next year.
4. Vanguard Research Initiative (VRI): 2014:08; Survey captures respondents' expected stock market returns, in percent, over a 1-year horizon.
5. Roper: 1974-1977, annual, observed June of each calendar year; Respondents provide the categorial opinion whether they expect stock prices to rise, or stay about where they are, or decline over the next year.
6. Lease, Lewellen, and Schlarbaum (1974, 1977): 1972-1973, annual, observed July of each calendar year; Survey captures respondents' expected stock market returns, in percent, over a 1-year horizon.

Among these sources, UBS/Gallup and VRI provide direct, point forecasts of expected stock returns, while SOC, CB, and Roper offer qualitative or probabilistic information that requires conversion to consistent return expectations. Nagel and Xu (2021) construct their final series using the following procedure:

1. Start with UBS/Gallup for 1998:06-2007:10 and VRI for 2014:08 since they capture the respondents' expected stock returns relatively closely (other surveys only provide qualitative measures).
2. Regress SOC on UBS/Gallup and VRI using periods of overlapping coverage (2002:04-2007:10). Use the fitted values from this regression to impute missing data for 2007:11-2023:12 (excluding 2014:08).
3. Regress CB on UBS/Gallup and VRI using periods of overlapping coverage (1998:06-2007:10). Use the fitted values from this regression to impute missing data for 1987:04-1998:05 (using CB) and 1974-1977 (using Roper).
4. Use the coefficients from regressing CB on UBS/Gallup and VRI (from step 3) to compute fitted values that convert the probabilistic forecast from Roper into point forecasts of stock returns.
5. Convert expected returns to expected excess returns by subtracting the average 1-year Treasury yield measured at the beginning of the survey month.
6. Aggregate monthly series to a quarterly frequency by taking the average expectation within calendar quarters.

C.4 Risk-Free Rates

Realized Risk-Free Rates As a measure of realized risk-free rates r_t^f , I obtain daily series for the annualized three-month Treasury bill rate (DTB3), downloaded from FRED on May 15, 2024. To match the definition used as the target variable in the Survey of Professional Forecasters (SPF), I time-aggregate the daily realized risk-free rate series to a quarterly frequency by taking the quarterly average, as discussed below.

Survey Expectations of Risk-Free Rates I obtain subjective expectations about risk-free rates from median forecasts for the annualized three-month Treasury bill rate from the Survey of Professional Forecasters (SPF). The SPF provides forecasts at the one and ten year horizons. For one year ahead forecasts (TBILL), respondents are asked to provide quarterly forecasts of the quarterly average three-month Treasury bill rate, in percentage points, where the forecasts are for the quarterly average of the underlying daily levels. I interpret the survey to be asking about annual net simple rates $\mathbb{F}_t[R_{t,t+1}^f]$, and approximate the expected log risk-free rate as $\mathbb{F}_t[r_{t,t+1}^f] \approx \log(1 + \mathbb{F}_t[R_{t,t+1}^f])$. For ten year ahead forecasts (BILL10), respondents are asked to provide forecasts for the annual-average rate of return to three-month Treasury bills over the next 10 years, in percentage points. The ten year ahead forecasts are available only for surveys conducted in the first quarter of each calendar year. I interpret the survey to be asking about annualized cumulative net simple rates compounded from the survey quarter to the same quarter that is ten years after the survey year $\mathbb{F}_t[R_{t,t+10}^f]$, and approximate the expected log risk-free rate as $\mathbb{F}_t[r_{t,t+10}^f] \approx \log(1 + \mathbb{F}_t[R_{t,t+10}^f])$. To obtain long-horizon survey expectations of annualized log three-month Treasury bill rates over the next $1 < h < 10$ years, I interpolate the forecasts across annualized 1 year and 10 year return expectations:

$$\mathbb{F}_t[r_{t,t+h}^f] = \frac{10 - h}{10 - 1} \mathbb{F}_t[r_{t,t+1}^f] + \frac{h - 1}{10 - 1} \mathbb{F}_t[r_{t,t+10}^f], \quad h = 1, 2, \dots, 10$$

Finally, I use the difference between the cumulative annualized long-horizon log three-month Treasury bill rate expectations between adjacent years (i.e., $\mathbb{F}_t[r_{t,t+h-1}^f]$ and $\mathbb{F}_t[r_{t,t+h}^f]$) to obtain $\mathbb{F}_t[r_{t+h}^f]$, the time t survey expectation of annualized forward log three-month Treasury bill rate h years ahead:

$$\mathbb{F}_t[r_{t+h}^f] = h \times \mathbb{F}_t[r_{t,t+h}^f] - (h - 1) \times \mathbb{F}_t[r_{t,t+h-1}^f], \quad h = 1, 2, \dots, 10$$

The surveys are sent out at the end of the first month of each quarter, and collected in the second or third week of the middle month of each quarter. When constructing machine learning forecasts for the risk-free rate, I assume that forecasters could have used all data released before the survey deadlines for the SPF, which are posted online at the Federal Reserve Bank of Philadelphia website. Since surveys are typically sent out at the end of the first month of each quarter, I make the conservative assumption that respondents only had data released by the first day of the second month of each quarter.

C.5 Earnings

C.5.1 Realized Earnings

I use IBES street earnings per share (EPS) data that start in 1983:Q4 as the forecast target for IBES analysts. Following the recommendation of Hillenbrand and McCarthy (2024), I use Street earnings as the forecast target for IBES analysts. Street earnings differ from GAAP earnings by excluding discontinued operations, extraordinary charges, and other non-operating items. According to the IBES user guide, analysts submit forecasts after backing out these transitory components, and IBES constructs the realized series to align with those forecasts. While analysts have some discretion over which items to exclude, Hillenbrand and McCarthy (2024) demonstrate that the target of these forecasts corresponds closely to earnings before special items in Compustat, suggesting that street earnings accurately reflect the measure analysts are targeting. To convert EPS to total earnings, I multiply the resulting quarterly EPS series by the quarterly S&P 500 divisor, available at: https://ycharts.com/indicators/sp_500_divisor. The final quarterly total earnings series spans the period 1983:Q4 to 2023:Q4. To extend the sample back to 1965Q1, I use quarterly Compustat data on earnings before special items. As noted in Hillenbrand and McCarthy (2024), this measure closely tracks IBES street earnings, indicating it accurately reflects analysts' forecast targets. IBES street earnings data and Compustat data has been downloaded from WRDS on July 19, 2025. The divisor data were downloaded on July 21, 2025.

C.5.2 Survey Expectations of Earnings

I obtain monthly survey data for the median analyst earnings per share forecast and actual earnings per share from the Institutional Brokers Estimate System (IBES) via Wharton Research Data Services (WRDS). The data spans the period 1976:01 to 2023:12.

Short-Term Growth (STG) Expectations I build measures of aggregate S&P 500 earnings expectations growth using the constituents of the S&P 500 at each point in time following De La O and Myers (2021). I first construct expected earnings expectations for aggregate earnings h -months-ahead as:

$$\mathbb{F}_t[E_{t+h}] = \Omega_t \sum_{i \in x_t} \mathbb{F}_t[EPS_{i,t+h}] \cdot S_{i,t}/Divisor_t$$

where \mathbb{F} is the median analyst survey forecast, E is aggregate S&P 500 earnings, EPS_i is earning per share of firm i among all S&P 500 firms x_t for which I have forecasts in IBES for $t + h$, S_i is shares outstanding of firm i , and $Divisor_t$ is calculated as the S&P 500 market capitalization divided by the S&P 500 index. I obtain the number of outstanding shares

for all companies in the S&P500 from Compustat. IBES estimates are available for most but not all S&P 500 companies. Following De La O and Myers (2021), I multiply this aggregate by Ω_t , a ratio of total S&P 500 market value to the market value of the forecasted companies at t to account for the fact that IBES does not provide earnings forecasts for all firms in the S&P 500 in every period.

IBES database contains earning forecasts up to five annual fiscal periods (FY1 to FY5) and as a result, I interpolate across the different horizons to obtain the expectation over the next 12 months. This procedure has been used in the literature, including De La O and Myers (2021). Specifically, if the fiscal year of firm XYZ ends nine months after the survey date, I have a 9-month earning forecast $\mathbb{F}_t[E_{t+9}]$ from FY1 and a 21-month forecast $\mathbb{F}_t[E_{t+21}]$ from FY2. I then obtain the 12-month ahead forecast by interpolating these two forecasts as follows,

$$\mathbb{F}_t[E_{t+12}] = \frac{9}{12} \mathbb{F}_t[E_{t+9}] + \frac{3}{12} \mathbb{F}_t[E_{t+21}].$$

To convert the monthly forecast to quarterly frequency, I use the forecast made in the middle month of each quarter, and construct one-year earnings expectations from 1976Q1 to 2023Q4 and the earning expectation growth is calculated as an approximation following following De La O and Myers (2021):

$$\mathbb{F}_t(\Delta e_{t+12}) \approx \ln(\mathbb{F}_t[E_{t+12}]) - e_t$$

where e_t is log earnings for S&P 500 at time t calculated as $e_t = \log(EPS_t \cdot Divisor_t)$, where EPS_t is the earnings per share for the S&P 500 obtained from Shiller's data depository and S&P Global, as described above.

Long-Term Growth (LTG) Expectations I construct long term expected earnings growth (LTG) for the S&P 500 following Bordalo et al. (2019). Specifically, I obtain the median firm-level LTG forecast from IBES, and aggregate the value-weighted firm-level forecasts,

$$LTG_t = \sum_{i=1}^S LTG_{i,t} \frac{P_{i,t} Q_{i,t}}{\sum_{i=1}^S P_{i,t} Q_{i,t}}$$

where S is the number of firms in the S&P 500 index, and where $P_{i,t}$ and $Q_{i,t}$ are the stock price and the number of shares outstanding of firm i at time t , respectively. $LTG_{i,t}$ is the median forecast of firm i 's long term expected earnings growth. The data spans the periods from 1981:12 to 2023:12. All data were downloaded in July 19, 2025.

Finally, I use the difference between survey expectations of log earnings between adjacent years (i.e., $\mathbb{F}_t[e_{t+h-1}]$ and $\mathbb{F}_t[e_{t+h}]$) to obtain $\mathbb{F}_t[\Delta e_{t+h}] = \mathbb{F}_t[e_{t+h}] - \mathbb{F}_t[e_{t+h-1}]$, the time t survey expectation of forward one-year log earnings growth $h = 1, 2$ years ahead. For the $h = 3, 4, 5$ year horizon, I interpret the IBES's Long-Term Growth (LTG) forecast as the forward annual log earnings growth:

$$\mathbb{F}_t[\Delta e_{t+h}] = \begin{cases} \mathbb{F}_t[e_{t+h}] - \mathbb{F}_t[e_{t+h-1}] & \text{if } h = 1, 2 \text{ years} \\ LTG_t & \text{if } h = 3, 4, 5 \text{ years} \end{cases}$$

To estimate any biases in IBES analyst forecasts, the dynamic machine algorithm takes as an input a likely date corresponding to information analysts could have known at the time of their forecast. IBES does not provide an explicit deadline for their forecasts to be returned. Therefore I instead use the “statistical period” day (the day when the set of summary statistics was calculated) as a proxy for the deadline. I set the machine deadline to be the day before this date. The statistical period date is typically between day 14 and day 20 of a given month, implying that the machine deadline varies from month to month. As the machine learning algorithm uses mixed-frequency techniques adapted to quarterly sampling intervals, while the IBES forecasts are monthly, I compare machine and IBES analyst forecasts as of the middle month of each quarter, considering 12-month ahead forecast from the beginning of the month following the survey month.

C.6 Price-Earnings Ratio

I construct a quarterly series for the price-earnings ratio $PE_t \equiv P_t/E_t$ using the end-of-quarter S&P 500 stock price index P_t and the S&P 500 quarterly total earnings E_t . I infer subjective expectations of the log price-earnings ratio $\mathbb{F}_t[pe_{t+h}]$ by combining the current log price-earnings ratio pe_t with h year ahead subjective expectations of annual log stock returns $\mathbb{F}_t[r_{t+h}]$ and annual log earnings growth $\mathbb{F}_t[\Delta e_{t+h}]$, following the approach used in De La O and Myers (2021). Rearrange the Campbell and Shiller (1988) present value identity for the price-earnings ratio in equation (A.51) to express the future log price-earnings ratio as a function of current log price-earnings, log earnings growth, and log stock returns:

$$pe_{t+h} = \frac{1}{\rho^h} pe_t - \frac{1}{\rho^h} \sum_{j=1}^h \rho^{j-1} (c_{pe} + \Delta e_{t+j} - r_{t+j})$$

where the equation holds both ex-ante and ex-post. Apply subjective expectations \mathbb{F}_t on both sides of the equation:

$$\mathbb{F}_t[pe_{t+h}] = \frac{1}{\rho^h} pe_t - \frac{1}{\rho^h} \sum_{j=1}^h \rho^{j-1} (c_{pe} + \underbrace{\mathbb{F}_t[\Delta e_{t+j}]}_{\text{Survey (IBES)}} - \underbrace{\mathbb{F}_t[r_{t+j}]}_{\text{Survey (CFO)}})$$
(A.81)

where subjective expectations about j years ahead forward annual log stock returns $\mathbb{F}_t[r_{t+j}]$ and forward annual log earnings growth $\mathbb{F}_t[\Delta e_{t+j}]$ use survey forecasts from the CFO survey and IBES, respectively. I construct firm-level price-earnings expectations by applying the same log-linear approximation to firm-level expectations of stock returns (from IBES and Value Line) and earnings growth (from IBES).

C.7 Earnings-Employment Ratio

The current earnings-employment ratio is defined as $EL_t \equiv E_t/L_{t+1}$, where E_t denotes quarterly total earnings for the S&P 500 and L_{t+1} is the employment stock at the beginning of period $t+1$. I measure L_{t+1} using end-of-period employment levels within each quarter. This timing assumption ensures that the measures are consistent with the timing conventions from Section B while still remaining known to firms by the end of period t .

C.8 Machine Learning Forecasts

For each survey forecast, I also construct their corresponding machine learning forecast by estimating a Long Short-Term Memory (LSTM) neural network:

$$\mathbb{E}_t[y_{t+h}] = G(\mathcal{X}_t, \boldsymbol{\beta}_{h,t})$$

where y_{t+h} denotes the variable y to be predicted h years ahead of time t , and \mathcal{X}_t is a large input dataset of right-hand-side variables including the intercept. $G(\mathcal{X}_t, \boldsymbol{\beta}_{h,t})$ denotes predicted values from a LSTM neural network that can be represented by a (potentially) high-dimensional set of finite-valued parameters $\boldsymbol{\beta}_{h,t}$. The machine learning model is estimated using an algorithm that takes into account the data-rich environment in which firms operate in (Bianchi et al., 2022 and Bianchi et al., 2024). When constructing machine learning forecasts of each variable, I allow the machine to use only information that would have been available to all survey respondents at the time of each forecast. See Section D for details about the machine learning algorithm and predictor variables. Machine expectations about the price-earnings ratio $\mathbb{E}_t[pe_{t+h}]$ is constructed similarly to the survey counterpart, by replacing the survey forecasts of stock returns and earnings growth on the right-hand side of equation (A.81) with the corresponding machine learning forecasts.

For the cross-sectional decomposition, I construct analogous machine learning forecasts of returns, earnings growth, and price-earnings ratios at the firm level using the same LSTM framework, applied to portfolio-specific predictors and outcomes. To keep the machine learning algorithm tractable, I re-estimate the model parameters and update the hyper-parameter cross-validation every four quarters.

D Machine Learning

D.1 Machine Algorithm Details

The basic dynamic algorithm follows the six step approach of Bianchi et al. (2022) of 1. Sample partitioning, 2. In-sample estimation, 3. Training and cross-validation, 4. Grid reoptimization, 5. Out-of-sample prediction, and 6. Roll forward and repeat. We refer the interested reader to that paper for details and discuss details of the implementation here only insofar as they differ. At time t , a prior sample of size \dot{T} is partitioned into two subsample windows: a *training sample* consisting of the first T_E observations, and a hold-out *validation sample* of T_V subsequent observations so that $\dot{T} = T_E + T_V$. The training sample is used to estimate the model subject to a specific set of tuning parameter values, and the validation sample is used for tuning the hyperparameters. The model to be estimated over the training sample is

$$y_{t+h} = G^e(\mathcal{X}_t, \boldsymbol{\beta}_{h,t}) + \epsilon_{t+h}.$$

where y_{t+h} is a time series indexed by j whose value in period $h \geq 1$ the machine is asked to predict at time t , \mathcal{X}_t is a large input dataset of right-hand-side variables including the intercept, and $G^e(\cdot)$ is a machine learning estimator that can be represented by a (potentially) high-dimensional set of finite-valued parameters $\boldsymbol{\beta}_{h,t}^e$. We consider two estimators for $G^e(\cdot)$: Elastic Net $G^{\text{EN}}(\mathcal{X}_t, \boldsymbol{\beta}_{j,h}^{\text{EN}})$, and Long Short-Term Memory (LSTM) network $G^{\text{LSTM}}(\mathcal{X}_t, \boldsymbol{\beta}_{j,h}^{\text{LSTM}})$. The $e \in \{\text{EN}, \text{LSTM}\}$ superscripts on $\boldsymbol{\beta}$ indicate that the parameters depend on the estimator being used (See the next section for a description of EN and LSTM). \mathcal{X}_t always denotes the most recent data that would have been in real time prior to the date on which the forecast was submitted. To ensure that the effect of each variable in the input vector is regularized fairly during the estimation, we standardize the elements of \mathcal{X}_t such that sample means are zero and sample standard deviations are unity. It should be noted that the most recent observation on the left-hand-side is generally available in real time only with a

one-period lag, thus the forecasting estimations can only be run with data over a sample that stops one period later than today in real time. The parameters $\beta_{h,t}^e$ are estimated by minimizing the mean-square loss function over the training sample with L_1 and L_2 penalties

$$L(\beta_{h,t}^e, \mathbf{X}_{T_E}, \lambda_t^e) \equiv \underbrace{\frac{1}{T_E} \sum_{\tau=1}^{T_E} (y_{\tau+h} - G^e(\mathcal{X}_\tau, \beta_{h,t}^e))^2}_{\text{Mean Square Error}} + \underbrace{\lambda_{1,t}^e \sum_{k=1}^K |\beta_{j,h,t,k}^e|}_{L_1 \text{ Penalty}} + \underbrace{\lambda_{2,t}^e \sum_{k=1}^K (\beta_{j,h,t,k}^e)^2}_{L_2 \text{ Penalty}}$$

where $\mathbf{X}_{T_E} = (y_{t-T_E}, \dots, y_t, \mathcal{X}'_{t-T_E}, \dots, \mathcal{X}'_t)'$ is the vector containing all observations in the training sample of size T_E . The estimated $\beta_{h,t}^e$ is a function of the data \mathbf{X}_{T_E} and a non-negative regularization parameter vector $\lambda_t^e = (\lambda_{1,t}^e, \lambda_{2,t}^e, \lambda_{0,t}^{LSTM})'$ where $\lambda_{0,t}^{LSTM}$ is a set of hyperparameters only relevant when using the LSTM estimator for $G^e(\cdot)$ (see below). For the EN case there are only two hyperparameters, which determine the optimal shrinkage and sparsity of the time t machine specification. The regularization parameters λ_t^e are estimated by minimizing the mean-square loss over pseudo-out-of-sample forecast errors generated from rolling regressions through the validation sample:

$$\hat{\lambda}_t^e, \hat{T}_E, \hat{T}_V = \underset{\lambda_t^e, T_E, T_V}{\operatorname{argmin}} \left\{ \frac{1}{T_V - h} \sum_{\tau=T_E}^{T_E+T_V-h} (y_{\tau+h} - G^e(\mathcal{X}_\tau, \hat{\beta}_{j,h,\tau}^e(\mathbf{X}_{T_E}, \lambda_t^e)))^2 + \underbrace{\lambda_{1,t}^e \sum_{k=1}^K |\beta_{j,h,t,k}^e|}_{L_1 \text{ Penalty}} + \underbrace{\lambda_{2,t}^e \sum_{k=1}^K (\beta_{j,h,t,k}^e)^2}_{L_2 \text{ Penalty}} \right\}$$

where $\hat{\beta}_{j,h,\tau}^e(\cdot)$ for $e \in \{\text{EN, LSTM}\}$ is the time τ estimate of $\beta_{j,h}^e$ given λ_t^e and data through time τ in a training sample of size T_E . Denote the combined final estimator $\hat{\beta}_{h,t}^e(\mathbf{X}_{\hat{T}_E}, \hat{\lambda}_t^e)$, where the regularization parameter $\hat{\lambda}_t^e$ is estimated using cross-validation dynamically over time. Note that the algorithm also asks the machine to dynamically choose both the optimal training window \hat{T}_E and the optimal validation window \hat{T}_V by minimizing the pseudo-out-of-sample MSE.

The estimation of $\hat{\beta}_{h,t}^e(\mathbf{X}_{\hat{T}_E}, \hat{\lambda}_t^e)$ is repeated sequentially in rolling subsamples, with parameters estimated from information known at time t . Note that the time t subscripts of $\hat{\beta}_{h,t}^e$ and $\hat{\lambda}_t^e$ denote one in a sequence of time-invariant parameter estimates obtained from rolling subsamples, rather than estimates that vary over time within a sample. Likewise, we denote the time t machine belief about y_{t+h} as $\mathbb{E}_t^e[y_{t+h}]$, defined by

$$\mathbb{E}_t^e[y_{t+h}] \equiv G^e(\mathcal{X}_t, \hat{\beta}_{h,t}^e(\mathbf{X}_{\hat{T}_E}, \hat{\lambda}_t^e))$$

Finally, the machine MSE is computed by averaging across the sequence of squared forecast errors in the true out-of-sample forecasts for periods $t = (\hat{T} + h), \dots, T$ where T is the last period of our sample. The true out-of-sample forecasts used for neither estimation nor tuning is the *testing subsample* used to evaluate the model's predictive performance.

On rare occasions, one or more of the explanatory variables used in the machine forecast specification assumes a value that is order of magnitudes different from its historical value. This is usually indicative of a measurement problem in the raw data. We therefore program the machine to detect in real-time whether its forecast is an extreme outlier, and in that case to discard the forecast replacing it with the historical mean. Specifically, at each t , the machine forecast $\mathbb{E}_t^e[y_{t+h}]$ is set to be the historical mean calculated up to time t whenever the former is five or more standard deviations above its own rolling mean over the most recent 20 quarters.

We include the contemporaneous survey forecasts $\mathbb{F}_t[y_{t+h}]$ for the median respondent only for inflation and GDP forecasts, following Bianchi et al. (2022). This procedure allows the machine to capture intangible information due to judgement or private signals. Specifically, for these forecasts of inflation and GDP growth, we consider the following machine learning empirical specification for forecasting y_{t+h} given information at time t , to be benchmarked against the time t survey forecast of respondent-type X , where this type is the median here:

$$y_{t+h} = G_{jh}^e(\mathbf{Z}_t) + \gamma_{jhM} \mathbb{F}_t[y_{t+h}] + \epsilon_{t+h}, \quad h \geq 1$$

where γ_{jhM} is a parameter to be estimated, and where $G_{jhM}(\mathbf{Z}_t)$ represents a ML estimator as function of big data. Note that the intercept α_{jh} from Bianchi et al. (2022) gets absorbed into the $G_{jh}^e(\mathbf{Z}_t)$ in LSTM via the outermost bias term.

D.1.1 Elastic Net (EN)

We use the Elastic Net (EN) estimator, which combines Least Absolute Shrinkage and Selection Operator (LASSO) and ridge type penalties. The model can be written as:

$$y_{t+h} = \mathcal{X}'_{tj} \beta_{j,h}^{\text{EN}} + \epsilon_{t+h}$$

where $\mathcal{X}_t = (1, \mathcal{X}_{1t}, \dots, \mathcal{X}_{Kt})'$ include the independent variable observations $(\mathbb{F}_t[y_{t+h}], \mathcal{Z}_{j,t})$ into a vector with "1" and $\beta_{j,h}^{\text{EN}} = (\alpha_{j,h}, \beta_{j,hF}, \text{vec}(\mathbf{B}_{j,hZ}))' \equiv (\beta_0, \beta_1, \dots, \beta_K)'$ collects all the coefficients.

It is customary to standardize the elements of \mathcal{X}_t such that sample means are zero and sample standard deviations are unity. The coefficient estimates are then put back in their original scale by multiplying the slope coefficients by their respective standard deviations, and adding back the mean (scaled by slope coefficient over standard deviation.) The EN estimator incorporates both an L_1 and L_2 penalty:

$$\widehat{\boldsymbol{\beta}}_{j,h}^{\text{EN}} = \underset{\beta_0, \beta_1, \dots, \beta_K}{\operatorname{argmin}} \frac{1}{T_E} \sum_{\tau=1}^{T_E} \left(y_{\tau+h} - \mathcal{X}'_{\tau} \boldsymbol{\beta}_{j,h} \right)^2 + \underbrace{\lambda_1 \sum_{k=1}^K |\beta_{j,h,k}|}_{\text{LASSO}} + \underbrace{\lambda_2 \sum_{k=1}^K (\beta_{j,h,k})^2}_{\text{ridge}}$$

By minimizing the MSE over the training samples, we choose the optimal λ_1 and λ_2 values simultaneously.

In the implementation, the EN estimator is sometimes used as an input into the algorithm using the LSTM estimator. Specifically, we ensure that the machine forecast can only differ from the relevant benchmark if it demonstrably improves the pseudo out-of-sample prediction in the training samples *prior* to making a true out-of-sample forecast. Otherwise, the machine is replaced by the benchmark calculated up to time t . In some cases the benchmark is a survey forecast, in others it could be a historical mean value for the variable. However, for the implementation using LSTM, we also use the EN forecast as a benchmark.

D.1.2 Long Short-Term Memory (LSTM) Network

An LSTM network is a type of Recurrent Neural Network (RNN), which are neural networks used to learn about sequential data such as time series or natural language. In particular, LSTM networks can learn long-term dependencies between across time periods by introducing hidden layers and memory cells to control the flow of information over longer time periods. The general case of the LSTM network with up to N hidden layers is defined as

$$\begin{aligned} \underbrace{G^{\text{LSTM}}(\mathcal{X}_t, \boldsymbol{\beta}_{j,h}^{\text{LSTM}})}_{1 \times 1} &= \underbrace{W^{(y h^N)}}_{1 \times D_{hN}} \underbrace{h_t^N}_{D_{hN} \times 1} + \underbrace{b_y}_{1 \times 1} && \text{(Output layer)} \\ \underbrace{h_t^n}_{D_{hN} \times 1} &= \underbrace{o_t^n}_{D_{hN} \times 1} \odot \tanh(\underbrace{c_t^n}_{D_{hN} \times 1}) && \text{(Hidden layer)} \\ \underbrace{c_t^n}_{D_{hN} \times 1} &= \underbrace{f_t^n}_{D_{hN} \times 1} \odot \underbrace{c_{t-1}^n}_{D_{hN} \times 1} + \underbrace{i_t^n}_{D_{hN} \times 1} \odot \underbrace{\tilde{c}_t^n}_{D_{hN} \times 1} && \text{(Final memory)} \\ \underbrace{\tilde{c}_t^n}_{D_{hN} \times 1} &= \tanh(\underbrace{W^{(c^n h^{n-1})}}_{D_{hN} \times D_{hN-1}} \underbrace{h_{t-1}^{n-1}}_{D_{hN-1} \times 1} + \underbrace{W^{(c^n h^n)}}_{D_{hN} \times D_{hN}} \underbrace{h_{t-1}^n}_{D_{hN} \times 1} + \underbrace{b_{c^n}}_{D_{hN} \times 1}) && \text{(New memory)} \\ \underbrace{f_t^n}_{D_{hN} \times 1} &= \sigma(\underbrace{W^{(f^n h^{n-1})}}_{D_{hN} \times D_{hN-1}} \underbrace{h_{t-1}^{n-1}}_{D_{hN-1} \times 1} + \underbrace{W^{(f^n h^n)}}_{D_{hN} \times D_{hN}} \underbrace{h_{t-1}^n}_{D_{hN} \times 1} + \underbrace{b_{f^n}}_{D_{hN} \times 1}) && \text{(Forget gate)} \\ \underbrace{i_t^n}_{D_{hN} \times 1} &= \sigma(\underbrace{W^{(i^n h^{n-1})}}_{D_{hN} \times D_{hN-1}} \underbrace{h_{t-1}^{n-1}}_{D_{hN-1} \times 1} + \underbrace{W^{(i^n h^n)}}_{D_{hN} \times D_{hN}} \underbrace{h_{t-1}^n}_{D_{hN} \times 1} + \underbrace{b_{i^n}}_{D_{hN} \times 1}) && \text{(Input gate)} \\ \underbrace{o_t^n}_{D_{hN} \times 1} &= \sigma(\underbrace{W^{(o^n h^{n-1})}}_{D_{hN} \times D_{hN-1}} \underbrace{h_{t-1}^{n-1}}_{D_{hN-1} \times 1} + \underbrace{W^{(o^n h^n)}}_{D_{hN} \times D_{hN}} \underbrace{h_{t-1}^n}_{D_{hN} \times 1} + \underbrace{b_{o^n}}_{D_{hN} \times 1}) && \text{(Output gate)} \end{aligned}$$

where $n = 1, \dots, N$ indexes each hidden layer. $h_t^n \in \mathbb{R}^{D_{hN}}$ is the n -th *hidden layer*, where D_{hN} is the number of *neurons* or *nodes* in the hidden layer. The 0-th layer is defined as the input data: $h_0^0 \equiv \mathcal{X}_t$. The memory cell c_t^n allows the LSTM network to retain information over longer time periods. The output gate o_t^n controls the extent to which the memory cell c_t^n maps to the hidden layer h_t^n . The forget gate f_t^n controls the flow of information carried over from the final memory in the previous timestep c_{t-1}^n . The input gate i_t^n controls the flow of information from the new memory cell \tilde{c}_t^n . The initial states for the hidden layers $(h_0^n)_{n=1}^N$ and memory cells $(c_0^n)_{n=1}^N$ are set to zeros. $\sigma(\cdot)$ and $\tanh(\cdot)$ are *activation functions* that introduce non-linearities in the LSTM network, applied elementwise. $\sigma : \mathbb{R} \rightarrow \mathbb{R}$ is the sigmoid function: $\sigma(x) = (1 + e^{-x})^{-1}$. $\tanh : \mathbb{R} \rightarrow \mathbb{R}$ is the hyperbolic tangent function: $\tanh(x) = \frac{e^{2x}-1}{e^{2x}+1}$. The \odot operator refers to elementwise multiplication. $\boldsymbol{\beta}_{j,h}^{\text{LSTM}} \equiv (((\text{vec}(W^{(g^n h^{n-1})})), \text{vec}(W^{(g^n h^n)}), b_{g^n}),_{g \in \{c,f,i,o\}})_{n=1}^N, \text{vec}(W^{(y h^N)}), b_y)$ are parameters to be estimated. We will refer to parameters indexed with W as *weights*; parameters indexed with b are *biases*. We estimate the parameters $\boldsymbol{\beta}_{j,h}^{\text{LSTM}}$ for the LSTM network using Stochastic Gradient Decent (SGD), which is an iterative algorithm for minimizing the loss function and proceeds as follows:

1. *Initialization.* Fix a random seed R and draw a starting value of the parameters $\boldsymbol{\beta}_{j,h}^{(0)}$ randomly, where the superscript (0) in parentheses indexes the iteration for an estimate of $\boldsymbol{\beta}_{j,h}^{\text{LSTM}}$.

- (a) Initialize input weights $W^{(g^n h^{n-1})} \in \mathbb{R}^{D_{h^n} \times D_{h^{n-1}}}$ for $g \in \{c, f, i, o\}$ using the *Glorot* initializer. Draw from a uniform distribution with zero mean and a variance that depends on the dimensions of the matrix:

$$W_{ij}^{(g^n h^{n-1})} \stackrel{iid}{\sim} U \left[-\sqrt{\frac{6}{D_{h^n} + D_{h^{n-1}}}}, \sqrt{\frac{6}{D_{h^n} + D_{h^{n-1}}}} \right]$$

for each $i = 1, \dots, D_{h^n}$ and $j = 1, \dots, D_{h^{n-1}}$.

- (b) Initialize the recurrent weights $W^{(g^n h^n)} \in \mathbb{R}^{D_{h^n} \times D_{h^n}}$ for $g \in \{c, f, i, o\}$ using the *Orthogonal* initializer. Use the orthogonal matrix obtained from the QR decomposition of a $D_{h^n} \times D_{h^n}$ matrix of random numbers drawn from a standard normal distribution.
- (c) Initialize biases $(b_{g^n})_{g \in \{c, f, i, o\}}$, hidden layers h_0^n , and memory cells c_0^n with zeros.

2. *Mini-batches*. Prepare the input data by dividing the training sample into a collection of *mini-batches*.

- (a) Suppose that we have a multi-variate time-series training sample with dimensions (T_E, K) whose time steps t are indexed by $t = 1, \dots, T_E$ and K is the number of predictors. We transform this training sample into a 3-D tensor with dimensions (N_S, M, K) where
- N_S = Total number of sequences in training sample
 - M = Sequence length, i.e., number of time steps in each sequence
 - K = Input size, i.e., number of predictors in each time step

This can be done by creating overlapping sequences from the time series:

- Sequence 1 contains time steps $1, \dots, M$
- Sequence 2 contains time steps $2, \dots, M + 1$
- Sequence 3 contains time steps $3, \dots, M + 2$
- \dots
- Sequence $T_E - M$ contains time steps $T_E - M, \dots, T_E - 1$
- Sequence $N_S = T_E - M + 1$ contains time steps $T_E - M + 1, \dots, T_E$

- (b) Randomly shuffle the N_S sequences by randomly sampling a permutation without replacement.

- (c) Partition the N_S shuffled sequences into $\lceil N_S / N_B \rceil$ mini-batches. We partition the N_S sequences in the training sample $((N_S, M, K)$ tensor) into a list of $\lceil N_S / N_B \rceil$ mini-batches. A mini-batch is a (N_B, M, K) -dimensional tensor containing N_B out of N_S randomly shuffled sequences. When N_S / N_B is not a whole number, $\lfloor N_S / N_B \rfloor$ of the mini-batches will be 3-D tensors with dimensions (N_B, M, K) . One batch will contain leftover sequences and will have dimensions $(N_S \% N_B, M, K)$ where $\%$ is the modulus operator. Let $B^{(1)}, \dots, B^{\lceil N_S / N_B \rceil}$ denote the list of mini-batches.

- N_S = Total number of sequences in training sample
- N_B = Mini-batch size, i.e., number of sequences in each partition.
- M = Sequence length, i.e., number of time steps in each sequence
- K = Input size, i.e., number of predictors in each time step

3. Repeat until the stopping condition is satisfied ($k = 1, 2, 3, \dots$):

- (a) *Dropout*. Apply dropout to the mini-batch. To obtain the n -th hidden layer under dropout, multiply the current value of the $n - 1$ -th hidden layer h_t^{n-1} and the lagged value of the n -th hidden layer h_{t-1}^n with binary masks $r_{t, h_t^{n-1}}^{(k)} \in \mathbb{R}^{D_{h^{n-1}}}$ and $r_{t, h_{t-1}^n}^{(k)} \in \mathbb{R}^{D_{h^n}}$, respectively:

$$\underbrace{h_t^{n-1}}_{D_{h^{n-1}} \times 1} = \underbrace{r_{t, h_t^{n-1}}^{(k)}}_{D_{h^{n-1}} \times 1} \odot \underbrace{h_{t-1}^n}_{D_{h^n} \times 1}, \quad r_{t, h_t^{n-1}, i}^{(k)} \stackrel{iid}{\sim} \text{Bernoulli}(p_{h_t^{n-1}}), \quad i = 1, \dots, D_{h^{n-1}}$$

$$\underbrace{h_{t-1}^n}_{D_{h^n} \times 1} = \underbrace{r_{t, h_{t-1}^n}^{(k)}}_{D_{h^n} \times 1} \odot \underbrace{h_{t-1}^n}_{D_{h^n} \times 1}, \quad r_{t, h_{t-1}^n, i}^{(k)} \stackrel{iid}{\sim} \text{Bernoulli}(p_{h_{t-1}^n}), \quad i = 1, \dots, D_{h^n}$$

where $t \in B^{(k)}$ and $n = 1, \dots, N$ indexes the hidden layer and it is understood that the 0-th layer is the input vector $h_t^0 \equiv \mathcal{X}_t$. $p_{h_t^{n-1}}, p_{h_{t-1}^n} \in [0, 1]$ is the probability that time t nodes in the $n - 1$ -th hidden layer and time $t - 1$ nodes in the n -th hidden layer are retained, respectively.

(b) *Stochastic Gradient*. Average the gradient over observations in the mini-batch

$$\nabla L(\boldsymbol{\beta}_{j,h}^{(k-1)}, \mathbf{X}_{B^{(k)}}, \boldsymbol{\lambda}^{\text{LSTM}}) = \frac{1}{M} \sum_{t \in B^{(k)}} \nabla L(\boldsymbol{\beta}_{j,h}^{(k-1)}, \mathbf{X}_t, \boldsymbol{\lambda}^{\text{LSTM}})$$

where $\nabla L(\boldsymbol{\beta}_{j,h}^{(k-1)}, \mathbf{X}_t, \boldsymbol{\lambda}^{\text{LSTM}})$ is the gradient of the loss function with respect to the parameters $\boldsymbol{\beta}_{j,h}^{(k-1)}$, evaluated at the time t observation $\mathbf{X}_t = (y_{t+h}, \hat{\mathcal{X}}'_t)'$ after applying dropout.

(c) *Learning rate shrinkage*. Update the parameters to $\boldsymbol{\beta}_{j,h}^{(k)}$ using the Adaptive Moment Estimation (Adam) algorithm. The method uses the first and second moments of the gradients to shrink the overall learning rate to zero as the gradient approaches zero.

$$\boldsymbol{\beta}_{j,h}^{(k)} = \boldsymbol{\beta}_{j,h}^{(k-1)} - \gamma \frac{m^{(k)}}{\sqrt{v^{(k)}} + \epsilon}$$

where $m^{(k)}$ and $v^{(k)}$ are weighted averages of first two moments of past gradients:

$$m^{(k)} = \frac{1}{1 - \pi_1^k} (\pi_1 m^{(k-1)} + (1 - \pi_1) \nabla L(\boldsymbol{\beta}_{j,h}^{(k-1)}, \mathbf{X}_{B^{(k)}}, \boldsymbol{\lambda}^{\text{LSTM}}))$$

$$v^{(k)} = \frac{1}{1 - \pi_2^k} (\pi_2 v^{(k-1)} + (1 - \pi_2) \nabla L(\boldsymbol{\beta}_{j,h}^{(k-1)}, \mathbf{X}_{B^{(k)}}, \boldsymbol{\lambda}^{\text{LSTM}})^2)$$

π^k denotes the k -the power of $\pi \in (0, 1)$, and $/$, $\sqrt{\cdot}$, and $(\cdot)^2$ are applied elementwise. The default values of the hyperparameters are $m^{(0)} = v^{(0)} = 0$ (initial moment vectors), $\gamma = 0.001$ (initial learning rate), $(\pi_1, \pi_2) = (0.9, 0.999)$ (decay rates), and $\epsilon = 10^{-7}$ (prevent zero denominators).

(d) *Stopping Criteria*. Stop iterating and return $\boldsymbol{\beta}_{j,h}^{(k)}$ if one of the following holds:

- *Early stopping*. At each iteration, use the updated $\boldsymbol{\beta}_{j,h}^{(k)}$ to calculate the loss from the validation sample. Stop when the validation loss has not improved for S steps, where S is a “patience” hyperparameter. By updating the parameters for fewer iterations, early stopping shrinks the final parameters $\boldsymbol{\beta}_{j,h}$ towards the initial guess $\boldsymbol{\beta}_{j,h}^{(0)}$, and at a lower computational cost than ℓ_2 regularization.
- *Maximum number of epochs*. Stop if the number of iterations reaches the maximum number of epochs E . An epoch happens when the full set of the training sample has been used to update the parameters. If the training sample has T_E observations and each mini-batch has M observations, then each epoch would contain $\lceil T_E/M \rceil$ iterations (after rounding up as needed). So the maximum number of iterations is bounded by $E \times \lceil T_E/M \rceil$.

4. *Ensemble forecasts*. Repeat steps 1. and 2. over different random seeds R and save each of the estimated parameters $\widehat{\boldsymbol{\beta}}_{j,h,T_E}^{LSTM}(\mathbf{X}_{T_E}, \boldsymbol{\lambda}^{\text{LSTM}}, R)$. Then construct out-of-sample forecasts using the top 10 out of 20 starting values with the best performance in the validation sample. Ensemble can be considered as a regularization method because it aims to guard against overfitting by shrinking the forecasts toward the average across different random seeds. The random seed affects the random draws of the parameter’s initial starting value $\boldsymbol{\beta}_{j,h}^{(0)}$, the sequences selected in each mini-batch $B^{(k)}$, and the dropout mask $r_t^{(k)}$.

Hyperparameters Let $\boldsymbol{\lambda}^{\text{LSTM}} \equiv [\lambda_1, \lambda_2, \gamma, \pi_1, \pi_2, p, N, (D_{h^n})_{n=1}^N, M, E, S]'$ collect all the hyper-parameters that control the LSTM network’s complexity and prevent the model from overfitting the data. The number of hidden layers N and the number of neurons D_{h^1}, \dots, D_{h^N} in each hidden layer are hyper-parameters that characterize the network’s architecture. To choose the number of neurons in each layer, we apply a geometric pyramid rule where the dimension of each additional hidden layer is half that of the previous hidden layer. We select the best LSTM architecture iteratively by minimizing the pseudo out-of-sample mean-squared error from rolling forecasts over the validation sample. Table A.11 reports the hyper-parameters for the LSTM network and its estimation. Hyper-parameters reported as a range or a set of values are cross-validated. The hyper-parameters are estimated by minimizing the mean-square loss over pseudo out-of-sample forecast errors generated from rolling regressions through the validation sample. The pseudo out-of-sample forecasts are ensemble averages implied by parameters based on different random seeds R .

Adaptive Architecture Selection We allow the LSTM architecture to evolve over time using a simple, adaptive updating procedure. At each period in the testing sample, the machine selects the architecture (number of hidden layers and neurons per layer) that minimized out-of-sample forecast errors in the preceding period. The candidate architectures considered span various combinations of hidden layers and neurons per layer, as listed in Table A.11. The architecture is updated quarterly by using the forecast performance from the most recent quarter. This approach allows the machine to adjust its specification over time based on evolving patterns in the data, while avoiding look-ahead bias or overfitting to future outcomes.

Table A.11: Candidate hyper-parameters for the machine learning forecast

Variable	Earnings Growth	Stock Returns
Horizon (Years)	1,2,3,4,5	1,2,3,4,5
(a) Elastic Net		
L_1 penalty λ_1		
L_1 penalty λ_1	$[10^{-2}, 10^1]$	$[10^{-6}, 10^{-2}]$
L_2 penalty λ_2	$[10^{-2}, 10^1]$	$[10^{-6}, 10^{-2}]$
Training window T_E	4, 6, 8, 10	5, 7
Validation window T_V	4, 6, 8, 10	5, 7, 20
(b) Long Short-Term Memory Network		
L_1 penalty λ_1	$[10^{-6}, 10^{-2}]$	$[10^{-6}, 10^{-2}]$
L_2 penalty λ_2	$[10^{-6}, 10^{-2}]$	$[10^{-6}, 10^{-2}]$
Learning rate γ	0.001	0.001
Gradient decay π_1, π_2	0.9, 0.999	0.9, 0.999
Dropout input p_x	0.5	0.5
Dropout recurrent p_h	0.5	0.5
Hidden layers N	1, 3, 5	1, 3, 5
Neurons per layer	16, 32, 64	4, 8, 16
Mini-batch size M	4	4
Max epochs E	10,000	10,000
Early stopping S	20	20
Random seeds R	1, ..., 20	1, ..., 20
Training window T_E	4, 8, 12	5, 7
Validation window T_V	4, 8, 12	5, 7, 20

Notes: This table reports the hyperparameters considered in the machine learning algorithm for each estimator.

D.2 Data Inputs for Machine Learning Algorithm

D.2.1 Macro Data Surprises

These data are used as inputs into the machine learning forecasts. I obtain median forecasts for GDP growth (Q/Q percentage change), core CPI (Month/Month change), unemployment rate (percentage point), and nonfarm payroll (month/month change) from the Money Market Service Survey. The median market survey forecasts are compiled and published by the Money Market Services (MMS) the Friday before each release. I apply the approach used in Bauer and Swanson (2023) and define macroeconomic data surprise as the actual value of the data release minus the median expectation from MMS on the Friday immediately prior to that data release. The GDP growth forecasts are available quarterly from 1990Q1 to 2023Q4. The core CPI forecast is available monthly from July 1989 to December 2023. The median forecasts for the unemployment rate and nonfarm payrolls are available monthly from January 1980 to December 2023, and January 1985 to December 2023, respectively. All survey forecasts were downloaded from Haver Analytics on December 17, 2022 and the Bloomberg Terminal on July 15, 2025. To pin down the timing of when the news was actually released I follow the published tables of releases from the Bureau of Labor Statistics (BLS), discussed below.

The macro news events are indexed by their date and time of the data release, while the machine learning algorithm is adapted to quarterly sampling frequencies. When including the macro data surprises as additional predictors for the machine forecast, I time-aggregate the macro data surprises to a quarterly frequency by taking the sum of the surprises across data releases that occurred before the response deadline set for the machine. For example, if the response deadline is set to the first day of the middle month of each quarter (e.g., February 1st), I take the sum of the surprises from data releases up to the day before the deadline, the last day of the first month of each quarter (e.g., January 31st).

D.2.2 FOMC Surprises

FOMC surprises are defined as the changes in the current-month, 1, 2, 6, 12, and 24 month-ahead federal funds futures (FFF) contract rate and changes in the 1, 2, 4, and 8 quarter-ahead Eurodollar (ED) futures contract rate, from 10 minutes before to 20 minutes after each U.S. Federal Reserve Federal Open Market Committee (FOMC) announcement. The data on FFF and ED were downloaded on July 15, 2025. When benchmarking against a survey, I use the last FOMC meeting before the survey deadline to compute surprises. For surveys that do not have a clear deadline, I compute surprises using from the last FOMC in the first month of the quarter. When benchmarking against moving average, I use the last FOMC meeting before the end of the first month in each quarter to compute surprises.

When including the FOMC surprises as additional predictors for the machine forecast, I time-aggregate the FOMC surprises to a quarterly frequency by taking the sum of the surprises across FOMC announcements that occurred before the response deadline set for the machine. For example, if the response deadline is set to the first day of the middle month of each quarter (e.g., February 1st), I take the sum of the surprises from FOMC announcements up to the day before the deadline, the last day of the first month of each quarter (e.g., January 31st).

D.2.3 S&P 500 Jumps

As a measure of the market's reaction to news shocks, I use the jump in the S&P 500 pre- and post- a 30-minute window around major news events. The events in our analysis include (i) 1,482 macroeconomic data releases for U.S. GDP, Consumer Price Index (CPI), unemployment, and payroll data spanning 1980:01-2023:12, (ii) 16 corporate earnings announcement days spanning 1999:03-2020:05, and (iii) 219 Federal Open Market Committee (FOMC) press releases from the Fed spanning 1994:02-2023:12. The corporate earnings news events are from Baker et al. (2019) who conduct textual analyses of *Wall Street Journal* articles to identify days in which there were large jumps in the aggregate stock market that could be attributed to corporate earnings news with high confidence. The jump in the S&P 500 for a given event is defined as $j_\tau = p_{\tau+\delta_{post}} - p_{\tau-\delta_{pre}}$, where τ indexes the time of an event and $p_\tau = \log(P_\tau)$ is the log S&P 500 index. δ_{pre} and δ_{post} denote the pre and post event windows, which is 10 minutes before and 20 minutes after the event, respectively. I obtain data on P_τ using tick-by-tick data on the S&P 500 index from tickdata.com. The series was purchased and downloaded on July 15, 2025 from <https://www.tickdata.com/>. I create the minutely data using the close price within each minute. I supplement the S&P 500 index using S&P500 E-mini futures for events that occur in off-market hours. I use the current-quarter contract futures. I purchased the S&P 500 E-mini futures from CME group on July 15, 2025 at <https://datamine.cmgroup.com/>. Our sample spans 1/2/1986 to 12/31/2023.

For each event, I separate out the events for which the S&P 500 increased over the window ($j_\tau^{(+)} \geq 0$) and those for which the market decreased ($j_\tau^{(-)} \leq 0$). I aggregate the event-level jumps to monthly time series by summing over all the relevant events within the month, where the events are partitioned into two groups based on the sign of the jump: $J_t^{(+)} = \sum_{\tau \in x(t)} j_\tau^{(+)}$, $J_t^{(-)} = \sum_{\tau \in x(t)} j_\tau^{(-)}$, where t indexes the month and $x(t)$ is the set of all events that occurred within month t . The procedure results in two monthly variables, $J_t^{(+)}$ and $J_t^{(-)}$, which capture total market reaction to news events in either direction during the quarter. The series spans the period 1994:02 to 2023:12. Separating out the events based on the sign of the jump allows us to capture any differential effects on return predictability based on whether the market perceived the news as good or bad. The partition also allows us to accurately capture the total extent of over- or underreaction. Otherwise, mixing all the events would only capture the net effect of the jumps and bias the market reaction towards zero.

When used as additional predictors in the for the machine forecast, the jumps need to be converted to quarterly time series because the machine learning algorithm is adapted to a quarterly sampling frequency. The set of events in $x(t)$ is chosen so that the machine only sees the news events that would have been available to the real-time firm. When combining the events within a quarter, I impose the response deadline used to produce the machine forecast. For example, if the response deadline is set to the first day of the middle month of each quarter (e.g., February 1st), I use the jumps from the events up to the day before the deadline, the last day of the first month of each quarter (e.g., January 31st).

D.2.4 Real-Time Macro Data

This section gives details on the real time macro data inputs used in the machine learning forecasts. A subset of these series are used in the structural estimation. At each forecast date in the sample, I construct a dataset of macro variables that could have been observed on or before the day of the survey deadline. I use the Philadelphia Fed's Real-Time Data Set to obtain vintages of macro variables. The real-time data sets are available at <https://www.philadelphiafed.org/research-and-data/real-time-center/real-time-data/data-files>. These vintages capture changes to historical data due to periodic revisions made by government statistical agencies. The vintages for a particular series can be available at the monthly and/or quarterly frequencies, and the series have monthly and/or quarterly observations. In cases where a variable has both frequencies available for its vintages and/or its observations, I choose one format of the variable. For instance, nominal personal consumption expenditures on goods is quarterly data with both monthly and quarterly vintages available; in this case, I use the version with monthly vintages.

Table A.12 gives the complete list of real-time macro variables. Included in the table is the first available vintages for each variable that has multiple vintages. I do not include the last vintage because most variables have vintages through the present. For variables BASEBASAQVMD, NBRBASAQVMD, NBRECBASAQVMD, and TRBASAQVMD, the last available vintage is 2013Q2. Table A.12 also lists the transformation applied to each variable to make them stationary before generating factors. Let $X_{i,t}$ denote variable i at time t after the transformation, and let $X_{i,t}^A$ be the untransformed series. Let $\Delta = (1 - L)$ with $LX_{i,t} = X_{it-1}$. There are seven possible transformations with the following codes:

- 1 Code *lv*: $X_{i,t} = X_{i,t}^A$
- 2 Code *Δ lv*: $X_{i,t} = X_{i,t}^A - X_{it-1}^A$
- 3 Code *Δ^2 lv*: $X_{i,t} = \Delta^2 X_{i,t}^A$
- 4 Code *ln*: $X_{i,t} = \ln(X_{i,t}^A)$
- 5 Code *Δ ln*: $X_{i,t} = \ln(X_{i,t}^A) - \ln(X_{it-1}^A)$
- 6 Code *Δ^2 ln*: $X_{i,t} = \Delta^2 \ln(X_{i,t}^A)$
- 7 Code *Δ lv/lv*: $X_{i,t} = (X_{i,t}^A - X_{it-1}^A)/X_{it-1}^A$

Table A.12: List of Macro Dataset Variables

No.	Short Name	Source	Tran	Description	First Vintage
Group 1: Output and Income					
1	IPMMVMD	Philly Fed	Δln	Ind. production index - Manufacturing	1962M11
2	IPTMVMD	Philly Fed	Δln	Ind. production index - Total	1962M11
3	CUMMVMD	Philly Fed	lv	Capacity utilization - Manufacturing	1979M8
4	CUTMVMD	Philly Fed	lv	Capacity utilization - Total	1983M7
5	NCPROFATMVQD	Philly Fed	Δln	Nom. corp. profits after tax without IVA/CCAdj	1965Q4
6	NCPROFATWMVQD	Philly Fed	Δln	Nom. corp. profits after tax with IVA/CCAdj	1981Q1
7	OPHMVQD	Philly Fed	Δln	Output per hour - Business sector	1998Q4
8	NDPIQVQD	Philly Fed	Δln	Nom. disposable personal income	1965Q4
9	NOUTPUTQVQD	Philly Fed	Δln	Nom. GNP/GDP	1965Q4
10	NPIQVQD	Philly Fed	Δln	Nom. personal income	1965Q4
11	NPSAVQVQD	Philly Fed	Δlv	Nom. personal saving	1965Q4
12	OLIQVQD	Philly Fed	Δln	Other labor income	1965Q4
13	PINTIQVQD	Philly Fed	Δln	Personal interest income	1965Q4
14	PINTPAIDQVQD	Philly Fed	Δln	Interest paid by consumers	1965Q4
15	PROPIQVQD	Philly Fed	Δln	Proprietors' income	1965Q4
16	PTAXQVQD	Philly Fed	Δln	Personal tax and nontax payments	1965Q4
17	RATESAVQVQD	Philly Fed	Δlv	Personal saving rate	1965Q4
18	RENTIQVQD	Philly Fed	Δlv	Rental income of persons	1965Q4
19	ROUTPUTQVQD	Philly Fed	Δln	Real GNP/GDP	1965Q4
20	SSCONTRIBQVQD	Philly Fed	Δln	Personal contributions for social insurance	1965Q4
21	TRANPFQVQD	Philly Fed	Δln	Personal transfer payments to foreigners	1965Q4
22	TRANRQVQD	Philly Fed	Δln	Transfer payments	1965Q4
23	CUUR0000SA0E	BLS	$\Delta^2 ln$	Energy in U.S. city avg., all urban consumers, not seasonally adj	
Group 2: Employment					
24	EMPLOYMVM	Philly Fed	Δln	Nonfarm payroll	1946M12
25	HMVMD	Philly Fed	lv	Aggregate weekly hours - Total	1971M9
26	HGMVMD	Philly Fed	lv	Agg. weekly hours - Goods-producing	1971M9
27	HSMVMD	Philly Fed	lv	Agg. weekly hours - Service-producing	1971M9
28	LFCMVMD	Philly Fed	Δln	Civilian labor force	1998M11
29	LFPARTMVMD	Philly Fed	lv	Civilian participation rate	1998M11
30	POPMVMD	Philly Fed	Δln	Civilian noninstitutional population	1998M11
31	ULCMVMD	Philly Fed	Δln	Unit labor costs - Business sector	1998Q4
32	RUCQVMD	Philly Fed	Δlv	Unemployment rate	1965Q4
33	WSDQVQD	Philly Fed	Δln	Wage and salary disbursements	1965Q4
Group 3: Orders, Investment, Housing					
34	HSTARTSMVMD	Philly Fed	Δln	Housing starts	1968M2
35	RINVBFMVQD	Philly Fed	Δln	Real gross private domestic inv. - Nonresidential	1965Q4
36	RINVCHIMVQD	Philly Fed	Δlv	Real gross private domestic inv. - Change in private inventories	1965Q4
37	RINVRESIDMVQD	Philly Fed	Δln	Real gross private domestic inv. - Residential	1965Q4
38	CASESHILLER	S&P	Δln	Case-Shiller US National Home Price index/CPI	1987M1
Group 4: Consumption					
39	NCONGMMVMD	Philly Fed	Δln	Nom. personal cons. exp. - Goods	2009M8
40	NCONHHMMVMD	Philly Fed	Δln	Nom. hh. cons. exp.	2009M8
41	NCONSHHMMVMD	Philly Fed	Δln	Nom. hh. cons. exp. - Services	2009M8
42	NCONSNPMMVMD	Philly Fed	Δln	Nom. final cons. exp. of NPISH	2009M8
43	RCONDMMVMD	Philly Fed	Δln	Real personal cons. exp. - Durables	1998M11
44	RCONGMMVMD	Philly Fed	Δln	Real personal cons. exp. - Goods	2009M8
45	RCONHHMMVMD	Philly Fed	Δln	Real hh. cons. exp.	2009M8
46	RCONMMVMD	Philly Fed	Δln	Real personal cons. exp. - Total	1998M11
47	RCONNDMMVMD	Philly Fed	Δln	Real personal cons. exp. - Nondurables	1998M11
48	RCONSHHMMVMD	Philly Fed	Δln	Real hh. cons. exp. - Services	2009M8
49	RCONSMMVMD	Philly Fed	Δln	Real personal cons. exp. - Services	1998M11
50	RCONSNPMMVMD	Philly Fed	Δln	Real final cons. exp. of NPISH	2009M8
51	NCONGMVQD	Philly Fed	Δln	Nom. personal cons. exp. - Goods	2009Q3
52	NCONHHMVQD	Philly Fed	Δln	Nom. hh. cons. exp.	2009Q3
53	NCONSHHMVQD	Philly Fed	Δln	Nom. hh. cons. exp. - Services	2009Q3
54	NCONSNPMVQD	Philly Fed	Δln	Nom. final cons. exp. of NPISH	2009Q3
55	RCOND MVQD	Philly Fed	Δln	Real personal cons. exp. - Durable goods	1965Q4
56	RCONGMVQD	Philly Fed	Δln	Real personal cons. exp. - Goods	2009Q3
57	RCONHHMVQD	Philly Fed	Δln	Real hh. cons. exp.	2009Q3
58	RCONMVQD	Philly Fed	Δln	Real personal cons. exp. - Total	1965Q4
59	RCONNDMVQD	Philly Fed	Δln	Real personal cons. exp. - Nondurable goods	1965Q4
60	RCONSHHMVQD	Philly Fed	Δln	Real hh. cons. exp. - Services	2009Q3
61	RCONSMVQD	Philly Fed	Δln	Real personal cons. exp. - Services	1965Q4
62	RCONSNPMVQD	Philly Fed	Δln	Real final cons. exp. of NPISH	2009Q3
63	NCONQVQD	Philly Fed	Δln	Nom. personal cons. exp.	1965Q4
Group 5: Prices					
64	PCONGMMVMD	Philly Fed	$\Delta^2 ln$	Price index for personal cons. exp. - Goods	2009M8

No.	Short Name	Source	Tran	Description	First Vintage
65	PCONHHMMVMD	Philly Fed	Δ^2ln	Price index for hh. cons. exp.	2009M8
66	PCONSHHMMVMD	Philly Fed	Δ^2ln	Price index for hh. cons. exp. - Services	2009M8
67	PCONSNPMMVMD	Philly Fed	Δ^2ln	Price index for final cons. exp. of NPISH	2009M8
68	PCPIMVMD	Philly Fed	Δ^2ln	Consumer price index	1998M11
69	PCPIXMVMD	Philly Fed	Δ^2ln	Core consumer price index	1998M11
70	PPPIMVMD	Philly Fed	Δ^2ln	Producer price index	1998M11
71	PPPIXMVMD	Philly Fed	Δ^2ln	Core producer price index	1998M11
72	PCONGMVQD	Philly Fed	Δ^2ln	Price index for personal cons. exp. - Goods	2009Q3
73	PCONHHMVQD	Philly Fed	Δ^2ln	Price index for hh. cons. exp.	2009Q3
74	PCONSHHMVQD	Philly Fed	Δ^2ln	Price index for hh. cons. exp. - Services	2009Q3
75	PCONSNPMVQD	Philly Fed	Δ^2ln	Price index for final cons. exp. of NPISH	2009Q3
76	PCONXMVQD	Philly Fed	Δ^2ln	Core price index for personal cons. exp.	1996Q1
77	CPIQVMD	Philly Fed	Δ^2ln	Consumer price index	1994Q3
78	PQVQD	Philly Fed	Δ^2ln	Price index for GNP/GDP	1965Q4
79	PCONQVQD	Philly Fed	Δ^2ln	Price index for personal cons. exp.	1965Q4
80	PIMPQVQD	Philly Fed	Δ^2ln	Price index for imports of goods and services	1965Q4
Group 6: Trade and Government					
81	REXMVQD	Philly Fed	Δln	Real exports of goods and services	1965Q4
82	RGMVQD	Philly Fed	Δln	Real government cons. and gross inv. - Total	1965Q4
83	RGFMVQD	Philly Fed	Δln	Real government cons. and gross inv. - Federal	1965Q4
84	RGSLMVQD	Philly Fed	Δln	Real government cons. and gross. inv. - State and local	1965Q4
85	RIMP MVQD	Philly Fed	Δln	Real imports of goods and services	1965Q4
86	RNXMVQD	Philly Fed	Δlv	Real net exports of goods and services	1965Q4
Group 7: Money and Credit					
87	BASEBASAQVMD	Philly Fed	Δ^2ln	Monetary base	1980Q2
88	M1QVMD	Philly Fed	Δ^2ln	M1 money stock	1965Q4
89	M2QVMD	Philly Fed	Δ^2ln	M2 money stock	1971Q2
90	NBRBASAQVMD	Philly Fed	$\Delta lv/lv$	Nonborrowed reserves	1967Q3
91	NBRECBASAQVMD	Philly Fed	$\Delta lv/lv$	Nonborrowed reserves plus extended credit	1984Q2
92	TRBASAQVMD	Philly Fed	Δ^2ln	Total reserves	1967Q3
93	DIVQVQD	Philly Fed	Δln	Dividends	1965Q4

D.2.5 Monthly Financial Data

The 147 financial series in this data set are versions of the financial dataset used in Jurado et al. (2015) and Ludvigson et al. (2021). It consists of a number of indicators measuring the behavior of a broad cross-section of asset returns, as well as some aggregate financial indicators not included in the macro dataset. These data include valuation ratios such as the dividend-price ratio and earnings-price ratio, growth rates of aggregate dividends and prices, default and term spreads, yields on corporate bonds of different ratings grades, yields on Treasuries and yield spreads, and a broad cross-section of industry equity returns. Following Fama and French (1992), returns on 100 portfolios of equities sorted into 10 size and 10 book-to-market categories. The dataset X^f also includes a group of variables we call “risk-factors,” since they have been used in cross-sectional or time-series studies to uncover variation in the market risk-premium. These risk-factors include the three Fama and French (1993) risk factors, namely the excess return on the market MKT_t , the “small-minus-big” (SMB_t) and “high-minus-low” (HML_t) portfolio returns, the momentum factor UMD_t , and the small stock value spread $R15 - R11$.

The raw data used to form factors are always transformed to achieve stationarity. In addition, when forming forecasting factors from the large macro and financial datasets, the raw data (which are in different units) are standardized before performing PCA. When forming common uncertainty from estimates of individual uncertainty, the raw data (which are in this case in the same units) are demeaned, but we do not divide by the observation’s standard deviation before performing PCA. Throughout, the factors are estimated by the method of static principal components (PCA). Specifically, the $T \times r_F$ matrix \hat{F}_t is \sqrt{T} times the r_F eigenvectors corresponding to the r_F largest eigenvalues of the $T \times T$ matrix $xx'/(TN)$ in decreasing order. In large samples (when $\sqrt{T}/N \rightarrow \infty$), Bai and Ng (2006) show that the estimates \hat{F}_t can be treated as though they were observed in the subsequent forecasting regression. All returns and spreads are expressed in logs (i.e., the log of the gross return or spread), are displayed in percent (i.e., multiplied by 100), and are annualized by multiplying by 12. That is, if x is the original return or spread, we transform to $1200 \times \log(1+x/100)$. Federal Reserve data are annualized by default and are therefore not re-annualized. Note that this annualization implies that the annualized standard deviation (volatility) is equal to the data standard deviation divided by $\sqrt{12}$. The data series used in this dataset are listed below by data source. Additional details on data transformations are given below the table.

We convert monthly data to quarterly by using either the beginning-of-quarter or end-of-quarter values. The decision to use beginning-of-quarter or end-of-quarter depends on the survey deadline of a particular forecast date. If the survey deadline is known to be in the middle of the second month of quarter t , then it is conceivable that the forecasters would have information about the first month of quarter t . Therefore, we use the first month of that quarter’s values. Alternatively, a few anomalous observations have unknown survey deadlines (e.g., the SPF deadlines for 1990Q1). In such cases, we allow

only information up to quarter $t - 1$ to enter the model. Thus, we use the last month of the previous quarter's values in these cases. Let $X_{i,t}$ denote variable i observed at time t after, e.g., logarithm and differencing transformation, and let $X_{i,t}^A$ be the actual (untransformed) series. Let $\Delta = (1 - L)$ with $LX_{i,t} = X_{i,t-1}$. There are six possible transformations with the following codes:

- 1 Code $lv : X_{i,t} = X_{i,t}^A$
- 2 Code $\Delta lv : X_{i,t} = X_{i,t}^A - X_{i,t-1}^A$
- 3 Code $\Delta^2 lv : X_{i,t} = \Delta^2 X_{i,t}^A$
- 4 Code $ln : X_{i,t} = \log(X_{i,t}^A)$
- 5 Code $\Delta ln : X_{i,t} = \log(X_{i,t}^A) - \log(X_{i,t-1}^A)$
- 6 Code $\Delta^2 ln : X_{i,t} = \Delta^2 \log(X_{i,t}^A)$
- 7 Code $\Delta lv / lv : X_{i,t} = \frac{X_{i,t}^A - X_{i,t-1}^A}{X_{i,t-1}^A}$

Table A.13: List of Financial Dataset Variables

No.	Short Name	Source	Tran	Description
Group 1: Prices, Yields, Dividends				
1	D_log(DIV)	CRSP	Δln	1 log D_t , see additional details below
2	D_log(P)	CRSP	Δln	1 log P_t , see additional details below
3	D_DIVreinvest	CRSP	Δln	1 log $D_t^{re,*}$, see additional details below
4	D_Preinvest	CRSP	Δln	1 log $P_t^{re,*}$, see additional details below
5	d-p	CRSP	ln	$\log D_t - P_t$, see additional details below
Group 2: Equity Risk Factors				
6	R15-R11	Kenneth French	lv	(Small, High) minus (Small, Low) sorted on (size, book-to-market)
7	Mkt-RF	Kenneth French	lv	Market excess return
8	SMB	Kenneth French	lv	Small Minus Big, sorted on size
9	HML	Kenneth French	lv	High Minus Low, sorted on book-to-market
10	UMD	Kenneth French	lv	Up Minus Down, sorted on momentum
Group 3: Industries				
11	Agric	Kenneth French	lv	Agric industry portfolio
12	Food	Kenneth French	lv	Food industry portfolio
13	Beer	Kenneth French	lv	Beer industry portfolio
14	Smoke	Kenneth French	lv	Smoke industry portfolio
15	Toys	Kenneth French	lv	Toys industry portfolio
16	Fun	Kenneth French	lv	Fun industry portfolio
17	Books	Kenneth French	lv	Books industry portfolio
18	Hshld	Kenneth French	lv	Hshld industry portfolio
19	Clths	Kenneth French	lv	Clths industry portfolio
20	MedEq	Kenneth French	lv	MedEq industry portfolio
21	Drugs	Kenneth French	lv	Drugs industry portfolio
22	Chems	Kenneth French	lv	Chems industry portfolio
23	Rubbr	Kenneth French	lv	Rubbr industry portfolio
24	Txtls	Kenneth French	lv	Txtls industry portfolio
25	BldMt	Kenneth French	lv	BldMt industry portfolio
26	Cnstr	Kenneth French	lv	Cnstr industry portfolio
27	Steel	Kenneth French	lv	Steel industry portfolio
28	Mach	Kenneth French	lv	Mach industry portfolio
29	ElcEq	Kenneth French	lv	ElcEq industry portfolio
30	Autos	Kenneth French	lv	Autos industry portfolio
31	Aero	Kenneth French	lv	Aero industry portfolio
32	Ships	Kenneth French	lv	Ships industry portfolio
33	Mines	Kenneth French	lv	Mines industry portfolio
34	Coal	Kenneth French	lv	Coal industry portfolio
35	Oil	Kenneth French	lv	Oil industry portfolio
36	Util	Kenneth French	lv	Util industry portfolio
37	Telcm	Kenneth French	lv	Telcm industry portfolio
38	PerSv	Kenneth French	lv	PerSv industry portfolio
39	BusSv	Kenneth French	lv	BusSv industry portfolio
40	Hardw	Kenneth French	lv	Hardw industry portfolio
41	Chips	Kenneth French	lv	Chips industry portfolio
42	LabEq	Kenneth French	lv	LabEq industry portfolio
43	Paper	Kenneth French	lv	Paper industry portfolio
44	Boxes	Kenneth French	lv	Boxes industry portfolio
45	Trans	Kenneth French	lv	Trans industry portfolio
46	Whlsl	Kenneth French	lv	Whlsl industry portfolio

No.	Short Name	Source	Tran	Description
47	Rtail	Kenneth French	<i>lv</i>	Rtail industry portfolio
48	Meals	Kenneth French	<i>lv</i>	Meals industry portfolio
49	Banks	Kenneth French	<i>lv</i>	Banks industry portfolio
50	Insur	Kenneth French	<i>lv</i>	Insur industry portfolio
51	RlEst	Kenneth French	<i>lv</i>	RlEst industry portfolio
52	Fin	Kenneth French	<i>lv</i>	Fin industry portfolio
53	Other	Kenneth French	<i>lv</i>	Other industry portfolio
Group 4: Size/BM				
54	1..2	Kenneth French	<i>lv</i>	(1, 2) portfolio sorted on (size, book-to-market)
55	1..4	Kenneth French	<i>lv</i>	(1, 4) portfolio sorted on (size, book-to-market)
56	1..5	Kenneth French	<i>lv</i>	(1, 5) portfolio sorted on (size, book-to-market)
57	1..6	Kenneth French	<i>lv</i>	(1, 6) portfolio sorted on (size, book-to-market)
58	1..7	Kenneth French	<i>lv</i>	(1, 7) portfolio sorted on (size, book-to-market)
59	1..8	Kenneth French	<i>lv</i>	(1, 8) portfolio sorted on (size, book-to-market)
60	1..9	Kenneth French	<i>lv</i>	(1, 9) portfolio sorted on (size, book-to-market)
61	1..high	Kenneth French	<i>lv</i>	(1, high) portfolio sorted on (size, book-to-market)
62	2..low	Kenneth French	<i>lv</i>	(2, low) portfolio sorted on (size, book-to-market)
63	2..2	Kenneth French	<i>lv</i>	(2, 2) portfolio sorted on (size, book-to-market)
64	2..3	Kenneth French	<i>lv</i>	(2, 3) portfolio sorted on (size, book-to-market)
65	2..4	Kenneth French	<i>lv</i>	(2, 4) portfolio sorted on (size, book-to-market)
66	2..5	Kenneth French	<i>lv</i>	(2, 5) portfolio sorted on (size, book-to-market)
67	2..6	Kenneth French	<i>lv</i>	(2, 6) portfolio sorted on (size, book-to-market)
68	2..7	Kenneth French	<i>lv</i>	(2, 7) portfolio sorted on (size, book-to-market)
69	2..8	Kenneth French	<i>lv</i>	(2, 8) portfolio sorted on (size, book-to-market)
70	2..9	Kenneth French	<i>lv</i>	(2, 9) portfolio sorted on (size, book-to-market)
71	2..high	Kenneth French	<i>lv</i>	(2, high) portfolio sorted on (size, book-to-market)
72	3..low	Kenneth French	<i>lv</i>	(3, low) portfolio sorted on (size, book-to-market)
73	3..2	Kenneth French	<i>lv</i>	(3, 2) portfolio sorted on (size, book-to-market)
74	3..3	Kenneth French	<i>lv</i>	(3, 3) portfolio sorted on (size, book-to-market)
75	3..4	Kenneth French	<i>lv</i>	(3, 4) portfolio sorted on (size, book-to-market)
76	3..5	Kenneth French	<i>lv</i>	(3, 5) portfolio sorted on (size, book-to-market)
77	3..6	Kenneth French	<i>lv</i>	(3, 6) portfolio sorted on (size, book-to-market)
78	3..7	Kenneth French	<i>lv</i>	(3, 7) portfolio sorted on (size, book-to-market)
79	3..8	Kenneth French	<i>lv</i>	(3, 8) portfolio sorted on (size, book-to-market)
80	3..9	Kenneth French	<i>lv</i>	(3, 9) portfolio sorted on (size, book-to-market)
81	3..high	Kenneth French	<i>lv</i>	(3, high) portfolio sorted on (size, book-to-market)
82	4..low	Kenneth French	<i>lv</i>	(4, low) portfolio sorted on (size, book-to-market)
83	4..2	Kenneth French	<i>lv</i>	(4, 2) portfolio sorted on (size, book-to-market)
84	4..3	Kenneth French	<i>lv</i>	(4, 3) portfolio sorted on (size, book-to-market)
85	4..4	Kenneth French	<i>lv</i>	(4, 4) portfolio sorted on (size, book-to-market)
86	4..5	Kenneth French	<i>lv</i>	(4, 5) portfolio sorted on (size, book-to-market)
87	4..6	Kenneth French	<i>lv</i>	(4, 6) portfolio sorted on (size, book-to-market)
88	4..7	Kenneth French	<i>lv</i>	(4, 7) portfolio sorted on (size, book-to-market)
89	4..8	Kenneth French	<i>lv</i>	(4, 8) portfolio sorted on (size, book-to-market)
90	4..9	Kenneth French	<i>lv</i>	(4, 9) portfolio sorted on (size, book-to-market)
91	4..high	Kenneth French	<i>lv</i>	(4, high) portfolio sorted on (size, book-to-market)
92	5..low	Kenneth French	<i>lv</i>	(5, low) portfolio sorted on (size, book-to-market)
93	5..2	Kenneth French	<i>lv</i>	(5, 2) portfolio sorted on (size, book-to-market)
94	5..3	Kenneth French	<i>lv</i>	(5, 3) portfolio sorted on (size, book-to-market)
95	5..4	Kenneth French	<i>lv</i>	(5, 4) portfolio sorted on (size, book-to-market)
96	5..5	Kenneth French	<i>lv</i>	(5, 5) portfolio sorted on (size, book-to-market)
97	5..6	Kenneth French	<i>lv</i>	(5, 6) portfolio sorted on (size, book-to-market)
98	5..7	Kenneth French	<i>lv</i>	(5, 7) portfolio sorted on (size, book-to-market)
99	5..8	Kenneth French	<i>lv</i>	(5, 8) portfolio sorted on (size, book-to-market)
100	5..9	Kenneth French	<i>lv</i>	(5, 9) portfolio sorted on (size, book-to-market)
101	5..high	Kenneth French	<i>lv</i>	(5, high) portfolio sorted on (size, book-to-market)
102	6..low	Kenneth French	<i>lv</i>	(6, low) portfolio sorted on (size, book-to-market)
103	6..2	Kenneth French	<i>lv</i>	(6, 2) portfolio sorted on (size, book-to-market)
104	6..3	Kenneth French	<i>lv</i>	(6, 3) portfolio sorted on (size, book-to-market)
105	6..4	Kenneth French	<i>lv</i>	(6, 4) portfolio sorted on (size, book-to-market)
106	6..5	Kenneth French	<i>lv</i>	(6, 5) portfolio sorted on (size, book-to-market)
107	6..6	Kenneth French	<i>lv</i>	(6, 6) portfolio sorted on (size, book-to-market)
108	6..7	Kenneth French	<i>lv</i>	(6, 7) portfolio sorted on (size, book-to-market)
109	6..8	Kenneth French	<i>lv</i>	(6, 8) portfolio sorted on (size, book-to-market)
110	6..9	Kenneth French	<i>lv</i>	(6, 9) portfolio sorted on (size, book-to-market)
111	6..high	Kenneth French	<i>lv</i>	(6, high) portfolio sorted on (size, book-to-market)
112	7..low	Kenneth French	<i>lv</i>	(7, low) portfolio sorted on (size, book-to-market)
113	7..2	Kenneth French	<i>lv</i>	(7, 2) portfolio sorted on (size, book-to-market)
114	7..3	Kenneth French	<i>lv</i>	(7, 3) portfolio sorted on (size, book-to-market)
115	7..4	Kenneth French	<i>lv</i>	(7, 4) portfolio sorted on (size, book-to-market)
116	7..5	Kenneth French	<i>lv</i>	(7, 5) portfolio sorted on (size, book-to-market)
117	7..6	Kenneth French	<i>lv</i>	(7, 6) portfolio sorted on (size, book-to-market)

No.	Short Name	Source	Tran	Description
118	7.7	Kenneth French	lv	(7, 7) portfolio sorted on (size, book-to-market)
119	7.8	Kenneth French	lv	(7, 8) portfolio sorted on (size, book-to-market)
120	7.9	Kenneth French	lv	(7, 9) portfolio sorted on (size, book-to-market)
121	8_low	Kenneth French	lv	(8, low) portfolio sorted on (size, book-to-market)
122	8_2	Kenneth French	lv	(8, 2) portfolio sorted on (size, book-to-market)
123	8_3	Kenneth French	lv	(8, 3) portfolio sorted on (size, book-to-market)
124	8_4	Kenneth French	lv	(8, 4) portfolio sorted on (size, book-to-market)
125	8_5	Kenneth French	lv	(8, 5) portfolio sorted on (size, book-to-market)
126	8_6	Kenneth French	lv	(8, 6) portfolio sorted on (size, book-to-market)
127	8_7	Kenneth French	lv	(8, 7) portfolio sorted on (size, book-to-market)
128	8_8	Kenneth French	lv	(8, 8) portfolio sorted on (size, book-to-market)
129	8_9	Kenneth French	lv	(8, 9) portfolio sorted on (size, book-to-market)
130	8_high	Kenneth French	lv	(8, high) portfolio sorted on (size, book-to-market)
131	9_low	Kenneth French	lv	(9, low) portfolio sorted on (size, book-to-market)
132	9_2	Kenneth French	lv	(9, 2) portfolio sorted on (size, book-to-market)
133	9_3	Kenneth French	lv	(9, 3) portfolio sorted on (size, book-to-market)
134	9_4	Kenneth French	lv	(9, 4) portfolio sorted on (size, book-to-market)
135	9_5	Kenneth French	lv	(9, 5) portfolio sorted on (size, book-to-market)
136	9_6	Kenneth French	lv	(9, 6) portfolio sorted on (size, book-to-market)
137	9_7	Kenneth French	lv	(9, 7) portfolio sorted on (size, book-to-market)
138	9_8	Kenneth French	lv	(9, 8) portfolio sorted on (size, book-to-market)
139	9_high	Kenneth French	lv	(9, high) portfolio sorted on (size, book-to-market)
140	10_low	Kenneth French	lv	(10, low) portfolio sorted on (size, book-to-market)
141	10_2	Kenneth French	lv	(10, 2) portfolio sorted on (size, book-to-market)
142	10_3	Kenneth French	lv	(10, 3) portfolio sorted on (size, book-to-market)
143	10_4	Kenneth French	lv	(10, 4) portfolio sorted on (size, book-to-market)
144	10_5	Kenneth French	lv	(10, 5) portfolio sorted on (size, book-to-market)
145	10_6	Kenneth French	lv	(10, 6) portfolio sorted on (size, book-to-market)
146	10_7	Kenneth French	lv	(10, 7) portfolio sorted on (size, book-to-market)
147	VXO	Fred MD	lv	VXOCLS

CRSP Data Details Value-weighted price and dividend data were obtained from the Center for Research in Security Prices (CRSP, Center for Research in Security Prices (1926–2022)). From the Annual Update data, we obtain the monthly value-weighted return series `vwretd` (with dividends) and `vwretx` (excluding dividends). These series have the interpretations: $VWRET_t = \frac{P_{t+1} + D_{t+1}}{P_t}$, $VWRETX_t = \frac{P_{t+1}}{P_t}$. From these series, a normalized price series P_t can be constructed recursively as: $P_0 = 1$, $P_t = P_{t-1} \times VWRETX_{t-1}$. A dividend series can then be constructed using: $D_t = P_{t-1} \times (VWRET_{t-1} - VWRETX_{t-1})$. In order to remove seasonality of dividend payments from the data, instead of D_t we use the series: $\bar{D}_t = \frac{1}{12} \sum_{j=0}^{11} D_{t-j}$, i.e., the moving average over the entire year. For the price and dividend series under “reinvestment,” we calculate the price under reinvestment, P_t^{re} , as the normalized value of the market portfolio under reinvestment of dividends, using the recursion: $P_0^{re} = 1$, $P_t^{re} = P_{t-1} \times VWRET_{t-1}$. Similarly, we can define dividends under reinvestment, D_t^{re} , as the total dividend payments on this portfolio (the number of “shares” of which have increased over time) using: $D_t^{re} = P_t^{re} \times (VWRET_{t-1} - VWRETX_{t-1})$. As before, we can remove seasonality by using: $\bar{D}_t^{re} = \frac{1}{12} \sum_{j=0}^{11} D_{t-j}^{re}$. Five data series are constructed from the CRSP data as follows: `D_log(DIV)`: $\Delta \log(\bar{D}_t)$; `D_log(P)`: $\Delta \log(P_t)$; `D_DIVreinvest`: $\Delta \log(\bar{D}_t^{re})$; `D_Preinvest`: $\Delta \log(P_t^{re})$; `d-p`: $\log(\bar{D}_t) - \log(P_t)$.

Kenneth French Data Details The following data are obtained from the data library of Kenneth French’s Dartmouth website (French (1926–2022)):

- Fama/French Factors: From this dataset we obtain the series `RF`, `Mkt-RF`, `SMB`, and `HML`.
- 25 Portfolios Formed on Size and Book-to-Market (5 x 5): From this dataset we obtain the series `R15-R11`, which is the return spread between the (small, high book-to-market) and (small, low book-to-market) portfolios.
- Momentum Factor (Mom): From this dataset we obtain the series `UMD`, which is equal to the momentum factor.
- 49 Industry Portfolios: From this dataset we use all value-weighted series, excluding any series that have missing observations from January 1960 onward. This yields the series `Agric` through `Other`. The omitted series are `Soda`, `Hlth`, `FabPr`, `Guns`, `Gold`, and `Softw`.
- 100 Portfolios Formed on Size and Book-to-Market: From this dataset we use all value-weighted series, excluding any series that have missing observations from January 1960 onward. This yields variables with names `X_Y`, where X denotes the size index (1, 2, ..., 10) and Y denotes the book-to-market index (Low, 2, 3, ..., 8, 9, High). The omitted series are `1_low`, `1_3`, `7_high`, `9_low`, `10_low`, `10_8`, `10_9`, and `10_high`.

VXO Data Details VXO data is obtained from the Monthly Database for Macroeconomic Research (FRED-MD, McCracken (2015–2022)).

D.2.6 Daily Financial Data

Daily Data and construction of daily factors These data are used in the machine learning forecasts. The daily financial series in this data set are from the daily financial dataset used in Andreou et al. (2013). I create a smaller daily database which is a subset of the large cross-section of 991 daily series in their dataset. Our dataset covers five classes of financial assets: (i) the Commodities class; (ii) the Corporate Risk category; (iii) the Equities class; (iv) the Foreign Exchange Rates class and (v) the Government Securities. The dataset includes up to 87 daily predictors in a daily frequency from 23-Oct-1959 to 31-Dec-2023 from the above five categories of financial assets. I remove series with fewer than ten years of data and time periods with no variables observed, which occurs for some series in the early part of the sample. For those years, I have less than 87 series. There are 39 commodity variables which include commodity indices, prices and futures, 16 corporate risk series, 9 equity series which include major US stock market indices and the 500 Implied Volatility, 16 government securities which include the federal funds rate, government treasury bills of securities from three months to ten years, and 7 foreign exchange variables which include the individual foreign exchange rates of major five US trading partners and two effective exchange rate. I choose these daily predictors because they are proposed in the literature as good predictors of economic growth.

I construct daily financial factors in a quarterly frequency in two steps. First, I use these daily financial time series to form factors at a daily frequency. The raw data used to form factors are always transformed to achieve stationarity and standardized before performing factor estimation (see generic description below). I re-estimate factors at each date in the sample recursively over time using the entire history of data available in real time prior to each out-of-sample forecast. In the second step, I convert these daily financial indicators to quarterly weighted variables to form quarterly factors by selecting an optimal weighting scheme according to the method described below (see the weighting scheme section). The data series used in this dataset are listed below in Table A.14 by data source. The tables also list the transformation applied to each variable to make them stationary before generating factors. The transformations used to stationarize a time series are the same as those explained in the section “Monthly financial factor data”.

Table A.14: List of Daily Financial Dataset Variables

No.	Short Name	Source	Tran	Description
Group 1: Commodities				
1	GSIZSPT	Data Stream	Δln	S&P GSCI Zinc Spot - PRICE INDEX
2	GSSBSPT	Data Stream	Δln	S&P GSCI Sugar Spot - PRICE INDEX
3	GSSOSPT	Data Stream	Δln	S&P GSCI Soybeans Spot - PRICE INDEX
4	GSSISPT	Data Stream	Δln	S&P GSCI Silver Spot - PRICE INDEX
5	GSIKSP	Data Stream	Δln	S&P GSCI Nickel Spot - PRICE INDEX
6	GSLCSPT	Data Stream	Δln	S&P GSCI Live Cattle Spot - PRICE INDEX
7	GSLHSPT	Data Stream	Δln	S&P GSCI Lean Hogs Index Spot - PRICE INDEX
8	GSILSPT	Data Stream	Δln	S&P GSCI Lead Spot - PRICE INDEX
9	GSGCSP	Data Stream	Δln	S&P GSCI Gold Spot - PRICE INDEX
10	GSCTSP	Data Stream	Δln	S&P GSCI Cotton Spot - PRICE INDEX
11	GSKCSP	Data Stream	Δln	S&P GSCI Coffee Spot - PRICE INDEX
12	GSCCSPT	Data Stream	Δln	S&P GSCI Cocoa Index Spot - PRICE INDEX
13	GSIASPT	Data Stream	Δln	S&P GSCI Aluminum Spot - PRICE INDEX
14	SGWTSPT	Data Stream	Δln	S&P GSCI All Wheat Spot - PRICE INDEX
15	EIAEBRT	Data Stream	Δln	Europe Brent Spot FOB U\$/BBL Daily
16	CRUDOIL	Data Stream	Δln	Crude Oil-WTI Spot Cushing U\$/BBL - MID PRICE
17	LTICASH	Data Stream	Δln	LME-Tin 99.85% Cash U\$/MT
18	CWFCS00	Data Stream	Δln	CBT-WHEAT COMPOSITE FUTURES CONT. - SETT. PRICE
19	CCFCFS00	Data Stream	Δln	CBT-CORN COMP. CONTINUOUS - SETT. PRICE
20	CSYCS00	Data Stream	Δln	CBT-SOYBEANS COMP. CONT. - SETT. PRICE
21	NCTCS20	Data Stream	Δln	CSCE-COTTON #2 CONT.2ND FUT - SETT. PRICE
22	NSBCS00	Data Stream	Δln	CSCE-SUGAR #11 CONTINUOUS - SETT. PRICE
23	NKCCS00	Data Stream	Δln	CSCE-COFFEE C CONTINUOUS - SETT. PRICE
24	NCCCS00	Data Stream	Δln	CSCE-COCOA CONTINUOUS - SETT. PRICE
25	CZLCS00	Data Stream	Δln	ECBOT-SOYBEAN OIL CONTINUOUS - SETT. PRICE
26	COFC01	Data Stream	Δln	CBT-OATS COMP. TRc1 - SETT. PRICE
27	CLDCS00	Data Stream	Δln	CME-LIVE CATTLE COMP. CONTINUOUS - SETT. PRICE
28	CLGC01	Data Stream	Δln	CME-LEAN HOGS COMP. TRc1 - SETT. PRICE
29	NGCCS00	Data Stream	Δln	CMX-GOLD 100 OZ CONTINUOUS - SETT. PRICE
30	LAH3MTH	Data Stream	Δln	LME-Aluminium 99.7% 3 Months U\$/MT
31	LED3MTH	Data Stream	Δln	LME-Lead 3 Months U\$/MT
32	LNI3MTH	Data Stream	Δln	LME-Nickel 3 Months U\$/MT
33	LTI3MTH	Data Stream	Δln	LME-Tin 99.85% 3 Months U\$/MT
34	PLNYD	www.macrotrends.net	Δln	Platinum Cash Price (U\$ per troy ounce)
35	XPDD	www.macrotrends.net	Δln	Palladium (U\$ per troy ounce)
36	CUS2D	www.macrotrends.net	Δln	Corn Spot Price (U\$/Bushel)
37	SoybOil	www.macrotrends.net	Δln	Soybean Oil Price (U\$/Pound)

No.	Short Name	Source	Tran	Description
38	OATSD	www.macrotrends.net	Δln	Oat Spot Price (US\$/Bushel)
39	WTIOilFut	US EIA	Δln	Light Sweet Crude Oil Futures Price: 1St Expiring Contract Settlement (\$/Bbl)
Group 2: Equities				
40	S&PCOMP	Data Stream	Δln	S&P 500 COMPOSITE - PRICE INDEX
41	ISPCS00	Data Stream	Δln	CME-S&P 500 INDEX CONTINUOUS - SETT. PRICE
42	SP5EIND	Data Stream	Δln	S&P500 ES INDUSTRIALS - PRICE INDEX
43	DJINDUS	Data Stream	Δln	DOW JONES INDUSTRIALS - PRICE INDEX
44	CYMC00	Data Stream	Δln	CBT-MINI DOW JONES CONTINUOUS - SETT. PRICE
45	NASCOMP	Data Stream	Δln	NASDAQ COMPOSITE - PRICE INDEX
46	NASA100	Data Stream	Δln	NASDAQ 100 - PRICE INDEX
47	CBOEVIX	Data Stream	lv	CBOE SPX VOLATILITY VIX (NEW) - PRICE INDEX
48	S&P500toVIX	Data Stream	Δln	S&P500/VIX
Group 3: Corporate Risk				
49	LIBOR	FRED	Δlv	Overnight London Interbank Offered Rate (%)
50	1MLIBOR	FRED	Δlv	1-Month London Interbank Offered Rate (%)
51	3MLIBOR	FRED	Δlv	3-Month London Interbank Offered Rate (%)
52	6MLIBOR	FRED	Δlv	6-Month London Interbank Offered Rate (%)
53	1YLIBOR	FRED	Δlv	One-Year London Interbank Offered Rate (%)
54	1MEuro-FF	FRED	lv	1-Month Eurodollar Deposits (London Bid) (% P.A.) minus Fed Funds
55	3MEuro-FF	FRED	lv	3-Month Eurodollar Deposits (London Bid) (% P.A.) minus Fed Funds
56	6MEuro-FF	FRED	lv	6-Month Eurodollar Deposits (London Bid) (% P.A.) minus Fed Funds
57	APFNF-AANF	Data Stream	lv	1-Month A2/P2/F2 Nonfinancial Commercial Paper (NCP) (% P.A.) minus 1-Month Aa NCP (% P.A.)
58	APFNF-AAF	Data Stream	lv	1-Month A2/P2/F2 NCP (% P.A.) minus 1-Month Aa Financial Commercial Paper (% P.A.)
59	TED	Data Stream, FRED	lv	3Month Tbill minus 3-Month London Interbank Offered Rate (%)
60	MAaa-10YTB	Data Stream	lv	Moody Seasoned Aaa Corporate Bond Yield (% P.A.) minus Y10-Tbond
61	MBaa-10YTB	Data Stream	lv	Moody Seasoned Baa Corporate Bond Yield (% P.A.) minus Y10-Tbond
62	MLA-10YTB	Data Stream, FRED	lv	Merrill Lynch Corporate Bonds: A Rated: Effective Yield (%) minus Y10-Tbond
63	MLAA-10YTB	Data Stream, FRED	lv	Merrill Lynch Corporate Bonds: Aa Rated: Effective Yield (%) minus Y10-Tbond
64	MLAAA-10YTB	Data Stream, FRED	lv	Merrill Lynch Corporate Bonds: AAA Rated: Effective Yield (%) minus Y10-Tbond
Group 4: Treasuries				
65	FRFEDFD	Data Stream	Δlv	US FED FUNDS EFF RATE (D) - MIDDLE RATE
66	FRTBS3M	Data Stream	Δlv	US T-BILL SEC MARKET 3 MONTH (D) - MIDDLE RATE
67	FRTBS6M	Data Stream	Δlv	US T-BILL SEC MARKET 6 MONTH (D) - MIDDLE RATE
68	FRTCM1Y	Data Stream	Δlv	US TREASURY CONST MAT 1 YEAR (D) - MIDDLE RATE
69	FRTCM10	Data Stream	Δlv	US TREASURY CONST MAT 10 YEAR (D) - MIDDLE RATE
70	6MTB-FF	Data Stream	lv	6-month treasury bill market bid yield at constant maturity (%) minus Fed Funds
71	1YTB-FF	Data Stream	lv	1-year treasury bill yield at constant maturity (% P.A.) minus Fed Funds
72	10YTB-FF	Data Stream	lv	10-year treasury bond yield at constant maturity (% P.A.) minus Fed Funds
73	6MTB-3MTB	Data Stream	lv	6-month treasury bill yield at constant maturity (% P.A.) minus 3M-Tbills
74	1YTB-3MTB	Data Stream	lv	1-year treasury bill yield at constant maturity (% P.A.) minus 3M-Tbills
75	10YTB-3MTB	Data Stream	lv	10-year treasury bond yield at constant maturity (% P.A.) minus 3M-Tbills
76	BKEVEN05	FRB	lv	US Inflation compensation: continuously compounded zero-coupon yield: 5-year (%)
77	BKEVEN10	FRB	lv	US Inflation compensation: continuously compounded zero-coupon yield: 10-year (%)
78	BKEVEN1F4	FRB	lv	BKEVEN1F4
79	BKEVEN1F9	FRB	lv	BKEVEN1F9
80	BKEVEN5F5	FRB	lv	US Inflation compensation: coupon equivalent forward rate: 5-10 years (%)
Group 5: Foreign Exchange (FX)				
81	US_CWBN	Data Stream	Δln	US NOMINAL DOLLAR BROAD INDEX - EXCHANGE INDEX
82	US_CWMN	Data Stream	Δln	US NOMINAL DOLLAR MAJOR Curr INDEX - EXCHANGE INDEX

No.	Short Name	Source	Tran	Description
83	US_CSFRR2	Data Stream	Δln	CANADIAN \$ TO US \$ NOON NY - EXCHANGE RATE
84	EU_USFR2	Data Stream	Δln	EURO TO US\$ NOON NY - EXCHANGE RATE
85	US_YFR2	Data Stream	Δln	JAPANESE YEN TO US \$ NOON NY - EXCHANGE RATE
86	US_SFRR2	Data Stream	Δln	SWISS FRANC TO US \$ NOON NY - EXCHANGE RATE
87	US_UKFR2	Data Stream	Δln	UK POUND TO US \$ NOON NY - EXCHANGE RATE

From Daily to Quarterly Factors: Weighting Schemes After we obtain daily financial factors $G_{D,t}$, we use weighting schemes proposed in the literature on Mixed Data Sampling (MIDAS) regressions to form quarterly factors, denoted $G_{D,t}^Q$. Let G_t^D denote a factor in daily frequency formed from the daily financial dataset, and let G_t^Q denote a quarterly aggregate of the corresponding daily factor time series. Let $G_{ND-j,d_t,t}^D$ denote the value of a daily factor on the j -th day counting backwards from the survey deadline d_t in quarter t . Hence, the day d_t of quarter t corresponds to $j = 0$, so the daily factor on the survey deadline is $G_{ND,d_t,t}^D$. For simplicity, we suppress the subscript d_t , writing $G_{ND-j,t}^D$.

We compute the quarterly aggregate of a daily financial factor as a weighted average of observations over the ND business days before the survey deadline. This means that the forecaster's information set includes daily financial data up to the previous ND business days before the survey deadline. The quarterly factor G_t^Q is defined as:

$$G_t^Q(w) = \sum_{j=1}^{ND} w_j \times G_{ND-j,t}^D$$

where w_j is a weight. We consider the following three types of weighting schemes to convert daily factor observations to quarterly aggregates. Each weighting scheme weights information by some function of the number of days prior to the survey deadline.

1. $w_i = 1$ for $i = 1$ and $w_i = 0$ otherwise. This weighting scheme places all weight on the data from the last business day before the survey deadline and zero weight on any data prior to that day.
2. $w_i = \delta^i / \sum_{j=1}^{ND} \delta^j$, where we consider a range of δ values with $\delta \in \{0.1, 0.2, 0.3, 0.7, 0.8, 0.9, 1.0\}$. The smaller the δ , the more rapidly information prior to the survey deadline is down-weighted. This down-weighting is progressive but not non-monotonic. The case $\delta = 1$ corresponds to a simple average of observations across all days.
3. The third parameterization uses two parameters $\theta = (\theta_1, \theta_2)'$ and allows for non-monotonic weighting of past information. The weights are defined as:

$$w(i; \theta_1, \theta_2) = \frac{f\left(\frac{i}{ND}; \theta_1, \theta_2\right)}{\sum_{j=1}^{ND} f\left(\frac{j}{ND}; \theta_1, \theta_2\right)}$$

where $f(x; a, b) = x^{a-1}(1-x)^{b-1} \cdot \frac{\Gamma(a+b)}{\Gamma(a)\Gamma(b)}$, and $\Gamma(a)$ is the gamma function $\Gamma(a) = \int_0^\infty x^{a-1} e^{-x} dx$. The weights $w(i; \theta_1, \theta_2)$ are the Beta polynomial MIDAS weights of Ghysels et al. (2007), based on the Beta function. This weighting scheme is flexible enough to generate a wide range of possible shapes with only two parameters.

We consider these possible weighting schemes and choose the optimal weighting scheme w^* from 24 candidate weighting schemes for each daily financial factor G_t^D by minimizing the sum of squared residuals in a regression of $y_{j,t+h}$ on G_t^Q :

$$y_{j,t+h} = \alpha + \beta \times G_t^Q(w) + u_{t+h}$$

This procedure is conducted in real time using recursive regressions. We re-estimate the weights at each date in the sample recursively over time, using the entire history of data available in real time prior to each out-of-sample forecast. We assume that $ND = 14$, which implies that forecasters use daily information from at most the past two weeks before the survey deadline. This process is repeated for each daily financial factor in $G_{D,t}$ to form quarterly factors $G_{D,t}^Q$.

D.2.7 LDA Data

The LDA data are used as inputs into the machine learning forecasts. The database for our Latent Dirichlet Allocation (LDA) analysis contains around one million articles published in *Wall Street Journal* between January 1984 to Dec 2023. The current vintage of the results reported here is based a randomly selected sub-sample of 200,000 articles over the same period, one-fifth size of the entire database. The sample selection procedure follows Bybee et al. (2021). First, I remove all articles prior to January 1984 and after June 2022 and exclude articles published in weekends. Second, I exclude articles with subject tags associated with obviously non-economic content such as sports. Third, I exclude articles with the certain headline patterns, such as those associated with data tables or those corresponding to regular sports, leisure, or books columns. I filter the articles using the same list of exclusions provided by Bybee et al. (2021). Last, I exclude articles with less than 100 words.

Processing of texts The processing of the texts can be summarized into five steps:

1. Tokenization: parse each article's text into a white-space-separated word list retaining the article's word ordering.
2. I drop all non-alphabetical characters and set the remaining characters to lower-case, remove words with less than 3 letters, and remove common stop words and URL-based terms. I use a standard list of stop words from the Python library *gensim.parsing.preprocessing*.
3. Lemmatization and Stemming: lemmatization returns the original form of a word using external dictionary *Textblob.Word* in Python and based on the context of the word. For instance, as a verb, “went” is converted to “go”. Stemming usually refers to a heuristic process that removes the trailing letters at the end of the words, such as from “assesses” to “assess”, and “really” to “real”. I use the Python library *Textblob.Word* to implement the lemmatization and *SnowballStemmer* for the stemming. The results are not very sensitive to the particular Python packages being used.
4. From the first three steps, I obtain a list of uni-grams which are a list of singular words. For example, “united” and “states” are uni-grams from “united states”. From the list of uni-grams, I generate a set of bi-grams as all pairs of (ordered) adjacent uni-grams. For example, “united states” together is one bi-gram. I then exclude uni-grams and bi-grams appearing in less than 0.1% of articles.
5. Last, I convert an article's word list into a vector of counts for each uni-gram and bi-gram. For example, the vector of counts [5, 7, 2] corresponds to the number of times the words [“federal”, “reserve”, “bank”] appear in the article.

The LDA Model The LDA model Blei et al. (2003) essentially achieves substantial dimension reduction of the word distribution of each article using the following assumptions. I assume a factor structure on the vectors of word counts. Each factor is a topic and each article is a parametric distribution of topics, specified as follows,

$$\underbrace{\begin{matrix} V \times 1 \\ w_i \end{matrix}}_{\text{word dist of article } i} \sim \text{Mult} \left(\underbrace{\begin{matrix} V \times K \\ \Phi' \end{matrix}}_{\text{topic-word dist}}, \underbrace{\begin{matrix} K \times 1 \\ \theta_i \end{matrix}}_{\text{topic dist.}}, \underbrace{N_i}_{\# \text{ of words}} \right)$$

where Mult is the multinomial distribution. In the above equation, w_i is a vector of word counts of each unique term (uni-gram or bi-gram) in article i , whose size is equal to the number of unique terms V . K is the number of factors in article i . In the estimation, I assume $K = 180$ following Bybee et al. (2021). Φ is a matrix sized $K \times V$, whose k th row and v th column is equal to the probability of the unique term v showing up in topic k . θ_i stores the weights of all k topics contained in article i , which sum up to one. Dimension reduction is achieved as long as $K \ll V$ (the number of topics are significantly smaller than the number of unique terms). More specifically, it reduces the dimension from $T \times V$ to $T \times K$ (the size of θ) + $K \times V$ (the size of Φ).

Real-time news factors. I also generate real-time news factors for each month t starting from January 1991. In theory, I could train the LDA model using each real-time monthly vintage but it is computationally challenging. Instead, I simplify the procedure by training the LDA model using quarterly vintages $t, t+3, t+6$, etc, and use the LDA model parameters estimated at t to filter news paper articles within the quarter and generate news factors for those months. More specifically, given every article's word distribution $w_{i,t+s}$, for $s = 0, 1, 2$, and the estimated real-time topic-word distribution parameters $\hat{\Phi}_t$ using articles till date t , one can obtain the filtered topic distribution of each article $\hat{\theta}_{i,t+s}$, as follows,

$$\underbrace{\begin{matrix} V \times 1 \\ w_{i,t+s} \end{matrix}}_{\text{word dist of article } i \text{ at time } t+s} \sim \text{Mult} \left(\underbrace{\begin{matrix} V \times K \\ \hat{\Phi}' \end{matrix}}_{\text{topic-word dist}}, \underbrace{\begin{matrix} K \times 1 \\ \hat{\theta}_{i,t+s} \end{matrix}}_{\text{topic dist.}}, \underbrace{N_{i,t+s}}_{\# \text{ of words}} \right).$$

LDA Estimation I use the built-in LDA model estimation toolbox in the Python library <https://pypi.org/project/gensim/> to implement the model estimation. The model requires following initial inputs and parameters and it is estimated using Bayesian methods. In theory, maximum-likelihood estimation is possible but it is computationally challenging.

1. I create a document-term matrix \mathbf{W} as a collection of w_i for all articles i in the sample. The number of rows in \mathbf{W} is equal to the number of articles in our sample and the number of columns in \mathbf{W} is equal to the number of unique uni-gram and bi-grams (after being filtered) across all articles. The matrix \mathbf{W} is used as an input for the LDA model estimation. I then follow Bybee et al. (2021) and set the number of topics K to be 180. The authors used Bayesian criteria to find 180 to be an optimal number of topics.

2. In the Python library Gensim, the key parameters of the LDA estimation are α and β . With a higher value of α , the documents are composed of more topics. With a higher value of β , each topic contains more terms (uni- or bi-grams). In the implementations, I do not impose any explicit restrictions on initial values of those parameters and set them to be “auto”. These two parameters, alongside Φ' and $\{\theta_i\}_i$, are estimated by the toolbox from Python library <https://pypi.org/project/gensim/>.

Real-time LDA Factors With the estimated topic weights $\theta_{i,t}$ of each article i from the LDA model, I further construct time series of the overall news attention to each topic, or a news factor. The value of the topic k at time t is the average weights of topic k of all articles published at t , specified as follows,

$$F_{k,t} = \frac{\sum_i \hat{\theta}_{i,k,t}}{\# \text{ of articles at } t}$$

for all topics k . We construct daily LDA factors by aggregating all articles published on each calendar day. The value of topic k at day t is the average weights of topic k across all articles published that day.

D.2.8 Machine Variables to Be forecast

Returns and price growth When evaluating the MSE ratio of the machine relative to that of a benchmark survey, we use the machine forecast for the return or price growth measure that most closely corresponds to the concept that survey respondents are asked to predict:

1. CFO survey asks respondents about their expectations for the S&P 500 return over the next 12 months. Following Nagel and Xu (2021), we interpret the survey to be asking about $r_{t,t+12}^d$, the one-year CRSP value-weighted return (including dividends) from the current survey month to the same month one year ahead.
2. Gallup/UBS survey respondents report the return (including dividends) they expect on their own portfolio one year ahead. We interpret the survey to be asking about $r_{t,t+12}^d$, the one-year CRSP value-weighted return (including dividends) from the current survey month to the same month one year ahead.
3. Livingston survey respondents provide 12-month ahead forecasts of the S&P 500 index. We convert the level forecast to price growth forecast by taking the log difference between the 12-month ahead level forecast and the nowcast of the S&P 500 index for the current survey month. Therefore, we interpret the survey to be asking about the one-year price growth in the S&P 500 index.
4. Bloomberg Consensus Forecasts asks survey respondents about the end-of-year closing value of the S&P 500 index. We interpret the survey to be asking about the h -month price growth in the S&P 500 index. The horizon of the forecast changes depending on when in the year the panelists are answering the survey.
5. Michigan Survey of Consumers (SOC) asks respondents about their perceived probability that an investment in a diversified stock fund would increase in value in the year ahead. We interpret the question to be asking about the one-year price growth in the S&P 500 index.
6. Conference Board (CB) survey asks respondents about their categorical belief on whether they expect stock prices to increase, decrease, or stay the same over the next year. We interpret the question to be asking about the one-year price growth in the S&P 500 index.

Earnings growth (IBES “Street” Earnings) For earnings growth forecasts, we use a quarterly S&P 500 total earnings series based on IBES street earnings per share (EPS), as described above. Street earnings exclude discontinued operations, extraordinary charges, and other non-operating items, making them better aligned with the earnings measure targeted by survey respondents. We convert EPS to total earnings using the S&P 500 index divisor and use the resulting quarterly series directly, prior to any monthly interpolation, since the machine learning algorithm operates at a quarterly frequency. The IBES street earnings series spans 1983Q4 to 2021Q4.

For Long-Term Growth (LTG) forecasts, IBES defines LTG as the “expected annual increase in operating earnings over the company’s next full business cycle. These forecasts refer to a period of between three to five years.” We compare survey responses of LTG against machine forecasts under alternative interpretations of LTG. First, we consider machine forecasts of annual five-year forward growth, i.e., annual earnings growth from four to five years ahead (Bianchi et al. (2024)). Second, we consider machine forecasts of annualized 5-year growth, i.e., annual earnings growth from current quarter to five years ahead, following the interpretation in Bordalo et al. (2019). Third, we consider machine forecasts of annualized earnings growth from one to 10 years ahead, following the interpretation in Nagel and Xu (2021).

Inflation We construct forecasts of annual inflation defined as $\pi_{t+4,t} = \log\left(\frac{PGDP_{t+4}}{PGDP_t}\right)$, where $PGDP_t$ is the quarterly level of the chain-weighted GDP price index. Following Coibion and Gorodnichenko (2015), we use the vintage of inflation data that is available four quarters after the period being forecast.

D.2.9 Machine Input Data: Predictor Variables

The vector $\mathbf{Z}_{jt} \equiv (y_{j,t}, \hat{\mathbf{G}}'_t, \mathbf{W}'_{jt})'$ is an $r = 1 + r_G + r_W$ vector which collects the data at time t with

$$\mathcal{Z}_{jt} \equiv (y_{j,t}, \dots, y_{j,t-p_y}, \hat{\mathbf{G}}'_t, \dots, \hat{\mathbf{G}}'_{t-p_G}, \mathbf{W}'_{jt}, \dots, \mathbf{W}'_{j,t-p_W})'$$

a vector of contemporaneous and lagged values of \mathbf{Z}_{jt} , where p_y, p_G, p_W denote the total number of lags of $y_{j,t}$, $\hat{\mathbf{G}}'_t$, \mathbf{W}'_{jt} , respectively. The predictors below are listed as elements of $y_{j,t}$, $\hat{\mathbf{G}}'_t$, or \mathbf{W}'_{jt} for variables.

Stock return and price growth predictor variables and specifications For y_j equal to CRSP value-weighted returns or S&P 500 price index growth, we first predict the one-year log stock return or price growth that is expected to occur h quarters into the future from time $t+h-4$ to $t+h$, i.e., $\mathbb{E}_t[r_{t+h-4,t+h}]$. For horizons longer than one year, since the h -quarter long horizon return is the sum of one-year returns between time t to $t+h$, we first forecast the forward one-year returns separately and then add the components together to get machine forecasts of h -quarter long horizon returns. The forecasting model considers the following variables. Lags of the dependent variable:

1. y_{t-1}, y_{t-2} one and two quarter lagged stock returns or price growth.

The factors in $\hat{\mathbf{G}}'_t$ are formed from three large datasets separately:

1. $\mathbf{G}_{M,t-k}$, for $k = 0, 1$ are factors formed from a real-time macro dataset \mathcal{D}^M with 92 real-time macro series; includes both monthly and quarterly series, with monthly series converted to quarterly according to the method described in the data appendix.
2. $\mathbf{G}_{F,t-k}$, for $k = 0, 1$ are factors formed from a financial data set \mathcal{D}^F with 147 monthly financial series.
3. $\mathbf{G}_{D,t-k}^Q$, for $k = 0$ are quarterly factors formed from a daily financial dataset \mathcal{D}^D of 87 daily financial indicators. The raw daily series are first converted to daily factors $\mathbf{G}_{D,t}(\mathbf{w})$ and the daily factors are aggregated up to quarterly observations $\mathbf{G}_{D,t}^Q(\mathbf{w})$ using a weighted average of daily factors, with the weights \mathbf{w} dependent on two free parameters that are chosen to minimize the sum of squared residuals in a regression of $y_{j,t+h}$ on $\mathbf{G}_{D,t}(\mathbf{w})$.

The variables in \mathbf{W}'_{jt} include:

1. *LDA topics* $F_{k,t-j}$, for topic $k = 1, 2, \dots, 50$ and $j = 0, 1$. The value of the topic k at time t is the average weights of topic k of all articles published at t .
2. *Macro data surprises* from the money market survey. The macro news include, GDP growth (Q/Q percentage change), core CPI (Month/Month change), unemployment rate (percentage point), and nonfarm payroll (month/month change). We include first release, second release, and final release for GDP growth. This constitutes six macro data surprises per quarter.
3. *FOMC surprises* are defined as the changes in the current-month, 1, 2, 6, 12, and 24 month-ahead federal funds futures (FFF) contract rate and the changes in the 1, 2, 4, and 8 quarter-ahead Eurodollar (ED) futures contracts, from 10 minutes before to 20 minutes after each FOMC announcement. When benchmarking against a survey, we use the last FOMC meeting before the survey deadline to compute surprises. For surveys that do not have a clear deadline, we compute surprises using from the last FOMC in the first month of the quarter. When benchmarking against moving average, we use the last FOMC meeting before the end of the first month in each quarter to compute surprises. This leaves 10 FOMC surprise variables per quarter.
4. *Stock market jumps* are accumulated 30-minute window negative and positive jumps in the S&P 500 around news events over the previous quarter.
5. *Long-term growth of earnings*: 5-year growth of the SP500 earnings per share.
6. *Short rates*. When forecasting returns or price growth, the machine controls for the current nominal short rate, $\log(1 + 3MTB_t/100)$, imposing a unit coefficient. This is equivalent to forecasting the future return minus the current short rate.

The 92 macro series in \mathcal{D}^M are selected to represent broad categories of macroeconomic time series. The majority of these are real activity measures: real output and income, employment and hours, consumer spending, housing starts, orders and unfilled orders, compensation and labor costs, and capacity utilization measures. The dataset also includes commodity and price indexes and a handful of bond and stock market indexes, and foreign exchange measures. The financial dataset \mathcal{D}^F is an updated monthly version of the 147 variables comprised solely of financial market time series used in Ludvigson and Ng (2007). These data include valuation ratios such as the dividend-price ratio and earnings-price ratio, growth rates of aggregate dividends and prices, default and term spreads, yields on corporate bonds of different ratings grades, yields on Treasuries and yield spreads, and a broad cross-section of industry, size, book-market, and momentum portfolio equity returns. A detailed description of the series is given in the Data Appendix of the online supplementary file at www.sydneyludvigson.com/succ_data_appendix.pdf. The 87 daily financial indicators in \mathcal{D}^D include daily time series on commodities spot prices and futures prices, aggregate stock market indexes, volatility indexes, credit spreads and yield spreads, and exchange rates.

Earning growth predictor variables and specifications For y_t equal to S&P 500 log earning growth, we construct a forecasted value for y_t , denoted $\hat{y}_{t|t-h}$, based on information known up to time t using the following variables. Lags of the dependent variable:

1. y_{t-1}, y_{t-2} one and two quarter lagged earnings growth.

The factors in $\hat{\mathbf{G}}'_{jt}$ are formed from three large datasets separately:

1. $\mathbf{G}_{M,t-k}$, for $k = 0, 1$ are factors formed from a real-time macro dataset \mathcal{D}^M with 92 real-time macro series; includes both monthly and quarterly series, with monthly series converted to quarterly according to the method described in the data appendix.
2. $\mathbf{G}_{F,t-k}$, for $k = 0, 1$ are factors formed from a financial data set \mathcal{D}^F with 147 monthly financial series.
3. $\mathbf{G}_{D,t-k}^Q$, for $k = 0$ are quarterly factors formed from a daily financial dataset \mathcal{D}^D of 87 daily financial indicators. The raw daily series are first converted to daily factors $\mathbf{G}_{D,t}(\mathbf{w})$ and the daily factors are aggregated up to quarterly observations $\mathbf{G}_{D,t}^Q(\mathbf{w})$ using a weighted average of daily factors, with the weights \mathbf{w} dependent on two free parameters that are chosen to minimize the sum of squared residuals in a regression of $y_{j,t}$ on $\mathbf{G}_{D,t}(\mathbf{w})$.

The variables in \mathbf{W}'_{jt} include:

1. *LDA factors* $F_{k,t-j}$, for topic $k = 1, 2, \dots, 50$ and $j = 0, 1$. The value of the topic k at time t is the average weights of topic k of all articles published at t .
2. *Macro data surprises* from the money market survey. The macro news include, GDP growth (Q/Q percentage change), core CPI (Month/Month change), unemployment rate (percentage point), and nonfarm payroll (month/month change). We include first release, second release, and final release for GDP growth. This constitutes six macro data surprises per quarter.
3. *FOMC surprises* are defined as the changes in the current-month, 1, 2, 6, 12, and 24 month-ahead federal funds futures (FFF) contract rate and the changes in the 1, 2, 4, and 8 quarter-ahead Eurodollar (ED) futures contracts, from 10 minutes before to 20 minutes after each FOMC announcement. When benchmarking against a survey, we use the last FOMC meeting before the survey deadline to compute surprises. For surveys that do not have a clear deadline, we compute surprises using from the last FOMC in the first month of the quarter. When benchmarking against moving average, we use the last FOMC meeting before the end of the first month in each quarter to compute surprises. This leaves 10 FOMC surprise variables per quarter.
4. *Stock market jumps* are accumulated 30-minute window negative and positive jumps in the S&P 500 around news events over the previous quarter.

Inflation predictor variables For y_j equal to inflation, the forecasting model considers the following variables. Lags of the dependent variable:

1. $y_{t-1,t-h-1}$ one quarter lagged inflation.

The factors in $\hat{\mathbf{G}}'_{jt}$ are formed from three large datasets separately:

1. $\mathbf{G}_{M,t-k}$, for $k = 0, 1$ are factors formed from a real-time macro dataset \mathcal{D}^M with 92 real-time macro series; includes both monthly and quarterly series, with monthly series converted to quarterly according to the method described in the data appendix.

2. $\mathbf{G}_{F,t-k}$, for $k = 0, 1$ are factors formed from a financial data set \mathcal{D}^F with 147 monthly financial series.
3. $\mathbf{G}_{D,t-k}^Q$, for $k = 0$ are quarterly factors formed from a daily financial dataset \mathcal{D}^D of 87 daily financial indicators. The raw daily series are first converted to daily factors $\mathbf{G}_{D,t}(\mathbf{w})$ and the daily factors are aggregated up to quarterly observations $\mathbf{G}_{D,t}^Q(\mathbf{w})$ using a weighted average of daily factors, with the weights \mathbf{w} dependent on two free parameters that are chosen to minimize the sum of squared residuals in a regression of $y_{j,t+h}$ on $\mathbf{G}_{D,t}(\mathbf{w})$.

The variables in \mathbf{W}'_{jt} include:

1. $\mathbb{F}_{jt-k}^{(i)}[y_{jt+h-k}]$, lagged values of the i th type's forecast, where $k = 1, 2$
2. $\mathbb{F}_{jt-1}^{(s \neq i)}[y_{jt+h-1}]$, lagged values of other type's forecasts, $s \neq i$
3. $var_N\left(\mathbb{F}_{t-1}^{(\cdot)}[y_{jt+h-1}]\right)$, where $var_N(\cdot)$ denotes the cross-sectional variance of lagged survey forecasts
4. $skew_N\left(\mathbb{F}_{t-1}^{(\cdot)}[y_{jt+h-1}]\right)$, where $skew_N(\cdot)$ denotes the cross-sectional skewness of lagged survey forecasts
5. Trend inflation measured as $\bar{\pi}_{t-1} = \begin{cases} \rho\bar{\pi}_{t-2} + (1-\rho)\pi_{t-1}, \rho = 0.95 & \text{if } t < 1991\text{Q4} \\ \text{CPI10}_{t-1} & \text{if } t \geq 1991\text{Q4} \end{cases}$, where CPI10 is the median SPF forecast of annualized average inflation over the current and next nine years. Trend inflation is intended to capture long-run trends. When long-run forecasts of inflation are not available, as is the case pre-1991Q4, we use a moving average of past inflation.
6. \dot{GDP}_{t-1} = detrended gross domestic product, defined as the residual from a regression of GDP_{t-1} on a constant and the four most recent values of GDP as of date $t - 8$. See Hamilton (2018).
7. \dot{EMP}_{t-1} = detrended employment, defined as the residual from a regression of EMP_{t-1} on a constant and the four most recent values of EMP as of date $t - 8$. See Hamilton (2018).
8. $\mathbb{N}_t^{(i)}[\pi_{t,t-h}]$ = Nowcast as of time t of the i th percentile of inflation over the period $t - h$ to t .

D.3 Cross-Sectional Forecasts

I construct machine learning forecasts of stock returns and earnings growth at the firm level using the Long Short-Term Memory (LSTM) framework described in Section D. The model is estimated using pooled panel data across all firms, with firm-specific predictors as inputs. I re-estimate model parameters and update hyperparameters every four quarters using a recursively expanding sample to maintain computational tractability while still incorporating new information. The stock universe consists of about 5,000 firms listed on the NYSE, AMEX, and NASDAQ with available IBES analyst coverage for one- and two-year ahead earnings expectations and long-term growth forecasts. Monthly total returns for these firms are obtained from CRSP. The sample spans March 1990 to December 2024.

To construct predictors, I follow the cross-sectional asset pricing literature and compile a broad set of stock-level characteristics. Specifically, I include 94 firm characteristics, of which 61 are updated annually, 13 quarterly, and 20 monthly. These characteristics span valuation ratios, profitability, investment, size, momentum, volatility, and other firm-level attributes, based on the definitions in Green et al. (2013). Book equity and operating profitability follow Fama and French (2015). I rank-transform each characteristic cross-sectionally within each month to the $[-1, 1]$ interval, as in Gu et al. (2020). I also include 74 industry dummies based on two-digit Standard Industrial Classification (SIC) codes. Table A.15 provides further details on these predictors. To avoid forward-looking bias, I apply realistic reporting lags: monthly characteristics are assumed available with a one-month delay, quarterly characteristics with at least a four-month delay, and annual characteristics with at least a six-month delay. Missing values are replaced with the cross-sectional median at each period.

Following Gu et al. (2020), I construct an expanded set of predictors that interact firm-level characteristics with aggregate macroeconomic state variables. Let $\mathcal{C}_{i,t}$ denote the vector of firm characteristics for firm i , and let \mathcal{X}_t denote the vector of aggregate predictors, which includes a constant and the same macroeconomic variables used to forecast aggregate returns, price growth, and earnings growth, respectively. The final predictor set for firm i at time t is given by $\mathcal{X}_{i,t} = \mathcal{X}_t \otimes \mathcal{C}_{i,t}$, where \otimes denotes the Kronecker product. This structure generates interaction terms that capture how aggregate economic conditions influence the effect of firm-level characteristics on expected returns and earnings growth.

Table A.15: Details of Firm Characteristics

No.	Acronym	Characteristic	Authors	Source	Freq.
1	absacc	Absolute accruals	Bandyopadhyay, Huang, Wirjanto 2010	Compustat	Y
2	acc	Working capital accruals	Sloan 1996	Compustat	Y
3	aeavol	Abnormal earnings ann volume	Lerman, Livnat, Mendenhall 2007	Compustat/CRSP	Q
4	age	Years since first coverage	Jiang, Lee, Zhang 2005	Compustat	Y
5	agr	Asset growth	Cooper, Gulen, Schill 2008	Compustat	Y
6	baspread	Bid-ask spread	Amihud, Mendelson 1989	CRSP	M
7	beta	Beta	Fama, MacBeth 1973	CRSP	M
8	betasq	Beta squared	Fama, MacBeth 1973	CRSP	M
9	bm	Book-to-market	Rosenberg, Reid, Lanstein 1985	Compustat/CRSP	Y
10	bm_ia	Industry-adj book-to-market	Asness, Porter, Stevens 2000	Compustat/CRSP	Y
11	cash	Cash holdings	Palazzo 2012	Compustat	Q
12	cashdebt	Cash flow to debt	Ou, Penman 1989	Compustat	Y
13	cashpr	Cash productivity	Chandrashekhar, Rao 2009	Compustat	Y
14	cfp	Cash flow to price ratio	Desai, Rajgopal, Venkatachalam 2004	Compustat	Y
15	cfp_ia	Industry-adj cash flow to price ratio	Asness, Porter, Stevens 2000	Compustat	Y
16	chatoia	Industry-adj chg asset turnover	Soliman 2008	Compustat	Y
17	chcsho	Chg shares outstanding	Pontiff, Woodgate 2008	Compustat	Y
18	chempia	Industry-adj chg employees	Asness, Porter, Stevens 1994	Compustat	Y
19	chinv	Chg inventory	Thomas, Zhang 2002	Compustat	Y
20	chmom	Chg 6-month momentum	Gettleman, Marks 2006	CRSP	M
21	chpmia	Industry-adj chg profit margin	Soliman 2008	Compustat	Y
22	chtx	Chg tax expense	Thomas, Zhang 2011	Compustat	Q
23	cinvest	Corporate investment	Titman, Wei, Xie 2004	Compustat	Q
24	convind	Convertible debt indicator	Valta 2016	Compustat	Y
25	currat	Current ratio	Ou, Penman 1989	Compustat	Y
26	depr	Depreciation over PP&E	Holthausen, Larcker 1992	Compustat	Y
27	divi	Dividend initiation	Michaely, Thaler, Womack 1995	Compustat	Y
28	divo	Dividend omission	Michaely, Thaler, Womack 1995	Compustat	Y
29	dolvol	Dollar trading volume	Chordia, Subrahmanyam, Anshuman 2001	CRSP	M
30	dy	Dividend-to-price ratio	Litzenberger, Ramaswamy 1982	Compustat	Y
31	ear	Earnings announcement return	Kishore, Brandt, Santa-Clara, Venkatachalam 2008	Compustat/CRSP	Q
32	egr	Gr common shareholder equity	Richardson, Sloan, Soliman, Tuna 2005	Compustat	Y
33	ep	Earnings-to-price ratio	Basu 1977	Compustat	Y
34	gma	Gross profitability	Novy-Marx 2013	Compustat	Y
35	grCAPX	Gr capex	Anderson, Garcia-Feijoo 2006	Compustat	Y
36	grltnoa	Gr long-term net operating assets	Fairfield, Whisenant, Yohn 2003	Compustat	Y
37	herf	Industry sales concentration	Hou, Robinson 2006	Compustat	Y
38	hire	Employee gr rate	Bazdresch, Belo, Lin 2014	Compustat	Y
39	idiivol	Idiosyncratic return volatility	Ali, Hwang, Trombley 2003	CRSP	M
40	ill	Illiquidity	Amihud 2002	CRSP	M
41	indmom	Industry momentum	Moskowitz, Grinblatt 1999	CRSP	M
42	invest	Capital expenditures and inventory	Chen, Zhang 2010	Compustat	Y
43	lev	Leverage	Bhandari 1988	Compustat	Y
44	lgr	Gr long-term debt	Richardson, Sloan, Soliman, Tuna 2005	Compustat	Y
45	maxret	Maximum daily return	Bali, Cakici, Whitelaw 2011	CRSP	M
46	mom12m	12-month momentum	Jegadeesh 1990	CRSP	M
47	mom1m	1-month momentum	Jegadeesh, Titman 1993	CRSP	M
48	mom36m	36-month momentum	Jegadeesh, Titman 1993	CRSP	M
49	mom6m	6-month momentum	Jegadeesh, Titman 1993	CRSP	M
50	ms	Financial statement score	Mohanram 2005	Compustat	Q
51	mvel1	Size	Banz 1981	CRSP	M
52	mve_ia	Industry-adj size	Asness, Porter, Stevens 2000	Compustat	Y
53	nincr	Number of earnings increases	Barth, Elliott, Finn 1999	Compustat	Q
54	operprof	Operating profitability	Fama, French 2015	Compustat	Y
55	orgcap	Organizational capital	Eisfeldt, Papanikolaou 2013	Compustat	Y
56	pchcapx_ia	Industry-adj % chg capex	Abarbanell, Bushee 1998	Compustat	Y
57	pchcurrat	% chg current ratio	Ou, Penman 1989	Compustat	Y
58	pchdepr	% chg depreciation	Holthausen, Larcker 1992	Compustat	Y
59	pchgm	% chg gross margin - % chg sales	Abarbanell, Bushee 1998	Compustat	Y
	pchsale				
60	pchquick	% chg quick ratio	Ou, Penman 1989	Compustat	Y
61	pchsale	% chg sales - % chg inventory	Abarbanell, Bushee 1998	Compustat	Y
	pchinvt				
62	pchsale	% chg sales - % chg receivables	Abarbanell, Bushee 1998	Compustat	Y
	pchrect				
63	pchsale	% chg sales - % chg SG&A	Abarbanell, Bushee 1998	Compustat	Y
	pchxsga				

No.	Acronym	Firm Characteristic	Authors	Source	Freq.
64	pchsaleinv	% chg sales-to-inventory	Ou, Penman 1989	Compustat	Y
65	pctacc	Percent accruals	Hafzalla, Lundholm, Van Winkle 2011	Compustat	Y
66	pricedelay	Price delay	Hou, Moskowitz 2005	CRSP	M
67	ps	Financial statement score	Piotroski 2000	Compustat	Y
68	quick	Quick ratio	Ou, Penman 1989	Compustat	Y
69	rd	R&D increase	Eberhart, Maxwell, Siddique 2004	Compustat	Y
70	rd_mve	R&D to market capitalization	Guo, Lev, Shi 2006	Compustat	Y
71	rd_sale	R&D to sales	Guo, Lev, Shi 2006	Compustat	Y
72	realestate	Real estate holdings	Tuzel 2010	Compustat	Y
73	retvol	Return volatility	Ang, Hodrick, Xing, Zhang 2006	CRSP	M
74	roaq	Return on assets	Balakrishnan, Bartov, Faurel 2010	Compustat	Q
75	roavol	Earnings volatility	Francis, LaFond, Olsson, Schipper 2004	Compustat	Q
76	roeq	Return on equity	Hou, Xue, Zhang 2015	Compustat	Q
77	roic	Return on invested capital	Brown, Rowe 2007	Compustat	Y
78	rsup	Revenue surprise	Kama 2009	Compustat	Q
79	salecash	Sales to cash	Ou, Penman 1989	Compustat	Y
80	saleinv	Sales to inventory	Ou, Penman 1989	Compustat	Y
81	salerec	Sales to receivables	Ou, Penman 1989	Compustat	Y
82	secured	Secured debt	Valta 2016	Compustat	Y
83	securedind	Secured debt indicator	Valta 2016	Compustat	Y
84	sgr	Sales gr	Lakonishok, Shleifer, Vishny 1994	Compustat	Y
85	sin	Sin stocks	Hong, Kacperczyk 2009	Compustat	Y
86	sp	Sales to price	Barbee, Mukherji, Raines 1996	Compustat	Y
87	std_dolvol	Volatility liquidity dollar volume	Chordia, Subrahmanyam, Anshuman 2001	CRSP	M
88	std_turn	Volatility liquidity share turnover	Chordia, Subrahmanyam, Anshuman 2001	CRSP	M
89	stdacc	Accrual volatility	Bandyopadhyay, Huang, Wirjanto 2010	Compustat	Q
90	stdcf	Cash flow volatility	Huang 2009	Compustat	Q
91	tang	Debt capacity / firm tangibility	Almeida, Campello 2007	Compustat	Y
92	tb	Tax income to book income	Lev, Nissim 2004	Compustat	Y
93	turn	Share turnover	Datar, Naik, Radcliffe 1998	CRSP	M
94	zerotrade	Zero trading days	Liu 2006	CRSP	M